

# **Industrial Chemicals via C<sub>1</sub> Processes**



A C S   S Y M P O S I U M   S E R I E S   **328**

# **Industrial Chemicals via C<sub>1</sub> Processes**

**Darryl R. Fahey, EDITOR**  
*Phillips Petroleum Company*

Developed from a symposium sponsored by  
the Division of Petroleum Chemistry, Inc.  
at the 191st Meeting  
of the American Chemical Society,  
New York, New York  
April 13-18, 1986



American Chemical Society, Washington, DC 1987



### Library of Congress Cataloging-in-Publication Data

Industrial chemicals via  $C_1$  processes.  
(ACS symposium series; 328)

“Developed from a symposium sponsored by the  
Division of Petroleum Chemistry, Inc. at the 191st  
Meeting of the American Chemical Society, New York,  
New York, April 13-18, 1986.”

Bibliography: p.  
Includes index.

1. Feedstock—Congresses. 2. Synthesis gas—  
Congresses. 3. Carbon compounds—Congresses.

I. Fahey, Daryl R. II. American Chemical Society.  
Division of Petroleum Chemistry. III. Series.

TP201.I46 1986 661.8 86-26616  
ISBN 0-8412-1009-8

Copyright © 1987

American Chemical Society

All Rights Reserved. The appearance of the code at the bottom of the first page of each chapter in this volume indicates the copyright owner's consent that reprographic copies of the chapter may be made for personal or internal use or for the personal or internal use of specific clients. This consent is given on the condition, however, that the copier pay the stated per copy fee through the Copyright Clearance Center, Inc., 27 Congress Street, Salem, MA 01970, for copying beyond that permitted by Sections 107 or 108 of the U.S. Copyright Law. This consent does not extend to copying or transmission by any means—graphic or electronic—for any other purpose, such as for general distribution, for advertising or promotional purposes, for creating a new collective work, for resale, or for information storage and retrieval systems. The copying fee for each chapter is indicated in the code at the bottom of the first page of the chapter.

The citation of trade names and/or names of manufacturers in this publication is not to be construed as an endorsement or as approval by ACS of the commercial products or services referenced herein; nor should the mere reference herein to any drawing, specification, chemical process, or other data be regarded as a license or as a conveyance of any right or permission, to the holder, reader, or any other person or corporation, to manufacture, reproduce, use, or sell any patented invention or copyrighted work that may in any way be related thereto. Registered names, trademarks, etc., used in this publication, even without specific indication thereof, are not to be considered unprotected by law.

PRINTED IN THE UNITED STATES OF AMERICA

**American Chemical Society**  
Library  
1155 16th St., N.W.  
Washington, D.C. 20036

# ACS Symposium Series

**M. Joan Comstock, *Series Editor***

## *Advisory Board*

**Harvey W. Blanch**  
University of California—Berkeley

**Alan Elzerman**  
Clemson University

**John W. Finley**  
Nabisco Brands, Inc.

**Marye Anne Fox**  
The University of Texas—Austin

**Martin L. Gorbaty**  
Exxon Research and Engineering Co.

**Roland F. Hirsch**  
U.S. Department of Energy

**Rudolph J. Marcus**  
Consultant, Computers &  
Chemistry Research

**Vincent D. McGinniss**  
Battelle Columbus Laboratories

**Donald E. Moreland**  
USDA, Agricultural Research Service

**W. H. Norton**  
J. T. Baker Chemical Company

**James C. Randall**  
Exxon Chemical Company

**W. D. Shults**  
Oak Ridge National Laboratory

**Geoffrey K. Smith**  
Rohm & Haas Co.

**Charles S. Tuesday**  
General Motors Research Laboratory

**Douglas B. Walters**  
National Institute of  
Environmental Health

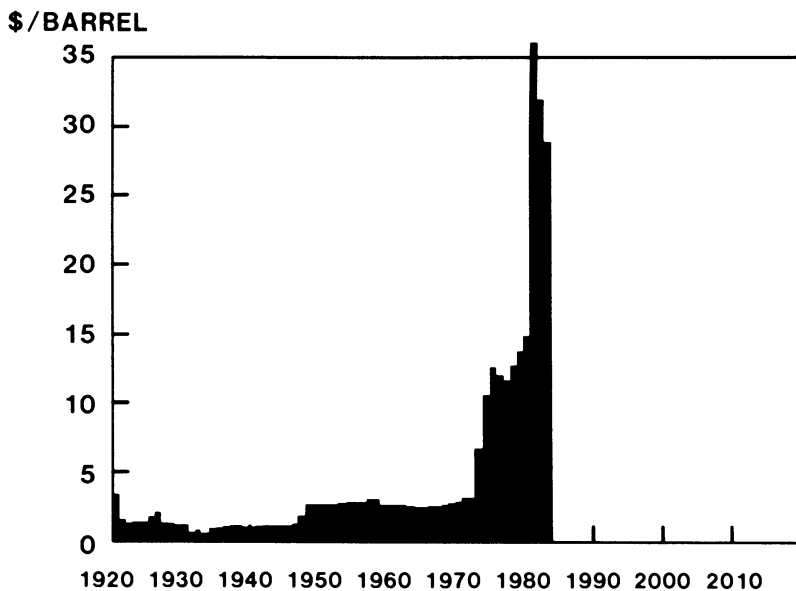
**C. Grant Willson**  
IBM Research Department

## Foreword

The ACS SYMPOSIUM SERIES was founded in 1974 to provide a medium for publishing symposia quickly in book form. The format of the Series parallels that of the continuing ADVANCES IN CHEMISTRY SERIES except that, in order to save time, the papers are not typeset but are reproduced as they are submitted by the authors in camera-ready form. Papers are reviewed under the supervision of the Editors with the assistance of the Series Advisory Board and are selected to maintain the integrity of the symposia; however, verbatim reproductions of previously published papers are not accepted. Both reviews and reports of research are acceptable, because symposia may embrace both types of presentation.

# Preface

ONE OF THE RESPONSES to the large increases in crude oil prices that began 13 years ago (see Figure) was an intensification of research and development activities in producing chemicals and fuels from nonpetroleum resources. Programs based on synthesis gas and methanol emerged in numerous U.S., European, and Japanese laboratories where these carbon sources were foreseen as feedstocks possessing long-term pricing and supply stability in contrast to the situation for crude oil. The fruits of these research and development efforts have been the discoveries of exciting new processes for industrial chemicals production. These discoveries range in development from early discoveries to full commercialization.



*Posted price of midcontinent crude oil at the well (yearly average).*

About midway through the 1980s, the escalating crude oil prices took a dramatic turnabout. Because of the difficulty in forecasting crude oil prices 5–10 years into the future, predicting the extent of synthesis gas and methanol use as feedstocks during the next decade is impossible. However, the long-term picture continues to look favorable for industrial chemical opportunities based on synthesis gas and methanol feedstocks. In some cases, processes are developing that could become economically competi-

tive in the near term with conventional petrochemical-based processes. These processes could become economically competitive even with lower priced crude oil.

The intent of the symposium upon which this book is based was to (1) identify the technical and economic forces that are crucial for the successful production of chemicals from synthesis gas and methanol within an ever-changing world economic climate, (2) delineate the present state of technical development for the chemicals most likely to be commercially produced from synthesis gas and methanol, and (3) provide useful new mechanistic insights into these and closely related processes that will speed development of the field. This volume contains chapters written by most of the speakers from that symposium. In addition, several complementary chapters have been added for subject balance. The result is a volume that covers technical and economic aspects of most of the new industrially interesting synthesis gas- or methanol-based chemical processes.

I sincerely appreciate the efforts of the authors and all others who have contributed their time and thought to the preparation of this book. Acknowledgment is made to the donors of the Petroleum Research Fund, administered by the American Chemical Society (ACS), for partial support of the symposium.

DARRYL R. FAHEY  
Research and Development  
Phillips Petroleum Company  
Bartlesville, OK 74004



# Chapter 1

## Synthesis Gas Feedstock for Chemicals

W. Keim

Institut für Technische Chemie und Petrolchemie der Rheinisch-Westfälischen  
Technischen Hochschule Aachen, Worringer Weg 1, D-5100 Aachen,  
Federal Republic of Germany

This paper deals with the application of synthesis gas as feedstock for chemicals. Distinction is made between a direct and indirect hydrogenation path of CO. The direct route leading to paraffins, olefins, oxygenates and N-containing derivatives is briefly discussed. Economics will favour reactions which retain at least one of the oxygen atoms of the original CO reactant and potential applications exist for alcohols. The indirect path considers methanol and methyl formate as intermediates. Starting from methanol, base and fine chemicals can be synthesized by carbonylation, reductive carbonylation and oxidative carbonylation. Special emphasis is given to the homologation of methanol to acetaldehyde. Finally various chemical reactions are discussed describing methyl formate as a potential building block.

The efforts to develop processes for fuels and chemicals from resources other than crude oil have seen a prodigious growth since 1973. The use of coal or natural gas derived synthesis gas has especially been considered to be a most promising route for the future production of fuel and chemicals. Numerous patents and papers have appeared and the reader is referred to the following books (1-6).

With the recent global decline in crude oil prices, the attractiveness of coal derived syngas as an alternate feedstock has ebbed bringing many efforts and considerations in this field back to the research stage.

Many arguments in favour of continuation of research and developments in syngas chemistry can be made on the following grounds: a) The long range availability of plentiful and low cost coal and natural gas will necessitate their utilization as raw materials. Since the development of a process from the bench scale to a commercial operation takes about 10-20 years, the need for doing research and development work today is obvious. b) The availability of alternative feedstocks and processes will ease monopoly positions of crude oil suppliers and will stabilize raw material prices. c) The shortage of foreign currency or strategic considerations will create regions where it is now sensible to produce fuels or chemicals starting from raw materials other than crude oil. d) Special situations can be envisioned where syngas derived chemicals can compete favourably as in the production of acetic acid, esters, and anhydrides.

Synthesis gas offers many routes to industrial chemicals. They can be classified in a direct and an indirect path as shown in Figure 1.

The direct conversion deals with the straight hydrogenation of carbon monoxide to paraffins, olefins and heteroatom (oxygen, nitrogen) containing products. The indirect conversion invokes intermediates such as methanol, methyl formate and formaldehyde. The latter ones in a consecutive reaction can yield a variety of desired chemicals. For instance, acetic acid can be synthesized directly from CO/H<sub>2</sub>, but for reasons of selectivity the carbonylation of methanol is by far the best commercial process.

For the synthesis of chemicals from CO/H<sub>2</sub> three considerations will influence the economics and process feasibility, namely the ratio of CO:H<sub>2</sub>, the loss of oxygen as by-product water or CO<sub>2</sub>, and the interrelation of chemicals/fuels. The two first points are exemplified in Table I.

Depending on the nature of the raw material (coal, natural gas, naphtha), both the reaction conditions of gasification, and the employment of reforming (shift conversion) will determine the composition of the syngas. For instance, synthesis gas produced from coal normally has a H<sub>2</sub>:CO ratio of unity and therefore the ratio has to be adjusted to 2.0 prior to the use of the gas for methanol synthesis. Accordingly, syngas derived from CH<sub>4</sub> bears a cost advantage for the needed ratio of 2.0. To remove oxygen atoms, water or CO<sub>2</sub> is formed as by-product, which in Table I is expressed in reactant loss as water. The synthesis of n-octane, representative for gasoline in the Fischer Tropsch synthesis, yields 57 % H<sub>2</sub>O indicating a poor raw material utilization. A similar picture is given for the ethene synthesis (Mobil route) from methanol. Therefore, both the ratio of CO:H<sub>2</sub> and the formation of water affect the economics of CO/H<sub>2</sub>

Table I. CO/H<sub>2</sub> usage

	ratio CO:H <sub>2</sub>	reactant loss (%) as H <sub>2</sub> O
<u>Direct conversion</u>		
CO + 2 H <sub>2</sub> → methanol	1:2	-
2 CO + 2 H <sub>2</sub> → acetic acid	1:1	-
2 CO + 2 H <sub>2</sub> → methyl formate	1:1	-
2 CO + 4 H <sub>2</sub> → ethanol	1:2	28
3 CO + 6 H <sub>2</sub> → propanol	1:2	38
2 CO + 3 H <sub>2</sub> → ethylene glycol	2:3	-
4 CO + 8 H <sub>2</sub> → isobutanol	1:2	50
2 CO + 4 H <sub>2</sub> → ethylene	1:2	56
8 CO + 34 H <sub>2</sub> → n-octane	1:2.1	57
<u>Indirect conversion</u>		
CH <sub>3</sub> OH + CO → acetic acid	-	-
CH <sub>3</sub> COOCH <sub>3</sub> + CO → acetic anhydride	-	-
2 CH <sub>3</sub> OH → ethylene	-	56

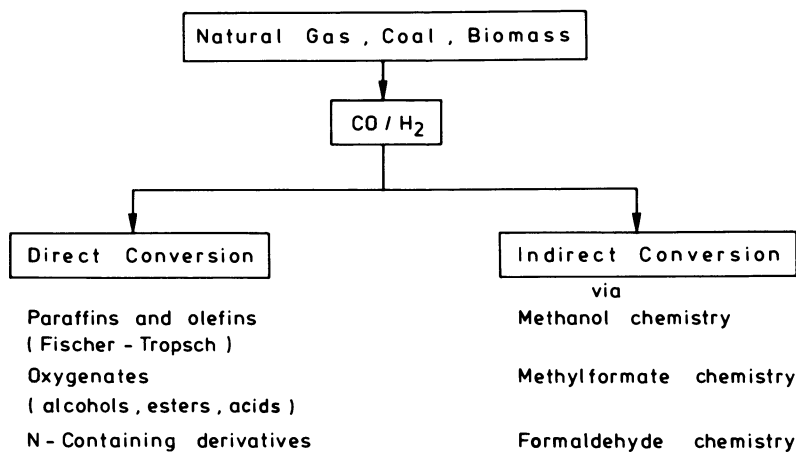


Figure 1. Direct and indirect conversion of synthesis gas

technology significantly. The chemical industry has always been tied very closely to the usage and development of energy whether it was coal in the past or crude oil today. Also in the future the fate of the chemical industry will be connected to the development of the energy resources. If methanol, ethanol or Fischer Tropsch products should ever enter into the energy sector, those products will be available as feedstocks for the chemical industry in practically any amount at rather low cost.

Within the frame work of this article special attention will be given to:

1. Direct conversion of synthesis gas
2. Indirect conversion of synthesis gas.

### Direct conversion of synthesis gas

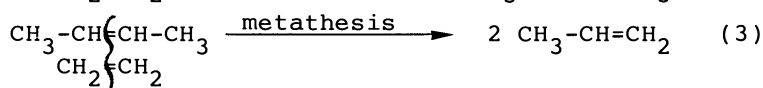
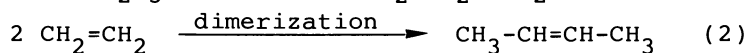
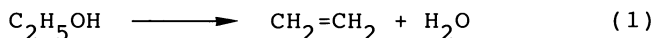
The direct conversion of synthesis gas can yield paraffins, olefins, oxygenates and nitrogen containing compounds. Best known here is the Fischer Tropsch synthesis yielding mixtures of mainly linear alkanes and/or alkenes. There have been many attempts to tailor the product slate to C<sub>2</sub>/C<sub>3</sub> olefins only. However, all data indicate, that the Schulz-Flory selectivity dominates. Mechanistically, the Fischer-Tropsch synthesis can be described as a reductive oligomerization of carbon monoxide following a geometric progression (Schulz-Flory distribution) in which the chain growth probability,  $\alpha$ , can possess various values (7). Prior to entering a costly research and development program, simple calculation can help to evaluate whether the mathematically determined product distribution can be balanced economically on the market. Tailoring the product distribution (selectivity) remains a challenging goal. Some research groups attack this problem by catalyst modifications (8). Other attempts aim at product adjustments by employing additional processes. Thus Shell has released details of its new process to transform natural gas to middle distillates, such as naphtha, gasoil and kerosene. In this scheme, methane is first converted to CO/H<sub>2</sub> followed by a Fischer-Tropsch type reaction using a proprietary catalyst. To adjust the product distribution the paraffins are hydrocracked to produce middle distillate (9). Another approach may be the conversion of Fischer-Tropsch olefins via methathesis similar to that practiced in the SHOP process by Shell (10). In this way, the low and high carbon number olefins may be convertible into the desired olefin range.

The synthesis of polymethylene directly from CO/H<sub>2</sub> was also attempted in various laboratories. However, great difficulties were encountered regarding catalyst activity and molecular weight distributions.

Based on economics (see Table I) the formation of oxygenates retaining at least one of the oxygen atoms of the original CO reactant is favoured. Potential applications exist here for the direct synthesis of alcohols, acids and esters. Methanol is by far the most promising chemical manufactured already from CO/H<sub>2</sub> in many millions of tons. The higher alcohols such as ethanol and propanol are potential candidates for chemicals or gasoline usage, alone or blended. Institute Francais Petrol (IFP) and Union Carbide, for instance, have disclosed catalysts, which synthesize quite selectively a spectrum of C<sub>1</sub>-C<sub>5</sub> alcohols. The IFP process currently is being further investigated together with Idemitsu in Japan and KFA Jülich in Germany (11-12). Also from Japan comes the message, that ethanol is being produced from syngas in a bench-scale unit by Kyowa Yuka. The vapor-phase process uses a supported rhodium catalyst and the production of 200 g/h of ethanol per g of catalyst is claimed.

In this connection the reduction of acetic acid to ethanol by Humphreys & Glasgow, Davy McKee and BASF must be quoted as an attractive route to ethanol. This route combines the high selectivity of the Monsanto acetic acid process with a hydrogenation step.

Based on ethanol, the olefins, ethene and propene, are accessible as outlined in equations 1-3.



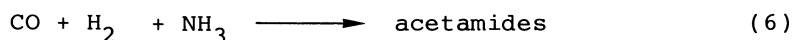
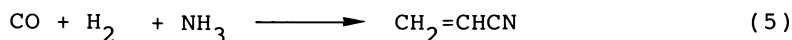
Also of potential interest is the direct hydrogenation of CO to isobutanol as it was practiced by BASF (13-14) or still is done in the German Democratic Republic. Again, a mixture of alcohols is obtained with isobutanol amounting up to 30 % (15). The latter one can be dehydrated to isobutene (chemical usage) or converted with methanol to fuel usage (MTBE).

Mention must also be made of the work of J.F. Knifton from Texaco who has demonstrated the use of ruthenium melt catalysis for the production of a wide range of commodity chemicals (alcohols, acids and esters) and fuels (16).

Also of great attractiveness is the direct synthesis of acetic acid from syngas, which would circumvent the two step process of Monsanto. Selectivities of up to 50 % are claimed. An economic analysis by Hoechst A.G. indicates (17) that this process is already economically feasible at a 80 % C<sub>2</sub>-oxygenate selectivity.

Most remarkable is the high pressure, rhodium catalyzed homogeneous reduction of carbon monoxide to ethylene glycol pioneered by Union Carbide (6, 18-19). As is evident from Table I, this reaction proceeds without losses due to formation of water or CO<sub>2</sub>. Furthermore, the great technical potential of this process is also obvious when considering the poor selectivity with which ethylene glycol is currently manufactured from ethene. From a technical point of view, however, the rhodium catalyzed synthesis of ethylene glycol possesses various disadvantages: First of all the high pressure being necessary for reasonable activities and selectivities has to be mentioned. (It can be postulated that the high pressure is needed to prevent the decomposition of the catalyst - presumably carbonyls - by the reaction temperature required). A very expensive metal, rhodium, is used. Catalyst recycle and circumvention of any rhodium loss will be difficult. To manufacture fibre grade ethylene glycol the purification costs will be high. Various attempts are known to use a less costly metal and/or to lower the pressure, but a breakthrough has not been reported, so far. It appears, that from all the metals tested, rhodium possesses the highest activity and selectivity followed by cobalt and ruthenium (20).

The incorporation of nitrogen-containing substrates into syngas chemistry offers a route to valuable nitrogen compounds. This field has not been explored extensively. By reacting syngas with ammonia the synthesis of acetonitrile is reported with 40 % conversion and 40-45 % selectivity (21). Other possible reactions are listed in Equations 4-6.



#### Indirect syngas conversion/methanol chemistry

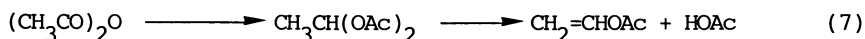
As is outlined in Figure 1, the indirect path using methanol, formaldehyde or methyl formate as intermediates can be used for the synthesis of chemicals from synthesis gas. Among organic chemicals, methanol belongs to industry's most significant products amounting to about 16 million tons in 1986. In addition to the traditional market, a very significant demand for methanol in new areas, such as energy or single cell proteins may emerge in the future. If energy prices develop in such a way that it becomes economically or industrially attractive to use methanol in gasoline or as a fuel for power production, the market potential in this area is almost unlimited. This development, however, will be governed by political decisions and so far predictions for the future are almost impossible. Many reactions are known

to use methanol for the synthesis of base chemicals as well as fine chemicals. Figure 2 gives some illustrative examples for the use of methanol to provide base chemicals. Applying ZSM-5 type zeolites (Mobil process) C<sub>2</sub>-C<sub>4</sub> olefins and C<sub>6</sub>-C<sub>10</sub> aromatics can be synthesized in good yields and conversions. Methanol can also be used to provide, upon catalytic decomposition, carbon monoxide and hydrogen or mixtures of both. The homologation of methanol to ethanol (see below) represents another route to ethene. As is outlined above (Equation 1-3), with ethene in hand the way to propene and butene/butadiene is paved. Finally, two other base chemicals which can be obtained from methanol are isoprene and toluene - the first by the reaction of methanol with 1-butene and the second by alkylation of benzene with methanol.

For the synthesis of fine chemicals, carbonylation, reductive carbonylation, and oxidative carbonylation of methanol can be applied as outlined in Table II.

The direct carbonylation of methanol yielding acetic acid, the Monsanto process, represents the best route for acetic acid. Carbonylation of methyl acetate, obtained from methanol and acetic acid, gives acetic anhydride, a technology commercialized by Tennessee Eastman (22). It is noteworthy that this process is based on coal derived synthesis gas to give as the final product cellulose acetate. A combination of Monsanto and Tennessee Eastman technology opens the door for the combined synthesis of acetic acid and acetic anhydride.

Starting from acetic anhydride, according to Equation 7, vinyl acetate can be obtained via ethylidene diacetate (22).



By adjusting the CO:H<sub>2</sub> ratio, catalytic systems for the reductive carbonylation of methyl acetate can be tuned to the production of acetic anhydride, ethylidene diacetate or acetaldehyde.

While the direct carbonylation is well accepted by industry, the reductive and oxidative carbonylations are still in the research and development stage. Using Texaco technology (16, 23) the combined synthesis of ethene and ethanol is feasible via homologation of acids according to Figure 3. Ethene can also be obtained from the reductive carbonylation of methyl acetate to ethyl acetate followed by pyrolysis (24). Both routes, so far, lack selectivity.

The oxidative coupling of CO in the presence of an alcohol to yield oxalate esters is under study by Ube Industries and Union Carbide. As oxidizing agent, oxygen or nitric oxide (Equation 8 and 9) can be used in the presence of a palladium catalyst (25).

Table II. Chemicals from methanol

---

<u>Carbonylation</u>			
CH <sub>3</sub> OH	$\xrightarrow{\text{CO}}$	methyl formate	
CH <sub>3</sub> OH	$\xrightarrow{\text{CO}}$	acetic acid	$\longrightarrow$ methyl acetate
methyl acetate	$\xrightarrow{\text{CO}}$	acetic anhydride	
<u>Reductive carbonylation</u>			
acetic acid	$\xrightarrow{\text{CO/H}_2}$	propionic acid	
CH <sub>3</sub> OH	$\xrightarrow{\text{CO/H}_2}$	acetaldehyde/ethanol	
methyl acetate	$\xrightarrow{\text{CO/H}_2}$	ethylidene diacetate	$\longrightarrow$
		vinyl acetate	
methyl acetate	$\xrightarrow{\text{CO/H}_2}$	ethyl acetate	
<u>Oxidative carbonylation</u>			
CH <sub>3</sub> OH	$\xrightarrow{\text{CO/O}_2}$	dimethyl carbonate	
CH <sub>3</sub> OH	$\xrightarrow{\text{CO/O}_2}$ or NO	dimethyl oxalate	$\longrightarrow$
		ethylene glycol	

---

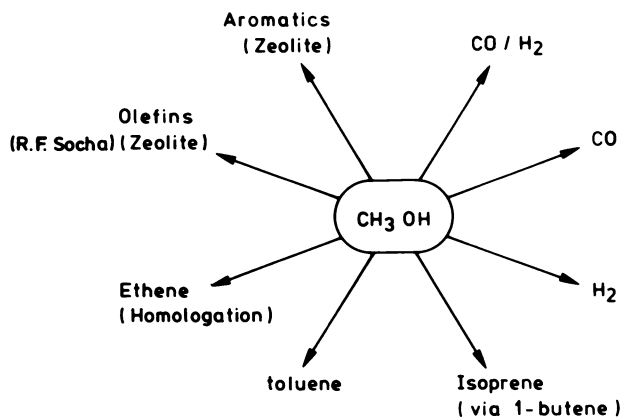
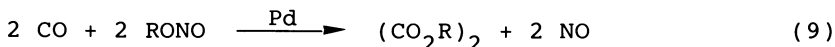
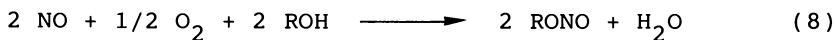


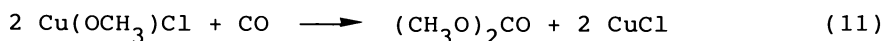
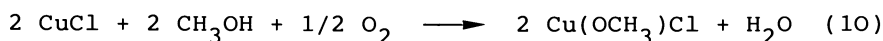
Figure 2. Base chemicals from methanol





In a subsequent reaction, the oxalate can be hydrogenated to ethylene glycol. Oxalate esters can also be reacted with  $\text{NH}_3$  giving oxamides, a fertilizer.

The oxidative carbonylation of methanol to dimethyl carbonate has found small industrial application (26-27). The reaction can be carried out in two steps following Equation 10 and 11 or also in one step.



#### Homologation of methanol to acetaldehyde

Although ethanol can be derived directly from synthesis gas alone - see above - reductive carbonylation (homologation) starting with methanol as a feed has received considerable attention, due to rates of conversion and better selectivity (see special chapters in ref. 3, 4, 6). In our laboratory, emphasis was placed on the synthesis of acetaldehyde (28, 29). Attempts to modify the  $\text{Co(OAc)}_2/\text{I}_2$  system by phosphorus-containing ligands resulted in a catalyst system  $[(\text{Ph}_3\text{P})_2\text{N}][\text{Co}(\text{CO})_4]/\text{I}_2$  in the presence of a polar solvent, such as sulfolane or dioxane. This catalyst yielded, at 97 % methanol conversions, ~ 80 % selectivities to acetaldehyde at rates of 1250  $\text{h}^{-1}$ . In cooperation with Union Rheinische Braunkohlen Kraftstoff AG, Wesseling a pilot plant was operated over 3 years. The data obtained and the results of the catalyst recycle looked very promising for a commercial operation. An engineering evaluation led to the following conclusions: In comparison to the Wacker process, the homologation of methanol is the more economical process. However, the costs of construction don't justify close-down economics for Wacker plants. In addition, due to the Monsanto process, which displaces the acetaldehyde oxidation to acetic acid, there is currently no need for a new acetaldehyde plant.

Detailed investigations were also carried out to understand the reaction mechanism. Based on kinetics and reactions with model complexes, the mechanism of Figure 4 is proposed. In a separate cycle methanol reacts with HI yielding methyl iodide, which alkylates  $[(\text{Co}(\text{CO})_3)]^-[(\text{Ph}_3\text{P})_2\text{N}]^+$  yielding complex 1. Hydrogenation of 1 gives acetaldehyde. Coordination of  $\text{CO}$  closes the catalytic cycle via elimination of HI and return to  $[(\text{Co}(\text{CO})_3)]^-$ . Kinetic measurements support that the alkylation of the cobalt complex with methyl iodide is the rate-determining step (30). Indeed, addition of  $\text{CH}_3\text{I}$  to a solution of  $[(\text{Ph}_3\text{P})_2\text{N}][\text{Co}(\text{CO})_4]$  at  $0^\circ\text{C}$  gives the novel anionic complex 1 (Equation 12) (31).

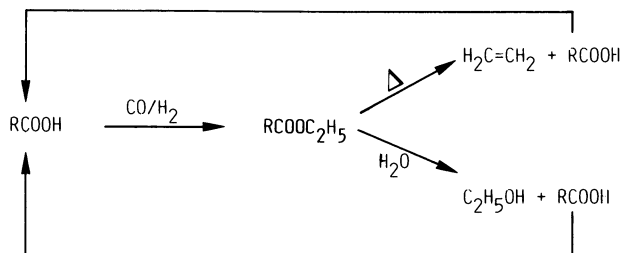


Figure 3. Homologation of acids

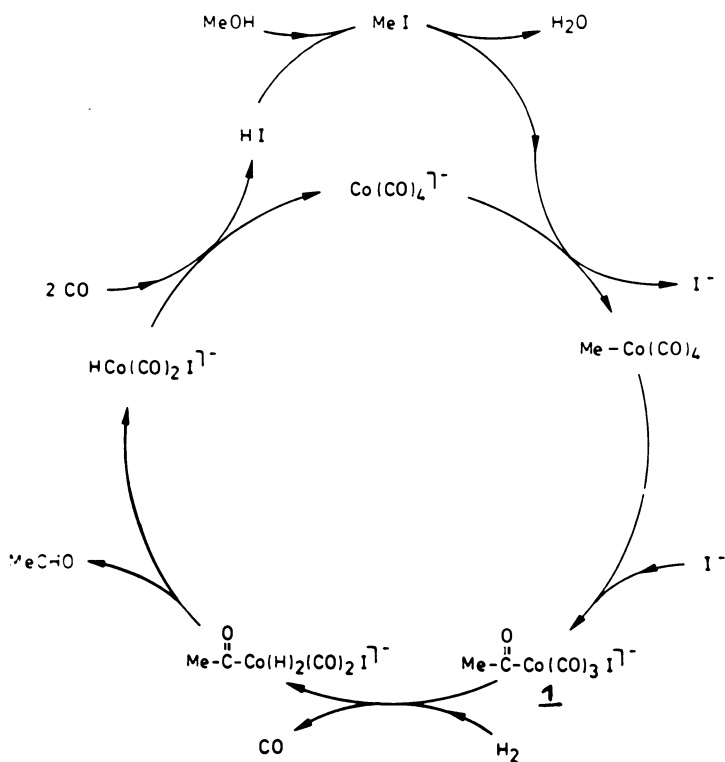
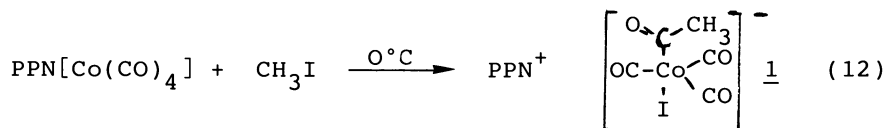


Figure 4. Proposed mechanism for methanol homologation



Complex 1 has a trigonal bipyramidal structure with three equivalent carbonyl ligands as could be confirmed by IR and x-ray analysis. The synthesis of complex 1 depends on the solvent and cation used.

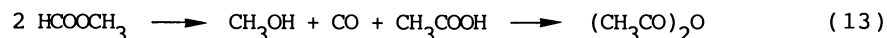
The chemical reactions of 1 are also in agreement with the proposed mechanism. Reaction with  $\text{Ph}_3\text{P}$  yields  $\text{Co}(\text{CO})_3[\text{C}(\text{O})\text{CH}_3]\text{Ph}_3\text{P}$ . Addition of hydrogen leads to acetaldehyde.

### Indirect syngas conversions/methyl formate chemistry

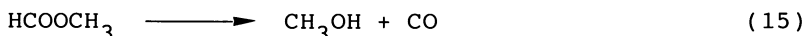
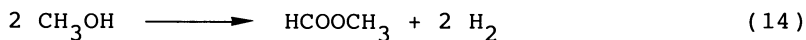
With syngas gaining importance, methyl formate could become a highly versatile and attractive intermediate (32-35). Figure 5 summarizes the routes leading to methyl formate.

Presently utilized processes are based on methanol carbonylation. As an alternative Mitsubishi Gas has developed a process involving dehydrogenation of methanol. Methyl formate can also be obtained by methanol oxydehydrogenation, direct homogeneous carbon monoxide hydrogenation, by disproportionating formaldehyde, or even from  $\text{CO}_2$ . Apart from some limited applications as a solvent and as an insect control agent, methyl formate is mainly used as an intermediate in the production of formic acid and formamides. However, around methyl formate various potential applications could revolve as depicted in Figure 6.

An interesting reaction of methyl formate is its isomerization to give acetic acid. Based on patent literature, a number of companies have recently reinvestigated this isomerization which has been known for over 30 years (36). It is unlikely that it can compete with the Monsanto process; however, since it doesn't need pure CO and may be operable at milder reaction conditions, some potential may be seen. Combining isomerization to acetic acid and decarbonylation to methanol and CO, could provide a direct synthesis for acetic anhydride starting directly from methyl formate (Equation 13).

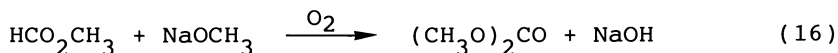


The decomposition of methyl formate to methanol and CO has been used by Mitsubishi Gas Chemical to synthesize high purity CO according to Equations 14 and 15 (35).



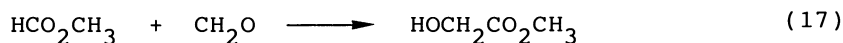
Usually, high-purity CO is manufactured on a large scale by means of costly cryogenic separation or absorption from syngas. The above approach could be attractive for small production. Also based on Equations 14 and 15, an easy source of oxogas (CO:H<sub>2</sub> = 1:1) can be imagined. Indeed, we could demonstrate that methyl formate and methanol can be used to hydroformylate olefins in good yields and selectivities (37).

The catalytic oxidation of methyl formate according to Equation 16 can be used to synthesize dimethyl carbonate (30).



The complete chlorination of methyl formate gives trichloromethylchloroformate (diphosgene), a liquid, which can easily be handled and transported. Thermal or catalytic treatment of diphosgene gives phosgene, thus making diphosgene a phosgene substitute, which is already commercially available.

Reactions of methyl formate with paraformaldehyde yields methyl glycolate (Equation 17).



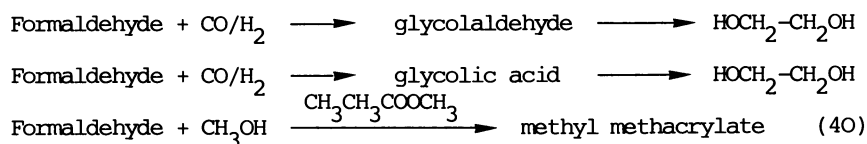
Methyl glycolate can be used to prepare a variety of fine chemicals exhibited in Figure 7.

Finally, mention should be made of the oxidative coupling to yield dimethyl oxalate, the isomerization into acetaldehyde and the reaction to acetone.

#### Indirect syngas conversions/formaldehyde chemistry

Instead of methanol, formaldehyde can be used as an intermediate derived from syngas. As is exemplified in Table III, various chemicals can be derived directly from formaldehyde.

Table III. Chemicals from formaldehyde



However, based on cost and lack of chemistry, it appears very unlikely that formaldehyde will develop into a major syngas intermediate, such as methanol is and methyl formate could become.

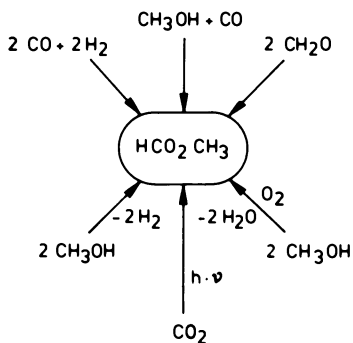


Figure 5. Synthesis of methyl formate

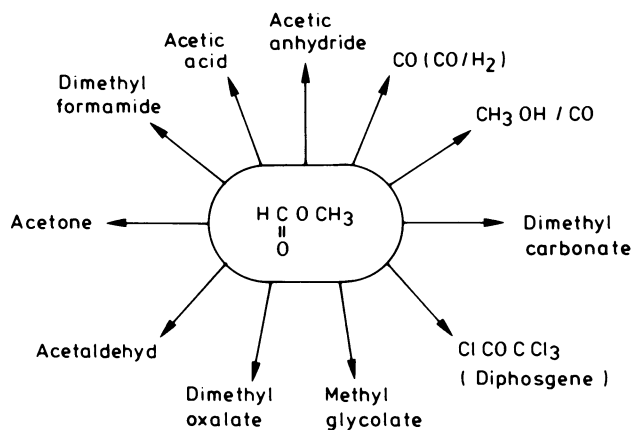


Figure 6. Potential applications to use methyl formate

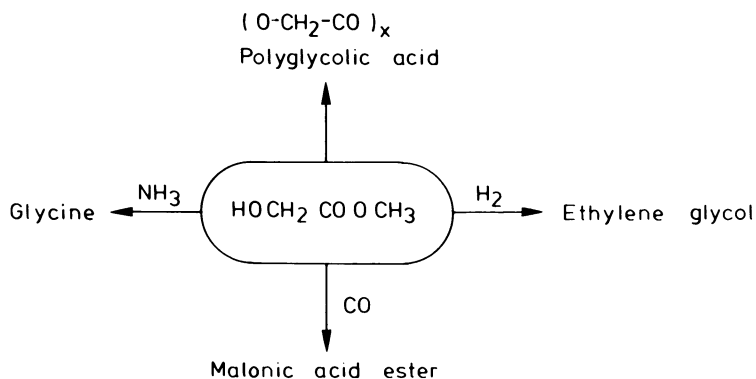


Figure 7. Potential applications for methyl glycolate

### Conclusions

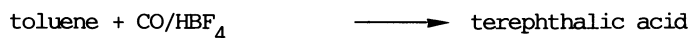
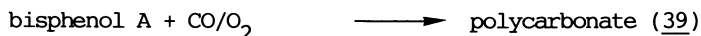
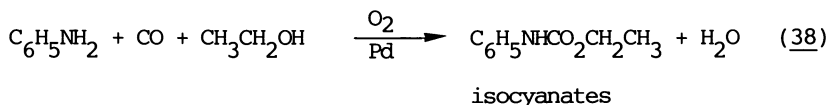
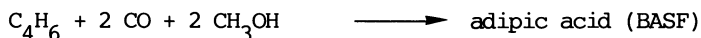
Based on syngas, direct and indirect paths are available to prepare a variety of chemicals. Among the industrialized nations, the future will be determined by the cost of crude oil versus natural gas and coal. However, even with low crude oil prices, we cannot afford to neglect research and developments in the field of C<sub>1</sub> chemistry. Long range syngas chemistry will come, only the timetable has changed. Here the research efforts in Japan deserve special mention. Within a National Research and Development Program sponsored by MITI, 14 companies collaborate aiming at four goals: ethylene glycol, ethanol, acetic acid and olefins. According to private communications all four groups have met their targets, and it will be interesting to see their results published.

It is reasonable to assume that prior to the exclusive use of chemicals derived from feedstocks other than crude oil, chemicals based on crude oil and chemicals based on alternate feedstocks will supplement each other. This situation has already arisen as is exemplified in the use of coal derived CO/H<sub>2</sub> to hydroformylate olefins originating from mineral oil. For instance, in West-Germany Hoechst converts coal into CO/H<sub>2</sub> which is used to prepare alcohols from naphtha derived olefins. Table IV summarizes a number of additional reactions in which this point is especially emphasized.

Table IV. Combination of crude oil derivatives with syngas

---

#### Hydroformylation



Literature Cited

1. Falbe, J. "New Synthesis with Carbon Monoxide"; Springer-Verlag, Berlin-Heidelberg-New York 1980.
2. Falbe, J. "Chemical Feedstocks from Coal"; John Wiley & Sons, New York 1982.
3. Herman, R.G. "Catalytic Conversions of Synthesis Gas and Alcohols to Chemicals"; Plenum Press, New York 1984.
4. Sheldon, R.A. "Chemicals from Synthesis Gas"; D. Reidel Publishing Company, Dordrecht-Boston-London 1983.
5. Gillies, M.T. "C<sub>1</sub> based Chemicals from Hydrogen and Carbon Monoxide"; Noyes Data Corporation, Park Ridge, N.J. 1982.
6. Keim, W. "Catalysis in C<sub>1</sub> Chemistry"; D. Reidel Publishing Company, Dordrecht-Boston-London 1983.
7. Huff, G.A.; Satterfield, C.N. J. of Catalysis 1984, 85, 370-379.
8. C & EN, 1985, Sept. 30, 75.
9. European Chemical News 1985, Nov. 25, 15.
10. Keim, W. Chem.-Ing.-Tech. 1984, 56, 850.
11. Keim, K.H.; Korff, J.; Keim, W.; Röper, M. Erdöl und Kohle-Erdgas-Petrochemie 1982, 35, 297-304.
12. Courty, P.; Durand, D.; Freund, E.; Sugier, A. J. of Mol. Catal. 1982, 17, 241-254.
13. "Ullmanns Enzyklopädie der Technischen Chemie", Urban & Schwarzenberg, München-Berlin 1957, 410.
14. Smith, K.J.; Anderson, R.B. Can. J. Chem. Eng. 1983, 61, 2, 40.
15. Seibring, J. Thesis RWTH Aachen 1985.
16. Knifton, J.F. Platinum Metals Rev. 1985, 29, 2, 63-72.
17. Dettmeier, U.; Leupold, E.I.; Pöll, H.; Schutz, J. Erdöl und Kohle-Erdgas-Petrochemie 1985, 38, 59-62.
18. King, D.L.; Cusumano, J.A.; Gorten, R.L. Catal. Rev. - Sci. Eng. 1981, 23, 233-263.
19. Dombeck, B.D. "In Catalytic Activation of Carbon Monoxide"; Ford, P.C.; Ed. ACS Symposium Series No. 152, American Chemical Society: Washington, D.C., 1981; pp. 213-225.
20. Keim, W.; Berger, M.; Schlupp, J. J. of Catal. 1980, 61, 359.
21. Olivé, S.; Olivé, G. Ger. Pat. 2.629.189.
22. Ehrler, J.L.; Juran, B. Hydrocarbon Processing February 1982, 109.
23. Knifton, J. J. of Catalysis 1983, 79, 147-155.
24. Braca, G. et al. J. of Mol. Catal. 1985, 32, 291-308.
25. Waller, F.J. J. of Mol. Catal. 1985, 31, 130.
26. Ugo, R.; Tesei, R.; Mauri, M.M.; Rebora, P. Ind. Eng. Chem. Prod. Res. Dev. 1980, 19, 396.
27. Chemical Week 1983, April 13, 18.
28. Röper, M. Habilitation RWTH Aachen 1985.

29. Union Rheinische Braunkohlen Kraftstoff AG, Ger. Offen. 3.343.519 (1.12.1983).
30. Röper, M.; Loevenich, H. C<sub>1</sub> Mol. Chem. 1984, 1, 155.
31. Röper, M.; Schieren, M.; Heaton, B.T. J. of Organomet. Chem. 1986, 299, 131-136.
32. Hiratani, T.; Noziri, S. Chem. Econ. & Eng. Rev. June 1985, 17, 6, p. 21-24.
33. Röper, M. Erdöl und Kohle-Erdgas-Petrochemie 1984, 37, 506.
34. Itatani, H. Chem. Econ. & Eng. Rev. April 1984, 16, 4, p. 21-28.
35. Ikarashi, T. Chem. Econ. & Eng. Rev. 1980, 12, 8, p. 31.
36. Röper, M.; Elvevoll, E.O.; Lütgendorf, M. Erdöl und Kohle-Erdgas-Petrochemie 1985, 1, 38.
37. Behr, A.; Kanne, U.; Keim, W. J. of Mol. Cat. April 1986
38. Fukuoka, S.; Chono, M.; Kohno, M. Chemtech. 1984, 14, 670.
39. General Electric, US Pat. 4 201 721 (1980).
40. Albanesi, G.; Moggi, P. Applied Cat. 1983, 6, 293-306.

RECEIVED July 29, 1986



## Chapter 2

# Chemicals Produced in a Commercial Fischer-Tropsch Process

Mark E. Dry

Sasol Technology (PTY) Limited, P.O. Box 1, Sasolburg 9570, Republic of South Africa

In this article a general review of the Fischer-Tropsch process is given, but since Sasol operates the only proven commercial plants the emphasis will fall on the Sasol operations.

The first Sasol plant (Sasol One) came on stream in 1955 and is still in production. The profitability of this operation initially was low because the price of crude oil remained depressed for many years due to the discovery and exploitation of the huge oil deposits in the Middle East. After 1973, however, the price of crude oil rose rapidly and consequently the profitability of the Fischer-Tropsch process in South Africa improved dramatically. This led to the construction of two much bigger plants (Sasol Two and Sasol Three) which came on stream in 1980 and 1982 respectively.

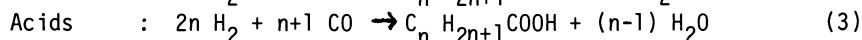
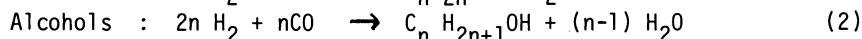
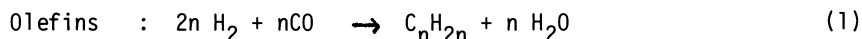
Sasol is now a public company and its shares are listed on the Johannesburg Stock Exchange. Despite the fluctuations in the price of crude oil, the commercial success of the process is reflected by the four-fold increase in the share prices since 1979. The reason for the viability of the process in South Africa is the combination of three factors:

- a) there are no petroleum deposits in the country
- b) the industrial activity (and therefore the market) is predominantly concentrated in the Witwatersrand area which is about 400 miles from the sea
- c) the huge deposits of coal which are in the same area are cheap to mine because the thick seams allow a high degree of mechanization.

The present plants are geared predominantly at the production of gasoline and diesel fuel but a significant fraction of chemicals are also produced in both the coal gasification and in the Fischer-Tropsch (FT) synthesis process. The latter process can be manipulated to increase the production of chemicals, should this be desired. For fuller detail of the production of fuels, the reader is referred to other reviews (1)(2).

The Fischer-Tropsch ProcessPrimary and Secondary Reactions

Examples of some of the primary reactions are:

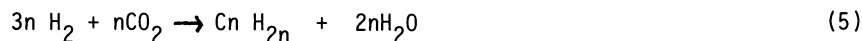


The primary products are linear. The formation of branched products probably result from secondary isomerization reactions. Ketones are also apparently secondary products.

If the catalyst used is active for the water gas shift reaction:



then  $\text{CO}_2$  can be formed in a secondary reaction. The extent to which this happens depends on the  $\text{H}_2/\text{CO}$  ratio inside the reactor and on the temperature. In principle therefore mixtures of  $\text{CO}_2$  and  $\text{H}_2$  or of  $\text{H}_2\text{O} + \text{CO}$  can be used as feed gases provided the water gas shift reaction is active. For instance, for the production of olefins



"Equation 5" is simply the sum of "Equation 1" and the reverse of "Equation 4".

Overall Process Scheme

A generalized scheme of the Sasol process is illustrated in Figure 1. The basic raw materials are coal, water and air. The plant is a complex operation consisting of many interlinked processes. This complexity is, however, not an important factor in the economics when it is borne in mind that the main cost is the production of synthesis gas, which accounts for over 50 % of the total.

Synthesis Gas Production

All the Sasol plants use Lurgi gasifiers to convert coal to raw synthesis gas. The units are fed counter currently (coal in at the top and the gasifying agents, oxygen and steam, in at the bottom). These gasifiers are well-suited to the low grade high-ash coal used by Sasol. The composition (volume percent) of the raw gas is approximately, 60 ( $\text{H}_2 + \text{CO}$ ); 9  $\text{CH}_4$ ; 29  $\text{CO}_2$ ; 1 Inerts ( $\text{A} + \text{N}_2$ ); 0.5  $\text{H}_2\text{S}$  and lesser amounts of components such as  $\text{C}_2\text{H}_6$  and tars etc.

The raw gas is purified in the Lurgi Rectisol process (cold methanol scrubbing) where various by-products (eg tar naphthas) and impurities (eg  $\text{CO}_2$  and  $\text{H}_2\text{S}$ ) are removed.

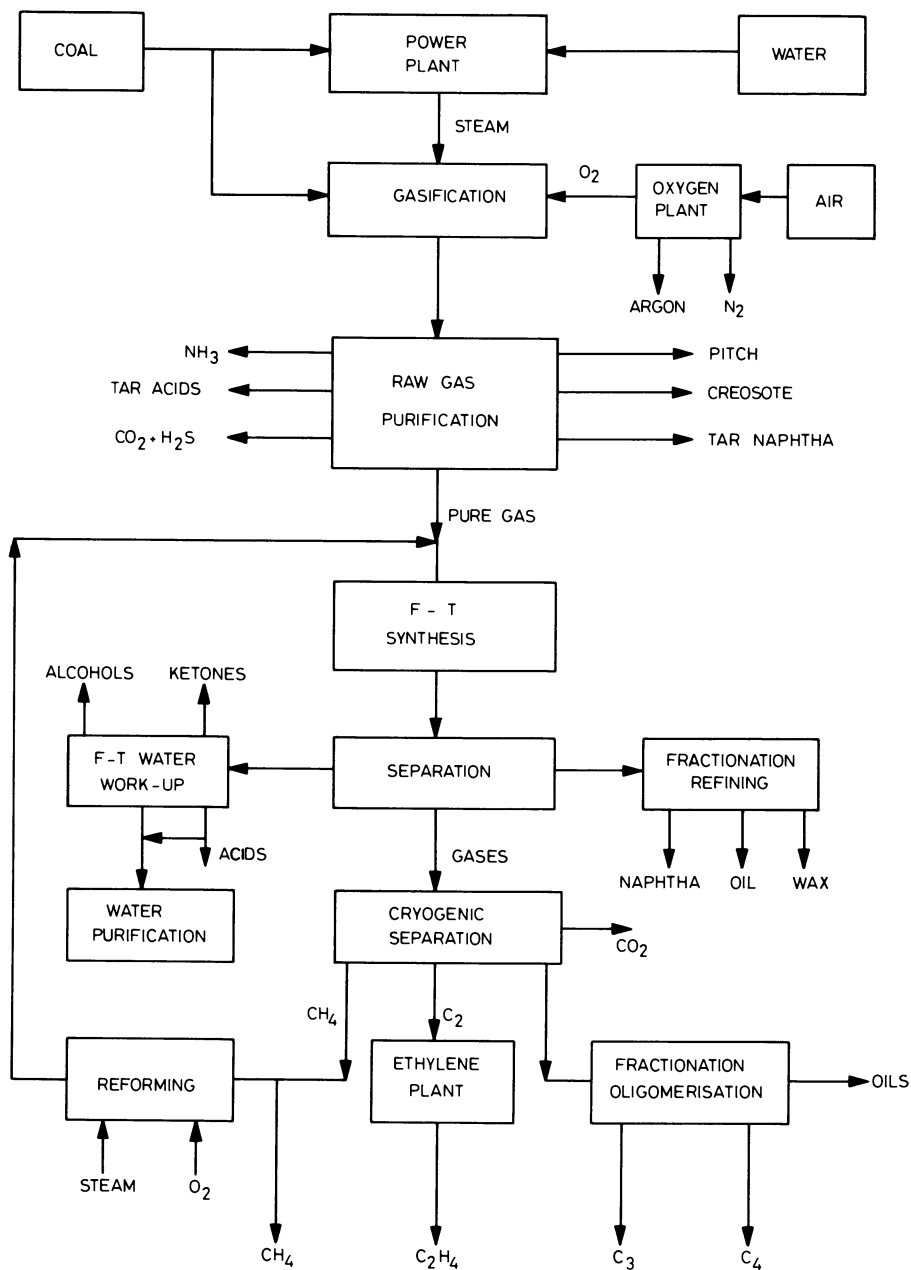
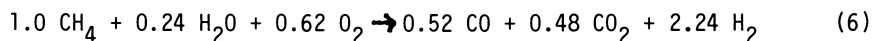


Fig. 1. Generalized Sasol process scheme

Other coal gasifiers, eg Shell-Koppers and Texaco, have been commercially tested elsewhere. These operate at higher temperatures than the Lurgi reactors and consequently produce a gas with a lower CH<sub>4</sub> content and a lower H<sub>2</sub>/CO ratio. They use less steam but more oxygen. A discussion of the pros and cons of the various coal gasifiers is beyond the scope of this review.

Unless there is a viable market for methane (eg as a fuel gas) the methane (both that from the coal gasifiers as well as that formed in the downstream FT process) is reformed using nickel catalyst at high temperatures to produce more CO and H<sub>2</sub> which is then recycled to the FT reactors (see Figure 1). The CH<sub>4</sub> reforming reaction is typically:



### Fischer-Tropsch Synthesis

#### Reactors

In its present commercial operations Sasol uses two types of reactors. In the fixed bed "low" temperature Arge reactors the gas enters at the top (see Figure 2). The catalyst is packed into the narrow tubes. The FT reaction heat is absorbed by the water surrounding the tubes and steam is generated. The desired reactor temperature is maintained by controlling the steam pressure above the water jacket. The catalyst formulation and the reactor process conditions are set for the maximum production of high quality paraffinic waxes. Only the Sasol One plant utilizes these reactors.

In the "high" temperature Synthol reactor (see Figure 3), the gas enters at the bottom where it picks up the powdered catalyst (flowing down the stand-pipe) and sweeps it up the right-hand side of the reactor where the FT reaction occurs. Two banks of heat exchangers (see Figure 3) remove some of the reaction heat. As for all well fluidized catalyst beds the whole reactor is near isothermal. At the top of the reactor the gas and catalyst disengage (in the wide settling hopper) and the gas leaves the reactor via cyclones while the catalyst flows back down the stand-pipe. The Synthol reactor is used for the production of low molecular weight olefins and light oils.

At the big new plants (Sasol Two and Three) only the Synthol reactors are used. Per unit cross-section of the reactors the Synthol reactor has a much higher gas throughput than the Arge reactor.

There are two other kinds of reactors which should be suitable for the FT reaction. In the slurry phase reactor finely divided catalyst is suspended in a heavy oil and the synthesis gas bubbles through the bed. The fixed fluidized bed (FFB) reactor is in principle the same as the slurry bed except that no oil medium is used. Like the Synthol reactor it operates at a "high" temperature. Sasol is currently investigating the feasibility of both these two alternative types of reactors.

More detail of the commercial and developmental reactors is published elsewhere (1) (2).

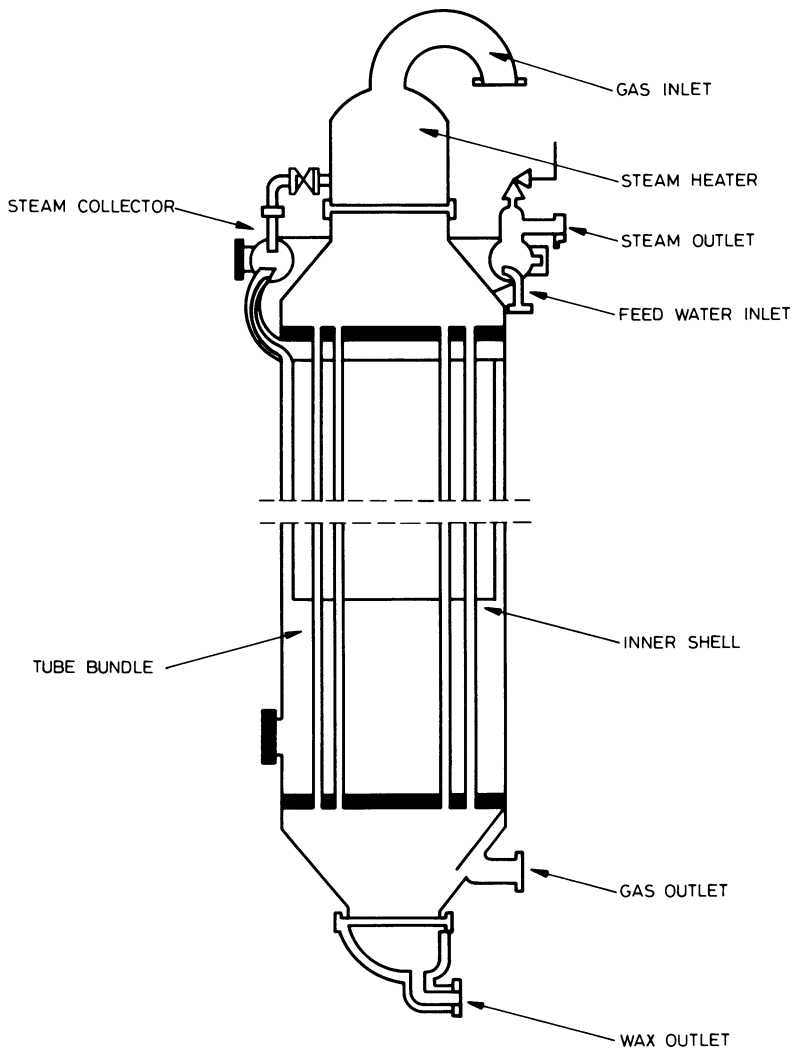


Fig. 2. Fixed-bed Arge reactor

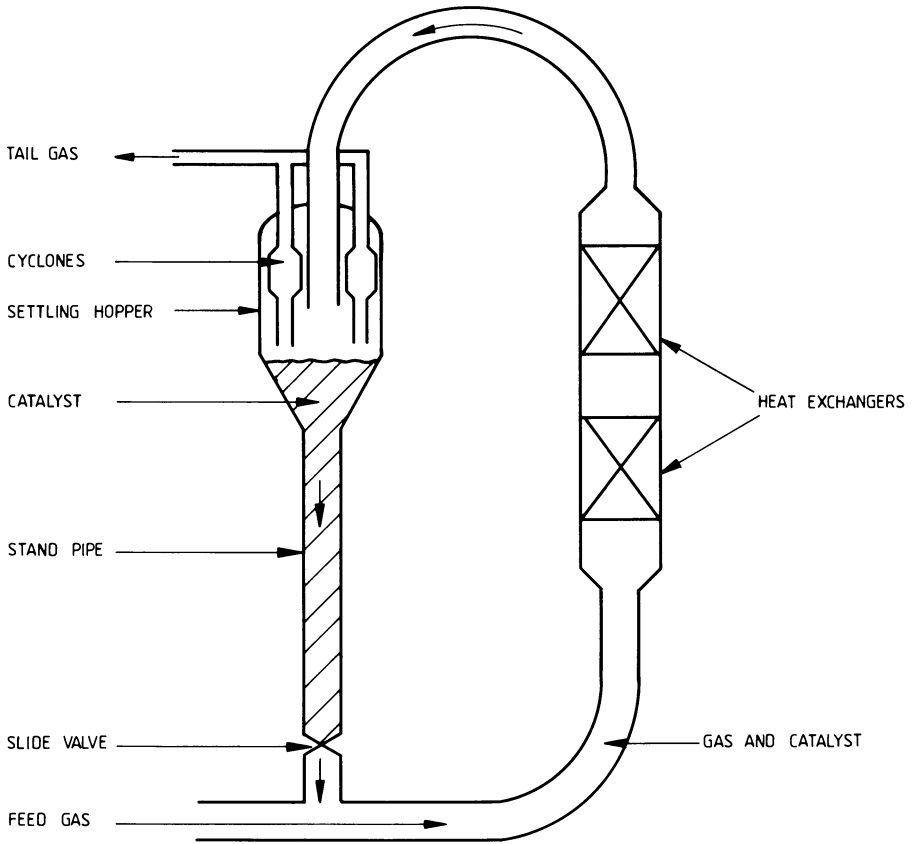


Fig. 3. Transported fluidized bed Synthol reactor

### Catalyst

The metals known to be active for hydrogenating carbon monoxide to hydrocarbons and alcohols are Fe, Ni, Co and Ru. Rhodium is also receiving considerable attention by many research workers for the production of alcohols. The relative prices of these metals are given in Table I.

Table I. The Relative Costs of Metals Active in CO Hydrogenation

Metal	Cost per unit mass (relative to Fe)
Fe	1.0
Ni	55
Co	325
Ru	35 000
Rh	320 000

In its commercial plants Sasol has to date used only iron based catalysts. (The preparation and properties of these catalysts have been reviewed elsewhere (2).) Not only is iron by far the cheapest of the metals (see Table I) but iron catalysts also produce large amounts of low molecular weight olefins which are important in the Sasol process. (These olefins are oligomerized to either gasoline or diesel fuel and this allows the production of these two liquid fuels to match the market requirement.) A major drawback of iron is that at high temperatures carbon deposition occurs which results in catalyst disintegration.

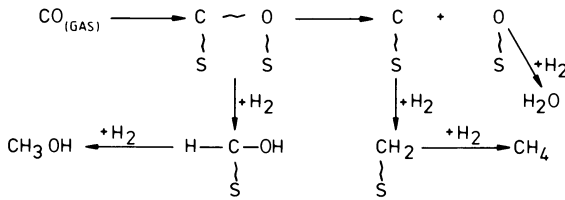
Of the metals listed in Table I nickel is the most hydrogenating and hence it is unsuitable for producing olefins or alcohols. Cobalt could be a good compromise between Fe and Ni and it has the advantage that under its normal operating conditions carbon deposition is much lower than for iron. Besides the very high cost of Ru, the present world stock of this metal is only sufficient to build a single Sasol size plant and then the catalyst would have to contain only about 0.5 % on a support. At the present cost of Rh it is very difficult to see that this metal could ever be used commercially. It should also be noted that the production of Ru and Rh is entirely linked to the demand for platinum.

Catalysts especially developed to produce low molecular weight alcohols can have complex formulations with cobalt and copper being the key components (3). The commercial viability of these catalysts has, however, not been fully proven.

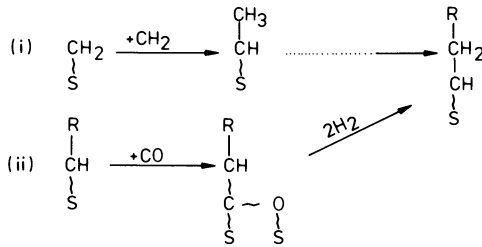
### Product Selectivity Control

Various mechanisms have been proposed for the FT reaction (1) (2) and (4-6). A generalized mechanism is illustrated in Figure 4. Irrespective of which mechanism is correct, or is dominant, there is general agreement that stepwise chain growth is involved. This inevitably results in a wide carbon number distribution of products, the particular distribution being determined by the probability of chain growth ( $\alpha$ ). The calculated effect of different  $\alpha$  values on

1. INITIATION AND C<sub>1</sub> COMPOUNDS



2. CHAIN GROWTH (INSERTION)



3. CHAIN TERMINATIONS

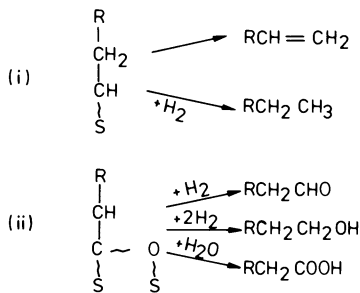


Fig. 4. Mechanism of FT process



product selectivity is illustrated in Figure 5. The carbon number distributions observed in practice agree well with the calculated ones.

The probability as well as the mechanism of chain growth will depend on both the number and the type of chemical species on the catalyst surface. From Figure 4 it can be seen that if the dominant, or more specifically, the most reactive surface species is "CH<sub>2</sub>" then olefins and paraffins will be the main products. If the surface coverage by undissociated CO is high, and this CO is capable of inserting into the hydrocarbon chain, large amounts of alcohols can result. If the coverage by hydrogen is high, this will increase the rate of chain termination and so shorter chained products will result. The nature and number of the surface species will depend on the chemical nature of the catalyst surface, the temperature and the composition of the gas inside the reactor.

The nature of the catalyst surface depends on the type of metal and on the type and amount of promoters and/or supports used. Under similar FT synthesis conditions Co and Ru are more hydrogenating than Fe and so the latter produces more olefins and alcohols. In the case of iron the "basicity" of the surface is a key factor in obtaining the desired selectivity (1) (2). The higher the "basicity" the higher the average molecular weight of the products, the higher the olefinity and the higher the production of alcohols and acids. The "basicity" is not only dependent on the amount of alkali (K<sub>2</sub>O) added but also on the interaction of the alkali with other components present in the catalyst (eg SiO<sub>2</sub> or Al<sub>2</sub>O<sub>3</sub>). The effect of alkali is not unique to metallic catalysts. For the oxide catalysts used in methanol synthesis it is also found that alkali promotion increases the production of longer chained alcohols (7) .

For most catalysts it is generally observed that as the temperature is increased, the selectivity shifts towards the lighter products, the olefinity of the products decrease and less alcohols are formed. Table II illustrates these effects for an experimental iron catalyst promoted with an intermediate amount of alkali.

Table II. The Effect of Temperature on Product Selectivity

Temp (°C)	Selectivity *1			$\frac{C_3H_6}{C_3H_8}$ ratio	Aromatic content of 80-160 °C cut
	CH <sub>4</sub>	Alcohols *2	Ketones *2		
330	14	2.3	0.8	10	8
350	17	1.6	1.1	9	10
360	20	1.1	1.3	8	13
370	23	0.8	1.2	6	18
380	28	0.5	0.8	4	26

\*1 Carbon atom basis

\*2 Present in the water phase

Publication Date: December 16, 1987 | doi: 10.1021/bk-1987-0328.ch002

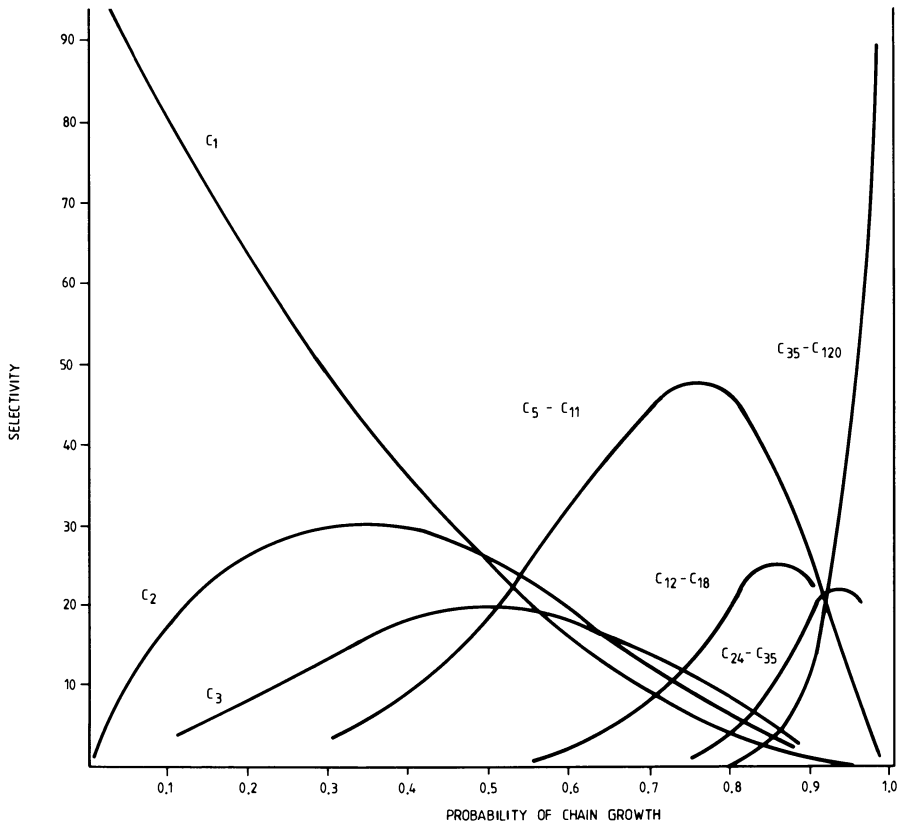


Fig. 5. Selectivity as a variable of the probability of chain growth

For FT catalysts operating below about 250 °C it is found that as the H<sub>2</sub>/CO ratio in the gas phase increases the average molecular weight of the product decreases, as well as the amounts of olefins formed. This is in keeping with the mechanism depicted in Figure 4. For iron catalysts operating at temperatures above 300 °C the simple H<sub>2</sub>/CO ratio does not correlate well with selectivity. A more complex factor  $p_{H_2}^{0.5}/(p_{CO} + p_{CO_2} + p_{H_2O})$  gives a better correlation (1).

The selectivities typically obtained in the fixed bed Arge and fluidized bed Synthol reactors as currently operated by Sasol are shown in Table III. If desired the selectivities can be varied over wide ranges. Thus in Arge the "hard wax" (the material boiling above 500 °C) can be varied from zero to over 50 % while in the Synthol reactors the CH<sub>4</sub> selectivity can be varied from 5 to 80 %.

Table III. Selectivity and Product Properties of Commercial FT Reactors

Product	Selectivity (C-atom basis)		Property of C <sub>12</sub> to C <sub>18</sub> cut	Synthol	Arge
	Synthol	Arge			
CH <sub>4</sub>	8	4	% Olefins	73	26
C <sub>2</sub> to C <sub>4</sub> olefins	26	5	% Paraffins	10	66
C <sub>2</sub> to C <sub>4</sub> paraffins	5	6	% Aromatics	10	0
C <sub>5</sub> to 350 °C	46	34	% Oxygenates	7	8
+350 °C	8	48	% Straight chain product	60	93
Water soluble oxygenates	7	3			

### Production of Chemicals

#### C<sub>1</sub> to C<sub>4</sub> Hydrocarbon Separation

In the newer Sasol plants the tailgas from the FT reactors is first water-washed (to extract the remnants of water-soluble oxygenated compounds), then treated in a Benfield unit (to remove all CO<sub>2</sub>) and then fed to a cryogenic unit where the gas is separated into four streams, a CH<sub>4</sub>-rich, a H<sub>2</sub>-rich, a C<sub>2</sub> and a C<sub>3</sub>/C<sub>4</sub> stream.

#### Methane

At Sasol the bulk of the CH<sub>4</sub> is either sold as fuel gas or is reformed to synthesis gas (see Figure 1). A portion is, however, sold as raw material for the production of NaCN and Ca(CN)<sub>2</sub> which are used to extract gold from the milled ore. (Gold mining is a major industry in South Africa). In the Shawinigan process CH<sub>4</sub> and NH<sub>3</sub> are passed through an electric arc and the HCN which is formed is absorbed by either NaOH or Ca(OH)<sub>2</sub> solutions.

Short Chain Alkenes

From the mechanistic scheme depicted in Figure 4 it can be deduced that in order to maximize the production of  $C_2$  to  $C_4$  olefins the combination of the following factors are required.

- After adsorption the CO molecule should dissociate to ensure that the dominant active surface species is " $CH_2$ " (the presence of a high level of active undissociated CO molecules would lead to CO insertion (see step 2 (ii) in Figure 4) which could result in the formation of alcohols in preference to hydrocarbons (see step 3 (ii) in Figure 4).
- The coverage of the surface by  $CH_2$  units should, however, not be too high as this would lead to a high chain growth rate (see step 2 (i) in Figure 4) and so lead to longer chained products at the expense of short chained olefins.
- Chemisorbed  $H_2$  is involved in both chain initiation and termination but the level of chemisorbed  $H_2$  must be such that the system is not too hydrogenating as this would lead to the formation of paraffins, and in the extreme case, to  $CH_4$  being the only product. Because of this, active hydrogenating catalysts, like Ni metal, are poor choices for FT synthesis.

The required balance of surface coverages by CO,  $CH_2$  and  $H_2$  is obtained by manipulation of the chemical nature of the catalyst surface (type of metal, metal-support interactions and chemical promotion) and by control of the gas composition inside the reactor.

As can be seen in Table III the Synthol process produces a large amount of  $C_2$  to  $C_4$  hydrocarbons which are predominantly olefins. At Sasol the  $C_2$  stream from the cryogenic separation unit is fed to a standard ethylene plant. The feed is first dried and then fractionated to remove the small amounts of  $C_1$  and  $C_3$  products. The  $C_2$  stream is then selectively hydrogenated to remove acetylene (formed in the down-stream  $C_2H_6$  cracking operation) and then fractionated to separate the  $C_2H_4$  and  $C_2H_6$ . The ethane is steam-cracked to  $C_2H_4$  and the product stream is recycled to the front end of the plant. The final  $C_2H_4$  product has a purity of 99.97% or better and is sold for the production of various grades of polyethylene, polyvinyl chloride, styrene etc.

The stream from the cryogenic unit which is rich in  $C_3/C_4$  olefins can be fractionated and selectively hydrogenated (to remove traces of dienes) to yield the pure olefins. Common uses of propene are the production of polypropylene, acrylonitrile, cumene etc. Butene can be catalytically dehydrogenated to butadiene which is used in the production of synthetic rubbers.

Long Chain Linear Alkenes

A feature of the FT process is that the primary hydrocarbon products are linear alpha olefins. Since chain branching is a temperature sensitive secondary reaction, a higher yield of linear  $\alpha$  olefins is obtained when the FT process is operated at lower temperatures (eg see the data in Table III comparing the low temperature Arge with the high temperature Synthol process).

The linear olefins are used in the production of biodegradable detergents. The C<sub>9</sub> to C<sub>15</sub> cuts are fed to alkylation units where the olefins react with benzene to form alkylbenzenes which are subsequently sulphonated. The paraffins present in the feed pass through unconverted. These are then chlorinated and used as plasticizers. The linear olefins can also be converted to linear aldehydes and alcohols by hydroformylation.

### Oils and Waxes

As already mentioned, the low temperature fixed bed FT synthesis produces almost exclusively straight chained products. In addition, these products are free of aromatics which is a very important feature from the health regulations point of view when the end uses of these chemicals are borne in mind.

The heavier waxes are fractionated into various cuts, deoiled and hydrofined (Ni catalyst at high pressure) to ensure the complete removal of all traces of olefins and oxygenated compounds. "Hard" waxes (> 500 °C) are also oxidised to yield a series of speciality waxes.

The refined waxes and oils have a wide variety of end uses eg in the manufacture of hand cleaners, hair pomades, milking creams, waxed food cartons, chewing gum, desensitiser in the explosives industry, crayons, candles, printing ink, industrial jellies, water proofing, carbon paper wax, hot melt adhesives, paints, varnishes and many others.

The oxidised waxes (containing various ratios of fatty acids, esters and alcohols) are used in the manufacture of various polishes, anti-corrosion coatings, tile glazing carriers, precision casting waxes, mould release agents, metal coatings etc.

### Alcohols, Ketones and Carboxylic Acids

From the proposed mechanism in Figure 4 the requirements for a high alcohol yield would appear to be as follows:

- a) a moderate amount of CO dissociation and subsequent CH<sub>2</sub> formation to ensure chain growth. If this does not occur then CH<sub>3</sub>OH will be the major product
- b) a high coverage of undissociated chemisorbed CO capable of inserting into the hydrocarbon complex (see step 2 (ii) in Figure 4).
- c) moderate hydrogenating conditions to avoid both the hydrogenation of the intermediate oxygenated surface complex or of the formed oxygenated products to paraffins.

For iron-based catalysts these requirements are enhanced by prenitriding the iron (1) (4) or by the combination of high alkali promotion, low temperature, low conversion, high pressure and low H<sub>2</sub>/CO ratio feed gas (2). Under the latter conditions it has been found that the alcohol content of the liquid product boiling below 160 °C can be as high as 86 % (8). Under such conditions large amounts of acids are also formed.

In the present commercial Sasol operations the tailgas leaving the reactors are cooled to ambient temperature and the liquid products separated into two phases, namely an oil and a water phase. The lower molecular weight oxygenated products are predominantly present in the water phase. Typical compositions of these oxygenated compounds are given in Table IV.

Table IV. Composition of Chemicals in FT Water Phase (Mass %)

Category	Compound	Synthol	Arge
Non-acid	Aldehydes	5	2
	CH <sub>3</sub> OH	1	25
	C <sub>2</sub> H <sub>5</sub> OH	55	50
	C <sub>3</sub> H <sub>7</sub> OH	16	11
	C <sub>4</sub> H <sub>9</sub> OH	7	6
	C <sub>5+</sub> alcohols	2	3
	Acetone	10	2
	MEK	3	1
	Higher ketones	1	
	Acids	Acetic	70
Propionic		16	
Butyric		9	

The recovery and work-up of these oxygenates is a complex process. The water is first fed to a "primary" distillation tower where the aldehydes, ketones and alcohols are removed overhead. The bottoms retain all the carboxylic acids. These acids can be extracted (eg by high boiling point alkyl phosphorus oxides such as TOPO, trioctyl phosphine oxide) and fractionated to produce high purity acetic, propionic and butyric acid. Due to the low acid concentrations in the FT water, this process has to date not been commercialized at Sasol and at present the diluted acid stream is sent to the water purification section where the acids are biologically destroyed in activated sludge units.

The overheads from the "primary" distillation column contain the C<sub>1</sub> to C<sub>6</sub> primary alcohols the lighter ketones (acetone, MEK etc) and the aldehydes. The individual chemicals are recovered and purified. The aldehydes are hydrogenated to the corresponding alcohols.

While alcohols and acids are considered to be primary products (see Figure 4) ketones are probably formed in secondary reactions which only occur at higher temperatures (2). In Table II it can be seen that as the temperature increases, ketone production increases at the expense of alcohols up to a point after which both decrease (due to hydrogenation to hydrocarbons which under FT conditions are thermodynamically more stable (2)). It has been suggested (2) that ketones result from the direct reaction between alcohols and surface carbon atoms and/or from the dehydrogenation of secondary alcohols (eg under high temperature FT conditions acetone and isopropyl alcohol are in thermodynamic equilibrium (2)).

### Phenols, Tars and Aromatics

The Lurgi gasifiers used by Sasol operate at "low" temperatures and consequently phenols, and "tars" are "distilled" from the coal at the top of the gasifier, and carried out with the raw gas. On condensation two liquid phases are formed, "tar" and "gas liquor" (water). The "tar acids" (phenol, cresols etc) are dissolved in the "gas liquor" which is fed to the Phenosolvan unit where the acids are recovered by counter current extraction with butyl acetate or diisopropyl ether. The crude tar acids are fractionated to yield phenol, ortho, meta and para cresol and xylenols. The phenol is further refined to produce a high purity, colourless and stable product. Phenol is used mainly in the production of formaldehyde resins while the cresols are used as flotation frothers and in the manufacture of pesticides etc.

The "tar" stream which is highly aromatic is made up of tar naphtha, creosote and pitch. The tar naphtha is hydrofined to remove N, S and O compounds. It consists mainly of toluenes and xylenes. The creosote can either be sold as such (eg for wood preservation) or be hydrofined to yield a product rich in higher aromatics. The tar pitch is used for impregnating cellulose fibre pipes or is converted to high quality coke (for the production of carbon electrodes).

In the FT synthesis itself, the production of aromatics is relatively low. The production does increase as the synthesis temperature is increased (see Table III) but this is accompanied by large increases in the undesirable CH<sub>4</sub> and so the FT synthesis itself is not a viable source of aromatics.

### Sulphur, Ammonia, Argon and CO<sub>2</sub>

#### Sulphur

In the gasifiers the sulphur present in the coal is converted to H<sub>2</sub>S which is scrubbed out, together with the CO<sub>2</sub>, in the downstream Rectisol unit. The effluent stream from this unit (typically 1.5 % H<sub>2</sub>S in CO<sub>2</sub>) is treated in a homogeneous catalytic process in which the H<sub>2</sub>S is converted to high grade elemental sulphur. The catalytic liquor consists essentially of an alkaline vanadium solution. In the absorber section the H<sub>2</sub>S is oxidised to S by V<sup>5+</sup> which in turn is reduced to V<sup>4+</sup>. The V<sup>4+</sup> is then reoxidized by air in a downstream unit and the regenerated liquor is returned to the absorber.

#### Ammonia

Chemically bound nitrogen in coal is converted to NH<sub>3</sub> in the gasifier and the ammonia ends up in the "gas liquor" (water) phase. After extraction of the tar acids in the Phenosolvan process, the liquor is steam-stripped to remove the NH<sub>3</sub> which is then purified.

### Argon

In the air liquefaction process used to produce the oxygen required in the coal gasifiers and the CH<sub>4</sub> reformers (see Figure 1) there is a side stream which is rich in Argon. This is further purified and is mainly used in arc welding.

### Carbon Dioxide

In the coal gasification, as well as in the FT process massive amounts of CO<sub>2</sub> are inevitably produced. CO<sub>2</sub> is the main component of the off-gas in the Sulphur recovery plant (see above) and in the Benfield plant (which scrubs CO<sub>2</sub> from the Synthol tailgas). The latter source is the purer of the two. CO<sub>2</sub> is used in fire extinguishers and the production of "dry ice".

### Literature Cited

1. Dry, M.E. In "Applied Industrial Catalysis"; Leach, B.E.; Ed. Academic: New York, 1983; Vol II p167
2. Dry, M.E. In "Catalysis Science and Technology"; Anderson, J.R. and Boudart, M.; Eds. Springer-Verlag: Berlin, 1981, Vol. I; p159
3. Courty, P.; Arlie, J.P.; Convers, A.; Mikitenko, P. and Sugier, A.; *Hydrocarbon Processing* 1984 (Nov), 105.
4. Anderson, R.B.; In "Catalysis"; Emmett, P.H.; Ed. Rheinhold: New York, 1956. Vol IV.
5. Anderson, R.B. In "The Fischer-Tropsch Synthesis" Academic : New York 1984
6. Sachtler, W.M.H; In "Proceedings 8th International Congress on Catalysis"; Schön & Wetzel Frankfurt A.M. Vol I p 151
7. Vedage, G.A.; Himelfarb, P.; Simmons, G.W. and Klier, K.; Symposium Role of Solid State Chemistry in Catalysis. Div. Pet. Chem. ACS Washington Aug 28 - Sept 2, 1983.
8. Kagan, Y.B.; Bashkirov, A.N. et al, Neftekhimija 1966, 6 (2), 262.

RECEIVED July 15, 1986



## Chapter 3

# Fluid-Bed Studies of Olefin Production from Methanol

R. F. Socha<sup>1</sup>, C. D. Chang<sup>1</sup>, R. M. Gould<sup>2</sup>, S. E. Kane<sup>2</sup>, and A. A. Avidan<sup>2</sup>

<sup>1</sup>Mobil Research and Development Corporation, Princeton, NJ 08540

<sup>2</sup>Mobil Research and Development Corporation, Paulsboro, NJ 08066

Studies at Mobil Research have shown that light olefins instead of gasoline can be made from methanol by modifying both the ZSM-5-type MTG (Methanol-to-Gasoline) catalyst and the operating conditions. Work carried out in micro-scale fluidized-bed reactors show that methanol can be completely converted to a mixture of hydrocarbons containing about 76 wt% C<sub>2</sub>-C<sub>5</sub> olefins. The remaining hydrocarbons are 9% C<sub>1</sub>-C<sub>5</sub> paraffins, of which the major component is isobutane, and 15% C<sub>6</sub>+, half of which is aromatic. It is likely that future commercialization of Methanol-to-Olefins (MTO) will take place in a fluid-bed reactor for many of the same reasons which encouraged fluid-bed MTG development, including better temperature control and constant product composition. The olefins produced by this process can be readily converted to gasoline, distillate and/or aviation fuels by commercially available technologies such as Mobil's MOGD process. Scale-up of MTO has proceeded through bench-scale and 4 BPD pilot units and has been tested in a 100 BPD reactor.

With newly developed technology, conversion of methanol to hydrocarbons represents the final link in the production of premium transportation fuels from coal or natural gas. The methanol-to-gasoline (MTG) process has been developed. The more readily scaled fixed-bed version is the heart of the New Zealand Gas-to-gasoline complex, which will produce 14,000 BPD high octane gasoline from 120 million SCFD gas. The fluid-bed version of the process, which is also available for commercial license, has a higher thermal efficiency and possesses substantial yield and octane advantages over the fixed-bed. Successful scale-up was completed in 1984 in a 100 BPD semi-works plant near Cologne, West Germany. The project was funded jointly by the U.S. and German governments and an industrial consortium comprised of Mobil; Union Rheinsche Braunkohlen Kraftstoff, AG; and Uhde, GmbH.

The 100 BPD MTG project was extended recently to demonstrate a related fluid bed process for selective conversion of methanol to light olefins (MTO). The products of the MTO reaction make an excellent feed to the commercially available Mobil Olefins to Gasoline and Distillate process (MOGD) which selectively converts olefins to premium transportation fuels (1). A schematic of the combined processes is shown in Figure 1. Total liquid fuels production is typically greater than 90 wt% of hydrocarbon in the feed. Distillate/gasoline product ratios from the plant can be adjusted over a wide range to meet seasonal demands.

This paper describes the initial scale-up of the MTO process from a micro-fluid-bed reactor (1-10 grams of catalyst) to a large pilot unit (10-25 kilograms of catalyst).

### Experimental

The catalysts used in this experimental program were variously modified ZSM-5-type catalysts. The ZSM-5 zeolite has a pore structure which allows the formation of olefins or gasoline-range hydrocarbons without the significant formation of heavier polymethylbenzenes. The feed in most cases was pure methanol, although in one of the micro-fluid-bed runs dimethyl ether was used as the feed. The MTO reaction has been investigated in the temperature range of 400-500°C and the pressure range of 1-6 atmospheres.

Figure 2 is a schematic drawing of the micro-fluid-bed reactor used in the study. It was fabricated from vycor and could hold as much as 10 grams of catalyst in an isothermal zone maintained in a vertically-mounted tube furnace. The catalyst bed was supported by a fritted glass disk. Temperature was monitored by means of thermocouple in an axial thermowell. A glass-wool plug in an expanded disengagement section at the top of the apparatus served as a filter to keep catalyst particles from exiting the reactor. Methanol or dimethyl ether feeds were fed from an ISCO positive-displacement pump. Liquid products were collected in a room-temperature trap and gaseous products were analyzed by on-line gas chromatography and volumes measured by a wet-test meter. The catalyst could be regenerated in-situ by switching to a nitrogen/air mixture.

This miniature fluid-bed reactor exhibited isothermicity far superior to that attainable in fixed-bed micro-units. Because of the highly exothermic nature of the MTO reaction (11.7 kcal/mole methanol, 49 kJ/mole), in an adiabatic reactor, there is a temperature profile as depicted in Figure 3. In a micro-scale laboratory fixed-bed reactor, where isothermicity is desired, a hot-spot developed (unless a very narrow reactor was used, for example 1/8 inch copper tubing in a sand bath). As the catalyst ages in its typical "band-aging" fashion (2), the hot-spot moves along the bed, as is also shown in Figure 3. In the micro-fluid-bed reactor, axial-mixing of the catalyst provides rapid heat transfer rates throughout the dense bed. As a result, a fairly isothermal zone several centimeters in length can be maintained with a single-zone tube furnace.

The fluid-bed pilot-plant is a 10.2 cm ID reactor, 7.6 m high, and is equipped for external catalyst recirculation and regeneration.

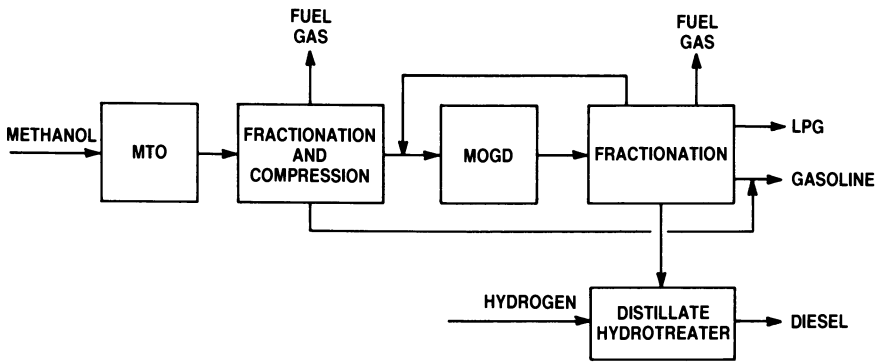


Figure 1. Schematic of combined MTO-MOGD process.

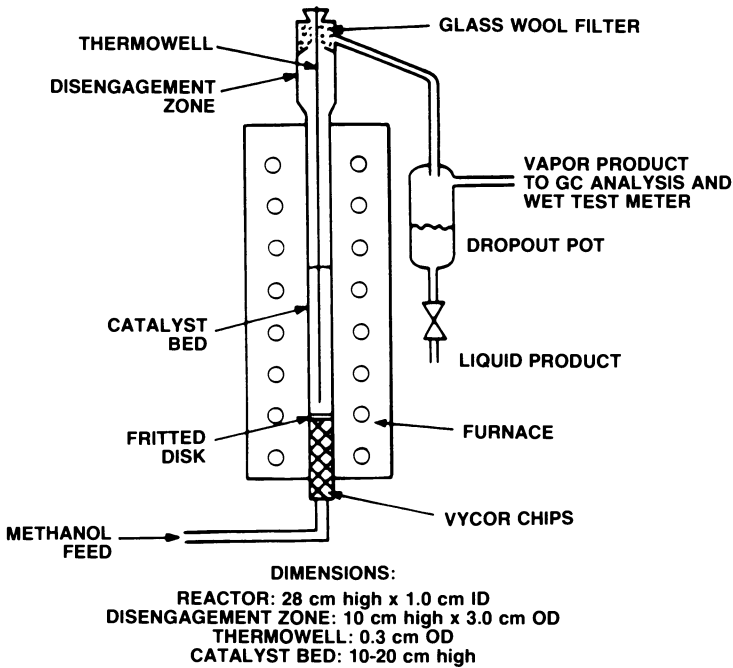
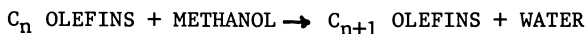


Figure 2. Schematic of micro fluid-bed reactor.

It was earlier used for fluid-bed MTG process development and is more fully described elsewhere (3). In the fluid-bed pilot-plant, uniform temperature profiles were obtained, with as little as 1°C ΔT over the entire 7.6 meter length.

### Results and Discussion

The reaction scheme of MTO is similar to that which describes methanol conversion to gasoline (MTG) (4,5):



It is necessary, however, to maximize the intermediate olefin product at the expense of the aromatic/paraffin product which makes up the gasoline (6). The olefin yield increases with increasing temperature and decreasing pressure and contact time. Judicious selection of process conditions result in high olefin selectivity and complete methanol conversion. The detailed effect of temperature, pressure, space velocity and catalyst silica/alumina ratio on conversion and selectivity has been reported earlier (6). The distribution of products from a typical MTO experiment is compared to MTG in Figure 4. Propylene is the most abundant species produced at MTO conditions and greatly exceeds its equilibrium value as seen in the table below for 482°C. It is apparently the product of autocatalytic reaction (7) between ethylene and methanol (8).

Olefins	Equil. (wt%)	Actual (wt%)
C <sub>2</sub>	8.3	8.1
C <sub>3</sub>	26.8	59.8
C <sub>4</sub>	39.0	19.2
C <sub>5</sub>	25.9	12.9

Since it is highly desirable to operate at complete methanol conversion so as to eliminate recycle of unconverted feed, most experimental results were obtained at conditions which gave complete conversion. The severity of reaction, in terms of position along the reaction pathway from methanol to paraffins and aromatics, was followed not by degree of methanol conversion, but by the ratio of propane to propene products. The higher this ratio, the further one is along the reaction path. Figure 5 shows how the olefin yield varies with propane/propene ratio, and also shows the good

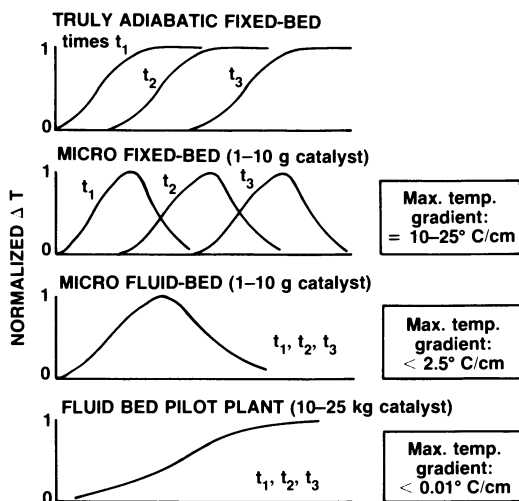


Figure 3. Temperature profiles in MTO reactors.

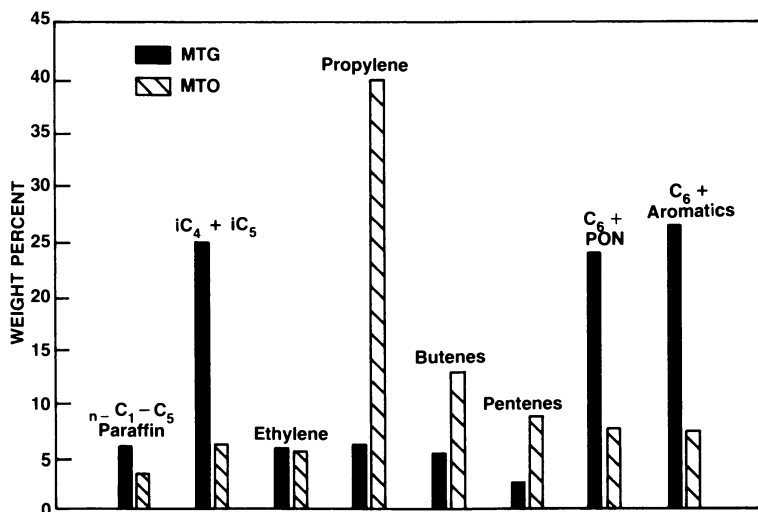


Figure 4. Comparison of product distribution from MTO and MTG reactions.

agreement that was obtained when the reaction was scaled up from 1-10 g catalyst to 10-25 kg. Figures 6 and 7 show that normal and isoparaffin yields also scaled up well from the micro-fluid-bed to the pilot plant.

One of the most important considerations in designing a process for converting methanol to olefins was to find the best way to remove the considerable heat of reaction. Despite the fact that we are stopping the reaction at the intermediate olefin product, the reactions leading to these intermediates give off almost 90% of the heat released in the overall MTG reaction scheme (49 vs. 56 kJ/mole of methanol converted for MTO vs. MTG). Efficient removal of the heat of reaction is one of the main reasons a fluid-bed reactor was selected for scale-up demonstration. A second advantage of the fluid-bed is that product composition can be kept constant, since optimum catalyst activity can be maintained by continuous make-up and regeneration.

Experimental work to date confirms that the MTO process, which is an extension of fluid-bed MTG technology, has been scaled up successfully in a 4 BPD fluid-bed pilot plant at Mobil's Paulsboro Laboratory. Product yields and catalyst performance were nearly identical to those of bench top microunits. The process is currently being demonstrated in the 100 BPD fluid-bed semi-works plant in Germany. The plant was started up February, 1985 after completing modifications required to enable extended operation at MTO conditions.

With completion of the 100 BPD MTO program, large scale testing will be completed for both steps of the MTO/MOGD process route, giving reliable scale-up information for a new and novel route for producing synthetic gasoline and diesel fuels.

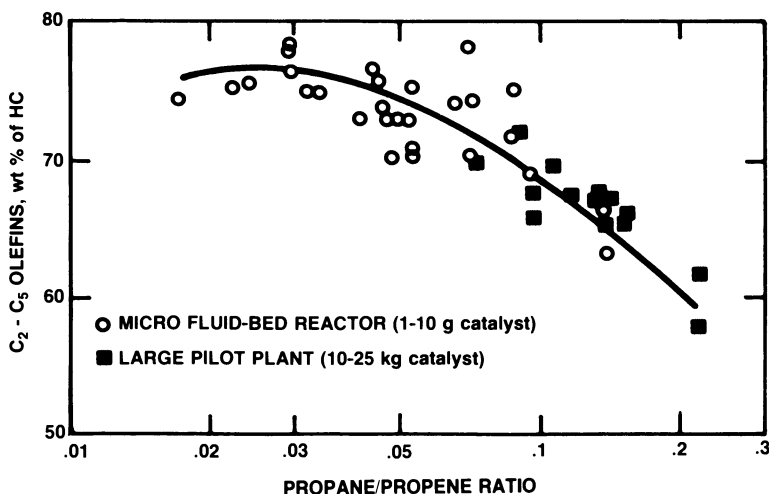


Figure 5. Comparison of olefin yield obtained in micro fluid-bed and large pilot plant

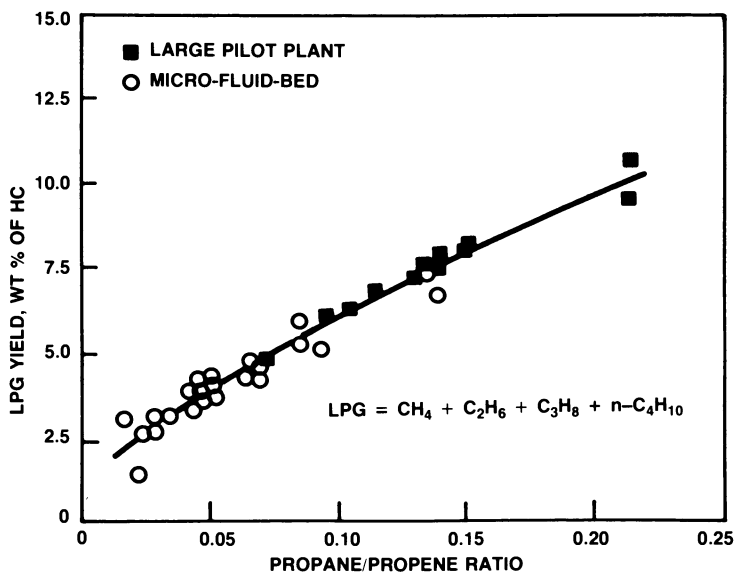


Figure 6. Comparison of normal paraffin yields obtained in micro fluid-bed and large pilot plant.

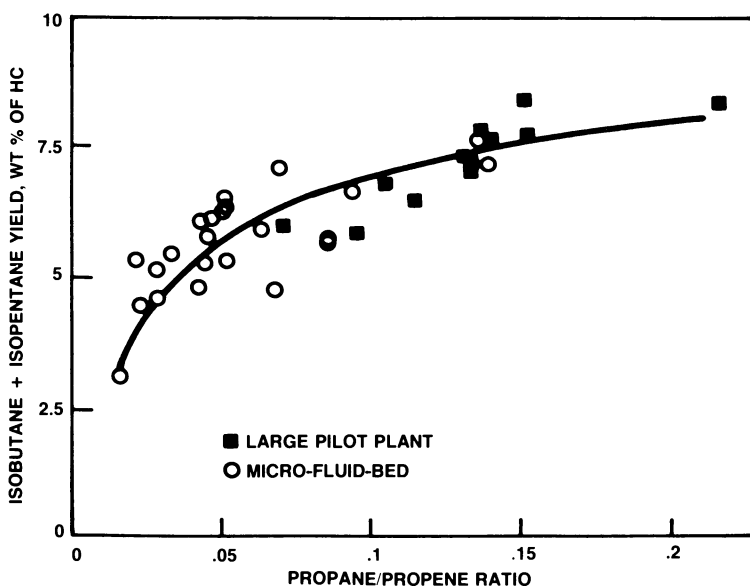


Figure 7. Comparison of isoparaffin yield obtained in micro fluid-bed and large pilot plant.

Literature Cited

1. Tabak, S. A.; AIChE 1984 Summer National Meeting, Preprint No. 42a.
2. Yurchak, S.; Voltz, S. E.; and Warner, J. P.; Ind. Eng. Chem. Process Des. Dev., 1979, 18 (3), 527-534.
3. Kam, A. Y.; and Lee, W.; Final Report "Fluid Bed Process Studies on Selective Conversion of Methanol to High Octane Gasoline", DOE Contract No. EX-76-C-01-2490, NTIS No. FE-2490-15 (1978).
4. Chang, C. D.; and Silvestri, A. J.; Journal of Catalysis, 1977, 47, 249.
5. Chang, C. D.; Chem. Eng. Sci., 1980, 35, 619.
6. Chang, C. D.; Chu, C. T-W.; Socha, R. F., Journal of Catalysis, 86, 289-296.
7. Chen, N. Y.; Reagan, W. J.; Journal of Catalysis, 1979, 59, 123-129.
8. Chu, C. T-W.; and Chang, C. D.; Journal of Catalysis, 1984, 86, 297.

RECEIVED July 15, 1986



## Chapter 4

# Production of C<sub>1</sub>-C<sub>6</sub> Alcohols from Synthesis Gas

Ph. Courty<sup>1</sup>, A. Forestiere<sup>1</sup>, N. Kawata<sup>2</sup>, T. Ohno<sup>2</sup>, C. Raimbault<sup>1</sup>, and M. Yoshimoto<sup>2</sup>

<sup>1</sup>Institut Français du Pétrole, B.P. 311, 92506 Reuil-Malmaison-Cédex, France

<sup>2</sup>Idemitsu Kosan Co. LTD, N°1-1,3-Chome, Marunouchi, Chiyoda-ku, Tokyo, Japan

Despite the current decrease of oil prices, the conversion of syngas to alcohols remains an attractive objective. Many companies are involved in alcohols synthesis projects, based on high pressure or low pressure technologies, with motor-fuels and octane boosters as targets. The I.F.P. (France), Idemitsu (Japan) R&D program is focused on the co-production of methanol and light C<sub>2+</sub> alcohols. These product mixtures yield favorable octane and methanol-compatibilizing properties. Pure linear saturated alcohols are selectively produced by highly-dispersed multi-metallic catalysts. The extent of chain-growth and related alcohols selectivity depend strongly on the steady-state active phases composition, which is determined by the operating parameters of reaction. Recent demonstration of the process, under the RAPAD R&D program, has proven its feasibility and good operability. Process economics are described. The development of such new technologies is of concern to countries lacking petroleum reserves or rich in natural gas. Syngas from natural gas is the most promising feedstock.

The development of new syngas-based processes is one of the objectives for the near future, despite the current low price of oil. Syngas can be produced from various carbonaceous sources, including coal, heavy residue, biomass and gas, the latter being the most economical and abundant feedstock. Chemical valorization of natural or associated gas is a priority objective, since liquefaction of remote gas via alcohol synthesis permits convenient shipping to markets not directly connected to the gas source by pipeline.

Another near future objective is to ensure development of technology that enables production of motor-fuel substitutes from non petroleum sources. The production of methanol-higher alcohols mixtures from natural gas, via syngas, remains a priority objective to obtain octane boosters capable of replacing lead alkyls and to allow the use of additional low-priced methanol.

I.F.P. (France) and Idemitsu Kosan (Japan), as a member of RAPAD (Research Association for Petroleum Alternative Development), are involved in process and catalysts development for alcohols synthesis. This paper details most of our recent results.

Present status of alcohols synthesis from syngas

Table I details most of the recent developments regarding direct synthesis of methanol-higher alcohol mixtures.

Chain-growth can be initiated with high operating temperatures and pressures, in the presence of alkalinized zinc-chromium mixed oxides (1,2) possibly modified with other metals (3). Such promoted catalysts allowed industrial scale production of alcohol mixtures containing up to 30 wt % of C<sub>2</sub><sup>+</sup> alcohols.

Low H<sub>2</sub>/CO ratios under more moderate temperatures and pressures, with copper-based methanol synthesis catalysts possibly alkalinized, yield methanol-higher alcohol mixtures (4-6) with rather high contents (5-12 wt %) of other oxygenated molecules (ketones, esters) - (7,8).

Copper-cobalt based catalysts induce a classical chain-growth mechanism (9-11). A heavier alcohol content ranging between 20 and 70 % wt can be obtained under moderate operating conditions. The actual target for scale-up studies is the production of alcohol mixtures containing 35-45 wt % of C<sub>2</sub><sup>+</sup> (12,13).

Sulfided and alkalinized molybdenum based catalysts have recently been claimed (14,15); mixed Mo(Co)K sulfides yield similar alcohol distributions under substoichiometric syngas and H<sub>2</sub>S (0.05-0.1 vol %), (16, 17).

Direct synthesis of alcohols on Cu-Co based catalysts

Reaction stoichiometry and mechanism. This process, which selectively produces linear alcohols ranging from C<sub>1</sub> to about C<sub>7</sub>, is based on the chemical reactions of Table II. Main reactions (a,b) produce alcohols and their related unavoidable by-products, CO<sub>2</sub> and H<sub>2</sub>O, the former being favored at low H<sub>2</sub>/CO ratios due to side or consecutive shift reaction (c). Secondary reactions produce light hydrocarbons (d,e). The reactions' stoichiometry (H<sub>2</sub>/CO) varies between 0.6 and 3, depending on the nature of the products and the number of carbon atoms involved. Most of these reactions are strongly exothermic.

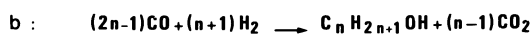
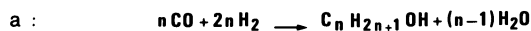
The reaction mechanism which obeys a Schultz-Flory polymerization law (9) leads to a simultaneous production of alcohols and hydrocarbons, according to the basic flow-scheme of Figure 1. On Cu-Co based catalysts, formation of formate and acetate species has been confirmed (18) by chemical trapping under reaction conditions. C-C bond formation could occur by reaction of RCH<sub>x</sub> species with either formyl or formate, yielding dioxymethylenic and acetate derivatives. Dioxymethylenic species have already been postulated, or isolated, as intermediates of direct synthesis of oxygenated compounds from syngas (19,20) and I.R. spectroscopy and chemical trapping have confirmed the appearance of methoxy, formyl, formate and acetate species in similar syngas-based reactions (21-23).

A similar chain-growth mechanism was said to occur with the first molybdenum-sulfur-potassium based catalysts of table I (15). For such a chain-growth mechanism, the heavier the average molecular weight of alcohols, the greater the formation of heavy compounds and, more often than not, the lower the alcohols' selectivity. Furthermore, in Fischer-Tropsch type catalysts (24,25) diffusion limitations, mostly due to the presence of liquid products condensed in the microporosity, increase with the size of diffusing molecules. These molecules are capable of

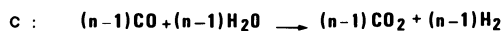
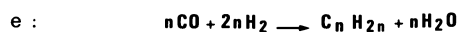
**TABLE I : PRESENT STATUS OF ALCOHOLS SYNTHESIS**

"CHAIN GROWTH" DUE TO:		RANGE OF OPERATING CONDITIONS			
Operating parameters	key elements of catalysts	T°C	P MPa	<sup>av.</sup> H <sub>2</sub> /CO <sub>mol.</sub>	C <sub>2+0H</sub> (wt%)
a/ high. op. temp. and pressure	Cr-Zn promoters alkali metals	380-420	12-25	2-3	20-30
b/ low H <sub>2</sub> /CO	• Cu-Zn (alkali metals)	~300	~10	~1 (or less)	20-30
c/ use of metals inducing chain-growth	• Cu-Co alkali metals • others	270-320	6-10	1.5 ± 0.5	35-45
d: b + c	• MoS <sub>2</sub> (a) promoter K	240-325(a)	10-28 (a)	~1(a)	20-70(a)

(a) PATENT DATA EP 119609

**TABLE II : METHANOL-HIGHER ALCOHOLS SYNTHESIS  
ON COPPER - COBALT BASED CATALYSTS****MAIN REACTIONS**

difference (b - a) :

**SIDE REACTIONS****REACTIONS' STOICHIOMETRY ( H<sub>2</sub>/CO required , vs.n )**

	<b>1 to 6</b>
<b>reactions :</b>	
a,e	(constant)
b	down to 0.63
d	down to 2.2

readsorbing and growing again. As a consequence the termination rates of the highest molecular weight species are lowered. This increased weight fraction of the heaviest products is undesirable for motor-fuel blending. This interpretation (24) explains why deviations from the expected straight line of the Schultz-Flory distribution are often observed for F.T. like catalysts. Figure 2 presents the predicted weight fractions of C<sub>7+</sub> alcohols (T<sub>B</sub> ≥ 176°C) and C<sub>8+</sub> alcohols (T<sub>B</sub> ≥ 195°C). vs. C<sub>2+</sub>OH wt %, for a theoretical straight line S.F. distribution. Since standard deviations suggest slightly higher heavy compound contents, a reasonable target is a C<sub>2+</sub>OH concentration between 35 and 45 % wt, which should provide alcohol mixtures that contain less than 1 % wt of C<sub>8+</sub> alcohols.

The catalysts. The catalysts are based on homogeneous spinel-type mixed oxides, modified by incorporating alkali metals. Among others, copper-cobalt-aluminum-zinc-sodium mixed oxides have been described earlier (9-13) as well as copper-cobalt-chromium-alkali metal oxides (26). When prepared by coprecipitation reactions, their hydrated precursors consist of highly homogeneous and lamellar, hydrotalcite like crystallized phases whose thermal decomposition, and related pseudomorphic transformation, lead to the spinel type mixed oxide phase sought after (9,27). Upon preliminary hydrogen reduction and further reconstruction under syngas reacting medium, the spinel phase is strongly depleted of its reducible metals and converted to highly dispersed clusters supported on the depleted mixed oxides support. Magnetic characterization (28,20) has confirmed the appearance of highly dispersed cobalt containing particles (av. diameter 2-4 nm) in stabilized catalysts.

CO<sub>2</sub> and H<sub>2</sub>O, unavoidable by-products of alcohols synthesis. Considering chemical reactions of table II, water and carbon dioxide appear as equivalent by-products due to shift conversion equilibrium, equation (1). Most other low temperature alcohol synthesis catalysts have a rather high shift activity as well. CO<sub>2</sub> removal from reacted syngas of synthesis loop, before recycling to reactor, leads to a significant decrease of water formation which, in turn, results in a lower water content in the raw alcohols, leading to simplified fractionation-dehydration processes.



$$p_{\text{H}_2\text{O}} = p_{\text{CO}_2} \cdot \frac{p_{\text{H}_2}}{p_{\text{CO}}} \cdot \frac{1}{K T_a} \quad (\text{Ta} = \text{temp. of approach}) \quad (2)$$

to equilibrium

Equation (2) confirms that lowering water partial pressure (p<sub>H<sub>2</sub>O</sub>) implies lowering p<sub>CO<sub>2</sub></sub> (CO<sub>2</sub> removal) and the H<sub>2</sub>/CO ratio. Decreasing reaction temperature displaces reaction (1) equilibrium to the right side. Provided that stable and active catalysts are available, water contents ranging between 2.5-5 wt % can be obtained while operating with reasonable (1.2-1.5) H<sub>2</sub>/CO ratios in the synthesis loop.

Although Cu-Co based catalysts can be used in a broad range of CO<sub>2</sub> partial pressures, our recent technico-economic analyses have pointed out some advantages of a "low CO<sub>2</sub>" operation, leading to a partial chemical removal of water rather than a total removal via fractionation and/or drying procedures. Furthermore, recent improvements in proven partial-oxidation technologies for production of substoichiometric syngas make feasible process improvements, provided that the CO<sub>2</sub> removed can be recycled to the syngas production section.

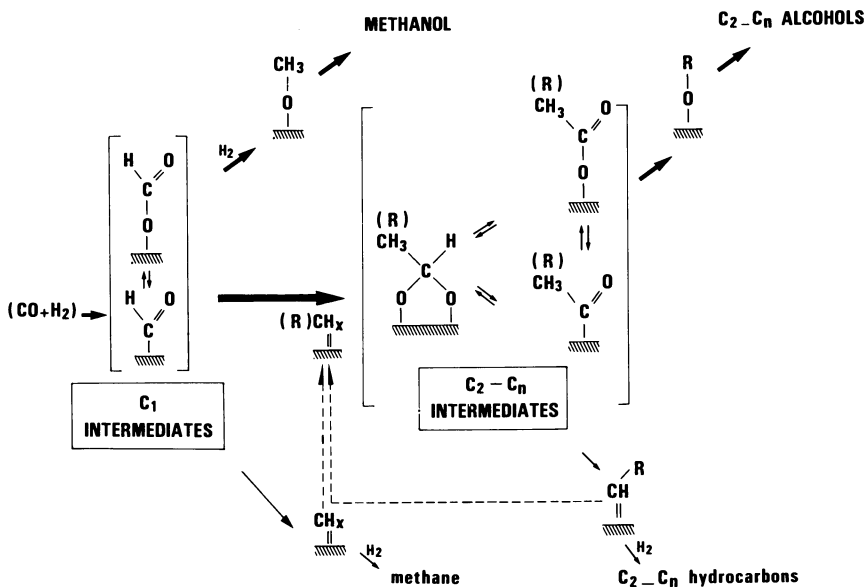


Figure 1 : Assumed reaction mechanism on Cu-Co based catalysts.

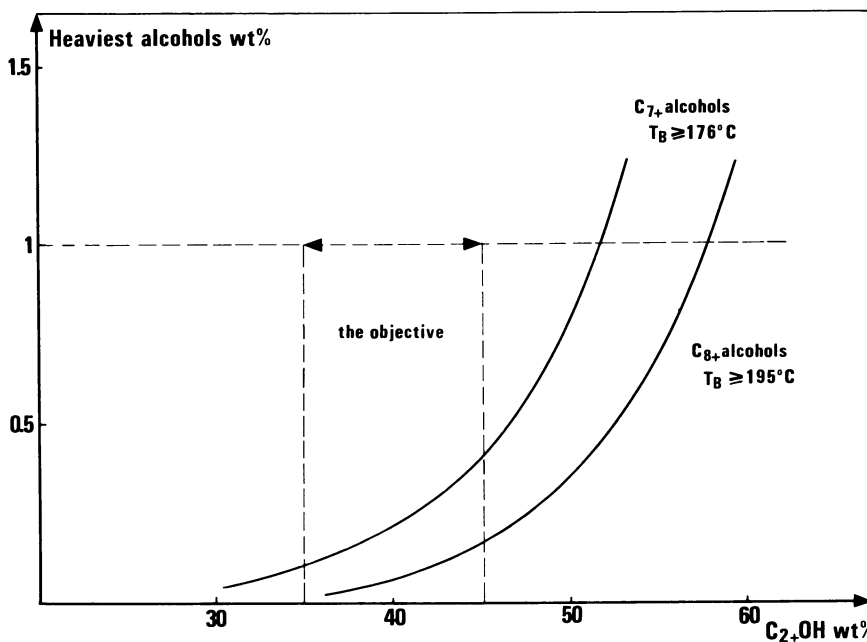


Figure 2 : Heaviest alcohols (wt%) vs. C<sub>2</sub>+OH (wt%) for a standard, straight-line Schultz-Flory distribution.

Performances of Cu-Co based catalysts. As disclosed earlier (10,11) modifications of either the catalyst formula or of its "in situ conditioning" allows varying the alcohol product phase composition from 20 to about 70 wt % of C<sub>2+</sub> alcohols at bench-scale. In connection with our target (35-45 wt % of C<sub>2+</sub> alcohols), table III details the range of typical performances under CO<sub>2</sub> removal and light substoichiometric conditions.

One of the advantages of copper-cobalt catalysts is the very high purity of the alcohol phase produced. Even though alcohol purity decreases slightly with C<sub>2+</sub>OH content (Figure 3), it remains rather high, since cobalt lowers the formation of esters and oxygenated impurities (ketones, aldehydes). This can be seen in table IV which details a typical composition of alcohols, along with comparative published data for copper-based cobalt-free catalysts operating under strong substoichiometric conditions (7).

Selectivity to alcohols varies vs. C<sub>2+</sub>OH as seen in Figure 4 ; the heavier the average molecular weight of alcohols, the lower their selectivity of formation. Current objectives for catalyst optimization deal mostly with selectivity improvements from A to D domain of performances, and even further. Same figure details the effects of H<sub>2</sub>/CO stoichiometry on chain-growth ; lower H<sub>2</sub>/CO favors higher C<sub>2+</sub> and slightly favors alcohol selectivities (without a significant deviation from general correlation). Higher H<sub>2</sub>/CO ratios (3.5 or more) have detrimental effects on both C<sub>2+</sub>OH content and alcohol selectivity. The activity slightly decreases when H<sub>2</sub>/CO decreases, a typical behaviour of F.T. like catalysts (24). Another procedure (H<sub>2</sub>/CO ratio being fixed) for adjusting the extent of chain-growth deals with the final hydrogen reduction temperature (200-500°C) before syngas admixtion. Higher temperatures (typical : 500°C) favor higher C<sub>2+</sub> (e.g. 50 wt %) without decreasing the activity compared to low temperature reduction (typical : 250°C - C<sub>2+</sub> = 20 % ; same catalyst as before). Lastly, at fixed operating conditions (e.g. : H<sub>2</sub>/CO = 2, CO<sub>2</sub> free syngas, medium range reduction temperature), it is feasible (Figure 5) to vary C<sub>2+</sub>OH and related selectivity between 20 % (or less) and 60 % (or more). Chain-growth is favored for higher cobalt concentration and/or alkali metal contents and/or lower Cu/Co ratios ; some specific promoters are also of prime importance in this way.

### Process development

Reaction section. The most important parameter for optimization in the reaction section involves heat transfer and removal in the catalyst beds in order to control temperature increases inside the catalyst particles and/or along the beds. To a lesser extent, thermodynamic limitations of methanol synthesis must also be considered, mostly at the lower operating H<sub>2</sub>/CO ratios.

Control of reaction temperature is achieved by using a multiquenched bed system rather than a multitubular "isothermal" reactor; the former is favored for large capacities. Two reactors are used in series with intermediate cooling (Figure 6). By recycling most of the untransformed syngas, after CO<sub>2</sub> removal, high CO conversions are realized.

Separation section. Owing to the fact that, except for methanol, azeotrops exist between alcohols and water, a simple fractionation technology cannot be considered for the production of pure and anhydrous alcohols from the raw liquid products of the reaction section. Among other

**TABLE III : DIRECT SYNTHESIS OF ALCOHOLS  
WITH COPPER - COBALT CATALYSTS****1 - RANGE OF OPERATING CONDITIONS**

T: 260-320°C

P: 6-10 MPa

G.H.S.V.: 3,000-6,000 h<sup>-1</sup> (STP)
$$\begin{array}{l} 1 < \text{H}_2/\text{CO} < 2 \\ 0.5 \leq \text{CO}_2 < 3 \end{array} \quad \left. \vphantom{\begin{array}{l} 1 < \text{H}_2/\text{CO} < 2 \\ 0.5 \leq \text{CO}_2 < 3 \end{array}} \right\} \% \text{ vol}$$
**2 - TYPICAL PERFORMANCES**CO conversion 90 (total)  
(CO conv. to CO<sub>2</sub> is excluded)Alcohols selectivity 70-80  
(at.g. C, CO<sub>2</sub> excluded)Alcohols productivity 0.10-0.15 kg.l<sup>-1</sup>.h<sup>-1</sup>**3 - RELATED COMPOSITION OF ALCOHOLS PRODUCED  
(before fractionation)**. Alcohols 97.5-99 wt %  
( anhydrous ). C<sub>2</sub>+Alcohols 35-45 wt %

. Breakdown :

C<sub>2</sub>H<sub>5</sub>OH 23-26 wt %C<sub>3</sub>H<sub>7</sub>OH 7.5-11C<sub>4</sub>H<sub>9</sub>OH 2.5-4.5C<sub>5</sub>H<sub>11</sub>OH 1-2C<sub>6</sub>+OH 1-2



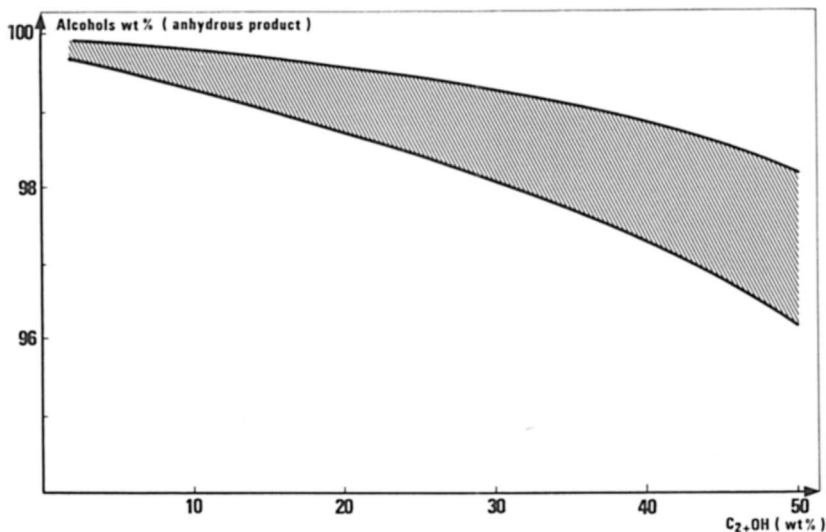


Figure 3 : Purity of raw alcohols (anhydrous base) vs. C<sub>2+</sub>OH (wt %).

**TABLE IV: TYPICAL COMPOSITIONS OF ALCOHOLS (wt%)**

	CuCo based catalyst (H <sub>2</sub> /CO = 2)	Cobalt free, copper based catalyst (a) (H <sub>2</sub> /CO < 1)
<b>CH<sub>3</sub>OH</b>	57.5	53.5
<b>C<sub>2</sub>OH</b>	28.5	3.9
<b>C<sub>3</sub>OH</b>	7.1	3.1
<b>C<sub>4</sub>OH</b>	2.8	6.2
<b>C<sub>5</sub>OH</b>	1.2	3.8
<b>C<sub>6+</sub>OH</b>	1.3	14.8
<b>Hydrocarbons</b>	0.3	4.3
<b>Esters</b>	0.7	} 10.1
<b>Other oxygenated compounds</b>	0.6	
	100.0 (anhydrous basis)	99.7 (+0.3% water)
<b>Alcohols purity</b>	98.3	85.3
<b>C<sub>2+</sub>OH</b>	40.9	31.9

(a) From ref. [7]

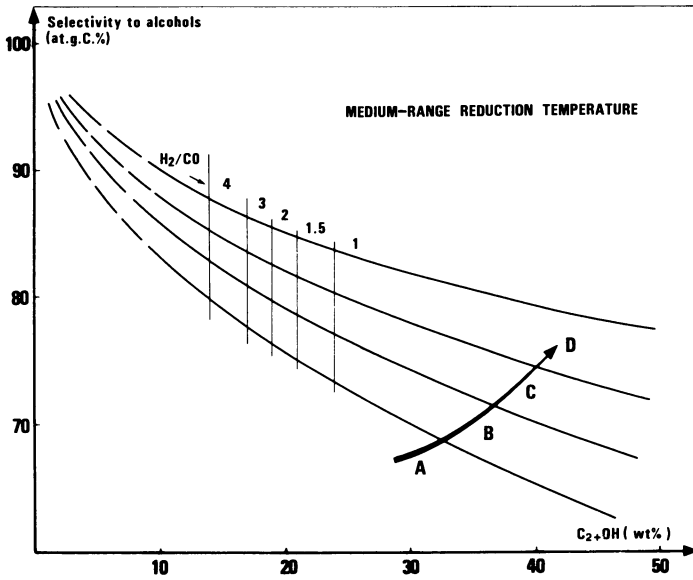


Figure 4 : Correlation between C<sub>2+</sub>OH wt % syngas stoichiometry and related alcohols selectivity.

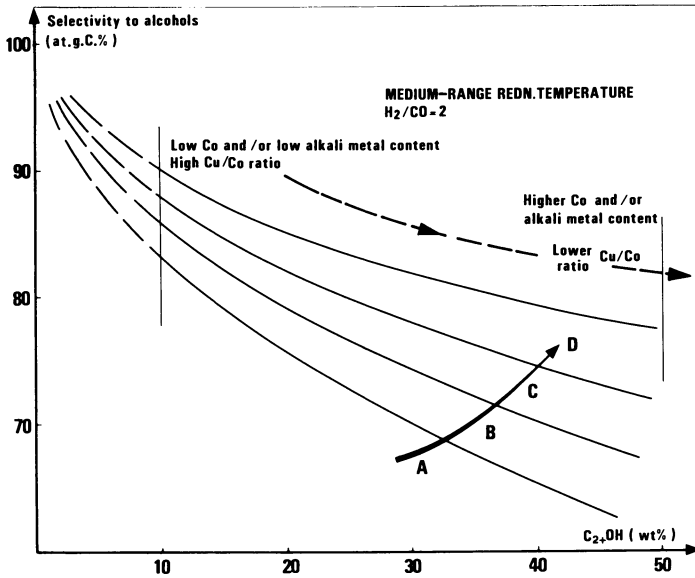


Figure 5 : Influence of catalyst's formula on its related performances.

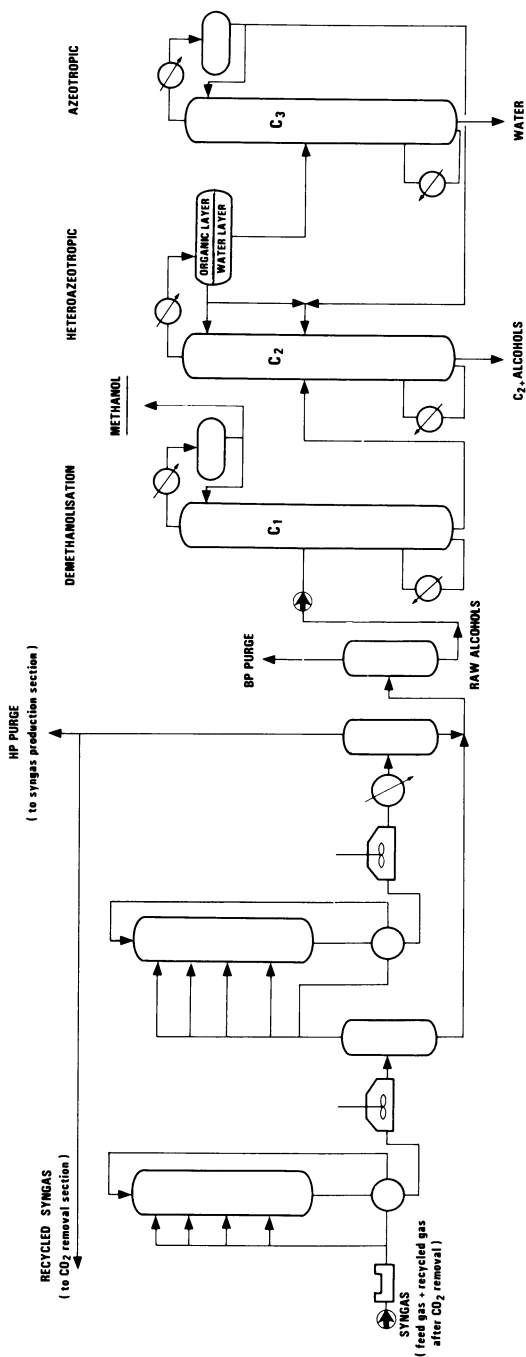


Figure 6 : Basic flow-scheme of the alcohols synthesis process.

technologies, the proven azeotropic distillation process is attractive for alcohol dehydration, considering the low water content (2.5-5wt %) which results from the new design of reaction section. Same Figure 6 presents the separation flow-scheme. In the first column C<sub>1</sub>, methanol is distilled from the heavier alcohols-water mixture. This mixture is then dehydrated in azeotropic columns C<sub>2</sub> and C<sub>3</sub> which are operated with a water entrainer. Benzene has been used for this purpose at bench scale to produce large samples of anhydrous alcohol mixtures (< 0.2 wt. % of water). Other entrainers well known for ethanol azeotropic dehydration may be used as well.

The integrated process. Figure 7 presents a typical block-diagram of the overall process. Syngas is produced via high temperature partial oxidation of natural gas. This technology yields very low contents of residual CH<sub>4</sub> and CO<sub>2</sub>, so that CO<sub>2</sub> removal from the feed gas is unnecessary. In order to minimize carbon losses, CO<sub>2</sub> purged from the CO<sub>2</sub> removal unit and most of the purge from the reaction section are recycled to syngas production section. The current performances of such an integrated process lead to the economics described later in the report.

#### First demonstration

Operation and results. Idemitsu Kosan Company, as a member of Rapad sponsored by the Japanese government, has built a 7000 bbl/y demonstration plant in Chiba, Japan, using IFP's process design. Figure 8 presents an overall view of the demonstration unit, which reaction section is very similar to that of Figure 6 ; the plant was operated from Dec. 84 to March 85 with first generation Cu-Co based catalyst without any major problem. Moderate operating pressures (6-10 MPa) and temperatures (260-300°) were used ; performance data are presented Figure 9. As the reaction temperature and pressure were raised to obtain the target productivity, the selectivity to alcohols (S<sub>Al</sub>) increased and stabilized at a fairly high level (29) ; in the same time, the weight proportion of C<sub>2+</sub> alcohols decreased to 36 wt %, then stabilized. This tendency is the same as was observed in bench and microplant studies, except that the stabilized value of C<sub>2+</sub> alcohols wt % was slightly higher ; there is a possibility that minor differences in reduction procedure of the catalyst might be the cause of this deviation. The overall alcohol content in the product was very high, more than 99 wt %, and was more than was predicted from bench scale and pilot studies.

Product characteristics and motor-fuel properties. The motor-fuel properties of bench-fractionated alcohols from the demonstration plant have also been examined. Table V presents the composition of the average representative fractionated sample. Its purity is 99.3 %, similar to that of the raw alcohols before fractionation, with 35.8 wt % C<sub>2+</sub> OH and 0.16 % water.

Several studies (12,13) have been carried out regarding auto-compatibilizing properties of C<sub>1</sub> and C<sub>2+</sub> alcohols in the C<sub>1</sub>-C<sub>6</sub> alcohols sample and, in parallel, motor-fuel properties after suitable blending with lead-free gasolines. It was found that compatibilizing properties of tertibutylalcohol (TBA) and C<sub>2</sub>-C<sub>6</sub> alcohols were almost the same, while typical octane blending values (T.O.B.V.) of C<sub>1</sub>-C<sub>6</sub> alcohols mixture

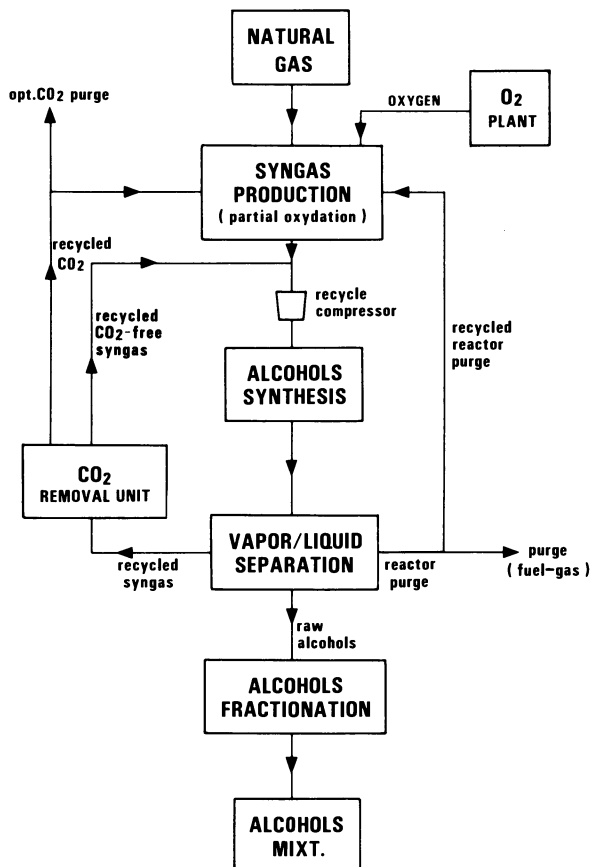


Figure 7 : Block diagram of the integrated natural gas to alcohols complex.

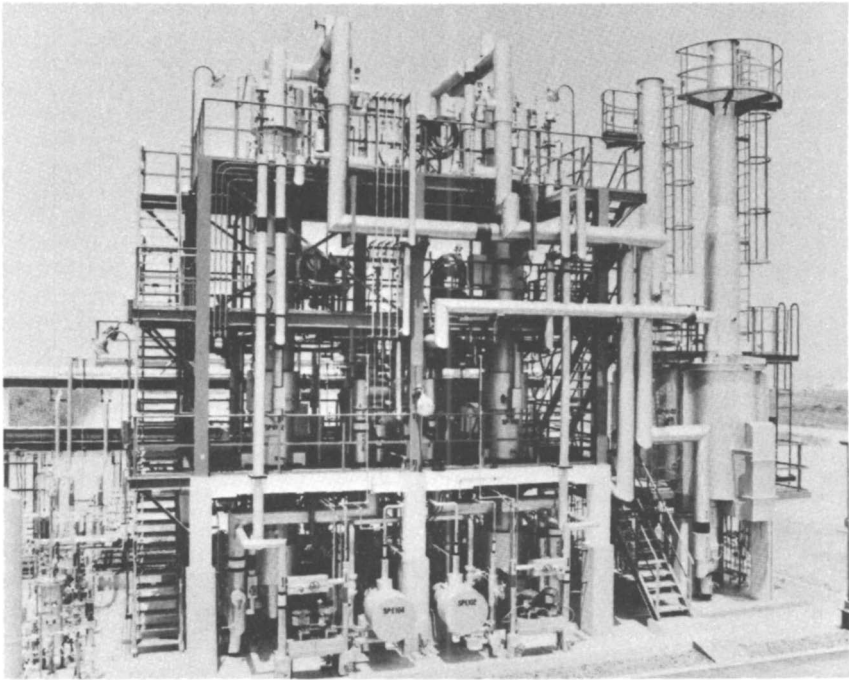


Figure 8 : A general view of the demonstration unit.

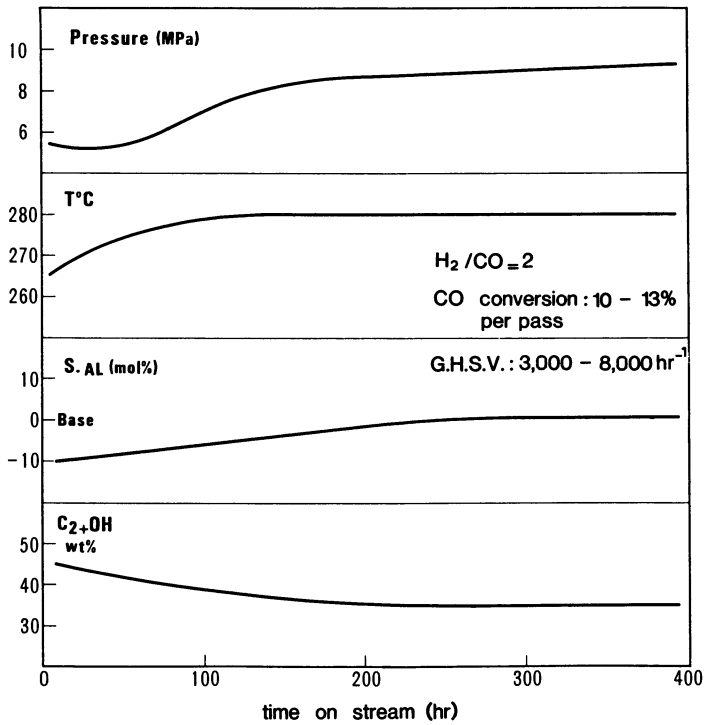


Figure 9 : Performance data of the demonstration.

**TABLE V: COMPOSITION OF FRACTIONATED ALCOHOLS (wt%)  
FROM DEMONSTRATION UNIT**

-	METHANOL	63.5	}	C <sub>2</sub>	69.5 %
-	C <sub>2</sub> +ALCOHOLS	35.8		C <sub>3</sub>	17
-	ALCOHOLS	99.3		C <sub>4</sub>	6.5
				C <sub>5</sub>	3
-	C <sub>5</sub> +HYDROCARBONS	0.2		C <sub>6+</sub>	4
-	ESTERS	0.3			100
-	OTHER OXYGENATES	0.2			
		100.0			water content 0.16 %

are located between those of ethanol and isopropanol. Field testing of such C<sub>1</sub>-C<sub>6</sub> alcohol blended motor-fuels is in progress.

#### The economics

These economics are based on alcohols production from natural gas, via syngas production, according to the block diagram of Figure 7. Cost of production of C<sub>1</sub>-C<sub>6</sub> alcohols is highly sensitive to that of natural gas. Low-priced gas is widely available, mostly in developing countries or remote areas. Most industrialized countries dispose of natural gas at significantly higher prices. Therefore two extreme situations are considered in table VI where estimated production costs are given for a typical 700,000 tons per year natural gas to alcohols integrated complex. Costs related to the investments are not the same for the different situations. For remote areas, it is reasonable to apply a location factor to the investments (here, 1.4). With a \$ 0.5/MMBTU gas price, production cost will be mainly sensitive to investment. Figure 10 illustrates the relative importance of raw material costs for the two situations.

Finally Figure 11 shows the breakdown between capital cost and production cost for the two situations. With a natural gas price as low as \$ 2/MMBTU like very recently in the U.S., the advantage of remote areas having very cheap gas, e.g. \$ 0.5/MM BTU, is significantly reduced.

**TABLE VI:**

**PRODUCTION COST OF C<sub>1</sub>-C<sub>6</sub> ALCOHOLS FROM NATURAL GAS**

plant capacity : 2,100 tons/d - 700,000 tons/y

stream factor : 8,000 h/y - 1986 data

Location	INDUSTRIAL AREA	REMOTE AREA
<b>CAPITAL COST (10<sup>6</sup>\$)</b>		
• Battery limit investments (B.L.I.)	320	450
• Storage, off.sites investments	160	220
• <b>FIXED CAPITAL (F.C.)</b>	<b>480</b>	<b>670</b>
<b>OPERATING COST</b>		
RAW MATERIALS		
• Natural gas - 3 \$ /MMBTU *	<b>132</b>	
• - 0.5\$ /MMBTU		<b>22</b>
CATALYST AND CHEMICALS	18	18
VARIABLE COSTS		
• Operating labor	2	2
• Maintenance labor **	6.86	9.57
• Control lab. labor	0.40	0.40
• Maintenance material **	6.86	9.57
• Plant overhead ***	7.40	9.58
• Taxes and Insurances ****	13.71	19.14
- DEPRECIATION (10% of F.C.)	68.57	95.71
<b>PRODUCTION COST \$/ton</b>	<b>256</b>	<b>186</b>
<b>SALE PRICE \$/ton</b> (at 10% ROI)	<b>324.6</b>	<b>281.7</b>

\*: H.H.V.    \*\*: 1.5% of B.L.I.    \*\*\*: 80% of total labor    \*\*\*\*: 2% of F.C.



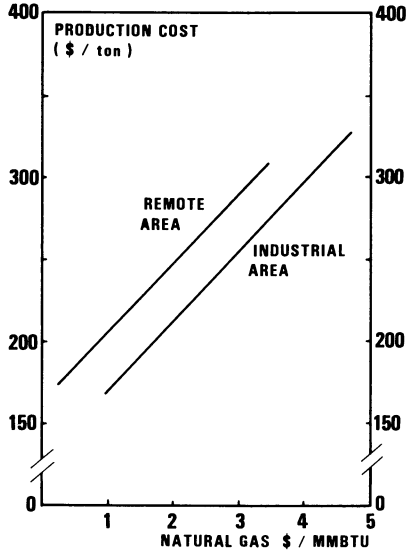


Figure 10 : Sensitivity to natural gas prices of production cost of alcohols.

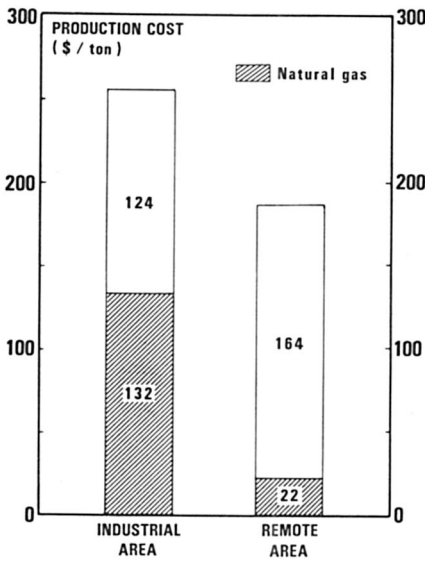


Figure 11 : Breakdown of production cost of C<sub>1</sub>-C<sub>6</sub> alcohols.

### Overall view

Compared to other technologies for alcohols production (e.g. ethanol from biotechnology), this new approach for the production of methanol-higher alcohol mixtures and its related economic data look rather promising for the near future. The C<sub>1</sub>-C<sub>6</sub> alcohols blend produced at demonstration scale which was further fractionated at bench scale offered both the high T.O.B.V. of ethanol and the high compatibilizing properties of similar methanol-TBA mixtures. Future additional improvements of both process and catalysts are strongly expected through the continuing R and D efforts of both partners.

Acknowledgments. The authors wish to thank RAPAD of Japan and Directory Boards of both Companies for allowing the publication of this paper, as well as all those who have contributed to its realization.

### Literature Cited

1. Natta G. Colombo U. Pasquon I. in "Catalysis" Reinhold Ed. New York 1957 ; vol.V, p. 131.
2. Montarani R. Aglietti B. Scarrosi A. Arpel Congress on Heavy Oils Caracas 8-11 oct 1984.
3. Paginni A., Sanfilippo D. American Institute of Chemical Engineers. Spring National Meeting, New Orleans - U.S. - 6-10 april 1986. paper nr. 25 b.
4. Hildebrand W., Supp E. Proc. 6th Int. Symp. on alcohol Fuel Techn. Ottawa (Canada) 1984, 2 pp. 140-146.
5. Cornelius G., Hildebrand W. et al. E.P. 152468, 1984.
6. Supp. E., in AICHE Meeting ref. 3 ; paper nr. 25c.
7. Hiller H., Supp. E. Erdöl u. Kohle 1985, 38 (1) pp. 19-22.
8. Elliott D.J. and Pennella F. in "Chemicals from syngas and methanol" 191st ACS National meeting (13-18 april 1986 New-York). American Chemical Society ; preprints vol 31 (1) pp. 39-45.
9. Courty P. Durand D. Freund E. Sugier A. J.Mol.Cat. 1982 17 pp.241-254.
10. Courty P. Arlie J.P. Convers A. Mikitenko P. Sugier A. Proc.11th World Petroleum Congress J. Wiley & Sons Ed. 1984.
11. Arlie J.P. Cariou J.P. Courty P. Forestière A. Travers P. Proc.6th Int. Symposium on Alcohol Fuel Techn. Ottawa (Canada) 1984 2pp 92-99.
12. Ohno T. Yoshimoto M. Asselinou L. Courty P. Travers P. in "Production of mixed alcohols from synthesis gas" ; AICHE Meeting ref.3 ; paper nr. 25e.
13. Courty P. Forestière A. Kawata N. Ohno T. Raimbault C. Yoshimoto M. in ACS Meeting ref. 8 ; preprints vol. 31 (1) pp. 38.
14. C.E.N. release of 12th nov. 1984.
15. Mintz M.J. Quarderer G.J. Alcohol Week Symposium. San Antonio (Texas) 1984.
16. Quarderer G.J., in "production of mixed alcohols from synthesis gas". AICHE Meeting ref. 3 ; paper nr. 25a.
17. Hakki A. Tellis C. in "Octane enhancers for motor-fuels" AICHE Meeting ref. 3 ; paper nr. 78d.
18. Kienemann A., Hindermann J.P., Breault R. Idriss H. in ACS Meeting ref. 8 ; preprints vol. 31 (1) pp 46-53.

19. Lavalley J.C., Lamotte J., Busca G., Lorenzelli O., J.C.S. Chem. Comm., 1985, pp. 1006.
20. Grandvallet P., PhD Thesis, Technip Ed., 1985.
21. Saussey J., Lavalley J.C., Lamotte J., Rais T., J. Chem. Soc., Chem. Comm., 1982, pp.278.
22. Breault R., Hindermann J.P., Kiennemann A., Laurin M., Catalysis on the Energy Scene, S. Kaliaguine & A. Mahay Ed. 1984, pp. 489.
23. Kikuzono Z., Kagami S., Naito S., Onishi T., Tamaru K., Faraday Discuss, Chem. Soc., 1981, 72, pp. 194.
24. Lucchesi P.J., Levine D.G., Priestley E.B., Proc. 11th W.P. Congress., J. Wiley & Sons, Ed. 1984.
25. Grandvallet P., Courty P., Freund E., Proc. 8th Int. Congress on Catalysis, Berlin (W), 1984, II, P. 81-92.
26. Courty P., Durand D., Freund E., Sugier A., F. Patent 2,523,957, 1982. Sugier A., Freund E., US P. 4,291,126, 1978, and 4,346,179, 1979.
27. Courty P., Marcilly C., Proc. 3rd Int. Symposium on Preparation of Cat., Louvain (Belgique), Elsevier Ed. 1983, pp. 485-520.
28. De Montgolfier P., Martin G.A., Dalmon J.A., J. Phys. Chem. Solids, 1973, 34, pp. 801 - Martin G.A., Primet M., Dalmon J.A., J. Cat., 1978, 53, pp. 321.
29. RAPAD (Japan) "Research and development on Synfuels" Annual Report, Sept. 1985.

RECEIVED July 29, 1986

## Chapter 5

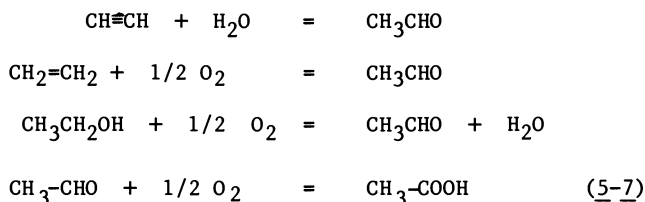
# Acetic Acid Production via Low-Pressure, Nickel-Catalyzed Methanol Carbonylation

Nabil Rizkalla<sup>1</sup>

The Halcon SD Group, Inc., Montvale, NJ 07645

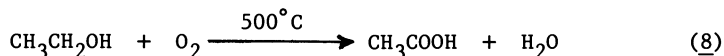
Nickel-catalyzed methanol carbonylation under high pressure and temperature has been known for decades. The parameters that bring the catalytic activity of the nickel catalyst to the same level of the rhodium process have been examined. Promoters stabilize the nickel catalyst and enhance the reaction rate under mild reaction conditions. The most efficient promoters are phosphines, alkali metals and tin. Combining two different promoters gives maximum reaction rate. Hydrogen and metals of group VIB promote reaction rate and catalyst stability. The reaction is first order with respect to iodine and nickel and is retarded by the presence of high water or methanol concentrations and high CO partial pressure. A mechanism is proposed to explain the function of the different promoters and reaction parameters.

Acetic acid is one of the oldest known chemicals. Dilute acetic acid, vinegar, has been made by aerobic bacterial oxidation of ethanol. It has also been reclaimed by extraction or extractive distillation from pyroligneous acid, which was obtained from the extractive distillation of wood (1). In the early nineteen hundreds, oxidation of acetaldehyde became the main source of acetic acid. The acetaldehyde has been obtained from acetylene (2), ethylene (3) or ethanol (4) as indicated below.



Alternatively, acetic acid was made by a high temperature direct oxidation of ethanol.

<sup>1</sup>Current address: 415 Faletti Circle, River Vale, NJ 07675



Beginning in the fifties, acetic acid was predominantly obtained from paraffin oxidation, especially n-butane (9). Acetic acid's chemical history has been rich and varied.

The concept that acetic acid can be prepared by carbonylation originated in use of routine acids. Carbonylation of methanol was first practiced in a high temperature and pressure process using boron trifluoride or phosphoric acid. A carbon monoxide pressure of 10,000 psi at 300°C was needed for the reaction (10). Metal salts came to replace acids as carbonylation catalysts. Carbonylation of methanol using a metal carbonyl catalyst was first discovered by Reppe and practised later by BASF. However, the process again required high pressure, 7500-10,000 psi, and the selectivity was low (11-14).

A substantial advance was made by discovery of the rhodium-catalyzed methanol carbonylation to acetic acid, developed by Monsanto. The rhodium process is highly selective and operates under mild reaction pressure, 400 to 1000 psig. However, because of the high price of rhodium, an efficient recovery of the catalyst is essential. An expensive rhodium recovery section is an integral part of any new acetic acid plant (15-16). This can be a substantial financial burden, especially in a smaller plant.

It is evident that the next improvement in this technology is to develop a process that utilizes a catalyst that is less expensive but just as selective and active as rhodium. This paper describes the development of nickel catalyzed carbonylation whose performance matches the current industry standard of rhodium.

#### Low Pressure Nickel Catalyzed Process

Use of Ni as a catalyst for carbonylation of methanol has been known for decades (11-14). The reaction was characterized by high temperature (200-300°C) and pressure (5000-10,000 psi). However, when BASF built methanol carbonylation plants in the early sixties, the catalyst of choice was cobalt, not nickel, in spite of its lower selectivity. Nickel was less reactive, more volatile as the carbonyl, and required higher temperature and pressure than cobalt.

Table I. Comparison Between Reppe System,  
High (I) Systems and the Rh System

Catalyst	Temp. °C	Press. psig	I %	Rate x 10 <sup>3</sup> <u>mol</u> l. sec	Ref.
Ni-P (Reppe)	200	10,000	9	0.15	(12), (13)
Ni-Aminophenol	275	10,000	4	(30% Conversion)	(12), (13)
Ni-P	150	725	20	1.08	(18)
Ni-Sn	150	725	20	0.18	(17)
Rh	175	1000	8.5	1.53	(15), (16)
Rh	175	400	7.5	1.17	(15), (16)

Our work in this area progressed in two steps. In the early phase of our program we were able to achieve an efficient methanol

carbonylation using nickel as the catalyst (17, 18). Reaction pressure and temperature were comparable with those of the rhodium reaction, 750 psi and 150°C. Tin, phosphine or amine promoters were needed for this activity. An essential requirement for the catalyst activity was a high concentration of iodide species. The reaction rate was still inferior to the rhodium system (Table I). However in subsequent studies, modification of the catalyst composition, solvent, and reaction parameters has allowed the elimination of the high iodide concentration with achievement of a reaction rate that matches that of the rhodium-catalyzed carbonylation. The following section describes the essential elements that were responsible for improving the catalytic activity of nickel.

### Catalyst Promoters

Nickel carbonyl charged, or formed in the carbonylation reaction mixture, can catalyze the carbonylation of methanol (11). To maintain the activity of the nickel carbonyl catalyst high temperature and pressure are required (12-14). However, certain promoters can maintain an active, soluble, nickel carbonyl species under much milder conditions. The most reactive promoters are phosphines, alkali metal salts, tin compounds, and 2-hydroxypyridine. Reaction rates of 2 to  $7 \times 10^{-3}$  (mol/l.sec) can be achieved without the use of high concentration of iodine (Table II). In addition, high reaction rates were, in most cases, associated with the presence of molybdenum, tungsten or chromium.

Table II. High Reaction Rates Acheived with Promoters

Catalyst	Press psig	Temp. °C	I %	Rate $\times 10^3$ $\frac{\text{mol}}{\text{l. sec}}$
Ni-P-Mo	1000	200	9.3	3.4
Ni-Sn-Li	1000	180	18	6.94
Ni-Sn-Li	400	160	18	2.6
Ni-Li-Mo	1200	200	10	5.8
Rh	1000	175	8.5	1.53
Rh	400	175	7.5	1.17

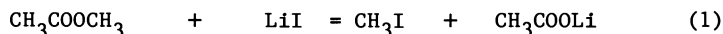
Catalyst (M):  $\text{NiI}_2(0.08-0.1)$ ,  $\text{LiI}(0.8)$ ,  $\text{Mo(CO)}_6(0.18)$ ,  $\text{P(Bu)}_3(0.4)$

In the case of phosphine, especially tri-n-butyl and triphenyl phosphines, an active phosphine complex is formed in the reaction medium via reaction with nickel carbonyl. This complex is a very active species provided that the optimum concentration of phosphine is used. Low phosphine concentration results in a loss of the effective nickel concentration through the formation of nickel tetracarbonyl, nickel metal or nickel iodide. The absolute concentration of phosphine is less important than the P/Ni ratio. In addition to form the stable Ni-P catalyst, the phosphine has to compete with other ligands in the reaction mixture for nickel. With high carbon monoxide partial pressure, there is more CO in solution to compete with phosphine favoring the formation of the carbonyl, which is inactive under the reaction conditions. Hence with high carbon mon-

oxide partial pressure, a high concentration of phosphine is needed to maintain catalyst activity. The dependence of the reaction rate on the balance between phosphine concentration and carbon monoxide partial pressure was demonstrated in a series of experiments. For experiments made under 1000 psig and with CO partial pressure of 550 psi, the reaction rate increased with higher P/Ni ratio, up to a ratio of 4/1. Thereafter, the effect of higher P concentration on reaction rate was nil (Figure 1). With increasing carbon monoxide partial pressure to 750 psi, total pressure was 1200 psig, the reaction rate increased linearly with higher P/Ni ratios up to a ratio of 8/1. At this point, the phosphine concentration was presumably high enough to overcome the higher carbon monoxide concentration. With higher CO partial pressure, the optimum P/Ni ratio was larger than 9/1. For each of the three different CO partial pressures used the reaction rate was independent of the phosphine concentration after the optimum P/Ni was achieved. Within the reaction parameters used the optimum reaction rates were all in the range  $1.3-1.6 \times 10^{-3}$  (mol/l.sec).

The effect of tin compounds, especially tetra-alkyl and tetra-aryl tin compounds, is similar to that of phosphine, though lower temperature and pressure are required for the catalyst's optimum activity. Tin can promote the activity of the nickel catalyst to a level that matches that of rhodium under mild conditions of system pressure and temperature e.g. 400 psig at 160°C. The tin-nickel complex is less stable than the phosphine containing catalyst. In the absence of carbon monoxide and at high temperature, as in carbonylation effluent processing, the tin catalyst did not demonstrate the high stability of the phosphine complex. As in the case of phosphine, addition of tin in amounts larger than required to maintain catalyst stability has no effect on reaction activity.

Lithium salts as well as those of other alkali metals can stabilize nickel complex anions as well as promote the consumption of any formed methylacetate.



This is in contrast with the rhodium system where alkali metal salts were reported to have no effect on methanol carbonylation (19). In spite of the promotion effect of lithium the nickel catalyst is not maintained in a soluble stable complex form. Precipitation of nickel iodide is common when one of the alkali metals is the only catalyst promoter.

### Promoters Synergism

Several combinations of promoters showed particular advantageous results. For example, addition of small amounts of group VI-B elements to tin, lithium or phosphine promoted reactions sharply increase the catalyst activity (Table III). Only the metals or the carbonyls are active for this function. It is presumed that part of the function of these elements is to assist in the reduction part of the catalyst cycle especially in the initial phase of the reaction.

Table III. Effect of Group VIB Metals on Reaction Rate

Promoter	Temp. °C	Press. psig	Rate x 10 <sup>3</sup> <u>mol</u> 1.sec
P	200	1000	2.5
P + Mo	200	1000	3.75
P + W	200	1000	2.8
Sn	180	1200	0.29
Sn + Cr	180	1200	1.9
Cs + Mo	200	1200	0.9
K + Mo	200	1200	1.0
Li + Cr	200	1200	2.8
Li + Mo	200	1200	3.1
Li + Mo	200	1200	5.8
Li	200	1200	2.2

Catalyst (M): NiI<sub>2</sub>(0.07), (Ph<sub>3</sub>)P (0.3), (Ph)<sub>4</sub>Sn (0.26), alkali metal iodides (1.3), Mo(CO)<sub>6</sub>(0.15), Cr(CO)<sub>6</sub> (0.15), W(CC)<sub>6</sub> (0.15).

Combining an alkali metal salt with a nickel complex, e.g. Ni-P carbonyl complex, increases the catalyst activity of the system. Presumably the alkali metal stabilizes a complex anion species. However, promoters which have similar promoting functions showed no sharp synergistic effect when added together e.g. phosphine and tin compounds. Promoters synergism was most pronounced in combining lithium with tin promoters which made it possible to obtain a reaction rate as high as  $7 \times 10^{-3}$  (mol/l.sec) at 1000 psig (Table IV) and  $2.6 \times 10^{-3}$  (mol/l.sec) at 160°C and 400 psig (Table VI) (twice as fast as the rate of the Rh system). Similarly, combining the phosphine with lithium gave enhanced reaction rates (Table IV). From the process point of view, the use of phosphine is preferred for practical efficient processing and catalyst stability.

Table IV. Promoters Synergism

Catalyst Promoters (M)			Reaction Rate x 10 <sup>3</sup> <u>mol</u> 1.sec
Li	Sn	P	
-	0.2	-	1.22
0.8	-	-	1.78
0.8	0.2	-	6.9
-	-	1.2	1.9
-	-	0.6	1.7
0.4	-	0.6	2.22

Solvent: Methyl Acetate, Pressure: 1000 psig, T: 180°C

One particularly interesting case was the addition of 2-hydroxypyridine to the lithium or phosphine promoted catalyst which showed



an abnormal increase in activity. 2-Hydroxypyridine is a resonance hybrid of the pyridine and the inner salt structures; it does not react as a tertiary amine and does not have strong phenolic properties. 2-Hydroxypyridine reacts with methyl iodide to give N-methyl-2-pyridone rather than the ammonium salt. These characteristics may explain the difference in activity between pyridine and 2-hydroxypyridine. This catalytic effect is independent of the pKa of the amines. In an earlier study (20) the nickel-catalyzed carbonylation of methyl acetate was effectively promoted with 2-hydroxypyridine or 8-hydroxyquinoline, and not by pyridine or quinoline. Since the pKa values of these compounds are 0.75, 5.02, 5.18, and 4.9 respectively; the catalytic activity is not related to their basic character but to their unique structure.

#### Effect of methanol concentration

With no solvent used the reaction proceeds rather slowly until the concentration of methanol is lower than 60% of the reaction mixture. In this case the competing reaction of methanol dehydration, especially at temperatures higher than 180°C, can predominate resulting in the formation of dimethyl ether which has a very high vapor pressure. At constant system pressure, dimethyl ether vapor will replace consumed carbon monoxide and reduce carbon monoxide partial pressure leading to further reaction retardation. For methanol concentration between 60 and 40%, the reaction rate is inversely proportional to the methanol concentration. The reaction is zero order in methanol for all concentrations below 40% until all the methanol is consumed. The retarding effect of high methanol concentration was very similar in either methyl acetate or acetic acid solvents (Figure 2). Rhodium catalyzed carbonylation is also retarded when methanol is present in high concentration (21). Similar deactivation is also reported for ethanol and isopropanol carbonylation (22, 23). One possible explanation for the reduced rate in the absence of other solvents is the formation of a stable nickel methoxy species. Also, the decrease in reaction rate is presumably related to the dielectric constants of the solvents as compared with that of methanol. The dielectric constants of acetic acid, methyl acetate and methyl iodide are all between 6.0 and 7.0 at 25°C, while that of methanol is 32.6. However, this does not explain why the addition of phosphoric acid to methanol brings the activity of the rhodium system up to a par with reactions in acetic acid solvent. By contrast addition of phosphoric acid to methanol does not affect the low activity of the nickel system in the absence of solvents.

#### Catalyst Concentration

The rate of reaction is directly proportional to nickel concentration (Figure 3). In order to define the effect of nickel concentration on the reaction rate, one should provide to the reaction mixture the optimum level of the complexing agent, e.g. phosphine, and the optimum carbon monoxide partial pressure.

The reaction rate is also directly proportional to the concentration of iodide (Figure 4). However, it is undesirable to maintain high concentrations of iodine because of its high molecular weight. With optimization of the other reaction parameters, the concen-

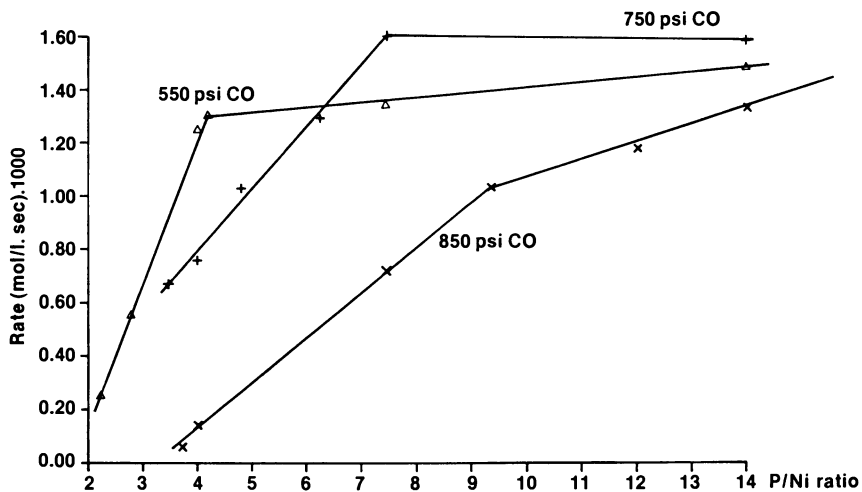


Figure 1. Effect of P/Ni ratio on reaction rate. Catalyst:  $\text{NiI}_2$ ,  $\text{Ph}_3\text{P}$ ,  $\text{Mo}(\text{CO})_6$ ,  $T=200^\circ\text{C}$ , solvent AcOH

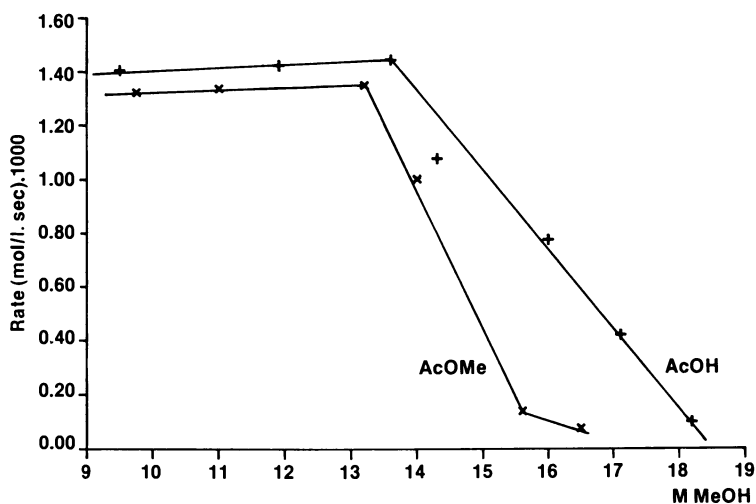


Figure 2. Effect of Methanol concentration on reaction rate. Catalyst:  $\text{NiI}_2$ ,  $\text{Bu}_3\text{P}$ ,  $\text{LiI}$ . Pressure: 1000 psig.  $T=180^\circ$ . Solvents: AcOH and AcOMe as indicated.

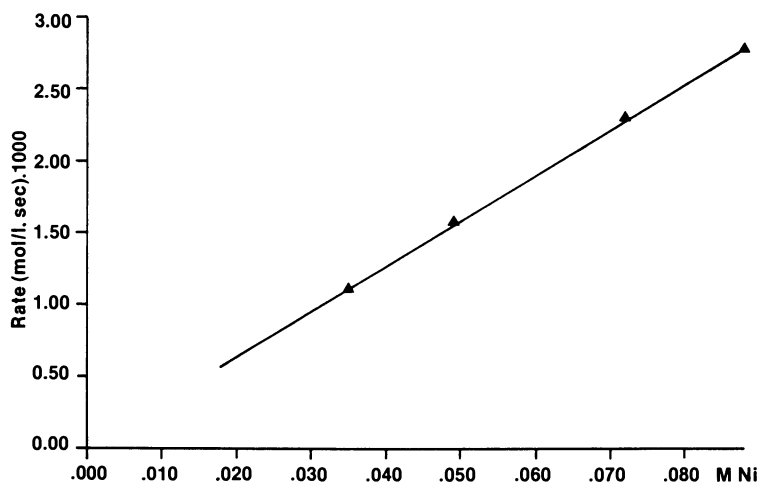


Figure 3. Effect of Ni concentration on reaction rate. Catalyst:  $\text{NiI}_2$ ,  $\text{Bu}_3\text{P}$ ,  $\text{Mo}(\text{CO})_6$ . Pressure: 1000 psig.  $T=200^\circ\text{C}$ . Solvent: AcOH

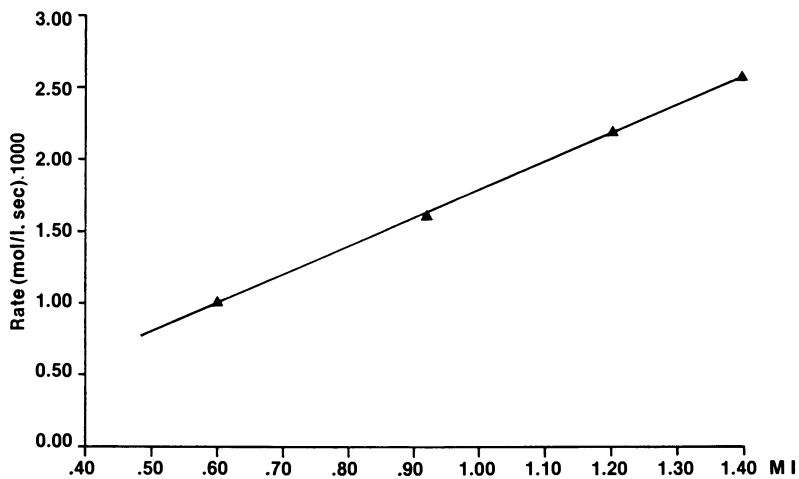


Figure 4. Effect of I concentration on reaction rate. Catalyst:  $\text{NiI}_2$ ,  $\text{LiI}$ ,  $\text{Mo}(\text{CO})_6$ . Pressure: 1000 psig.  $T: 180^\circ\text{C}$ , Solvent: AcOH

tration of I was reduced to 10 wt% and an efficient reaction was still obtained. This includes all the forms of iodine in the reaction mixture. The activity is the same for reaction mixtures containing ionic, covalent or mixed iodide. This is in contrast with the rhodium carbonylation system where alkali metal iodides are inactive (19).

#### Carbon Monoxide Partial Pressure

The activity of the nickel catalyst is affected by major variations in carbon monoxide partial pressure. With very low carbon monoxide partial pressure, nickel precipitates as a metal powder and occasionally as nickel iodide. Stability of the catalyst is improved with higher CO partial pressure up to a point above which the catalyst activity drops linearly. The optimum level of carbon monoxide is different from one catalyst mixture to another. This behavior is characteristic of all the nickel catalyzed carbonylation reactions we studied. In the Li-P system, optimum carbon monoxide partial pressure is in the range of 700 to 800 psi (Table V). On the other hand, the optimum carbon monoxide partial pressure for the Li-Sn system is in the range of 220 to 250 psi, at 160°C, and 450 psi at 180°C (Table VI). It is presumed that the retarding effect of higher carbon monoxide partial pressure is associated with stabilizing an inactive carbonyl species.

Table V. Effect of CO Partial Pressure

Press. psig	CO Partial Pressure psi	Rate x 10 <sup>3</sup> <u>mol</u> l.sec
800	450	1.2
1000	650	1.7
1400	850	2.4
1200	900	1.6
1400	1100	1.2
1600	1200	0.75
1800	1400	0.33
1800	1500	0.04

Catalyst (M): NiI<sub>2</sub>(0.08), LiI(0.26), (Bu)<sub>3</sub>P(0.4), [I]=(1.4)  
Solvent: Acetic acid, T: 200°C

#### Effect of Hydrogen:

In anhydrous mixtures, the rhodium catalyzed carbonylation is enhanced by the presence of hydrogen. Introduction of hydrogen to a rhodium catalyzed carbonylation of methyl acetate increases the reaction rate and maintains catalyst stability (26) when the hydrogen partial pressure is rather low. It leads to reduced products formation, e.g. acetaldehyde and ethylidene diacetate, with higher hydrogen partial pressure, in excess of 50 psi (27, 28). This is a clear indication that hydrogen is added to the coordination sphere of the rhodium catalyst. However, in the case of methanol carbonylation, the presence of hydrogen does not enhance the reaction rate or lead

to reduced products. Not even a trace of acetaldehyde was formed when hydrogen was present in a rhodium catalyzed methanol carbonylation (24, 25).

Table VI. Effect of CO Partial Pressure

Temp. °C	System Press. psig	CO Partial Pressure psi	Rate x 10 <sup>3</sup> <u>mol</u> l.sec
160	400	220	2.6
160	600	250	2.7
160	600	450	1.8
160	1000	500	1.6
160	1000	700	0.64
180	1450	1250	1.7
180	1000	800	3.4
180	1000(H <sub>2</sub> )	450	6.9

Catalyst (M): NiI (0.08), LiI(0.78), Ph<sub>4</sub>Sn(0.26), [I]=(1.4)  
Solvent: Methyl Acetate

Unlike rhodium, the activity of the nickel catalyst is greatly enhanced if hydrogen is present. This is true for both methanol and methyl acetate carbonylation. The presence of hydrogen enhances the reaction rate by 50 to 400% depending on catalyst promoters and reaction parameters (Tables VII, VIII). With a 50/50 syn-gas mixture, a reaction rate of  $4.2 \times 10^{-3}$  (mol/l.sec) was obtained at 180°C and 1000 psig, using the Ni-P-Mo catalyst mixture, with no reduced products formed. Syngas or carbon monoxide contaminated with large amounts of hydrogen are cheaper than pure carbon monoxide. It is presumed that hydrogen promotes the reduction step of the catalyst cycle particularly in the initial stage of the reaction.

Table VII. Effect of Hydrogen on Reaction Rate

P psig	T °C	H <sub>2</sub> Partial Pressure psi	Rate x 10 <sup>3</sup> <u>mol</u> l.sec
400	160	65	2.3
400	160	0	2.6
600	160	200	2.75
600	160	0	1.8
1000	180	450	6.9
1000	180	0	3.4

Catalyst (M): NiI<sub>2</sub>(0.08), LiI(0.78), Ph<sub>4</sub>Sn(0.26), [I]=(1.4)  
Solvent: Methyl Acetate

Within the reaction parameters used, the nickel catalyst is highly selective towards carbonylation. With the exception of trace amounts of methane formed, no other hydrogenation product is found. This is in contrast with cobalt whose carbonylation catalytic activity is enhanced by hydrogen but generally associated with aldehyde formation and homologation.

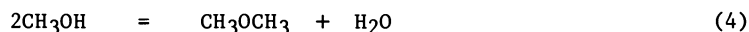
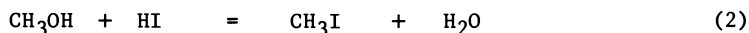
Table VIII. Effect of Hydrogen on Reaction Rate

Press. psig	Partial Pressure psi		Rate x 10 <sup>3</sup> $\frac{\text{mol}}{\text{l. sec}}$
	CO	H <sub>2</sub>	
800	300	150	0.9
800	450	-	1.2
1000	550	150	2.7
1000	650	-	1.7
1200	600	350	3.3
1200	700	200	3.33
1400	1100	-	1.1
1400	900	-	2.5
1400	900	200	4.4
1400	800	200	4.7
1400	700	400	4.2
1600	1200	-	0.75
1600	700	600	5.1
1800	1500	-	0.03
1800	1200	400	1.06
1800	1000	900	2.36

Catalyst (M): NiI<sub>2</sub>(0.1), (Bu)<sub>3</sub>P(0.26), [I]=(1.3)  
T=200°C, Solvent: Acetic Acid

#### Effect of Water

Water is indigenous to the methanol carbonylation reaction. It is introduced to the reaction as a part of the solvent, reactants, or catalyst. It can also be formed in situ through steps of the main reaction pathway or via other competing reactions.



Water is essential, since acetic acid is formed by the reaction between water and acetyl iodide or the Ni-acetyl complex. Acetic acid is also formed via the hydrolysis of any methyl acetate that is formed by methanol attack on acetyl iodide or the Ni-acetyl complex. Since these reactions are in equilibrium at any time, the concentration of water in the reaction mixture is a function of the concentrations of the other reactants and products. In the extreme case when water was a major part of the reaction mixture, the catalyst was completely inactive. Even when water was only a part of the solvent (more than 10%), or with methanol as the solvent, the reaction was sluggish.

The retarding effect of water varies from one catalyst system to another. The tin system particularly is highly affected by water (Table IX). At 160°C no activity was observed when water was added to the solvent. The catalyst activity was rather low also when

acetic acid was used as solvent; water was formed via esterification. However, the exceptional high activity of the tin system was obtained with methyl acetate as the main solvent. Methyl acetate here is a dehydrating agent; its saponification consumes most of the free water leaving the optimum concentration of water needed for acetic acid formation.

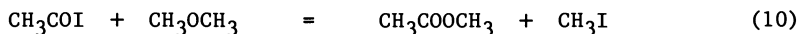
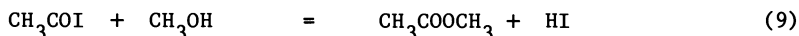
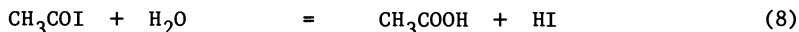
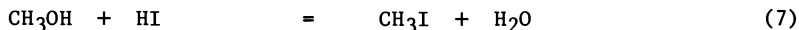
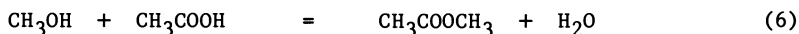
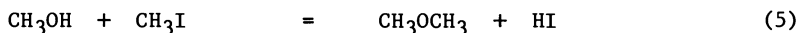
Table IX. Effect of Water on Reaction Rate

Solvent(%)	Press. psig	Temp. °C	Rate x 10 <sup>3</sup> $\frac{\text{mol}}{\text{l. sec}}$
Methanol (100)	400	160	0
Methanol (55) Acetic Acid (45)	400	160	0.04
Methanol(55) Methylacetate (35) Water (10)	400	160	0
Methanol (55) Methylacetate (13) Acetic Acid (32)	400	160	2.5
Methanol (55) Methylacetate (45)	400	160	2.6

Catalyst (M): NiI<sub>2</sub>(0.08), LiI(0.78), Ph<sub>4</sub>Sn(0.26), [I]=1.4

#### Reaction Pathways

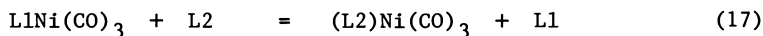
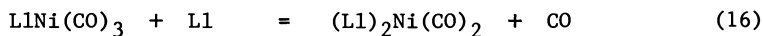
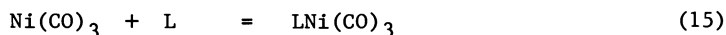
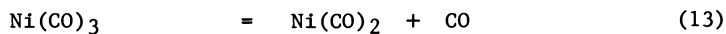
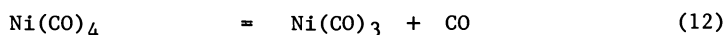
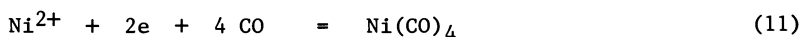
Methanol, acetic acid, reaction intermediates and catalyst components are involved in several pathways that are controlled by complex equilibria:



These reactions are in equilibrium at any time. When the carbonylation reaction's rate is low, side reactions, e.g. ether and ester formation, can predominate. On the other hand a high carbonylation rate results in removing the available methanol from the reaction mixture and sub-

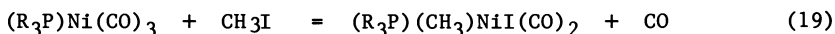
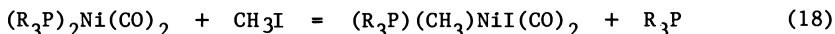
sequent drop in dimethyl ether, methyl acetate and water concentrations. Elimination of water and ether improves the carbonylation rate as discussed earlier.

The active catalyst is presumably formed through reduction of the Ni species, aided by hydrogen or group VIB metals and their carbonyls, to the nickel carbonyl. Nickel carbonyl is converted to the active catalyst by ligand dissociation. The exact nickel species is the result of complex equilibria, equations 11-17. The zero valent complex adds methyl iodide, after CO dissociation. This is believed to be the rate-determining step and has first order kinetics with respect to both iodide and Ni. It was found that temperature greater than 100°C is needed for the oxidative addition (29).



The formation of the active catalyst can be retarded with high carbon monoxide partial pressure. High CO partial pressure leads to more CO in solution which competes with the ligand over the tricarbonyl species,  $\text{Ni}(\text{CO})_3$ , and forms the inactive nickel tetracarbonyl. The active complex stability was retained by increasing the promoter concentration. The complex formed between nickel and promoters is more stable than  $\text{Ni}(\text{CO})_4$ . In addition, promoters may impart higher electron density to the central atom and increase its nucleophilic character towards methyl iodide.

In the case of phosphine, the active catalyst is presumably either bisphosphine dicarbonyl or the phosphine tricarbonyl complex. Kinetically the bis-phosphine nickel complex cannot be the predominant species. However, in the presence of very high phosphine concentration it may have an important role in the catalyst cycle. After ligand loss and methyl iodide oxidative addition, both complexes presumably give the same 5 coordinate alkyl species.

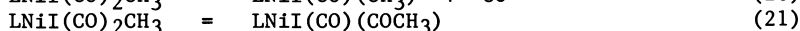
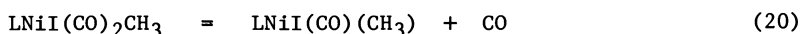


Strengthening of the Ni-C bond by electron charge donation of a trans phosphine ligand in the bisphosphine complex (equation 18) retards the elimination of CO prior to the oxidative step (30, 31). This is not the case for the phosphine nickel tricarbonyl (equation 19) where carbon monoxide is easier to eliminate (32).

Formation of five-coordinate nickel intermediates via oxidative addition of alkyl halides has been reported (33). This type of



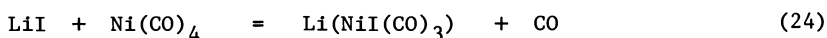
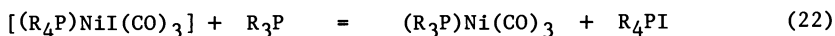
complex is unstable and undergoes either elimination of CO to give four-coordinate square planar alkyl complex or an insertion (alkyl migration) to give four-coordinate acyl complex (equation 20, 21).



The four-coordinate alkyl complex,  $\text{LNiI(CO)CH}_3$ , may coordinate with carbon monoxide to regenerate the five coordinate alkyl species, and this leads to insertion to form Ni-acyl complex. This complex,  $\text{LNiI(CO)(COCH}_3)$ , can be cleaved either by water yielding acetic acid or by methanol to give methyl acetate. However, in the presence of high iodide concentration formation of acetyl iodide may predominate (29). This step is reversible and can lead to decarbonylation under low carbon monoxide partial pressure. Similar decarbonylations of acyl halides by nickel complexes are known (34).

Acetyl iodide is very reactive and it reacts efficiently with water or methanol leading to acetate compounds. Hydrolysis of acetyl iodide along with the subsequent conversion of methanol to methyl iodide are very rapid under the reaction conditions leading to a complete mechanistic cycle.

The phosphine in the reaction mixture is partially in the form of the quaternary salt. In highly polar solvents, e.g. water and methanol, the salt formation can predominate leading to total loss of electron-donating phosphine and to catalyst deactivation. In protic solvents the iodide may form a stable iodotricarbonyl nickel complex,  $(\text{PR}_4)\text{NiI(CO)}_3$ . This type of complex is more stable than nickel carbonyl. The salt reacts irreversibly with free phosphine giving the tricarbonyl phosphine complex (35). The proposed formation of iodotricarbonyl nickel complex is consistent with the catalytic activity of alkali metal salts, alone or in addition to other promoters.



Triphenylstannide anion is isoelectronic with triphenyl antimony. Both form nickel carbonyl complexes (36). The lithium salt of triphenylstannide, which can readily be formed from tetraphenyltin and lithium salts, reacts violently with nickel carbonyl to give the presumably efficient catalyst  $\text{Li(Ni(CO)}_3\text{Sn(Ph)}_3)$ . This complex possibly catalyzes the carbonylation of methyl iodide in a manner similar to that of the phosphine complex.

### Economics

The Ni-catalyzed methanol carbonylation has the following advantages:

1. High reaction rate which allows a smaller reactor
2. Low water level in the reaction medium which simplifies the separation train especially for the HI-H<sub>2</sub>O-AcOH mixture
3. The high reaction rate with low water levels is associated with a highly exothermic reaction pattern. The reactor is actually, in part, an energy source for the rest of the plant

4. The reaction effluent of the rhodium process is subjected to flash distillation under mild conditions in order to maintain the activity of the sensitive catalyst and to contain the costly metal in a limited section of the plant. The effluent of the nickel process is subjected directly to distillation of the products with considerable savings.
5. Complete conversion of methanol is achieved. Acetic acid concentration can reach up to 70 wt% in the effluent, i.e. more product is made per pass
6. 96% of the world reserves of rhodium are in the USSR and South Africa. At \$10,000/lb, it is essential to have an elaborate reclamation section to recover rhodium from the heavies purge. Nickel at \$3.30/lb does not require this step.

Several economic evaluations of the nickel process as compared with the rhodium process, made by Halcon and by independent consultants, agreed that there is savings of about 1¢/lb of acetic acid in favor of the nickel process. The difference is derived essentially from utility savings due to the higher reaction rate, simplified separation and lower water concentration. The nickel process consumes less than half the energy needed for the rhodium-catalyzed process. The catalyst inventory, and the equipment needed for its recovery contribute to the higher cost of production in the rhodium case.

#### General experimental procedure

Charged to a one liter Hastelloy-C autoclave (Autoclave Engineer), provided with a magnet-drive stirrer, a mixture of methanol (5.4 mole), methylacetate (3.5 mole), methyl iodide (350 mmole), nickel iodide (40 mmole), lithium iodide (380 mmole) and tetraphenyl tin (130 mmole). The autoclave was sealed, flushed 3 times with carbon monoxide and then charged with carbon monoxide up to 300 psig. The reactor was heated up with steam until the stirred mixture was 180°C. The heating period was 10 minutes. The pressure of the reactor at that point of time was 400 psig. An additional charge of carbon monoxide was added to bring the reactor to the desired pressure of 600 psig. This was considered as the zero point of time. The pressure was maintained at this level through the entire reaction duration by feeding carbon monoxide through a "Brook" mass flow meter. The progress of reaction and reaction rate were determined by monitoring the flow rate of gas through the mass flow meter and by withdrawing liquid samples periodically from the reaction mixture. The samples were quenched in cold water bath and analyzed immediately using a Varian 3700 gas chromatograph.

#### Literature Cited

1. Othmer, D.F. (Tenn. Eastman Corp.), U.S. Patent 2 050 234, U.S. Patent 2 227 979.
2. Nieuwland, J.A., "The Chemistry of Acetylene", Amer. Chem. Soc. Monograph No 99; reinhold, 1945, 115.
3. Smidt, J., Angew. Chem., 71, 1959, 176.
4. Faith, W.L.; Keyes, D.B., Ind. and Eng. Chem., 1931, 23, 1250
5. Bludworth, J. (Celanese), U.S. Patent 2 369 710.

6. Reppe, W. (I.G. Fabenindustrie), German Patent 705 273.
7. Sieber, R.H.; Miller, S.A.; "Ethylene and its industrial derivatives", Ernest Benn, 1969, 668.
8. Blutworth, J. (Eastman Kodak), U.S. Patent 2 287 803.
9. Saunby (Union Carbide), German Patent 2 311 224.
10. Weymouth, F.J.; Millidge, A.F., Chem. Ind., 1966, 887.
11. Reppe, J.W., "Acetylene Chemistry", Charles A. Meyer (1949), 171.
12. Reppe, J.W., et al. (BASF), U.S. Patent 2 729 651.
13. Reppe, J.W., et al. (BASF), U.S. Patent 3 014 962.
14. Thomas, E.B., et al. (British Celanese), U.S. Patent 2 650 245
15. Leach, H.S., et al. (Monsanto) U.S. Patent 4 007 130.
16. Faunin, L.W., et al. (Monsanto) U.S. Patent 3 887 489.
17. Rizkalla, N., Naglieri, A., (Halcon International), U.S. Patent 4 134 912.
18. Rizkalla, N., Naglieri, A., (Halcon International), U.S. Patent 4 356 320
19. Forster, D., J. Mol. Catal. 1982, 17, 299.
20. Rizkalla, N., Naglieri, A., (Halcon International) U.S. Patent 4 002 678
21. Matsumoto, T., et al., Bul. Chem. Soc., Jp. (1977), 50, 2337.
22. Hjortkjaer, J., et al., J. Mol. Catal. (1978), 4, 199.
23. Hjortkjaer, J., et al., J. C. S. Perkin II, (1978), 763.
24. Roth, J., Craddock, J., Hershman, A., Paulik, F., Chem. Tech., 1971, 600.
25. Roth, J., et al, (Monsanto), U.S. Patent 3 769 329.
26. Rizkalla, N., (Halcon International), U.S. Patent 4 115 444.
27. Porcelli, R., (Halcon Research & Development), U.S. Patent 4 302 611.
28. Rizkalla, N., Winnick, C., (Halcon International), Ger. Offen, 2 610 035.
29. Chiusoli, G., Cassar, L., Angew. Chem. Int. Ed., 1967, 6, 124.
30. Basdo, F.; Wojciki, A., J. Amer. Chem. Soc., 83, 1961, 520.
31. Meriwether, L.S.; Fiene M.L., J. Am. Chem. Soc., 81, 1959, 4200.
32. Jolly, P.W.; Wilke, G., "The Organic Chemistry of Nickel", Academic Press, 1974, 63.
33. Otsuka, S., Nakamura, A., Yoshida, Y., J. Am. Chem. Soc., 1969, 91, 7196.
34. Ashley-Smith, J., Green, M., J.C.S. A, 1969, 3019.
35. Casser, L., Foa, M., Inorg. Nucl. Chem. Lett., 1976, 6, 291.
36. Kruck, Th., Herker, B., Angew Chem. Int. Ed., 1969, 8, 679.

RECEIVED August 14, 1986

## Chapter 6

# Oxidative Carbonylation

## A New Synthesis Gas Route to Adipic and Sebacic Acids

H. S. Kesling, Jr.

ARCO Chemical Company, Division of Atlantic Richfield Company,  
3801 West Chester Pike, Newtown Square, PA 19073

Adipic and sebacic acid are prepared from butadiene and the elements of synthesis gas using palladium catalyzed oxidative carbonylation technology. Dicarboxylation to give dimethyl hex-3-enedioate adipic acid precursor is promoted by high carbon monoxide pressure (1800 psig) and chloride as the palladium counter-ion. Monocarbonylation to give methyl 2,4-pentadienoate, which is the precursor to pelargonic and sebacic acid, is promoted by low carbon monoxide pressure (<1000 psig) and use of a Lewis Acid co-catalyst with iodide as the palladium counter-ion. Dimethyl hex-3-enedioate hydrogenation and subsequent hydrolysis yields adipic acid. Methyl 2,4-pentadienoate reacts with butadiene to give an unsaturated pelargonic acid precursor or can undergo palladium catalyzed dimerization to yield an unsaturated sebacic acid precursor. Hydrogenation and hydrolysis affords commercially attractive routes to pelargonic or sebacic acids. In the oxidative carbonylation reaction a dehydration agent, which can give controlled methanol release and remove water formed during catalytic reoxidation, is necessary for high product yield. Palladium/copper redox catalyst recovery and recycle are also critical for viable commercial technology.

In an era of decreasing oil reserves, new technology development to synthesize large volume oxygenated chemicals from readily available synthesis gas and methanol is a research area of increasing intensity. Current research interest is primarily focused on small molecules. Larger molecules with high volume potential have received little attention(51). Two representative

larger molecules, which potentially can be prepared from syngas and methanol, are adipic and sebacic acid. Both are commercially important aliphatic dicarboxylic acids and serve as basic raw materials for poly(amide) engineering resins, plasticizers, lubricants, poly(urethanes), and poly(esters). In 1985, adipic acid had a 2 billion pound per year market in the United States.

Adipic acid is prepared commercially by oxidative processes using either benzene or phenol as the raw material base. Since both benzene and phenol prices track with the price of crude oil, future adipic acid price will increase as the oil reserve decreases(1). Thus, there is a need for a new process to produce adipic acid from cheap, and readily available, raw materials such as butadiene, synthesis gas, and methanol.

Conventional technology for sebacic acid manufacture involves caustic soda decomposition of ricinoleic acid at high temperature(2). Principal co-products include 2-octanol and glycerine. Castor oil, which is the natural source for ricinoleic acid, is subject to price fluctuation due to cyclic crop production and protectionist policies by foreign governments. Castor oil technology is also at disadvantage because the overall product yield is low (<80%) and co-product 2-octanol must compete with cheap 2-ethyl hexanol in plasticizer applications. These and other factors have resulted in a significant decline in the United States sebacic acid market from about 30MM lbs. per year in the 70's to less than 5MM lbs. in the 80's. Again, there is a clear need for a new process to produce sebacic acid from cheap and readily available chemicals.

### Adipic Acid

One process that capitalizes on butadiene, synthesis gas, and methanol as raw materials is BASF's two-step hydrocarbonylation route to adipic acid(3-7). The butadiene in the C<sub>4</sub> cut from an olefin plant steam cracker is transformed by a two-stage carbonylation with carbon monoxide and methanol into adipic acid dimethyl ester. Hydrolysis converts the diester into adipic acid. BASF is now engineering a 130 million pound per year commercial plant based on this technology(8,9). Technology drawbacks include a requirement for severe pressure (>4500 psig) in the first cobalt catalyzed carbonylation step and dimethyl adipate separation from branched diester isomers formed in the second carbonylation step.

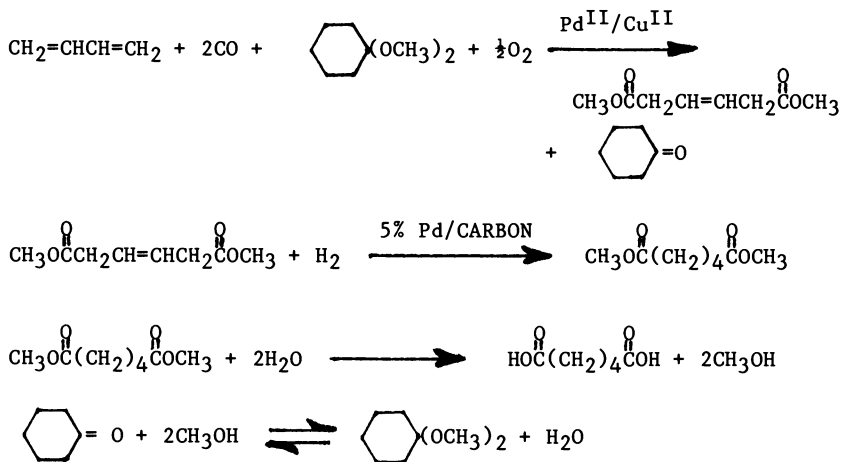
Although butadiene hydrocarbonylation chemistry has been extensively researched, little or no prior art exists on adipic acid precursor preparation using oxidative carbonylation technology. Fenton at Union Oil is well known for his olefin oxidative carbonylation(10,11) work, but he did not apply this technology to oxidative carbonylation of conjugated diolefins such as 1,3-butadiene. This is surprising since Fenton has a patent on adipic acid preparation *via* butadiene hydrocarbonylation(12). The only known prior art is a Japanese Kokai(13) which describes the preparation of unsaturated carboxylic acid esters by reacting a conjugated diene, carbon monoxide, excess methanol, and molecular oxygen in the presence of a Group 8 noble metal catalyst. The

primary product from butadiene was methyl 4-methoxypent-2-enoate with only a trace of the desired dicarbonylation adipic acid precursor.

After ARCO patents issued, Stille and coworkers published on butadiene oxycarbonylation(14-16). Palladium was utilized as the oxidative carbonylation catalyst and copper(II) chloride was employed as a stoichiometric reoxidation agent for palladium. Although the desired hex-3-enedioate is the exclusive product, commercial technology which uses stoichiometric copper is not practical. Once the copper(II) is consumed, the monoatomic palladium spent catalyst agglomerates affording polymeric palladium which is not easily reoxidized to an active form.

Recently, Monsanto has developed a carbonylation route(50) to prepare adipic acid from butenes. The process is based on dicarbonylation of 1,4-dimethoxy-2-butene with a palladium catalyst containing chloride ligands. This approach could achieve commercial potential if an economically viable 1,4-disubstituted 2-butene synthesis can be developed. A direct butene carbonylation route to adipic acid is a desirable research target.

The adipic acid process we have developed involves butadiene oxidative carbonylation in the presence of methanol, a 1,1-dimethoxycyclohexane dehydration agent, and a palladium(II)/copper(II) redox catalyst system (Equation 1.). The reaction sequence includes an oxycarbonylation, hydrogenation and hydrolysis step(17-19). The net result is utilization of butadiene, the elements of synthesis gas, 1,1-dimethoxycyclohexane and air to give adipic acid, cyclohexanone and methanol. Recovered methanol and cyclohexanone are used to regenerate the 1,1-dimethoxycyclohexane dehydration agent.



(1)

The main raw materials for the ARCO adipic acid process are butadiene, carbon monoxide and hydrogen. Process economics will be attractive in the next decade provided scenarios regarding the price of butadiene versus benzene come to fruition. Table I. shows raw material cost for the ARCO adipic acid process versus conventional oxidation technology. For the time frame of this evaluation, the

Table I. Comparative Adipic Acid Raw Materials

Raw Materials- ¢/Lb	300 MM Lbs/Yr - 1990's Operation	
	Cyclohexane Oxidation	Butadiene Oxycarbonylation
Butadiene	50.0	22.6
Carbon Monoxide	21.7	11.1
Oxygen	2.6	0.4
Methanol	26	1.0
Hydrogen	125	2.0
Cyclohexane	70.4	---
Nitric Acid	13.2	14.5
Pd (\$/Ounce)	375	---
Other	5.3	2.6
<u>By-Product Credit</u>	---	<u>(6.0)</u>
<u>Total Raw Materials</u>	<u>70.5</u>	<u>36.4</u>

carbon monoxide and hydrogen are derived from natural gas. Butadiene from a world scale olefin plant at 50¢ per pound is also derived from natural gas. Cyclohexane is assumed to be derived from \$4.17 per gallon benzene and is priced at 70.4¢ per pound. This significant difference in projected feedstock price is key to a large raw material economic advantage for butadiene oxycarbonylation technology. Recent softening of worldwide oil prices has resulted in \$0.85 per gallon benzene and \$0.26 per pound butadiene. Butadiene oxycarbonylation economics based on these feedstock prices are less attractive. It may be well into the year 2000 before decreased oil reserves make a synthesis gas route to adipic acid economically attractive.

From a chemistry standpoint a dehydration agent, which can give controlled alcohol release and remove water formed during catalytic reoxidation of palladium(0), to palladium(II), is key in obtaining a high product yield. After one hour at 100°C, 1800 psig total carbon monoxide/air pressure and 1500 ppm palladium catalyst concentration, conversion based on butadiene is 30 mole %. Selectivity to linear unsaturated diester carbonylation product is 79 mole %. About 10 mole % methyl 2,4-pentadienoate is formed along with 11% various other by-products (Table II.).

The speculative mechanism(20-21) as outlined in Equation 2 involves initial reaction between palladium(II) and butadiene to form a  $\pi$ -complex 2 followed by a nucleophilic reaction with carbon monoxide and methanol to give 3.

Table II. Butadiene Oxycarbonylation  
Dicarbonylation Product Distribution

---

<u>Reaction Conditions</u>	
o Redox Catalyst Couple	Copper(II)/Palladium(II)
o Catalyst Ratio (Molar)	2.3
o Palladium Concentration (ppm)	1500
o Temperature (°C)	100
o Pressure (psig)	1800
o Residence Time (hours)	1
o Dehydration Agent	<u>1,1</u> Dimethoxycyclohexane
o Solvent (weight %)	Sulfolane (10)

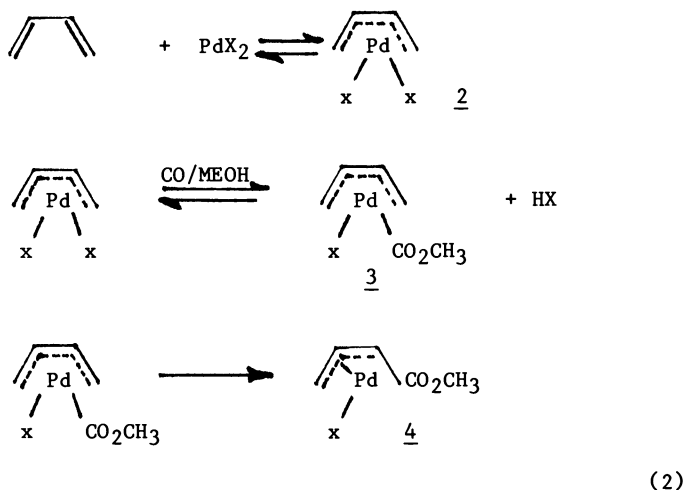
  

<u>Product Distribution</u> - CSTR result after 12 catalyst recycle passes.	
o <u>Conversion</u> (on butadiene; mole %)	30
o <u>Selectivity</u> (on butadiene; mole %)	
Adipic Acid Precursor	79
Diene Ester	10
Pelargonic Acid Precursors	5
Sebacic Acid Precursors	4
Others	2
o <u>Selectivity</u> (on carbon monoxide; mole %)	
Adipic Acid Precursor	82
Other Carbonylation Products	11
Carbon Dioxide	4
Dimethyl Oxalate	3
o <u>Dehydration Agent Loss</u> (mole %; per pass)	0.5

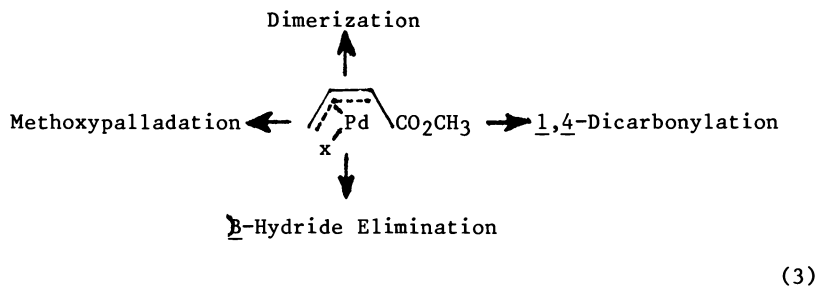
---



The  $\eta^2$ -diene carbomethoxy-palladium complex 2 then undergoes rearrangement to give  $\eta^1$ -allyl carbomethoxy-palladium complex 3.



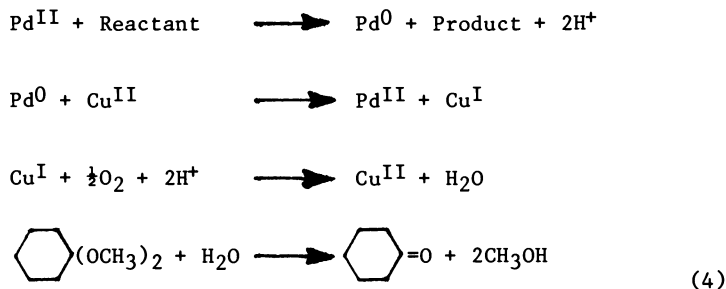
$\eta^1$ -allyl carbomethoxy palladium complex 4 is the key reaction intermediate and can be used to explain the formation of all the observed products. (Equation 3.)



Carbon monoxide insertion into the carbon-palladium bond of 4, followed by nucleophilic displacement with methoxide, gives a 4:1 mixture of trans and cis-dimethyl hex-3-endoate which is the desired 1,4-dicarbonylation precursor to adipic acid.

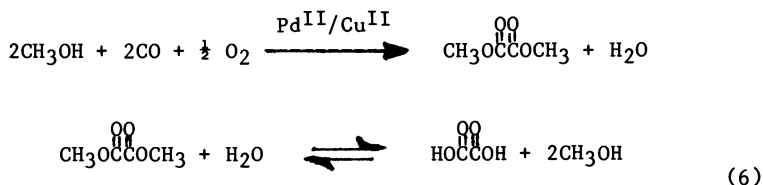
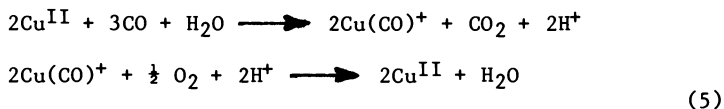
$\beta$ -palladium hydride elimination from 4 gives rise to trans and cis-methyl penta-2,4-dienoate which is a monocarbonylation by-product. Nucleophilic attack by methoxide on the palladium carbon bond on 4 gives non-selective methoxypalladation. Formation of trans and cis-4-methoxy pent-2-enoate can be controlled by using a dehydration agent capable of controlled

alcohol release. Excess methanol gives high selectivity to this by-product and, therefore, lower adipic acid precursor selectivity. Finally, the  $\pi$ -allyl carbomethoxy palladium complex 4 can react with either butadiene or methyl penta-2,4-dienoate to give unsaturated precursors to pelargonic acid and sebacic acid. In general, the desired 1,4-dicarbonylation reaction is promoted by high pressure (1800 psig) and the use of chloride as the palladium counter-ion.



The chemistry of the palladium(II)/copper(II) redox cycle (Equation 4.) is intimately linked to the dehydration agent chemistry(22). For every catalytic turnover, one equivalent of water is formed. This water reacts with 1,1-dimethoxycyclohexane to give cyclohexanone and two equivalents of methanol. Controlled alcohol release prevents the non-selective methoxypalladation side reaction as well as preventing other side reactions such as oxidation of carbon monoxide (Equation 5.) and hydrolysis of by-product dimethyl oxalate (Equation 6.). Carbon monoxide oxidation to carbon dioxide can be catalyzed by either palladium(II)(23) or by copper(II)(24) and can represent a major side reaction in the absence of the dehydration agent. Another major side-reaction in the absence of the dehydration agent is hydrolysis of dimethyl oxalate formed via non-selective oxycarbonylation of methanol (Equation 6.)(25-26). Oxalic acid formed by hydrolysis will react with the copper to give insoluble copper oxalate. Loss of soluble copper results in the destruction of the catalytic redox cycle. Since monoatomic palladium(0) cannot be reoxidized, it quickly agglomerates to give palladium metal which precipitates out of solution. Without the dehydration agent, catalytic activity is rapidly lost.

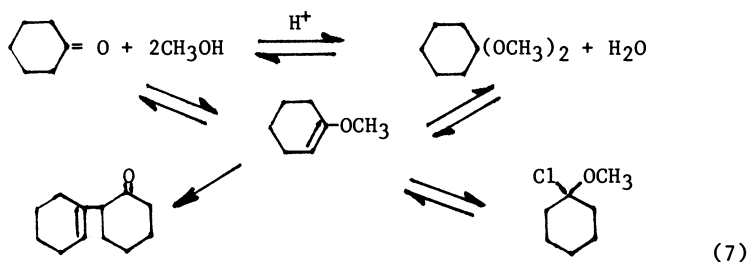
Di- $\mu$ -chloro-di- $\pi$ -(dimethyl hex-3-endoate) di-palladium is the preferred palladium catalyst and was used in the pilot plant studies outlined in Table II. Synthesis is easily accomplished by reaction of dimethyl hex-3-endoate with palladium chloride. In actual butadiene oxycarbonylation runs catalyzed



with palladium chloride or tetrachloropalladate salts, this  $\pi$ -allyl complex was isolated from the reaction products. Advantages over palladium(II) chloride include high initial catalyst solubility and a significant reduction in reactor corrosion. The major disadvantage for homogeneous palladium catalysis is ease of catalyst recovery and recycle. To overcome these problems supported palladium catalysts including palladium on silica, alumina, carbon, and graphite were evaluated. Although recent work by Knifton(52) indicate that catalysts of this type function well, our results show that these catalysts leach, thus negating their potential advantages. More recent work at ARCO with a special type of supported palladium catalyst(26) indicated greater potential for operability in oxycarbonylation processes. While these catalysts are being developed, focus is being placed on the homogeneous palladium catalyst system.

An oxidative environment is also an essential element in maintaining catalytic activity. Air is used as the copper(I) reoxidant for safety reasons. Oxygen partial pressure must be held between 2 volume % and 6 volume % during the redox cycle. If the oxygen partial pressure falls below 2 volume %, monoatomic palladium(0) does not reoxidize to palladium(II) at a sufficient rate, and some catalytic activity is lost due to polymeric palladium metal formation. Under typical oxycarbonylation conditions, copper(II) cannot reoxidize polymeric palladium metal. An oxygen partial pressure greater than 6 volume % affords a potentially explosive gas mixture with carbon monoxide. Oxygen partial pressure control within these limits was easily achieved in the oxidative-carbonylation pilot plant reactor.

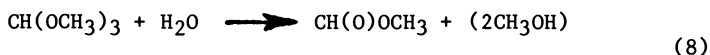
Although many dehydration agents function effectively in butadiene oxycarbonylation, ketals proved to be easily regenerated and recycled. Cyclohexanone was chosen because of its more favorable equilibrium constant during regeneration(27,28) (Equation 7.).



Ketal regeneration proceeds step-wise through an enol ether intermediate. This intermediate is capable of several side reactions including a copper catalyzed aldol condensation, heavies formation and addition reactions with hydrochloric acid. Hydrochloric acid addition to 1-methoxycyclohexene is of no consequence since this side reaction proved to be thermally reversible under oxycarbonylation reaction conditions.

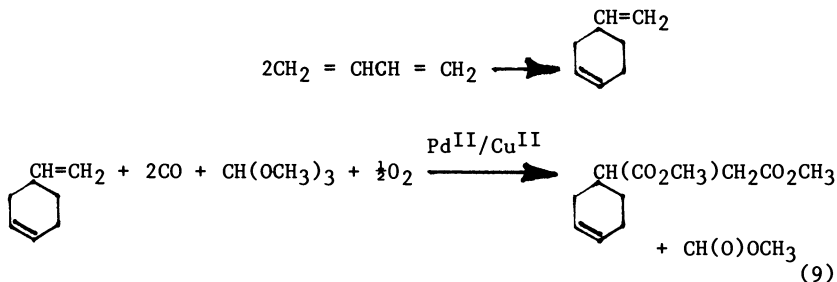
Aldol condensation and subsequent heavies formation are minimized by using a low concentration of the copper reoxidant. It is well known that soluble copper or other transition metals will catalyze Aldol condensation reactions(29). The optimum copper(II)/palladium(II) molar ratio is 2.3. Normally, about 1500 ppm palladium is used in the butadiene oxycarbonylation reaction. Under typical oxycarbonylation process conditions, around .5 mole % 1,1-dimethoxycyclohexane is lost to heavies per pass.

When trimethylorthoformate is utilized as the dehydration agent (Equation 8.), heavies due to Aldol condensation are eliminated. Methyl formate can be easily recovered from the reaction products, but synthetic routes to regenerate trimethylorthoformate are very involved and costly. An advancement to improve trimethylorthoformate synthesis would enhance the attractiveness of the homogeneous oxycarbonylation route to adipic acid.



In the absence of Aldol condensation, the only heavies forming reactions involve a butadiene Diels-Alder reaction to form 4-vinylcyclohexene and subsequent oxidative carbonylation.

Typically, little butadiene is dimerized to 4-vinylcyclohexene under actual reaction conditions(30,31). The butadiene used in the process, however, can contain up to .5 weight % Diels-Alder product, and at this level oxidative carbonylation can become a significant heavies forming reaction (Equation 9.). The major product from this reaction comes from 1,2-dicarbonylation of the 4-vinylcyclohexene exocyclic double bond.



Palladium catalyst stability, recovery and recycle are the key to viable commercial technology. Continuous palladium recovery and recycle at 99.9% efficiency is critical to the economics of the process. Traditional catalyst recovery methods fail since the adipic acid precursor, dimethyl hex-3-enedioate, is high boiling and the palladium catalytic species are thermally unstable above 125°C. Because of this problem, a non-traditional solvent extraction approach to catalyst recovery has been worked out and implemented at the pilot plant scale. Since patents have not issued, process detail on catalyst separation, secondary palladium recovery, and product recovery cannot be included in this review.

Following hydrogenation over palladium on carbon(33), dimethyl adipate hydrolysis to adipic acid is carried out using a strong mineral acid such as sulfuric acid. Hydrolysis is nearly quantitative with a selectivity of 99.5%. Since the adipic acid from the oxycarbonylation process contains no branched by-product acids, as is the case with the commercial oxidation process, extensive recrystallization is not required to produce a polymer grade material. Results indicate that the dried adipic acid crystals contain less than .5 weight % moisture and are 99.95 weight % pure on a dry basis.

Direct use of dimethyl adipate from the oxycarbonylation process to produce nylon 6,6 could be an attractive alternative to current adipic acid/nylon 6,6 technology. Dimethyl adipate condensation with hexamethylene diamine would give methanol rather than water. Reactors, which currently use caprolactam to prepare nylon 6, could also easily be retrofitted to produce nylon 6,6. Dimethyl hex-3-enedioate or dimethyl adipate are also useful raw materials for preparation of other high volume chemicals including hexamethylene diamine, caprolactam, and 1,6-hexanediol.

### Sebacic Acid

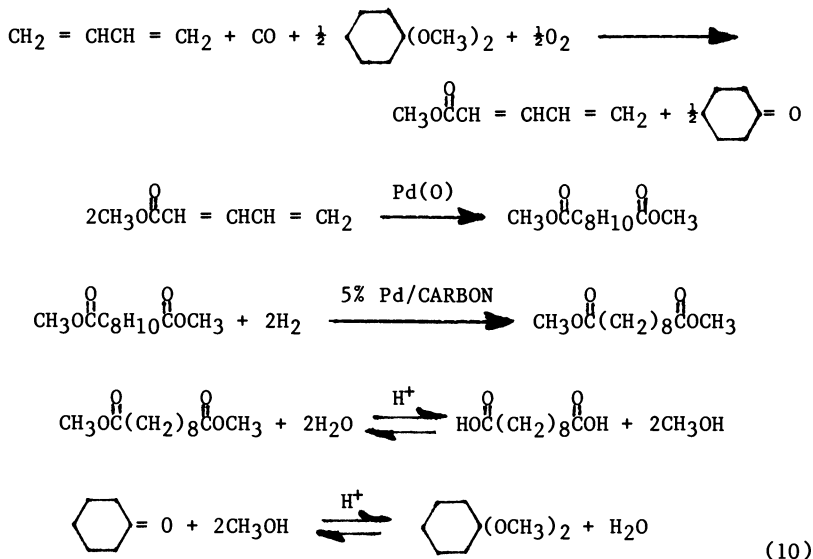
In Japan the need for new technology was answered by the development of an electrolytic route to sebacic acid(33). The Kolbe type electrolytic process developed by Asahi involves dimerization of adipic acid half methyl ester salt to give dimethyl sebacate(34). The dimerization proceeds in 92% yield with 90% selectivity based on the adipate half ester. The main drawbacks of this process are the cost of energy utilized by the electrolytic process and the cost of adipic acid. A Chem Systems report indicates a small advantage for the Asahi electrolytic process with ample room for new technology development(35).

Because 1,3-butadiene is predicted to be an increasingly important petrochemical building block in the 80's, Knifton(36) and others(37,38) have developed a palladium catalyzed dimerization-carbonylation reaction which gives 3,8-nonadienoate acid esters from butadiene in 80 mole % yield with approximately 90% selectivity. Isolation and further carbonylation under OXO conditions using cobalt carbonyl as the catalyst affords an unsaturated sebacic ester precursor which upon hydrogenation and hydrolysis gives sebacic acid. This process is at a disadvantage because the carbonylation with an OXO catalyst gives a significant yield of branched carbonylation isomers which are difficult to separate from sebacic acid.

Sebacic acid is readily available as a co-product from the three step ARCO adipic acid process (See Equation 1.). In this process about 10 mole % methyl 2,4-pentadienoate is formed along with 11% various other by-products. The 11% selectivity to various by-products include primarily unsaturated precursors to pelargonic and sebacic acid. Isolation, hydrogenation, and hydrolysis gives pelargonic and sebacic acid. A world scale adipic acid plant capable of producing 300 MM pounds per year adipic acid would also give 15 MM pounds per year pelargonic acid and 12 MM pounds per year sebacic acid as co-products. This sebacic acid volume would be enough to meet current United States demand and would result in more favorable economics than can be obtained using the castor oil process.

Adipic acid overcapacity, softening worldwide oil prices, and the increased investment necessary to establish a novel chemical process has made implementation of a world scale adipic acid plant based on butadiene oxycarbonylation technology less attractive. An attractive alternative to building a world scale adipic acid plant is to construct a specialty smaller volume oxycarbonylation plant which is capable of exclusively producing the more valuable precursors for pelargonic and sebacic acid. Oxycarbonylation process conditions can be controlled to give methyl 2,4-pentadienoate which is the product from butadiene mono-carbonylation(39,40). Methyl 2,4-pentadienoate can react in a subsequent step with butadiene to give an unsaturated pelargonic acid precursor in high yield(41). Methyl 2,4-pentadienoate

self-dimerization using a zero-valent palladium complex, hydrogenation, and hydrolysis affords a commercially attractive route to sebacic acid(42) (Equation 10.).



To understand how to control process conditions to give methyl 2,4-pentadienoate, the reaction mechanism must be examined. (See Equation 2.).  $\beta$ -palladium hydride elimination from 4 gives rise to trans and cis-methyl penta-2,4-dienoate which is the desired monocarbonylation intermediate for sebacic acid. The desired mono-carbonylation reaction is promoted by low carbon monoxide pressure ( $\leq 1000$  psig) while high pressure (1800 psig) gives excellent 1,4-dicarbonylation product yield. The mono-carbonylation reaction is also facilitated by using a Lewis Acid as a co-catalyst and iodide as the preferred palladium counter-ion (Table III.). Chloride is the preferred palladium counter-ion for 1,4-dicarbonylation.

Although several Lewis Acids were evaluated, including titanium(IV) chloride, aluminum(III) chloride and tin(IV) chloride, ferric(III) chloride proved to be the most effective co-catalyst. We believe that in the presence of a Lewis Acid, the rate of  $\beta$ -palladium hydride elimination (H-Pd-X) from the  $\pi$ -allyl carbomethoxy palladium complex 4 can be enhanced. A good leaving group such as iodide attached to  $\pi$ -allyl carbomethoxy palladium complex 4 would facilitate iodopalladium hydride elimination to selectively form methyl 2,4-pentadienoate (Equation 11.).

Table III. Butadiene Oxycarbonylation  
Mono-Carbonylation Product Distribution

---

Reaction Conditions

o Redox Catalyst (mmoles)	
Palladium Chloride	5.0
Copper (I) Iodide	25.0
Lithium Iodide	10.0
Ferric Chloride	7.5
o Dehydration Agent (mole %)	48.0
o Solvent (weight %)	10.0
o Temperature (°C)	100
o Pressure (psig)	1000
o Residence Time (hours)	2

Product Distribution - CSTR result after 7 catalyst recycle passes.

o <u>Conversion (mole %; on butadiene)</u>	32.2
o <u>Selectivity (mole %; on butadiene)</u>	
4-vinyl cyclohexene	Trace
Methyl-3-pentenoate	1.8
Methyl-2,4-pentadienoate	83.2
Dimethyl hex-3-enedioate	11.2
Others	3.8

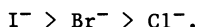
---





(11)

Mono carbonylation product yield is very sensitive to the leaving group. Leaving group preference is as follows:

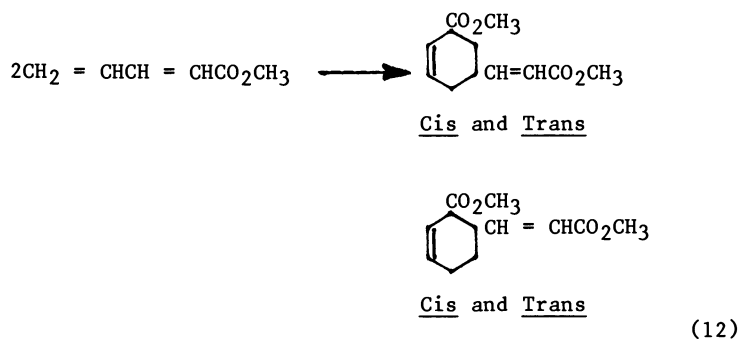


The optimum catalyst system for high butadiene conversion and high methyl 2,4-pentadienoate selectivity is palladium chloride, copper(I) iodide, lithium iodide, and ferric(III) chloride in a mole ratio of 5/25/10/7.5 mmoles catalyst per 500 mmoles of butadiene. No advantage is observed when palladium iodide is used in place of palladium chloride as long as lithium iodide is present to serve as an iodide pool. Reoxidation rate for the mixed chloride/iodide catalyst system appears to be nearly identical to either the all chloride or iodide systems. Di- $\mu$ -chloro-di- $\pi$ -(dimethyl hex-3-endoate) di-palladium can also be used in place of palladium chloride with no impact on overall yield. This  $\pi$ -allyl palladium complex improves process operability by increasing initial catalyst solubility and reducing reactor corrosion. Copper(I) iodide, however, is critical for high methyl 2,4-pentadienoate yield and cannot be replaced by either copper(II) chloride or copper(II) bromide. Although copper(II) iodide is unstable and not commercially available, it is assumed to be formed "in-situ" from copper(I) iodide.

We have observed with the above catalyst system that both butadiene conversion and methyl 2,4-pentadienoate selectivity increase when the catalyst is recycled. Over a series of seven recycle experiments, conversion increases from the low 20's to 32.2 mole % and selectivity increases from the low 70's to 83.2 mole % (See Table III.). Conversion and selectivity reach steady state after the third catalyst recycle.

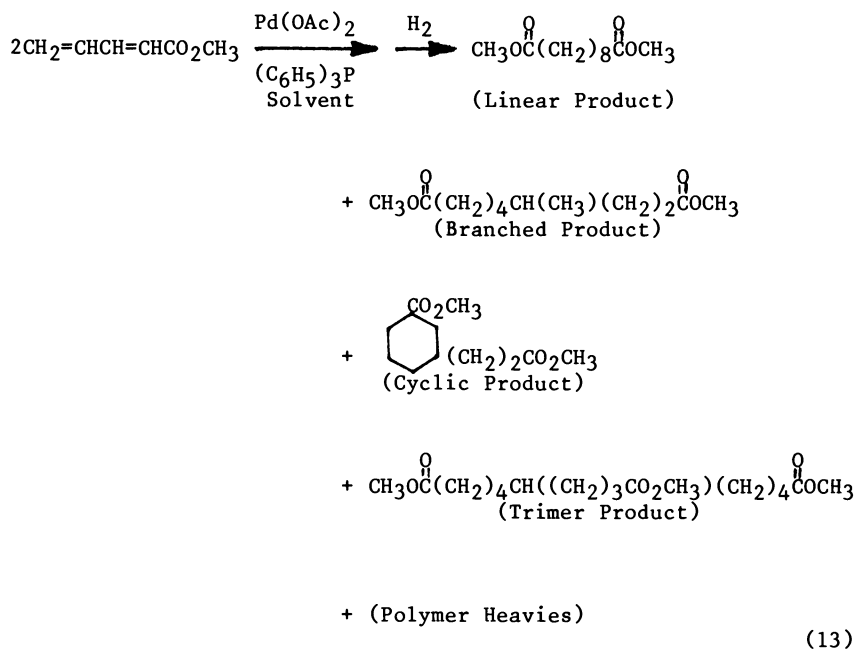
Methyl 2,4-pentadienoate self-dimerization as a potential route to sebacic acid precursors was extensively evaluated. Homogeneous metal catalyzed dimerization of compounds containing conjugated double bonds is known to give cyclic, branched, and linear dimers(43-45). At higher temperatures or in the presence of many zero-valent metal catalysts, cyclodimerization (Equation 12.) is the only observable reaction.

Under thermal conditions, the Diels-Alder reaction is bimolecular with a 18 Kcal/mole activation energy. Analysis shows 98.5% 1,3-dicarboxylate and 1.5% of the 1,2-dicarboxylate product.



Hydrogenation of the 1,3-cyclodimer followed by  $^{13}\text{C}$  NMR analysis reveals a 74/26 cis to trans geometric isomer ratio.

Dimerization(46,47) with a palladium acetate/tertiary phosphine complex (di-acetate-bis-[tri-phenylphosphine] palladium) in the absence of air gives primarily the desired linear dimer with smaller amount of branched, cyclic, and heavy product (Equation 13.). The reaction product is a complex mixture of cis and trans geometric isomers which makes analysis difficult. In order to simplify this problem, the product analysis is made after hydrogenation over 5% palladium on carbon.



In high polarity solvents, such as acetonitrile, dimethyl sulfoxide, methyl acetate, and methanol, the branched dimer, 4-methyl azelate precursor, is formed in high yield. In methanol, a methoxy dimer ( $\text{CH}_3\text{O}_2\text{CC}_8\text{H}_{14}(\text{OCH}_3)\text{CO}_2\text{CH}_3$ ) is also formed in moderate yield. Heavies contain both an acyclic methyl 2,4-pentadienoate trimeric product and high molecular weight methyl 2,4-pentadienoate homopolymer. Polymerization in the absence of air(48) appears to be catalyzed by traces of the tertiary phosphine which is used to prepare the palladium dimerization catalyst.

Under optimum reaction conditions (See Table IV.), selectivity to linear dimer is controlled by the choice of temperature, solvent and tertiary phosphine. Toluene and tetrahydrofuran are the best solvents. Temperatures between 25 to 60°C with a triphenyl or tributylphosphine/palladium acetate catalyst give linear dimer selectivities in the 80's. At 25°C in toluene, a palladium acetate/tributylphosphine catalyst gave 98.7% conversion and 89.6% linear, 4.7% branched, 1.9% cyclic, and 3.8% heavies selectivity. The linear dimerization reaction was second order in diene with a 3.6 Kcal/mole activation energy.

After dimerization and separation of the product mixture from the palladium catalyst complex, the reaction mixture is hydrogenated over a 1% palladium on activated carbon catalyst. A 50 psig hydrogen pressure and a 100-125°C reaction temperature are

Table IV. Methyl-2,4-Pentadienoate Dimerization

<u>Reaction Conditions*</u>			
o Reactants (mmoles)			
Methyl-2,4-pentadienoate	25.0	25.0	25.0
Palladium Acetate	0.5	0.5	0.5
Triphenyl Phosphine	.98	--	--
Tributyl Phosphine	--	.98	.98
Solvent (Toluene; ml)	20	20	20
o Temperature (°C)	60	60	60
o Residence Time (Hours)	2	2	8
<u>Product Distribution</u>			
o <u>Conversion (mole %)</u>	92.0	78.2	98.7
o <u>Selectivity (mole %)</u>			
Linear Dimer	76.1	81.1	89.6
Branched Dimer	8.9	6.5	4.7
Cyclic Dimer	2.0	2.0	1.9
Heavies**	13.0	10.4	3.8

\* Reaction carried out under nitrogen using degassed feeds.

\*\* Includes branched trimer and high molecular weight oligomers.

employed. Batch or continuous fixed bed conditions both give quantitative conversion. In the fixed bed reactor, hydrogenated product containing mostly dimethyl sebacate is recycled to the catalyst bed in order to control the temperature of the exothermic hydrogenation reaction. Purification to separate dimethyl sebacate from hydrogenated cyclic dimer, branched dimer, and heavies is carried out prior to hydrolysis to sebacic acid.

An excellent yield of high purity dimethyl sebacate may be recovered from the hydrogenation product mixture using a fractional crystallization approach(49). Recrystallization involves two steps. The first recovery step is preferably carried out at 0° to 20°C and second step is carried out at a temperature of 0° to -15°C. In general, the higher the dimethyl sebacate content in the mixture, the higher the recrystallization temperature that may be employed. Moreover, the higher the dimethyl sebacate purity desired, the greater the number of fractional recrystallization steps required. The following example illustrates a typical purification sequence.

A methyl ester C<sub>10</sub>-dicarboxylate mixture containing dimethyl sebacate (81.5%), branched isomer (10.3%), cyclic isomer (1.1%), and other by-products (7.1%) was mixed with an equal weight of pentane at ambient temperature. The mixture was then cooled with an ice-water bath until the temperature lowered to 0°-2°C, at which time white crystals dropped out of solution. The crystals were isolated from the liquid layer by decantation. The crystals were then heated until a liquid was obtained and were mixed with an equal weight of pentane. After cooling to 0°C, the crystals reformed and were isolated by decanting from pentane. The crystals were remelted and entrained pentane was stripped off by evaporation under vacuum. Gas chromatographic analysis of the isolated product indicated 99% pure dimethyl sebacate which contained only 1% branched isomer. No cyclic dimer or heavy products were detected. The overall isolated yield of dimethyl sebacate after two fractional recrystallizations was 96%. In an actual commercial process additional dimethyl sebacate would be recovered from the concentrated pentane solutions.

The isolated dimethyl sebacate can be sold commercially as is or optionally hydrolyzed to sebacic acid. If a higher molecular weight plasticizer diester is required, a transesterification with 2-ethyl hexanol, for example, gives the desired product plus two equivalents of methanol which is recycled back to the oxycarbonylation reaction. If the free acid is desired, dimethyl sebacate hydrolysis to sebacic acid is carried out using a strong mineral acid such as sulfuric acid. Hydrolysis is nearly quantitative with a selectivity of about 99.5% to diacid and .5% to the half-ester acid product. Additional recrystallization is used to improve purity if required.

### Summary

A commercially attractive palladium catalyzed oxidative carbonylation route to adipic and sebacic acid has been developed which uses butadiene and the elements of synthesis gas as the raw

materials. In an era of decreasing oil reserves, new technology development to synthesize large volume chemicals from readily available synthesis gas and methanol will become increasingly important. Process economics for the oxidative carbonylation route to adipic and sebacic acid will be attractive in the next decade provided butadiene and synthesis gas from natural gas are cheap and readily available while benzene feedstock increases in price due to decreasing crude oil reserves. Adipic acid overcapacity, softening worldwide oil prices, and the increased investment necessary to establish novel chemical processes have made implementation of a world scale adipic acid plant based on butadiene oxycarbonylation technology less attractive in the near term.

#### Acknowledgment

Acknowledgment is made to E. A. Hazbun, C. Y. Hsu, C. Johnson, H. F. Lawson, J. J. McCoy, F. S. Pinault, W. W. Wentzheimer, J. G. Zajacek, T. S. Zak, L. R. Zehner, and the many others who have made significant contributions in developing this technology.

#### Literature Cited

1. Chemical Week August 29, 1984, 46.
2. Chem Systems, Quarterly Report 2nd Quarter 1986, 116.
3. Matsuda, A. Bull. Chem. Soc. JPN. 1973, 46, 524.
4. Kummer U.S. Patent 4,259,50, 1981 to BASF.
5. Forster, D. Catal. Rev. Sci. Eng. 1981, 23, 89.
6. Milstein, D.; Huckalsy, J.L. J. Am. Chem. Soc. 1982, 104, 6150.
7. Brewis, S.; Hughes, P.R. Chem. Communications 1965, 8, 157.
8. Chemical Week July 4, 1984, 36.
9. Waller, F. J. J. Mol. Catal. 1985, 31, 128.
10. Fenton, D. M. J. Org. Chem. 1983, 38, 3192.
11. Fenton, D. M. U.S. Patent 3,397,225, 1968 to Union Oil.
12. Fenton, D. M. U.S. Patent 3,509,209, 1970 to Union Oil.
13. Japanese Kokai 75,120,714, 1975.
14. Stille, J. K.; James, D. E. J. Am. Chem. Soc. 1976, 98, 1810.
15. Stille, J. K.; Divakaruni, R. J. Org. Chem. 1979, 20, 3474.
16. Stille, J. K. U.S. Patent 4,259,519, 1981 to Polymer Sciences Corp.
17. Kesling, H. S.; Zehner, L. R. U.S. Patent 4,171,450, 1979 to Atlantic Richfield.
18. Kesling, H. S.; Zehner, L. R. U.S. Patent 4,166,913, 1979 to Atlantic Richfield.
19. Kesling, H. S. U.S. Patent 4,281,173, 1981 to Atlantic Richfield.
20. Heck, R. F. J. Am. Chem. Soc. 1972, 94, 2712.
21. Backvall, J. E. J. Chem. Soc. Chem. Comm. 1980, 943.
22. Fenton, D. M. J. Org. Chem. 1972, 37, 2034.
23. Lloyd, W. G. J. Org. Chem. 1967, 32, 2816.
24. Golodov, V. A. J. Mol. Catal. 1980, 383.

25. Fenton, D. M. J. Org. Chem. 1974, 39, 701.
26. Leonard, J. J.; et. al. J. Catal. 1984, 90, 261.
27. Bell, J. M. J. Org. Chem. 1965, 30, 4284.
28. Meskens, F. A. Synthesis 1981, 501.
29. Watanake, K. Bull. Chem. Soc. JPN. 1980, 53, 1356.
30. Schwartz, J. J. Am. Chem. Soc. 1984, 106, 5028.
31. Schwartz, J. Organometallics 1985, 4, 415-419.
32. Kesling, H. S.; Zehner, L. R. U.S. Patent 4,189,599, 1980 to Atlantic Richfield.
33. German Patent 2,404,560, 1974 to Asahi Chemical.
34. German Patent 1,802,865, 1970 to BASF.
35. Chem Systems Quarterly Report 2nd Quarter 1976, 125.
36. Knifton, J. F. J. Catal. 1979, 60, 27.
37. Tsuji, J. Tetrahedron 1972, 28, 3721.
38. Kiji, J. J. Mol. Catal. 1983, 18, 109.
39. Kesling, H. S.; Zehner, L. R. U.S. Patent 4,236,023, 1980 to Atlantic Richfield.
40. Kesling, H. S.; Zehner, L. R. U.S. Patent 4,195,184, 1980 to Atlantic Richfield.
41. Kesling, H. S.; Hsu, C. Y. U.S. Patent 4,318,860, 1982 to Atlantic Richfield.
42. Kesling, H. S.; Hsu, C. Y. U.S. Patent 4,299,976, 1981 to Atlantic Richfield.
43. Katagui, T. Nippon Kagaku Kaishi 1977, 4, 1742.
44. Tolstikov, G. A. Doki. Akad. Nank. USSR 1975, 224, 609.
45. Akhmedov, U. M. Zh. Org. Khim. 1972, 8, 1779 and 1795.
46. Smutny, E. J. J. Am. Chem. Soc. 1967, 86, 6973.
47. Wright, D. Tetrahedron Letters 1972, 163.
48. Minoura, Y. J. Polym. Sci. Polym. Chem. Ed. 1976, 14, 693, 1183.
49. Kesling, H. S.; Hsu, C. Y. U.S. Patent 4,365,079, 1982 to Atlantic Richfield.
50. C&E News April, 30, 1984, 28.
51. C&E News May 19, 1986, 7.
52. Lin Jiang-Jen; Knifton, J. F. U.S. Patent 4,552,976, 1985 to Texaco Inc.

RECEIVED July 29, 1986

## Chapter 7

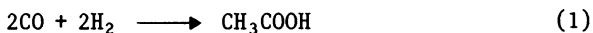
# The Selective Generation of Acetic Acid Directly from Synthesis Gas

John F. Knifton

Texaco Chemical Company, P.O. Box 15730, Austin, TX 78761

Acetic acid has been generated directly from synthesis gas (CO/H<sub>2</sub>) in up to 95 wt % selectivity and 97% carbon efficiency using a Ru-Co-I/Bu<sub>4</sub>PBr "melt" catalyst combination. The critical roles of each of the ruthenium, cobalt and iodide catalyst components in achieving maximum selectivity to HOAc have been identified. C<sub>1</sub>-Oxygenate formation is observed only in the presence of ruthenium carbonyls; [Ru(CO)<sub>3</sub>I<sub>3</sub>] is here the dominant species. Controlled quantities of iodide ensure that initially formed MeOH is rapidly converted to the more reactive methyl iodide. Subsequent cobalt-catalyzed carbonylation to acetic acid may be preparatively attractive (>80% selectivity) relative to competing syntheses where the [Co(CO)<sub>4</sub>] concentration is optimized; that is, where the Co/Ru ratio is >1, the syngas feedstock is rich in CO and the initial iodide/cobalt ratios are close to unity.

Acetic acid is an important commodity chemical (U. S. demand ca. 2.9MMM lb/yr) already targeted for generation directly from CO/H<sub>2</sub> (1). Here we describe a new application for ruthenium "melt" catalysis, where synthesis gas is for the first time converted directly to acetic acid in >80 wt % selectivity in the crude liquid product (eq. 1) (2,3).



Ruthenium, cobalt and halogen are the key elements of this catalysis (2), although ruthenium in combination with halogen-containing zirconium and titanium derivatives is also effective (3). In the case of the Ru-Co couple, the highest yields of acetic acid may generally be achieved with ruthenium oxide, carbonyls and complex derivatives in combination with various cobalt halides dispersed in low-melting quaternary phosphonium halide salts (2).

A significant enhancement in both acetic acid productivity and selectivity is normally realized in the presence of controlled quantities of iodide.

## Results

Data in Table I illustrate the production of acetic acid from 1/1 syngas catalyzed by ruthenium-cobalt halide bimetallic combinations dispersed in tetrabutylphosphonium bromide (m.p. 100°C).

The ruthenium(III) acetylacetonate-cobalt(II) iodide couple, for example, when dispersed in tetrabutylphosphonium bromide (ex. 1) and treated with 1/1 CO/H<sub>2</sub> at 220°C, generates a liquid product containing 76 wt % acetic acid plus 1.1 wt % propionic acid (111 mmol total acid). The liquid yield increase is 66% and the estimated carbon selectivity to acetic plus propionic acids and their esters is 84%. There is normally no metallic residue at this stage, ruthenium and cobalt recovery is essentially quantitative at the end of the run, and the product acids may be recovered in >90% purity by fractional distillation. Methane and water are the major by-products (4).

In a more detailed examination of the ruthenium-cobalt-iodide "melt" catalyst system, we have followed the generation of acetic acid and its acetate esters as a function of catalyst composition and certain operating parameters, and examined the spectral properties of these reaction products, particularly with regard to the presence of identifiable metal carbonyl species.

A typical reaction profile is illustrated in Figure 1 for the Ru<sub>3</sub>(CO)<sub>12</sub>-CoI<sub>2</sub>/Bu<sub>4</sub>PBr catalyst precursor. Under the selected operating conditions, acetic acid is the major product fraction; here it may comprise up to 85 wt % of the liquid product fraction (molar selectivity to HOAc is 86%, initial turnover frequency ca. 2.0x10<sup>-3</sup>s<sup>-1</sup> per g atom Ru charged). Methyl and ethyl acetates are also in evidence.

Figure 2 illustrates the effect of incremental changes in ruthenium catalyst content upon the production of acetic acid and its C<sub>1</sub>-C<sub>2</sub> alkyl acetate esters. Acetic acid production is maximized at Ru/Co ratios of ca. 1.0 → 1.5; however, the data in Figure 2 do show an approximate first order dependence of ΣOAc (acetic acid plus acetate esters) upon initial ruthenium content--at least up to the 2/1, Ru/Co stoichiometry under the chosen conditions. Selectivity to acetic acid in the liquid product peaks at 92 wt % (carbon efficiency 95 mol %) for a catalyst combination with initially low Ru/Co ratios (e.g. 1:4). The formation of C<sub>1</sub>-C<sub>2</sub> alkanols and their acetate esters rapidly exceeds acetic acid productivity when the Ru/Co atomic ratio is raised above 1.5, although two-carbon oxygenates continue to be the predominant fraction. Smaller quantities of glycol may also be in evidence.

The effect of varying cobalt concentration has been examined for two classes of catalyst precursor, viz. Ru<sub>3</sub>(CO)<sub>12</sub>-CoI<sub>2</sub>/Bu<sub>4</sub>PBr and Ru<sub>3</sub>(CO)<sub>12</sub>-Co<sub>2</sub>(CO)<sub>8</sub>-I<sub>2</sub>/Bu<sub>4</sub>PBr. The highest acetic acid selectivity in the liquid product (84%) was again achieved for both experimental series at Co/Ru molar ratios exceeding unity (see for example Figure 3). Maximum ΣOAc content was achieved at Co/Ru ratios of ca. 0.5, while the highest turnover frequencies



Table I. Carboxylic Acids from Synthesis Gas<sup>a,b</sup>

Ex.	Catalyst precursor	Quaternary salt	Product composition (mmol) <sup>c</sup>					Liquid yield (%)		
			CH <sub>3</sub> COOH	C <sub>2</sub> H <sub>5</sub> COOH	CH <sub>3</sub> COOMe	CH <sub>3</sub> COOEt	CH <sub>3</sub> COOPr			
1	Ru(acac) <sub>3</sub> - CoI <sub>2</sub>	Bu <sub>4</sub> PBr	110	1	2	9	2	20	53	66
2	RuO <sub>2</sub> - 2CoI <sub>2</sub> <sup>d</sup>	"	33	5	0.2	4	2	7	22 <sup>d</sup>	24
3	Ru <sub>3</sub> (CO) <sub>12</sub> - CoI <sub>2</sub> <sup>e</sup>	"	58	0.4	3	9	2	10	18	41
4	Ru <sub>3</sub> (CO) <sub>12</sub> - CoI <sub>2</sub>	"	116	5	4	34	6	10	37	84
5	RuO <sub>2</sub> - CoBr <sub>2</sub>	"	132	2	32	81	20	25	156	204
6	RuO <sub>2</sub> - CoCl <sub>2</sub>	"	50	7	39	66	11	382	678	358 <sup>f</sup>
7	RuO <sub>2</sub> - CoCO <sub>3</sub>	"	60	2	31	47	9	225	374	299 <sup>g</sup>
8	Ru <sub>3</sub> (CO) <sub>12</sub> - Co <sub>2</sub> (CO) <sub>8</sub> <sup>h</sup>	"	34		2	5		6	1	29
9	RuO <sub>2</sub> - Co <sub>2</sub> (CO) <sub>8</sub> - I <sub>2</sub>	"	113	3	6	23	6	19	122	108
10	RuO <sub>2</sub> - CoI <sub>2</sub> - I <sub>2</sub>	"	20			1		1	15 <sup>j</sup>	11
11	RuO <sub>2</sub> - CoI <sub>2</sub> - 4MeI	"							24	<2
12	CoI <sub>2</sub>	"								<2
13	Ru <sub>3</sub> (CO) <sub>12</sub> <sup>e</sup>	"			23	16	3	14	141	192 <sup>i</sup>

<sup>a</sup>Operating conditions: 482 bar; 220°C; 18 hr; CO/H<sub>2</sub>, 1:1.

<sup>b</sup>Reaction charge: Ru, 4.0 mmol; Co, 4.0 mmol; Ru<sub>4</sub>PBr, 10.0 g.

<sup>c</sup>Analysis of gas and liquid samples by glc; CH<sub>3</sub>COOEt and CH<sub>3</sub>COOPr fractions contain small quantities of C<sub>2</sub>H<sub>5</sub>COOMe and C<sub>2</sub>H<sub>5</sub>COOEt

<sup>d</sup>respectively, liquid products may also contain smaller quantities of MeOH, EtOH, PrOH, MeOOCH, and (CH<sub>2</sub>OH)<sub>2</sub>.

<sup>e</sup>Reaction charge: Ru, 4.0 mmol; Co, 8.0 mmol; product CO<sub>2</sub>, 317 mmol.

<sup>f</sup>Run time, 6 hr.

<sup>g</sup>Product also contains: MeOH, 150 mmol; EtOH, 136 mmol; PrOH, 29 mmol; liquid product comprises two phases.

<sup>h</sup>Product also contains: MeOH, 107 mmol; EtOH, 104 mmol; PrOH, 23 mmol.

<sup>i</sup>Run conditions: see Reference 2.

<sup>j</sup>Product also contains: MeOH, 244 mmol; EtOH, 110 mmol; PrOH, 11 mmol.

<sup>k</sup>Product CO<sub>2</sub>, 381 mmol.

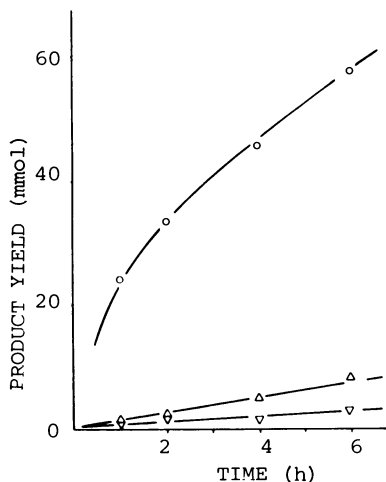


Figure 1. Typical Reaction Profile. Reactor charge: Ru<sub>3</sub>(CO)<sub>12</sub>, 4.0 mmol Ru; CoI<sub>2</sub>, 4.0 mmol Co; Bu<sub>4</sub>PBr, 10.0 g. Reaction conditions: 480 bar pressure; 220°C; 1:1 CO/H<sub>2</sub>. Legend: CH<sub>3</sub>COOH, ○; CH<sub>3</sub>COOCH<sub>3</sub>, ▽; CH<sub>3</sub>COOC<sub>2</sub>H<sub>5</sub>, △. Reproduced with permission from Ref. 5. Copyright 1985, Academic Press.

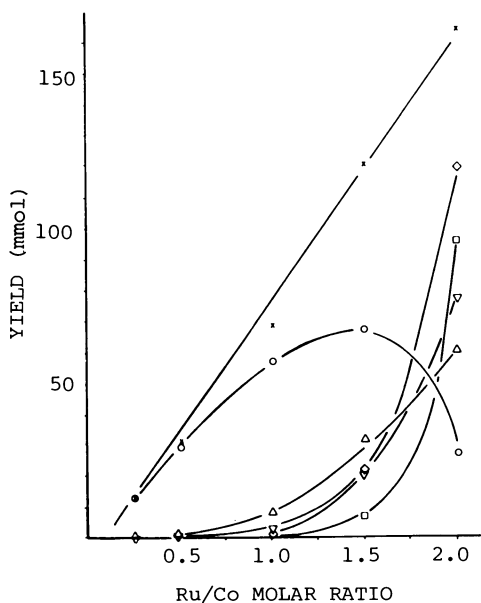


Figure 2. Effect of Varying [Ru]. Reactor charge: CoI<sub>2</sub>, 4.0 mmol; Bu<sub>4</sub>PBr, 10.0 g. Reaction conditions: as per Figure 1; reaction time, 6 hr. Legend: CH<sub>3</sub>COOH, ○; CH<sub>3</sub>COOCH<sub>3</sub>, ▽; CH<sub>3</sub>COOC<sub>2</sub>H<sub>5</sub>, △; ΣCH<sub>3</sub>COO<sup>-</sup>, ×; CH<sub>3</sub>OH, □; C<sub>2</sub>H<sub>5</sub>OH, ◇. Reproduced with permission from Ref. 5. Copyright 1985, Academic Press.

( $5 \times 10^{-3} \text{ s}^{-1}$  per g atom Ru charged) were measured at CoI<sub>2</sub>/Ru molar ratios of 1/4. No significant quantities of acetic acid are detected in the absence of the cobalt (see also Table I, ex. 13), although acetate esters may be generated in moderate yields, together with larger quantities of C<sub>1</sub>-C<sub>2</sub> alkanol.

The presence of an iodide component appears to be essential to the formation of acetic acid in >70 wt % selectivity (2). A series of comparative experiments using a ruthenium-cobalt catalyst of the general composition Ru<sub>3</sub>(CO)<sub>12</sub>-Co<sub>2</sub>(CO)<sub>8</sub>-I<sub>2</sub>/Bu<sub>4</sub>PBr has been completed with different iodine contents. Selectivity to acetic acid reaches 95 wt % of the liquid product (97% carbon efficiency) for the Ru-Co-3I formulation (see Figure 4). This is the highest HOAc selectivity achieved to date in this work. However, the heightened selectivity is generally realized at the expense of reactor productivity. Lower I/(Ru+Co) atomic ratios (e.g. 0.25) ensure a rise in productivity (turnover frequency  $2.9 \times 10^{-3} \text{ s}^{-1}$  per g atom Ru), while HOAc selectivity dips to 10 wt % as methanol formation and homologation activity increases. Essentially no liquid oxygenates are formed as the initial I/(Ru+Co) atomic ratios approach two (see also Figure 3 and Table 1, ex. 11).

### Discussion

It is clear that ruthenium-cobalt-iodide catalyst dispersed in low-melting tetrabutylphosphonium bromide provides a unique means of selectively converting synthesis gas in one step to acetic acid. Modest changes in catalyst formulation can, however, have profound effects upon liquid product composition.

The new data illustrate how preparatively attractive yields of acetic acid (and maximum rates of HOAc formation) may be realized when the following criteria are met:

- a) Ruthenium-cobalt atomic ratios range from ca. 0.5:1 → 2:1 (see Figures 2 and 3).
- b) Transition metal-iodide ratios (Ru:Co:I) are ca. 1:1:1 (Figure 4).
- c) Carbon monoxide partial pressures exceed ca. 70 bar (5).

Spectroscopic studies of typical Ru<sub>3</sub>(CO)<sub>12</sub>-Co<sub>2</sub>(CO)<sub>8</sub>-I<sub>2</sub>/Bu<sub>4</sub>PBr catalyst solutions have served to aid considerably in unraveling the differing roles of the ruthenium, cobalt and iodide-containing catalyst components in these syntheses. A typical solution spectrum in the metal-carbonyl region (5) shows the presence of significant concentrations of both [Ru(CO)<sub>3</sub>I<sub>3</sub>]<sup>-</sup> (2108 and 2036 cm<sup>-1</sup>) (6) and [Co(CO)<sub>4</sub>]<sup>-</sup> (1886 cm<sup>-1</sup>). Most of the ruthenium charged can be accounted for on the basis of the strength of the [Ru(CO)<sub>3</sub>I<sub>3</sub>]<sup>-</sup> absorptions. The importance of this species to the CO hydrogenation syntheses is evident from the close parallel we find between the yields of liquid oxygenate and acetic acid (ΣOAc), and the increase in ruthenium carbonyl iodide, [Ru(CO)<sub>3</sub>I<sub>3</sub>]<sup>-</sup>, content--as determined by its characteristic absorption at 2036 cm<sup>-1</sup>. The relationships are illustrated in Figure 5. NMR spectra of these typical product solutions show no hydride signals to δ -20 ppm. As in Table I, ex. 12, no aliphatic oxygenates are formed in the absence of the ruthenium catalyst component. The data (particularly the relationships of Figures 2 and 5) are in keeping with our

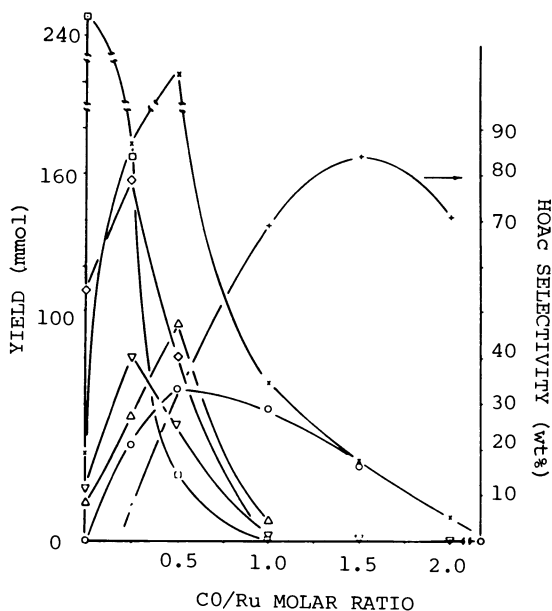


Figure 3. Effect of Varying  $[\text{CoI}_2]$ . Reactor charge:  $\text{Ru}_3(\text{CO})_{12}$ , 4.0 mmol Ru;  $\text{Bu}_4\text{PBr}$ , 10.0 g. Reaction conditions: as per Figure 1; reaction time, 6 hr. Legend as per Figures 1 and 2,  $\text{CH}_3\text{COOH}$  selectivity, +. Reproduced with permission from Ref. 5. Copyright 1985, Academic Press.

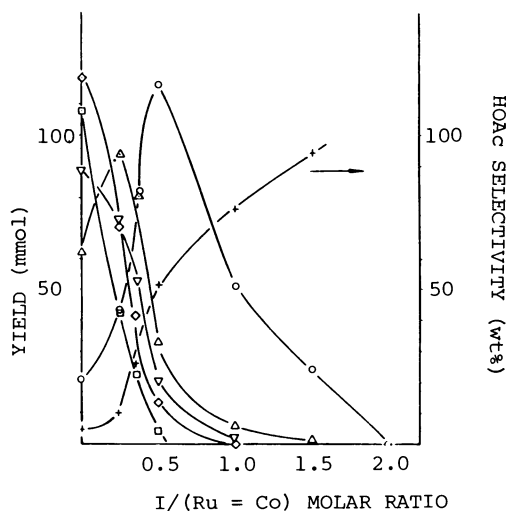


Figure 4. Effect of Varying  $[\text{I}_2]$ . Reactor charge:  $\text{Ru}_3(\text{CO})_{12}$ , 4.0 mmol Ru;  $\text{Co}_2(\text{CO})_8$ , 4.0 mmol Co;  $\text{Bu}_4\text{PBr}$ , 10.0 g. Reaction conditions: as per Figure 1; reaction time, 6 hr. Legend as per Figures 1-3. Reproduced with permission from Ref. 5. Copyright 1985, Academic Press.

earlier spectral correlations (7), pointing to initial C<sub>1</sub>-oxygenate (methanol) formation being associated with the presence of the [Ru(CO)<sub>3</sub>X<sub>3</sub>]<sup>-</sup> anion.

Regarding the function of the cobalt component, we find for different iodide charges (at fixed Ru, Co) there is a close parallel between HOAc productivity and the presence of the cobalt carbonyls, and a linear relationship between ΣOAc<sup>-</sup> and [Co(CO)<sub>4</sub>]<sup>-</sup> anion content (see Figure 6). This linear correspondence, taken together with the [Co], HOAc selectivity correlation of Figure 3, is indicative of cobalt carbonyl--or a derivative thereof--being responsible for the formation of the desired acetic acid.

Additional evidence regarding the role played by the cobalt carbonyl in the carbonylation sequence comes from the following observations:

1) Acetic acid may be readily synthesized from methanol (eq. 2) in the absence of ruthenium, in 96% selectivity, using the Co<sub>2</sub>(CO)<sub>8</sub>-I<sub>2</sub>/Bu<sub>4</sub>PBr "melt" catalyst alone; the rate of this cobalt-catalyzed carbonylation is >3 times faster than the rate of acetic acid formation via reaction (1) using the Ru-Co-I/Bu<sub>4</sub>PBr couple. Similarly, acetic acid may be generated from methyl iodide using cobalt octacarbonyl-tetrabutylphosphonium bromide as catalyst precursor.

2) Starting from <sup>13</sup>C-enriched methanol, the Co<sub>2</sub>(CO)<sub>8</sub>-I<sub>2</sub>/Bu<sub>4</sub>PBr "melt" catalyst carbonylates to acetic acid in accord with eq. 2, enrichment being detected only on the methyl carbon.



3) In competitive experiments, although Ru<sub>3</sub>(CO)<sub>12</sub>/Bu<sub>4</sub>PBr and its cobalt-containing analog, Ru<sub>3</sub>(CO)<sub>12</sub>-CoI<sub>2</sub>/Bu<sub>4</sub>PBr, both exhibit rapid rates of ΣC<sub>1</sub> oxygenate formation, the yield of HOAc is a factor of >10<sup>2</sup> higher for the Ru-Co combination (see Table 1, cf. ex. 3 and 13, and Figure 3). Cobalt--in the absence of ruthenium--does not, on the other hand, convert syngas to liquid oxygenates (Table 1, ex. 12).

Regarding the sensitivity of HOAc selectivity to catalyst structure, we find that preparatively attractive selectivities to acetic acid (>80 wt %) in the liquid product may be realized for the Ru-Co-I/Bu<sub>4</sub>PBr "melt" catalysts when the following general conditions are met: a) Cobalt:ruthenium atomic ratios are ca. unity or greater (see Figures 2 and 3); b) iodide/(Ru+Co) ratios are ca. 1.5:1 or greater (Figure 4); c) the synthesis gas feedstock is rich in CO (5).

For example, at fixed ruthenium content, increases in cobalt charge lead to significant changes in [Co(CO)<sub>4</sub>]<sup>-</sup> content, and for both the Ru<sub>3</sub>(CO)<sub>12</sub>-CoI<sub>2</sub>/Bu<sub>4</sub>PBr and Ru<sub>3</sub>(CO)<sub>12</sub>-I<sub>2</sub>/Bu<sub>4</sub>PBr formulations, there is a linear correlation between acetic acid selectivity and changes in [Co(CO)<sub>4</sub>]<sup>-</sup> content (over limited [Co]) (5). This relationship provides further evidence implicating the cobalt carbonyls, or their derivatives, as responsible for the carbonylation activity leading to HOAc formation.

Nevertheless, the critical role of the iodide fraction in ensuring a selective acetic acid synthesis is illustrated by the

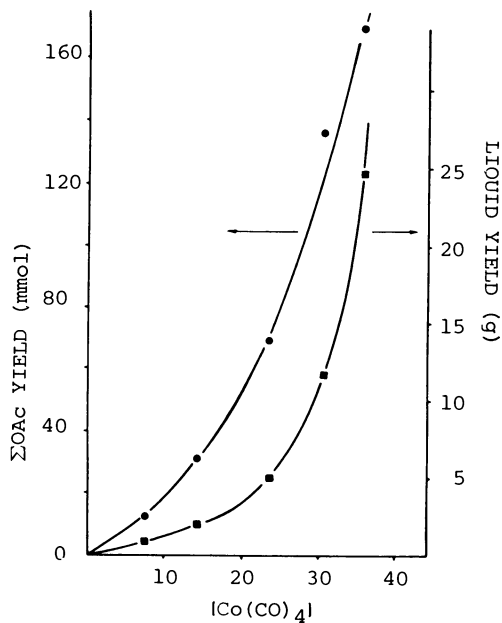


Figure 5.  $\Sigma\text{OAc}$  and Liquid Yield Versus  $[\text{Ru}(\text{CO})_3\text{I}_3]^-$ . Reactor charge and conditions as per Figure 2. Reproduced with permission from Ref. 5. Copyright 1985, Academic Press.

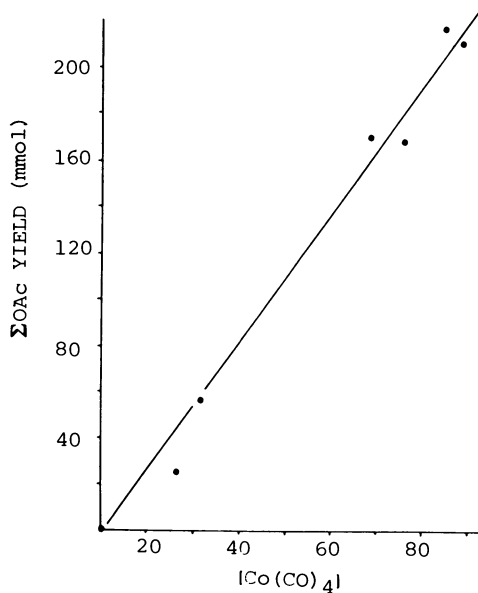


Figure 6.  $\Sigma\text{OAc}$  Versus  $[\text{Co}(\text{CO})_4]^-$ . Reactor charge and conditions as per Figure 4. Reproduced with permission from Ref. 5. Copyright 1985, Academic Press.

data in Figure 4. Here it can be seen that the introduction of controlled quantities of iodide component may bring about a greater than 20-fold improvement in acetic acid selectivity (from 4.3 to 94.8 wt %) in the liquid product. While the acetic acid productivity peaks at I/Co ratios of ca. unity, a further increase in this ratio dramatically lowers the HOAc productivity so that by 4/1 there is essentially no liquid product. Significantly, at this I/Co ratio, the infrared spectrum of the catalyst complex shows essentially complete elimination of the absorption at 1886 cm<sup>-1</sup> due to [Co(CO)<sub>4</sub>]<sup>-</sup>, while the presence of [CoI<sub>4</sub>]<sup>2-</sup> is confirmed by its characteristic (8) strong absorption in the visible spectrum at ca. 700 mμ. Chromatographic separation of these crude liquid products allows isolation of fractions containing [CoI<sub>4</sub>]<sup>2-</sup>. Once again, then, carbonylation activity leading to acetic acid tracks the presence of cobalt tetracarbonyl anion. Somewhat similar observations have been reported for cobalt-iodide catalyzed methanol homologation (9).

To achieve, then, high acetic acid selectivity directly from synthesis gas (eq. 1) it is necessary to balance the rates of the two consecutive steps of this preparation - ruthenium-carbonyl catalyzed methanol formation (10) (Figures 2 and 5) and cobalt-carbonyl catalyzed carbonylation to acetic acid (Figure 6) - such that the instantaneous concentration of methanol does not build to the level where competing secondary reactions, particularly methanol homologation (7, 11), ester homologation (12, 13), and acid esterification (14), become important.

The iodide content of the catalyst formulation is the key to avoiding these problems of competing reactions and achieving maximum acetic acid selectivity. The addition of iodide ensures that any initially formed methanol (7) is rapidly (11) converted to the more electrophilic methyl iodide. However, further increases in the quantities of iodide beyond that needed for methanol conversion to methyl iodide may lead to a portion, or all, of the catalytically active cobalt carbonyl reverting to catalytically inactive cobalt iodide species - e.g. the [CoI<sub>4</sub>]<sup>2-</sup> anion identified in this work, or possibly the cationic [Co(MeOH)<sub>x</sub>(CO)<sub>y</sub>I<sub>z</sub>]<sup>n+</sup> species (9).

### Conclusions

We conclude that each of the ruthenium, cobalt and iodide-containing catalyst components have very specific roles to play in the "melt" catalyzed conversion of synthesis gas to acetic acid. C<sub>1</sub>-Oxygenate formation is observed only in the presence of ruthenium carbonyls - [Ru(CO)<sub>3</sub>I<sub>3</sub>]<sup>-</sup> is here the dominant species - and there is a direct relationship between liquid yield, ΣOAc productivity and [Ru(CO)<sub>3</sub>I<sub>3</sub>]<sup>-</sup> content (see Figures 2 and 5). Controlled quantities of iodide ensure that initially formed MeOH is rapidly converted to the more reactive methyl iodide. Subsequent cobalt-catalyzed carbonylation to acetic acid may be preparatively attractive (>80% selectivity, good yields) relative to competing syntheses, where the [Co(CO)<sub>4</sub>]<sup>-</sup> concentration is maximized (Figure 6) that is where the Co/Ru ratio is >1, the syngas feedstock is rich in CO, and the initial iodide/cobalt ratios are ca. unity. Formation of cobalt-iodide species appears to be a competing, inhibitory step in this catalysis.

### Acknowledgments

The author wishes to thank Texaco Inc. for permission to publish this paper, Messrs. M. R. Swenson, R. Gonzales, R. D. Czimskey and D. W. White for experimental assistance and Messrs. J. M. Schuster and C. L. LeBas for FTIR and nmr data.

### Literature Cited

1. See for example: Chem Systems PERP Fourth Quarterly Report 1979 Program, July 1980, p. 386, and cited references therein.
2. Knifton, J. F.; Lin, J. J. U.S. Patent 4 366 259, 1982 to Texaco Develop. Corp.
3. Knifton, J. F. U.S. Patent 4 362 822, 1982 to Texaco Develop. Corp.
4. All liquid organic products (acids, esters and alkanols) plus methane have been considered in this work in estimating carbon efficiency for each of the individual experiments described in Table 1 and in the following Figures. The quantity of CO<sub>2</sub> formed is not included in carbon selectivity calculations since this component can be readily recycled to the synthesis gas generator as a source of additional CO. See: Chem. Eng. News, Nov. 12, 1984, p. 29. For previous examples of ruthenium-catalyzed water gas shift activity in acidic media see: Yarrow, P.; Cohen, H.; Ungermann, C.; Vandenberg, D.; Ford, P. C. *J. Mol. Catal.*, 1983, 22, 239.
5. Knifton, J. F. *J. Catal.*, 1985, 96, 439.
6. Knifton, J. F. *J. Mol. Catal.*, 1981, 11, 91.
7. Knifton, J. F.; Grigsby, R. A.; Lin, J. J. *Organometallics*, 1984, 3, 62.
8. Mizoroki, T.; Nakayama, M. *Bull. Chem. Soc. Jpn.* 1965, 38, 1876.
9. Pretzer, W. R.; Kobylinski, T. P. *Ann, N.Y. Acad. Sci.* 1980, 333 58.
10. Knifton, J. F. *J. Amer. Chem. Soc.*, 1981, 103, 3959.
11. Fakley, M. E.; Head, R. A. *Appl. Catal.*, 1983, 5, 3.
12. Knifton, J. F. *J. Catal.*, 1983, 79, 147.
13. Hidai, M.; Koyasu, Y.; Yokota, M.; Orisaku, M.; Uchida, Y. *Bull. Chem. Soc. Jpn.*, 1982, 55, 3951.
14. Braca, G.; Paladini, L.; Sbrana, G.; Valentini, G.; Andrich, G.; Gregorio, G. *Ind. Eng. Chem. Prod. Res. Dev.* 1981, 20, 115.

RECEIVED July 15, 1986



## Chapter 8

# Preparation of Ethylene Glycol Esters from Synthesis Gas

## Use of Promoted Homogeneous Ruthenium-Rhodium Catalysts

R. Whyman, K. Gilhooley, S. Rigby, and D. Winstanley

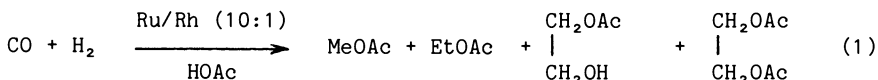
Imperial Chemical Industries plc, New Science Group, P.O. Box 11, The Heath,  
Runcorn, Cheshire, WA7 4QE United Kingdom

C<sub>2</sub>-oxygenated products, particularly the acetate esters of ethylene glycol, may be prepared in good selectivities directly from synthesis gas in the presence of composite bimetallic homogeneous catalysts which contain mixtures of ruthenium and rhodium, as major and minor components respectively, together with promoters in the form of nitrogen-containing bases or alkali metal cations, in acetic acid as solvent/co-reactant. These are the first catalyst systems containing ruthenium as the major metallic component which have been demonstrated (i) to provide good molar selectivities (e.g. C<sub>2</sub>/C<sub>1</sub> ~ 1-2) to specific C<sub>2</sub>-oxygenates, with no hydrocarbon formation, and (ii) to match the previously-documented behavior of mono-metallic rhodium catalysts in respect of both activity and selectivity.

A feature which is a key to any wider utilisation of chemistry based on synthesis gas is an understanding of, and more particularly, an ability to control, those factors which determine the selectivity of the C<sub>1</sub> to C<sub>2</sub> transformation during the hydrogenation of carbon monoxide. With the exception of the rhodium-catalysed conversion of carbon monoxide and hydrogen into ethylene glycol and methanol, in which molar ethylene glycol/methanol selectivities of ca 2/1 may be achieved, other catalyst systems containing metals such as cobalt or ruthenium exhibit relatively poor selectivities to ethylene glycol (1).

Our initial studies in this area were based on the reasoning that, since the reduction of carbon monoxide to C<sub>2</sub> products is a complex, multi-step process, the use of appropriate combinations of metals could generate synergistic effects which might prove more effective (in terms of both catalytic activity and selectivity) than simply the sum of the individual metal components. In

particular, the concept of the combination of a good hydrogenation catalyst with a good carbonylation, or "CO insertion", catalyst seemed particularly germane. As a result of this approach we discovered an unprecedented example of the effect of catalyst promoters, particularly in the enhancement of C<sub>2</sub>/C<sub>1</sub> selectivity, and one which has led to the development of composite mixed-metal homogeneous catalyst systems for the conversion of CO/H<sub>2</sub> into ethylene glycol esters (2,3) (Equation 1) and ethanol (4).



Other recent reports have also indicated that mixed-metal systems, particularly those containing combinations of ruthenium and rhodium complexes, can provide effective catalysts for the production of ethylene glycol or its carboxylic acid esters (5-9). However, the systems described in this paper are the first in which it has been demonstrated that composite ruthenium-rhodium catalysts, in which rhodium comprises only a minor proportion of the total metallic component, can match, in terms of both activity and selectivity, the previously documented behavior (1) of mono-metallic rhodium catalysts containing significantly higher concentrations of rhodium. Some details of the chemistry of these bimetallic promoted catalysts are described here.

### Experimental

Chemicals. Synthesis gas, as an equimolar mixture of carbon monoxide and hydrogen, was purchased from either Air Products Ltd or British Oxygen Company Ltd. Ru(acac)<sub>3</sub> was purchased from Johnson Matthey Chemicals Ltd and used without further purification; Ru<sub>3</sub>(CO)<sub>12</sub>, Rh<sub>6</sub>(CO)<sub>16</sub> and Rh(CO)<sub>2</sub>acac were prepared according to literature procedures (10-12). Glacial acetic acid and the various additives/promoters were purchased from BDH Ltd and used without further purification. Tetraglyme (ex-Aldrich Chemical Company Ltd) was dried over activated 3A molecular sieves before use.

High Pressure Experimentation. A typical autoclave experiment was carried out as follows. Ru(acac)<sub>3</sub> (0.80g, 2.0 mmol), Rh(CO)<sub>2</sub>(acac) (0.052g, 0.2 mmol), Cs<sub>2</sub>CO<sub>3</sub>·2H<sub>2</sub>O (0.362g, 2.0 mmol Cs) and glacial acetic acid (52.5g, 50 ml), were charged into a 100ml capacity silver-lined stainless steel autoclave fitted with a flip-flop stirrer. The autoclave was sealed, purged four times with a CO/H<sub>2</sub> mixture, pressurised to ca 500 atm CO/H<sub>2</sub> (1:1), stirred and heated to 230°C whereupon the pressure was increased to 1000 atm with further CO/H<sub>2</sub>. After 2 hr at 230°C, during which a further 210 atm CO/H<sub>2</sub> was added (in 25-30 atm increments) to maintain the total pressure at 1000 (±25) atm, the autoclave was allowed to cool to ambient temperature and carefully vented. After discharge from the autoclave the initially clear yellow-orange product solution rapidly became cloudy as excess dissolved carbon monoxide escaped. The organic reaction products were analysed by gas chromatography using a 15% Carbowax 20M on Chromosorb W HP column. In situ spectroscopic measurements were carried out using a Hastelloy C-276 high pressure

infrared cell, the details of which have been described previously (13). Very narrow pathlengths, ca 20-30 $\mu$ , between the cell windows were used in order to minimise the very strong background absorptions due to glacial acetic acid itself. Even under these conditions the maximum useful window only covered the range 2200-1900  $\text{cm}^{-1}$  and thus did not allow the detection of absorptions in the typical "bridging" carbonyl region of the infrared spectrum.

### Results and Discussion

Preliminary Studies. Initial work carried out at 1500 atm pressure and 230-245°C using bulky steel autoclaves with the reactants contained in glass liners indicated that combinations of ruthenium and rhodium, in which rhodium comprised the minor component, could give good selectivities to C<sub>2</sub> products (with molar ethylene glycol/methanol selectivities frequently greater than 1.5/1) particularly when the reaction was carried out in the presence of alkali metal cations as promoters. Subsequently these systems have been studied in greater detail at lower pressures (ca 1000 atm) in silver-lined autoclaves, the use of which has facilitated a high degree of temperature control and has ensured the generation of reliable, highly reproducible data under these severe reaction conditions.

The Ru/Rh/Cs/HOAc Catalyst Composition. Table I illustrates the effect, on product distribution and catalytic activity, of the incremental addition of cesium ions to a catalyst precursor composition containing ruthenium and rhodium, in the molar ratio of 10:1, dissolved in glacial acetic acid. The results of control experiments, in which no cesium is present, are also included. Several points emerge from this Table. First, a small but experimentally significant synergism is observed on the addition of ruthenium to rhodium in the absence of cesium. However, the selectivity to C<sub>2</sub> products is very poor and typical of those reported in other investigations, particularly those in which ruthenium has been used as a catalyst (1). Secondly, the addition of only a very small amount of cesium to this ruthenium/rhodium combination has a profound effect upon the course of the reaction - not only is the selectivity to ethylene glycol acetates dramatically enhanced, partly at the expense of methyl acetate production, but the overall catalytic activity, based on carbon monoxide conversion, almost doubles. The addition of cesium has therefore resulted in the generation of a true promotional effect. Thirdly, both the selectivity to ethylene glycol and the total CO conversion approach a maximum at approximately stoichiometric ratios of cesium to metal; further addition of cesium results in a gradual decrease in both selectivity and activity. Finally, replacement of acetic acid by tetraglyme as solvent at the optimum Ru/Rh/Cs ratio results in a dramatic reduction in both the selectivity to C<sub>2</sub> products and the overall catalyst productivity, the catalyst becoming inferior to that of the unpromoted Ru/Rh/HOAc system. Clearly the combination of metals, acetic acid solvent and promoter are all essential constituents of the composite catalyst for the selective production of C<sub>2</sub> esters.

Table I. Effect of the Addition of Cesium Ions on the Catalytic Activity and Selectivity of the Ru/Rh/HOAc System for the Hydrogenation of Carbon Monoxide<sup>a</sup>

Ru (mmol)	Rh (mmol)	Cs <sup>b</sup> (mmol)	Products (mol/l/hr)			Total CH <sub>2</sub> OH   CH <sub>2</sub> OH	Molar <sup>c</sup> Selectivity	Activity <sup>d</sup>	
			MeOAc	EtOAc	CH <sub>2</sub> OAc   CH <sub>2</sub> OAc				
2.0	-	-	0.180	0.008	0.015	0.002	0.017	0.09	0.23
-	0.2	-	0.175	0.009	0.011	-	0.011	0.06	0.22
2.0	0.2	-	0.419	0.013	0.030	0.008	0.038	0.09	0.52
2.0	0.2	0.2	0.388	0.025	0.214	0.020	0.234	0.60	0.91
2.0	0.2	0.5	0.293	0.024	0.262	0.051	0.313	1.07	0.97
2.0	0.2	1.0	0.250	0.033	0.295	0.054	0.349	1.40	1.01
2.0	0.2	2.0	0.226	0.044	0.307	0.058	0.365	1.62	1.04
2.0	0.2	4.0	0.219	0.060	0.282	0.053	0.335	1.53	1.01
2.0	0.2	8.0	0.212	0.092	0.220	0.037	0.257	1.21	0.91
2.0	0.2	2.0 <sup>e</sup>	0.340	0.010	-	-	0.013	0.04	0.39

a Reaction conditions: 50ml glacial acetic acid solvent, 1000 atm pressure, CO/H<sub>2</sub>(1:1), 230°C, 2-4 hr

b Cesium added as Cs<sub>2</sub>CO<sub>3</sub>·2H<sub>2</sub>O

c Selectivity defined as mol(  $\frac{\text{CH}_2\text{OAc}}{\text{CH}_2\text{OAc} + \frac{\text{CH}_2\text{OAc}}{\text{CH}_2\text{OH}}}$  ) / mol. MeOAc

d Activity defined as CO consumed mol/l/hr

e Acetic acid replaced by tetraglyme; the products are methanol, ethanol and ethylene glycol rather than acetate esters

Ru/Rh/Promoter/HOAc Catalyst Compositions. The behavior described in the previous section is however by no means limited to cesium ions as promoters, nor is it confined to cations of the alkali metal group. It is indeed quite a general phenomenon and some representative examples of the wide range of reaction promoters, which operate with varying degrees of efficacy, are included in Table II. The classes of promoter which have been shown to be effective thus include Groups IA, IIA and IIB metal salts, both weak and strong nitrogen-containing bases, ammonium and tetraalkylammonium salts. The N-bases presumably exist in the quaternised form when dissolved in glacial acetic acid. These catalyst systems are thermally robust and they appear truly homogeneous. The thermodynamically most preferred CO reduction reaction, namely methanation, the occurrence of which is a clear indication of heterogeneously-catalysed behavior, is not observed. The catalyst systems are also highly selective, methyl formate and *n*-propyl acetate being the only other products formed in significant quantities (at typical rates of 0.001-0.005 mol/ℓ/hr) under most reaction conditions, together with trace amounts of carbon dioxide. It is significant that strong nitrogen-containing bases provide effective promoters of these composite catalyst systems because they are normally believed to act as poisons of homogeneously-catalysed reactions e.g. the cobalt-catalysed hydroformylation and hydroesterification of olefins (14). The chemistry of these systems has therefore been investigated in more detail, particularly for the case of triethylamine.

The Ru/Rh/Et<sub>3</sub>N/HOAc Catalyst Composition. Figure 1 illustrates the product distribution as a function of added triethylamine at 1000 atm CO/H<sub>2</sub> (1:1) and 230°C. A comparison between Figure 1 and Table I highlights the strong similarity between cesium and triethylamine as promoters of the reaction. Although the latter is not quite as active or as selective as the former, the most obvious difference is the enhancement in the rate of production of ethyl acetate. Since the ethyl group of triethylamine could potentially act as a source of ethyl acetate, as could the acetic acid solvent, this poses a question concerning the origin of the products and whether or not they are genuinely derived from carbon monoxide. In order to answer this question a radiotracer study using <sup>14</sup>C was undertaken and the results are summarised in Table III. This data is consistent with the presence of the <sup>14</sup>C label on the methyl carbon of methyl acetate and on the methylene carbons of ethylene glycol diacetate respectively, thus conclusively demonstrating that they are indeed primary products of CO hydrogenation. Although the results are not quite as definitive in the case of ethyl acetate, it is clear that at least 90% of this product is derived from carbon monoxide. No radiolabelled hydrocarbons are observed either in the gas phase or in solution and only traces of <sup>14</sup>CO<sub>2</sub> are detected.

Pressure Dependence Studies. The variation of the product distribution as a function of total pressure for the optimum Ru/Rh/Et<sub>3</sub>N/HOAc system at 1000 atm and 230°C is illustrated in Figure 2. As found in much previous work this once again highlights the very strong pressure requirement for the formation of C<sub>2</sub> products, particularly ethylene glycol esters. In contrast however, the rate of formation of methyl acetate is relatively independent of

Table II. Representative Data on the Effect of a Range of Promoters on the Catalytic Activity and Selectivity of the Ru/Rh/HOAc System for the Hydrogenation of Carbon Monoxide<sup>a</sup>

Promoter	Products (mol/l/hr)				Total CH <sub>2</sub> OH   CH <sub>2</sub> OH	Molar Selectivity	Activity
	MeOAc	EtOAc	CH <sub>2</sub> OAc   CH <sub>2</sub> OAc	CH <sub>2</sub> OAc   CH <sub>2</sub> OH			
-	0.419	0.013	0.030	0.008	0.038	0.09	0.52
NaOAc.3H <sub>2</sub> O	0.318	0.037	0.242	0.063	0.305	0.96	1.00
Mg(OAc) <sub>2</sub> .4H <sub>2</sub> O	0.268	0.023	0.137	0.018	0.155	0.58	0.62
Zn(OAc) <sub>2</sub> .2H <sub>2</sub> O	0.318	0.023	0.119	0.022	0.141	0.45	0.65
NH <sub>4</sub> OAc	0.201	0.037	0.238	0.047	0.285	1.42	0.85
pyridine	0.329	0.036	0.251	0.068	0.319	0.97	1.04
2,2'-bipyridyl	0.296	0.085	0.115	0.015	0.130	0.44	0.73
4,4'-bipyridyl	0.218	0.055	0.242	0.067	0.309	1.42	0.95
diethylformamide	0.232	0.062	0.298	0.041	0.339	1.47	1.03
triethylamine	0.211	0.065	0.240	0.036	0.276	1.31	0.89
ethylenediamine	0.219	0.054	0.327	0.036	0.363	1.66	1.05
N,N',N'-tetraethyl- ethylenediamine	0.183	0.085	0.276	0.034	0.310	1.69	0.97
ethylenediaminetetra- acetic acid	0.307	0.035	0.212	0.046	0.258	0.84	0.89

<sup>a</sup> Reaction conditions: Ru(2.0 mmol), Rh (0.2mmol), promoter (2.0 mmol) glacial acetic acid (50 ml) 1000 atm pressure, CO/H<sub>2</sub> (1:1), 230°C, 2-4 hr reaction time.

Selectivity and activity definitions are the same as in Table 1.

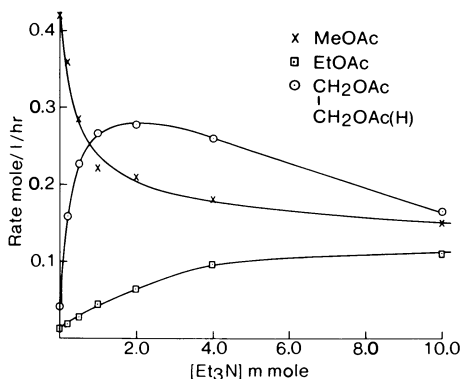


Figure 1 Product distribution as a function of added triethylamine in the Ru/Rh/Et<sub>3</sub>N/HOAc catalyst composition. Reaction conditions: Ru (2.0 mmol), Rh (0.2 mmol), glacial acetic acid (50 ml), 1000 atm CO/H<sub>2</sub> (1:1), 230°C.

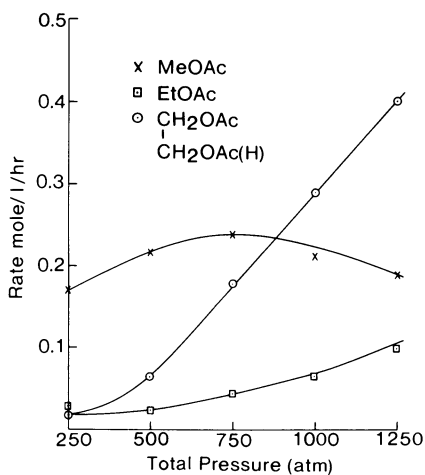


Figure 2 Product distribution as a function of pressure in the Ru/Rh/Et<sub>3</sub>N/HOAc catalyst composition. Reaction conditions: Ru (2.0 mmol), Rh (0.2 mmol), Et<sub>3</sub>N (2.0 mmol), glacial acetic acid (50 ml), CO/H<sub>2</sub> (1:1), 230°C.

Table III.  $^{14}\text{C}$ -Radiotracer Study of the Ru/Rh/ $\text{Et}_3\text{N}$ /HOAc System for the Hydrogenation of Carbon Monoxide<sup>a, b</sup>Specific activity of CO feed: 0.705  $\mu\text{Ci}/\text{mmol}$ 

Products	Yield (g)	mmol	Specific Activity ( $\mu\text{Ci}/\text{mmol}$ )	Product S.A./CO S.A.
MeOAc	1.58	21.3	0.72	1.02
EtOAc	0.53	6.0	1.31	1.86
CH <sub>2</sub> OAc	4.84	33.1	1.46	2.07
CH <sub>2</sub> OAc				

<sup>a</sup> With D.G. Parker and R.A. McReddie, ICI Physics and Radioisotopes Services, Billingham

<sup>b</sup> Reaction conditions: Ru(2.0 mmol), Rh(0.2 mmol),  $\text{Et}_3\text{N}$  (2.0 mmol), glacial acetic acid (50 ml), 1000 atm  $\text{CO}/\text{H}_2$ , 230°C, 2 hr.

pressure over the range 250-1250 atm. This behavior is quite distinct from that exhibited by separate rhodium and ruthenium catalysts where both  $\text{C}_1$  and  $\text{C}_2$  products show very similar pressure dependence (1).

Temperature Dependence Studies. Figure 3 illustrates the effect of temperature on the product distribution of the Ru/Rh/ $\text{Et}_3\text{N}$ /HOAc system at 1000 atm total pressure. Thus the rate of product formation increases steadily with increasing temperature over the range 190-245°C, at which point the rate of formation of ethylene glycol acetates passes through a maximum. This is not accompanied by any evidence of catalyst decomposition and must be a consequence of a change in reaction mechanism. Such behavior is not paralleled in the cesium promoted system where the rate of formation of all products increases up to temperatures in excess of 260°C. This difference could possibly be accounted for by an irreversible reaction/loss of the organic promoter, e.g. by Hofmann degradation of the triethylammonium cation, occurring at the higher temperatures (above 245°C). Arrhenius plots on the triethylamine-promoted catalyst yield apparent activation energies of ca 26 and 37 kcal/mole for ethylene glycol acetate and methyl acetate formation respectively. Both are quite high in relation to the values of ca 18 kcal/mole observed with rhodium catalysts and 32 kcal/mole for methanol formation with ruthenium (1).

Concentration Dependence Studies. The variation of the product distribution as a function of total metal concentration, at a fixed ruthenium:rhodium:triethylamine ratio of 10:1:10, under the standard reaction conditions of 1000 atm and 230°C is illustrated in Figure 4. Thus the rate of product formation increases linearly with respect to increasing concentration up to ca 2.5 mmoles total metal above which the rate levels off. A plot of turnover (total carbon monoxide



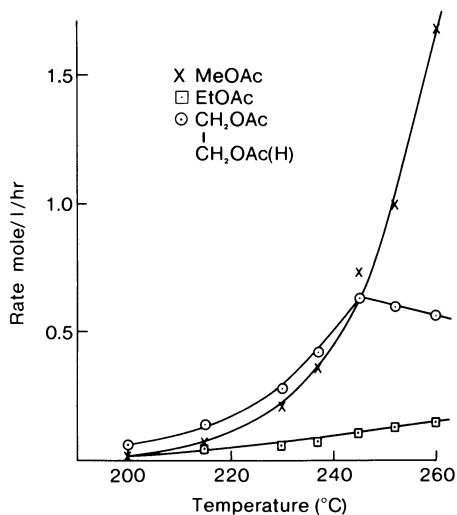


Figure 3 Product distribution as a function of temperature in the Ru/Rh/Et<sub>3</sub>N/HOAc catalyst composition. Reaction conditions: Ru(2.0 mmol), Rh(0.2mmol), Et<sub>3</sub>N(2.0 mmol), glacial acetic acid (50ml), 1000 atm CO/H<sub>2</sub> (1:1)

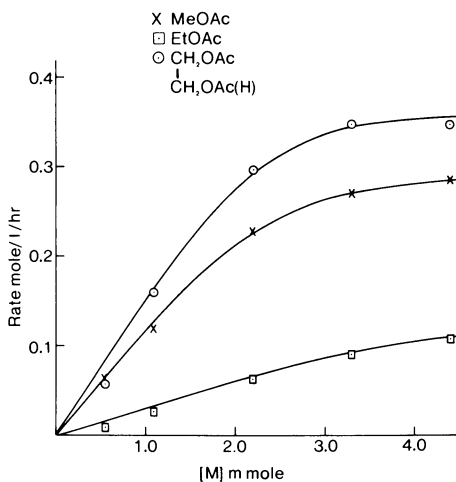


Figure 4 Product distribution as a function of metal concentration in the Ru/Rh/Et<sub>3</sub>N/HOAc catalyst composition. Reaction conditions: 1000 atm CO/H<sub>2</sub>(1:1), 230°C; Ru:Rh:Et<sub>3</sub>N::10:1:10

consumed per unit metal) against metal concentration shows an approximately linear decrease with increasing  $[M]$ , behavior which is perhaps consistent with catalysis by more highly dissociated metal centres (as distinct from clustered species) (15).

Ru/Et<sub>3</sub>N/HOAc and Rh/Et<sub>3</sub>N/HOAc Catalyst Compositions. As will be apparent from the previously-described behavior these are very complex catalyst systems and the origins of the promoter effects on catalytic activity and selectivity are not understood. In an attempt to unravel some of the chemistry we have investigated the behavior of the separate ruthenium and rhodium catalyst components under similar reaction conditions. The results (Figure 5) indicate that the major influence of the promoter on the product selectivity is associated with the rhodium component. Thus the effect of the incremental addition of triethylamine (Figure 5a) closely parallels that observed with the composite ruthenium/rhodium catalyst (Figure 1). By contrast, in the corresponding series of experiments with ruthenium (Figure 5b) the addition of triethylamine has essentially no effect. It is significant that the catalytic activity of the Rh/Et<sub>3</sub>N system, at the relatively low rhodium concentrations used, is quite high in comparison with previously published work.

A closer inspection of Figures 1 and 5 also serves to emphasise the lack of additive behavior when the two metal/promoter components are combined; the total catalytic activity in particular is significantly enhanced. Truly synergistic effects are therefore occurring. Thus, although the minor component (Rh/promoter) of the composite catalyst is apparently controlling the product selectivity, the presence of the major component (Ru) has the effect of doubling the activity displayed by the rhodium/promoter system alone. This behavior contrasts directly with that of Knifton's work on homogeneous bimetallic ruthenium/rhodium melt catalyst compositions for the production of oxygenates directly from synthesis gas (6). Here the presence of ruthenium was considered to be essential for the formation of ethylene glycol whereas the presence of rhodium contributed to improved productivity.

High Pressure Fourier Transform Infrared Spectroscopic Data. Infrared spectroscopic measurements were made, with difficulty, in glacial acetic acid solutions of the separate ruthenium and rhodium components, and of the composite catalyst system, at pressures and temperatures approaching those under which the catalytic reactions were investigated. The effective spectral range was limited to the window 2200-1900 cm<sup>-1</sup> imposed by the strongly absorbing background spectrum of glacial acetic acid. Some typical spectra for the ruthenium systems and for the composite Ru/Rh/Et<sub>3</sub>N catalyst are illustrated in Figures 6 and 7 respectively; a summary of our interpretation of the spectroscopic data is presented in Table IV.

A qualitative correlation between the catalytic and spectroscopic data is apparent. For example, the Ru and Ru/Et<sub>3</sub>N systems display both very similar catalytic behavior (see Figure 5b) and spectra at 180-200°C (Figure 6); the major species present in solution appears to be  $[\text{Ru}(\text{CO})_3\text{OAc}]_2$  (16) in both cases together with  $\text{Ru}(\text{CO})_5$  and small amounts of  $\text{Ru}_3(\text{CO})_{12}$ . Indeed, a mixture of yellow  $[\text{Ru}(\text{CO})_2(\text{OAc})]_n$  and orange  $\text{Ru}_3(\text{CO})_{12}$  crystallises from the reaction solution after cooling and venting the excess pressure from a typical

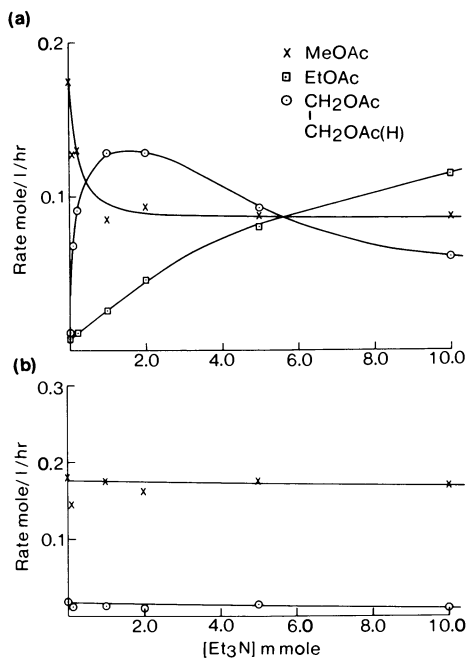


Figure 5 Product distribution as a function of added triethylamine in a) the Rh/Et<sub>3</sub>N/HOAc and b) Ru/Et<sub>3</sub>N/HOAc catalyst compositions. Reaction conditions: a) Rh (0.2 mmol), b) Ru (2.0 mmol), glacial acetic acid (50 ml), 1000 atm CO/H<sub>2</sub> (1:1), 230°C.

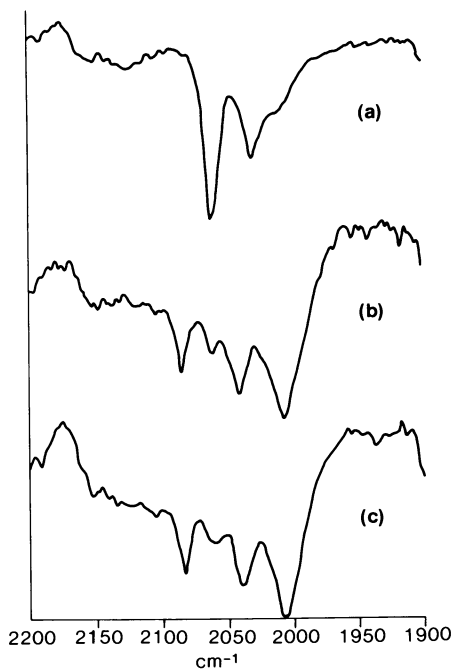


Figure 6 High pressure Fourier transform infrared spectroscopic data. Catalyst precursors: (i)  $\text{Ru}_3(\text{CO})_{12}$  in glacial acetic acid, a) 600 atm  $\text{CO}/\text{H}_2$ , 100°C, b) 760 atm, 180°C; (ii)  $\text{Ru}_3(\text{CO})_{12}/\text{Et}_3\text{N}$  in glacial acetic acid, c) 700 atm  $\text{CO}/\text{H}_2$ , 200°C.

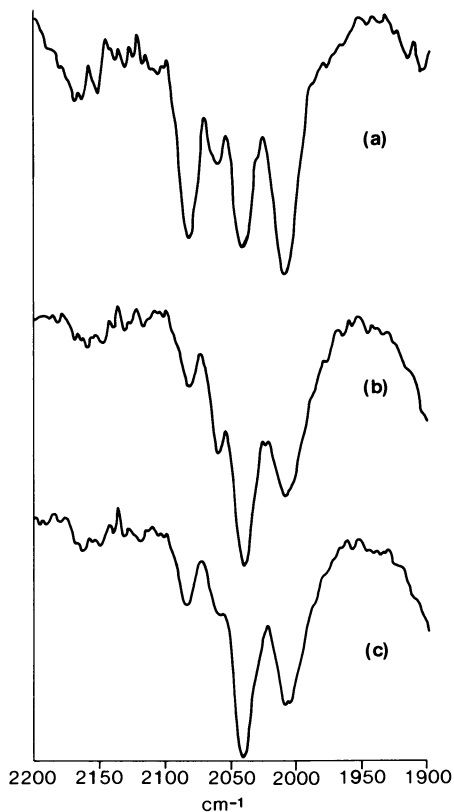


Figure 7 High pressure Fourier transform infrared spectroscopic data. Catalyst precursor:  $\text{Ru}_3(\text{CO})_{12}$ ,  $\text{Rh}(\text{CO})_2\text{acac}$ ,  $\text{Et}_3\text{N}$  (Ru:Rh: $\text{Et}_3\text{N}$ ::10:1:10) in glacial acetic acid. Reaction conditions: (a) 750 atm, 100°C, (b) 850 atm, 175°C, (c) 880 atm, 200°C

Table IV. Summary of Interpretation of High Pressure FT IR Data

Catalyst Components	Pressure (atm)	Temp (°C)	Species Present
Ru	600	100	$\text{Ru}_3(\text{CO})_{12}$
Ru	760	180	$[\text{Ru}(\text{CO})_3\text{OAc}]_2, \text{Ru}(\text{CO})_5, \text{Ru}_3(\text{CO})_{12}$
Ru/ $\text{Et}_3\text{N}$	700	200	$[\text{Ru}(\text{CO})_3\text{OAc}]_2, \text{Ru}(\text{CO})_5, \text{Ru}_3(\text{CO})_{12}$
Rh	680	175	$\text{Rh}_6(\text{CO})_{16}$
Rh/ $\text{Et}_3\text{N}$	750	200	$\text{Rh}_6(\text{CO})_{16}, [\text{Rh}_6(\text{CO})_{15}\text{X}]^-$
Ru/Rh	740	200	$[\text{Ru}(\text{CO})_3\text{OAc}]_2, \text{Ru}(\text{CO})_5, \text{Ru}_3(\text{CO})_{12}, \text{HRu}(\text{CO})_3\text{OAc}?, [\text{Rh}_6(\text{CO})_{15}\text{X}]^-?$
Ru/Rh/ $\text{Et}_3\text{N}$	880	200	$\text{HRu}(\text{CO})_3\text{OAc}, \text{Ru}(\text{CO})_5, [\text{Ru}(\text{CO})_3\text{OAc}]_2, \text{Ru}_3(\text{CO})_{12}, [\text{Rh}_6(\text{CO})_{15}\text{X}]^-?$

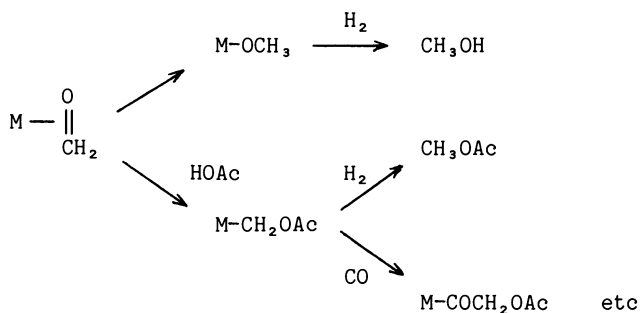
autoclave run. By contrast, in the rhodium system, where the addition of triethylamine to rhodium results in an abrupt change in selectivity in favour of the  $\text{C}_2$  products (Figure 5a), distinct spectroscopic differences are apparent. In the unpromoted system rhodium appears to be present in solution in the form  $\text{Rh}_6(\text{CO})_{16}$  whereas the addition of triethylamine results in the appearance of a new absorption at  $2040\text{ cm}^{-1}$  and a reduction in intensity of the  $2077\text{ cm}^{-1}$  peak due to  $\text{Rh}_6(\text{CO})_{16}$ . This new absorption has been interpreted in terms of the presence of the species  $[\text{Rh}_6(\text{CO})_{15}\text{X}]^-$ ,  $\text{X} = \text{H}$  and/or  $\text{OAc}$  (17), in which the counterion is presumably triethylammonium.

In the composite Ru/Rh catalyst (Figure 7), a peak at  $2040\text{ cm}^{-1}$  dominates the spectrum. Absorptions which are consistent with the presence of small amounts of species observed in the separate experiments are also noted in the spectra of the composite systems. The most likely assignment of the  $2040\text{ cm}^{-1}$  band is to a ruthenium species (the concentration of ruthenium is, of course, tenfold in excess over rhodium), which is closely related to the dimer  $[\text{Ru}(\text{CO})_3\text{OAc}]_2$  identified in the experiments containing ruthenium alone. After due consideration of absorption positions and band intensities, the most likely candidate appears to be a species of the type  $\text{HRu}(\text{CO})_n\text{OAc}$  ( $n=3$  or  $4$ ) formed by a homolytic cleavage reaction between  $[\text{Ru}(\text{CO})_3\text{OAc}]_2$  and hydrogen, presumably mediated by the presence of the rhodium complex in solution. Alternative species such as mixed-metal clusters of the type  $\text{H}_2\text{Ru}_2\text{Rh}_2(\text{CO})_{12}$  (18, 19), are unlikely to be major components of the solution, for the following reasons. First, the inconsistency between the observed spectra and the strongest  $\nu(\text{CO})$  absorptions reported for  $\text{H}_2\text{Ru}_2\text{Rh}_2(\text{CO})_{12}$  ( $2084, 2064$  and  $2056\text{ cm}^{-1}$ ) and  $\text{HRuRh}_3(\text{CO})_{12}$  ( $2077, 2067\text{ cm}^{-1}$ ) in hexane solution. Secondly, such neutral mixed species are unlikely to be stable (relative to mixtures of homonuclear ruthenium and rhodium derivatives, which would contain higher  $\text{CO}/\text{M}$  ratios) in acetic acid solution under the severe reaction conditions used, particularly the

high pressures of carbon monoxide and hydrogen (20). Finally, the preferred Ru/Rh stoichiometry of 10:1 is inconsistent with the presence of such mixed clusters. There is no spectroscopic evidence for the presence of  $[\text{Rh}(\text{CO})_4]^-$ , recently implicated by Japanese workers (21) in the production of ethylene glycol from synthesis gas.

Origin of Synergistic Effects. The question arises concerning the origin of the observed synergism in catalytic activity in these complex systems. A positive dependence on hydrogen partial pressure for all the products, which has been demonstrated in separate experiments, suggests that hydrogen activation is a key feature, and probably the rate-determining step, in the catalytic cycle for the reduction of carbon monoxide. The most likely explanation of the origin of the co-operative effects therefore resides in an acceleration of this hydrogen activation step, presumably through intermolecular interactions. Some support for this conclusion derives from the high pressure infrared spectroscopic data discussed above. Thus the predominance, in the composite catalyst system, of species of the type  $\text{HRu}(\text{CO})_n\text{OAc}$  under reaction conditions may result in the facilitation of hydride transfer to a coordinated carbonyl group, probably (although not necessarily) of the rhodium-containing moiety, with a consequent acceleration of the overall reaction rate.

The explanation of the key role played by acetic acid itself may be as proposed by Dombek (1). In this, the presumed coordinated formaldehyde intermediate, as the primary product of CO reduction, is preferentially acylated to produce a carbon bound acyloxymethyl group leading to the sequence of reactions shown in the lower half of the reaction scheme:



The acylation and subsequent "CO insertion" steps may be catalysed by the promoter. Thus the formation of  $\text{CH}_3\text{OH}$  (or  $\text{CH}_3\text{OAc}$ ) via a methoxide intermediate is suppressed. Finally, the CO-labilising ability of the acetate ion (22) almost certainly plays an important role in these reactions.

### Conclusions

Although the mechanistic details are far from clear, these bimetallic promoted catalysts combine some inherent advantages of the separate ruthenium- and rhodium-based systems (1). For example, comparable

activities and selectivities to those of the rhodium-based catalysts are achieved but at approximately only one quarter of the rhodium concentration. In addition the enhanced thermal stability associated with ruthenium dominates the behavior of the composite catalyst and thus the instability which is a characteristic of the rhodium systems is not a problem. The generation of products as acetate esters gives a more versatile product stream in terms of subsequent processing, eg the conversion into ethylene oxide and vinyl acetate, in addition to ethylene glycol. Against this has to be set the additional processing step required and the corrosive nature of acetic acid. Finally, the pressure constraint on the production of C<sub>2</sub> molecules is a problem which has yet to be overcome in any of these homogeneously-catalysed reductions of carbon monoxide.

#### Acknowledgments

The authors gratefully acknowledge the help of Dr. D.G. Parker and Mr. R.A. McReddie of ICI Physics and Radioisotope Services, Billingham, in the <sup>14</sup>C radiotracer experiment.

#### Literature Cited

1. Dombek, B.D. J. Catal. 1983, 32, 326, and references therein.
2. Whyman, R. European Patent 1981, 33,425, to ICI plc.
3. Whyman, R. J.C.S. Chem. Comm. 1983, 1439.
4. Head, R.A.; Whyman, R. European Patent 1983, 98,031, to ICI plc.
5. Knifton, J.F. U.S. Patent 1982, 4,315,994, to Texaco, Inc.
6. Knifton, J.F. J.C.S. Chem. Comm. 1983, 729.
7. Kiso, Y.; Nakamura, H.; Saeki, K. Japanese Patent Application 1982, 57/128,644, to Mitsui Petrochemical Industries.
8. Dombek B.D.; Hart, P.W.; O'Connor, G.L. European Patent Applications 1983, 75,937; 85,191, to Union Carbide Corporation.
9. Dombek, B.D. Organometallics 1985, 4, 1707.
10. Johnson, B.F.G.; Lewis, J. Inorg Syntheses 1972, 13, 92.
11. Chaston, S.H.H.; Stone, F.G.A. J. Chem. Soc. (A) 1969, 500.
12. Bonati, F.; Wilkinson, G. J. Chem. Soc. 1964, 3156.
13. Whyman, R.; Hunt, K.A.; Page, R.W.; Rigby, S. J. Phys. E: Sci. Instrum. 1984, 17, 559.
14. Forster, D.; Hershman, R.; Morris, D.E. Catal. Rev. - Sci. Eng. 1981, 23, 89.
15. Laine, R.M. Preprints, ACS Division of Petroleum Chemistry 1980, 25, 704.
16. Crooks, G.R.; Johnson, B.F.G.; Lewis, J.; Williams, I.G.; Gamlen, G. J. Chem. Soc. (A) 1969, 2761.
17. Chini, P.; Martinengo, S.; Giordano, G. Gazz. Chim. Ital. 1972, 102, 330, 344.
18. Pursiainen, J.; Pakkanen, T.A. J.C.S. Chem. Comm. 1984, 252.
19. Pursiainen, J.; Pakkanen, T.A.; Jääskeläinen, J. J. Organometal. Chem. 1985, 290, 85.



20. Gladfelter, W.L.; Geoffroy, G.L. Adv. Organometal. Chem. 1980, 18, 207.
21. Watanabe, E.; Murayama, K.; Hara, Y.; Kobayashi, Y.; Wada, K.; Onoda, T. J.C.S. Chem. Comm. 1986, 227.
22. Cotton, F.A.; Darensbourg, D.J.; Kolthammer, B.W.S. J. Am. Chem. Soc. 1981, 103, 398.

RECEIVED July 29, 1986

## Chapter 9

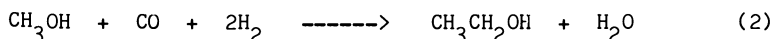
# Acetaldehyde Production by Reductive Carbonylation of Methanol, Methyl Ketals, and Methyl Esters

Richard W. Wegman, David C. Busby, and John B. Letts

Union Carbide Corporation, P.O. Box 8361, South Charleston, WV 25303

Acetaldehyde is obtained from the reaction of synthesis gas with methanol, methyl ketals or methyl esters. The reactions are carried out with an iodide-promoted Co catalyst at 180–200 °C and 2000–5000 psig. In comparing the various feedstocks, the best overall process to make acetaldehyde involves the reductive carbonylation of methyl esters. In this case, acetaldehyde selectivities are > 95% at acceptable rates and conversion.

The reductive carbonylation (Equation 1) and homologation (Equation 2) of methanol are reactions of considerable interest to the chemical industry (1). These reactions provide a route to

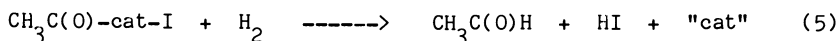
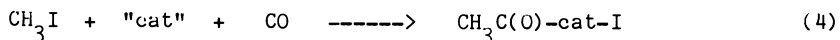


acetaldehyde and ethanol from non-petroleum-derived synthesis gas. Acetaldehyde can be used as a building block for numerous chemicals, for instance (i) condensation to higher aldehydes and alcohols, (ii) esters via the Tischenko reaction, specifically formation of ethyl acetate which can be readily cracked to ethylene and acetic acid, and (iii) vinyl ethers from various acetal derivatives. The main thought with ethanol is that it would provide a synthesis gas based route to ethylene.

The homologation reaction was first reported nearly 40 years ago (2). The catalyst precursor was  $\text{Co}_2(\text{CO})_8$ . Subsequent workers utilized cobalt catalysts but also employed iodide promoters (3,4), a Ru co-catalyst (5), and trivalent phosphines (6) to increase the yield. The reaction is carried out at 180–200 °C and 4000–8000 psig. In the better cases, the ethanol rate and selectivity are 1–6 M/hr and 50–80 %. Unsatisfactory conversion, selectivity, and the required high operating pressure have prevented commercialization of the current homologation technology. Additionally, fermentation routes to ethanol have now

become economically competitive with a synthesis gas-based process (7,8).

Less attention has been given to the reductive carbonylation reaction in the literature. The reaction is catalyzed, at least to some extent, by most Group VIII metals used in conjunction with an iodide promoter (9). The highest rates and selectivities are obtained with cobalt-based catalysts. In addition to Co-I, promoters of the form ER<sub>3</sub> (E = N, P, As, Sb, Bi; R = organic moiety) are frequently used. Several studies have been published that describe the effect of catalyst concentration, solvent, temperature, and pressure on the Co-I-ER<sub>3</sub> catalyzed reaction (6,10-13). In general, reasonable rates are obtained when the reaction is carried out at 160-180 °C and 3000-5000 psig. A simplified version of the generally accepted mechanism leading to the formation of acetaldehyde is shown in Equations 3-5 (14).



"Cat" represents the catalyst and is thought to be a cobalt compound containing iodide, CO, and, if applicable, ER<sub>3</sub> ligands. The homologation reaction proceeds via a similar mechanism except acetaldehyde is further reduced in situ to ethanol.

We have studied the Co-I-PPh<sub>3</sub> catalyzed reductive carbonylation of methanol, dimethyl ketals, dimethyl carbonate and methyl esters (10,15,16). Our goal was to achieve high acetaldehyde selectivity while maintaining a reasonable rate of product formation. The effect of reaction variables and the advantages and disadvantages of each feedstock are discussed.

### Experimental

All chemicals were reagent grade and used without further purification. The batch experiments were carried out in a 300 ml Hastelloy C autoclave. In a typical experiment Co(OAc)<sub>2</sub> · 4H<sub>2</sub>O (8.0 mmol), I<sub>2</sub> (14.0 mmol) and PPh<sub>3</sub> (30.8 mmol) are charged under N<sub>2</sub> to a clean reactor containing 150 ml CH<sub>3</sub>OH. The reactor is sealed, purged with synthesis gas and pressured to 2000 psig with synthesis gas. Agitation (750 rpm) is begun and the reactor heated to the desired temperature in 40 min. At reaction temperature the reactor is pressured to 5250 psig. The reaction is allowed to consume gas until the pressure has fallen to 4750 psig. The reactor is repressured to 5250 psig and cycled in this manner for 10000 psi total uptake. The reactor contents are then cooled via internal cooling coils to 10 °C. A vapor phase sample is taken for analysis, and the liquid contents are placed in a chilled bottle. A similar procedure was utilized with dimethylketals, dimethyl carbonate, and methyl ester feedstocks.

The liquid products obtained in the batch and semicontinuous experiments were analyzed with a Hewlett-Packard Model 5880 gas chromatograph equipped with two 1/8 in x 10 ft 60/70 mesh Chromasorb 101 columns connected in series.

Rates and selectivities were calculated as previously described (10).

### Discussion

Reductive Carbonylation of Methanol. The reductive carbonylation of methanol (solvent free) was studied at variable I/Co,  $\text{PPh}_3/\text{I}$ , temperature, pressure, synthesis gas ratio and methanol conversion (gas uptake) in the batch reactor. A summary of the results is given in Table I. In general, the acetaldehyde rate and selectivity increase with increasing I/Co. The  $\text{PPh}_3/\text{I}$  ratio has little effect except in run #7 where the rate is drastically reduced at I/Co = 3.5 and  $\text{PPh}_3/\text{I} = 2$ . A good set of conditions is I/Co = 3.5 and  $\text{PPh}_3/\text{I} = 1.1$  where the acetaldehyde rate and selectivity is 7.6 M/hr and 76% at 170 °C and 5000 psig. The effect of methanol conversion at these conditions is obtained by comparing runs 13, 14, and 15. The gas uptake was varied from 14000 to 4000 psi, which corresponds to observed methanol conversions of 68% to 38%.

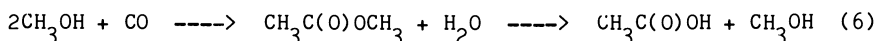
The most notable feature about the data is the acetaldehyde rate, which increases with decreasing methanol conversion. For example, a rate of 17.5 M/hr is obtained at a conversion of 38%. There are numerous explanations for this trend, including product inhibition of the catalyst or rate dependence on methanol concentration. However, the important point is that when comparing any data dealing with this reaction, the conversions must be similar in order to draw meaningful conclusions.

Increasing the temperature from 170–210 °C at I/Co = 3.5,  $\text{PPh}_3/\text{I} = 1.1$  and  $\text{H}_2/\text{CO} = 1.5$  results in lower acetaldehyde rate and selectivity. At 170 °C acetaldehyde and methyl acetate account for 91% of the products. Other products include ethanol (4%), dimethyl ether (2%), methane (1%), and trace amounts of crotonaldehyde, *n*-butanol and other minor components. At the higher temperatures, dimethyl ether and methane markedly increase. For example, at 210 °C their selectivities are 30 and 20%, respectively. This change in selectivity to less desirable products is accompanied by a reduction in the overall rate of conversion of methanol. Similar results were reported by Roper, Loevenich, and Korff for  $\text{Co}(\text{OAc})_2/\text{I}_2/\text{PPh}_3$  and cobalt-phosphine complexes such as  $\text{CoI}_2(\text{PPh}_3)_2$  (12). Our investigation of cobalt complexes  $\text{CoI}_2(\text{PPh}_3)_2$ ,  $\text{CoI}_2(\text{OPPh}_3)_2$ , and  $[\text{MePPh}_3]_2[\text{CoI}_4]$  also found declining activity as temperature increased above 190 °C, but the effect was more severe with the latter two indicating catalyst instability is a likely cause (10). The formation of cobalt metal would explain the increased production of methane observed.

Reaction pressure is also a significant variable. The reaction is best carried out at 5000 psig but will proceed at 3000 psig with reduced acetaldehyde rate and the same overall response to the reaction variables reported in Table I for 5000 psig. Below 2000 psig the acetaldehyde rate is less than 1.0 M/hr.

Methyl acetate is the principal by-product in the reductive carbonylation of methanol. As indicated in Table I, decreasing the  $\text{H}_2/\text{CO}$  increases the methyl acetate selectivity. In the limit of pure CO, methyl acetate is obtained in 90–95% selectivity.

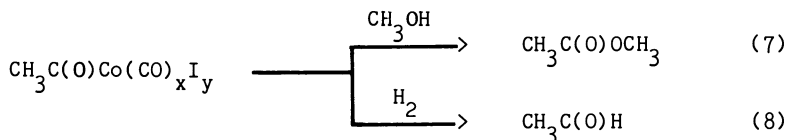
Carbonylation of methanol, Equation 6, is a well-known reaction.



BASF operates a commercial process with a Co-I catalyst at 210 °C and 10000 psig (17). The main product is acetic acid with rates and selectivities of 1-4 M/hr and 90-93%. In the late 1960s, Monsanto developed a Rh-I catalyst that operates at significantly lower pressure (18). In their process, the reaction is carried out at 180-200 °C and 500 psig with acetic acid rates and selectivities of 10-30 M/hr and 95-99%.

Since there is little known about Co-I-PPh<sub>3</sub> as a carbonylation catalyst, we studied the reaction of methanol with CO in some detail. A summary of the results is given in Table II.

The overall response to the reaction variables is very similar in the carbonylation and reductive carbonylation reactions. This may indicate similar catalysts and reaction mechanisms. In the carbonylation reaction Co(CO)<sub>4</sub><sup>-</sup> was identified by its characteristic CO stretching frequency (ν(CO) = 1890 cm<sup>-1</sup>) as the dominant species present in high pressure infrared experiments carried out at 170 °C and 5000 psig. Similar results were obtained in the reductive carbonylation of methanol. It is known that Co(CO)<sub>4</sub><sup>-</sup> rapidly reacts with CH<sub>3</sub>I to yield CH<sub>3</sub>C(O)Co(CO)<sub>4</sub> (19); however, in the carbonylation and reductive carbonylation reactions acyl-cobalt complexes are not observed by infrared under catalytic conditions. This indicates that once formed, the acyl complex rapidly reacts as outlined by Equations 7 and 8.



Methyl acetate probably originates from the reaction of methanol with the intermediate cobalt-acyl complex. The reaction leading to the formation of acetaldehyde is not well understood. In Equation 8, H<sub>2</sub> is shown as the reducing agent; however, metal carbonyl hydrides are known to react with metal acyl complexes (20-22). For example, Marko et al. has recently reported on the reaction of n-butyryl- and isobutyrylcobalt tetracarbonyl complexes with HCo(CO)<sub>4</sub> and H<sub>2</sub> (23). They found that at 25 °C rate constants for the reactions with HCo(CO)<sub>4</sub> are about 30 times larger than those with H<sub>2</sub>; however, they observed that under hydroformylation conditions, reaction with H<sub>2</sub> is the predominant pathway because of the greater concentration of H<sub>2</sub> and the stronger temperature dependence of its rate constant. The same considerations apply in the case of reductive carbonylation. Additionally, we have found that CH<sub>3</sub>C(O)Co(CO)<sub>3</sub>L (L = PBu<sub>3</sub>, PPh<sub>2</sub>CH<sub>3</sub>) reacts with H<sub>2</sub> (Equation 8) but not with the corresponding HCo(CO)<sub>3</sub>L and that the reaction of CH<sub>3</sub>C(O)Co(CO)<sub>3</sub>PPh<sub>3</sub> with HCo(CO)<sub>4</sub> and HCo(CO)<sub>3</sub>PR<sub>3</sub> (R = Bu, Ph) results only in the decomposition of the cobalt hydrides. The reaction of CH<sub>3</sub>C(O)Co(CO)<sub>3</sub>PPh<sub>3</sub> with HSiR<sub>3</sub>, HSnR<sub>3</sub> or H<sub>2</sub> yields acetaldehyde according to the following postulated mechanism (X = SiR<sub>3</sub>, SnR<sub>3</sub>, H) (24).

Table I. The Effect of Reaction Variables in the Reductive Carbonylation of Methanol

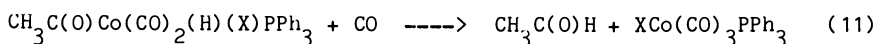
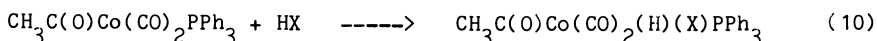
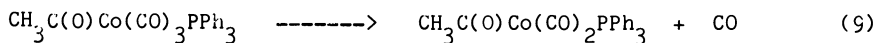
Run#	I/Co	P/I	Temp., °C.	H <sub>2</sub> /CO	Uptake, psi	ACh rate	Sel %	
							ACh	MeOAc
1	1.0	0.5	170	1:1	10000	4.2	68	20
2	1.0	2.0	170	1:1	10000	3.8	73	17
3	2.0	0.5	170	1:1	10000	5.4	79	14
4	2.0	2.0	170	1:1	10000	5.3	78	14
5	3.5	0.5	170	1:1	10000	6.1	74	18
6	3.5	1.1	170	1:1	10000	7.6	76	15
7	3.5	2.0	170	1:1	10000	0.9	76	15
8	3.5	1.1	170	1.5:1	10000	6.1	83	9
9	3.5	1.1	170	0.75:1	10000	11.4	72	20
10	3.5	1.1	170	0.5:1	10000	10.1	52	41
11	3.5	1.1	190	1.5:1	10000	1.2	48	16
12	3.5	1.1	210	1.5:1	10000	0.5	23	14
13	3.5	1.1	170	1:1	14000	3.8	75	17
14	3.5	1.1	170	1:1	7000	12.2	76	13
15	3.5	1.1	170	1:1	4000	17.5	76	13

All runs at 5000 psig with [Co] = 0.052 M, P = PPh<sub>3</sub>, and I = total iodide charged. Rates are reported as M/hr.

Table II. The Effect of Reaction Variables in the Carbonylation of Methanol

I/Co	P/I	Temp., °C	CH <sub>2</sub> OH Conv., %	MeOAc	
				Rate	Sel., %
2.0	0.5	170	60.7	2.0	93.3
2.0	1.1	170	61.6	2.9	92.8
3.5	0.5	170	60.2	1.7	87.7
3.5	1.1	170	61.5	4.0	94.1
3.5	1.1	170	25.1	7.4	95.7
3.5	1.1	170	47.2	5.3	95.4
3.5	1.1	170	83.4	2.6	93.2
3.5	1.1	210	59.5	4.7	93.5
3.5	1.1	180	61.7	3.2	93.9

All runs = 5000 psig CO; [Co]=0.052M, P=PPh<sub>3</sub>, and I = total iodide. Rates are reported as M/hr.



At constant CO partial pressure, the rate determining step is a function of the HX bond strength. In the case of  $\text{HSnR}_3$ , the rate determining step is CO dissociation, Equation 9. For  $\text{HSiR}_3$  and  $\text{H}_2$ , it is the oxidative addition step, Equation 10.

Assuming the reductive carbonylation of methanol proceeds according to the generalized Equations 3-5 and 7-8, then we can speculate on the nature of the acetaldehyde producing step under catalytic conditions. According to high-pressure infrared (170 °C and 5000 psig)  $\text{Co}(\text{CO})_4^-$  accounts for approximately 95% of the charged cobalt in the Co-I-PPh<sub>3</sub> catalyzed reaction (10). Trace amounts of  $\text{HCo}(\text{CO})_4$  are observed with no indication of a cobalt acyl complex. If we assume that the upper limit concentrations of the cobalt-acyl species and  $\text{HCo}(\text{CO})_4$  are 1 and 4% of the total cobalt charged (0.053 M), then, with a partial pressure of 2500 psi  $\text{H}_2$ , concentrations will vary as  $[\text{H}_2] (0.9 \text{ M}) \gg [\text{HCo}(\text{CO})_4] (0.002 \text{ M}) \gg [\text{cobalt-acyl}] (0.00053 \text{ M})$ .  $\text{H}_2$  and possibly  $\text{HCo}(\text{CO})_4$  are in relatively large excess so that once formed, the cobalt-acyl complex is rapidly cleaved. This step may occur as outlined in Equations 9-11. Based on the reported work of Marko et al. (23), cleavage should be at least an order of magnitude faster with  $\text{HCo}(\text{CO})_4$ ; however, the  $\text{H}_2:\text{HCo}(\text{CO})_4$  mole ratio is at least 100:1 so it is more likely that cleavage via  $\text{H}_2$ , as shown in Equation 8, is the dominant reaction. Therefore,  $\text{H}_2$  competes with methanol for reaction with the cobalt-acyl complex. Decreasing the  $[\text{H}_2]$  by decreasing the  $\text{H}_2/\text{CO}$  ratio increases the amount of methyl acetate formed. In the absence of added  $\text{H}_2$ , methyl acetate is the sole product.

The methyl acetate forming reaction can be suppressed by increasing the  $\text{H}_2$  partial pressure or by decreasing the initial methanol concentration. Increasing the  $\text{H}_2$  partial pressure requires an overall increase in the operating pressure and also increases the amount of by-product ethanol. A significant gain in acetaldehyde selectivity is not observed. Decreasing the methanol concentration is readily accomplished by utilizing a solvent. In this case the acetaldehyde selectivity is improved. The results of experiments carried out with various solvents are given in Table III.

In general, the best acetaldehyde rates and selectivities, typically 3-5 M/hr and 80-90%, are obtained in ethers and polyethers. Relative to the solvent-free case (methanol only) the rate is somewhat lower and the selectivity is normally 10% higher.

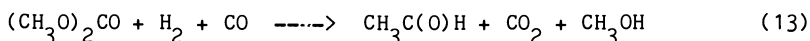
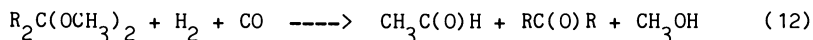
The problem with solvents is that in most cases they decompose under the reaction conditions used in the reductive carbonylation reaction. Solvent decomposition can occur in a variety of ways including (i) acid cleavage of ether linkages by HI and  $\text{HCo}(\text{CO})_4$ , (ii) well known hydrolysis and halogenation reactions,

(iii) participation in condensation reactions with acetaldehyde or other products produced in the reaction, and (iv) conversion by hydrogenation, reductive carbonylation, homologation or carbonylation. A good illustration is tetraglyme. With this solvent the acetaldehyde rate is 6.6 M/hr at 170 °C, 5000 psig and a methanol conversion of 61%; however, tetraglyme rapidly decomposes to triethylene glycol and methoxytetraethylene glycol. Triethylene glycol is a reasonably good solvent, but it eventually decomposes to ethylene glycol and diethylene glycol. Ethylene glycol is a poor solvent giving acetaldehyde rate and selectivity of 0.2 M/hr and 45%.

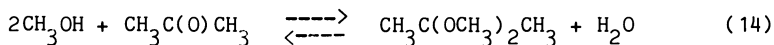
Ester, alcohol, and most ketone solvents also decompose. For example, with the Co-I-PPH<sub>3</sub> catalyst, methyl acetate reacts with synthesis gas to form ethyl acetate. All of the primary and secondary alcohols tested (C<sub>2</sub> thru C<sub>6</sub>) decompose during long-term operation. The major decomposition products include aldehydes, alkyl iodides, and ethers. Ketones are readily hydrogenated and the resulting alcohols decompose. Good solvents in terms of stability are diphenyl ether and alkanes. The acetaldehyde rate is somewhat low (1.8 M/hr) in diphenyl ether, and the selectivity is low in alkanes. In addition, these solvents do not have good solubility properties, especially in product refining.

#### Reductive Carbonylation of Dimethoxy Ketals and Dimethyl Carbonate.

Acetaldehyde is obtained via the reductive carbonylation of dimethyl ketals, Equation 12, and dimethyl carbonate, Equation 13 (15).



In each case, the products other than acetaldehyde must be recycled to reform the substrate. For example, 2,2-dimethoxypropane yields acetaldehyde, acetone, and methanol according to Equation 12. The reaction is carried out at 135 °C and 2250 psig with a cobalt catalyst. Iodide promoters are not required. The acetaldehyde rate is typically 4.0 M/hr and the selectivity is 60-70%. The co-produced acetone and methanol are recycled in a separate step via the equilibrium represented by Equation 14.



Relative to the reductive carbonylation of methanol, the added recycle step is a disadvantage with dimethyl ketals. This disadvantage is offset by the lower pressure of operation and the noncorrosive halide-free catalyst, which permits cheaper materials of construction.

The reaction of dimethyl carbonate with synthesis gas requires a cobalt-iodide catalyst and operating conditions of 180 °C and 4000 psig. The acetaldehyde rate approaches 30 M/hr with selectivities greater than 85%. The productivities are much better than with methanol; however, recycle of the CO<sub>2</sub> and methanol back to dimethyl carbonate is very difficult.



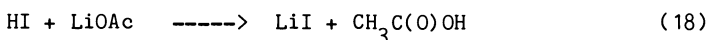
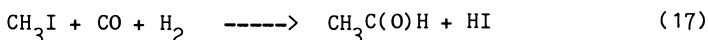
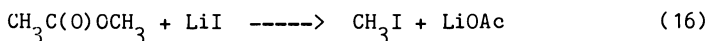
Reductive Carbonylation of Methyl Esters. The best alternative, and in our opinion, the best reported synthesis gas based process to produce acetaldehyde, is the reductive carbonylation of methyl esters, Equation 15 (16).



For example, the reaction of methyl acetate and synthesis gas at 170 °C and 5000 psig with a Co-LiI-NPh<sub>3</sub> catalyst results in the formation of acetaldehyde and acetic acid. The rate of acetaldehyde formation is 4.5 M/hr, and the yield based on Equation 15 is nearly 100%. Methane (1-2%) and ethyl acetate (1-2%) are the only by-products. The product mixture does not contain water, methanol or 1,1-dimethoxyethane. The acetic acid can easily be recycled by esterification with methanol in a separate step. Thus, the overall acetaldehyde selectivity approaches 98%. The utility of methyl acetate as an alternative feedstock has been previously illustrated by the reported carbonylation to acetic anhydride (25) and homologation (26) to ethyl acetate via reaction with synthesis gas.

A summary of the results we have obtained for the reductive carbonylation of methyl acetate is given in Table IV.

Amine promoters tend to give higher acetaldehyde rates relative to phosphines. Increasing the temperature to 200 °C increases the rate to 7.1 M/hr whereas decreasing the pressure to 2000 psig markedly lowers the rate. LiI is a critical component of the catalyst. Substituting LiI with NaI, KI, I<sub>2</sub> or CH<sub>3</sub>I results in a substantial loss in catalytic activity. A key step in the postulated reaction mechanism, as outlined in Equations 16-18, is cleavage of methyl acetate by LiI to yield CH<sub>3</sub>I and LiOAc (27).



Other alkali/alkaline earth metal iodides either cleave esters less efficiently or form insoluble carboxylate salts and are therefore not as effective as LiI. Addition of Li<sup>+</sup> and I<sup>-</sup> compounds capable of forming LiI under reaction conditions works as well as initially charging LiI (Table IV). The acetaldehyde producing step, Equation 17, is carried out with the cobalt-based catalyst. Since the carboxylate half of the ester is not involved with the cobalt center, any methyl ester which can be cleaved by LiI should also show activity. We have found that methyl isobutyrate, dimethyl malonate, methyl propionate, and dimethyl succinate yield acetaldehyde and the corresponding carboxylic acids in high yield under the same conditions utilized with methyl acetate.

### Summary and Conclusions

Acetaldehyde is obtained from the reaction of methanol, methyl

Table III. The Use of Solvents in the Reductive Carbonylation of Methanol

Solvent	Rx. Time	MeOH Conv.	AcH		EtOH		MeOAc	
			Rate	Sel	Rate	Sel	Rate	Sel
nonane	1.68	56	3.1	84	0.2	4.8	0.2	5.8
toluene	0.91	62	4.2	86	0.2	3.7	0.2	5.6
2,5-hexanedione	0.82	66	1.9	74	0.03	1.2	0.4	2.1
methyl ethyl ketone	0.51	52	4.4	86	0.06	1.0	0.3	8.0
diphenyl ether	1.15	66	1.8	88	0.07	3.4	0.05	3.5
THF	0.38	45	3.6	90	0.0	0.0	0.2	4.0
2-ethoxyethyl ether	0.48	64	5.4	86	0.2	2.5	0.2	5.9
1,4-dioxane	0.51	71	3.5	87	0.09	2.3		trace
n-propanol	0.45	56	1.8	73	0.2	7.1		a
iso-propanol	0.58	53	3.9	89	0.3	6.6	0.03	3.0
ethylene glycol	1.23	45	0.2	low	0.03	7.5	0.1	3.6
1,4-butanediol	0.98	72	1.9	25		b		b
2,5-hexanediol	0.53	65	3.8	87	0.1	4.3	0.1	3.6

All runs at 170 °C and 5000 psig with [Co] = 0.052 M, I/Co = 4, and I/P = 2. Rates reported as M/hr and the reaction time is hr.

a = not well resolved via GC.

b = complex reaction mixture due to solvent decomposition.

Table IV. Reductive Carbonylation of Methyl Acetate

CoI <sub>2</sub> mmol	ER <sub>3</sub> mmol	I	Temp., °C C	Pressure psig	AcH Rate, M/hr	
8	NBu <sub>3</sub>	(16)	LiI (32)	180	5000	4.7
8	NPh <sub>3</sub>	(16)	LiI (32)	180	5000	4.5
8	PCy <sub>3</sub>	(16)	LiI (32)	180	5000	3.9
8	PPh <sub>3</sub>	(16)	LiI (32)	180	5000	2.7
8	PPh <sub>3</sub>	(16)	LiI (32)	180	2000	0.2
8	NPh <sub>3</sub>	(16)	LiI (32)	200	5000	7.1
8	NPh <sub>3</sub>	(16)	NaI (32)	200	5000	0.5
8	NPh <sub>3</sub>	(16)	KI (32)	200	5000	0.2
8	NPh <sub>3</sub>	(16)	LiOAc (32)+CH <sub>3</sub> I (32)	200	5000	7.4
8	NPh <sub>3</sub>	(16)	Li <sub>2</sub> CO <sub>3</sub> (16)+I <sub>2</sub> (16)	200	5000	3.6

All runs = 150 mL methyl acetate

ketals, dimethyl carbonate or methyl esters with synthesis gas and a cobalt-based catalyst. Each feedstock has its advantages and disadvantages. Ketals suffer from low acetaldehyde selectivity and dimethyl carbonate requires a difficult recycle step. Good acetaldehyde rates and selectivities are obtained with methanol; however, achieving high selectivity (>90% while maintaining adequate methanol conversion) requires the use of a solvent. The solvent must be recycled, and that may require an additional refining step. The major problem with most solvents is that they eventually decompose which requires additional refining of the product and the costly replacement of the solvent. Overall, the best process is based on methyl esters. Good rates and, more importantly, high selectivity (>95%) are obtained in the absence of a solvent. In the case of methyl acetate, product refining consists of separating acetaldehyde from acetic acid and unreacted methyl acetate. An important feature of the methyl ester system is the absence of water and methanol in the product mixture. In contrast, with methanol the minimum separation involves acetaldehyde, methanol, dimethyl acetal, methyl acetate, acetic acid and water. The benefits obtained from the high acetaldehyde selectivity and the easy product refining more than compensate for the additional esterification step required with a methyl ester feedstock.

#### Acknowledgments

We thank Union Carbide Corporation for permission to publish this information.

#### Literature Cited

1. Bahrmann, H.; Cornils, B. In New Syntheses with Carbon Monoxide; Falbe, J., Ed.; Springer-Verlag: New York, 1980; Chap. 2.
2. Wender, I.; Levine, R.; Orchin, M. J. Am. Chem. Soc. 1949, 71, 4160.
3. Berty, J.; Marko, L.; Kallo, D. Chem. Tech. 1956, 3, 3260.
4. Mizorogi, T.; Nakayoma, N. Bull. Chem. Soc. Jpn. 1964, 37, 236.
5. Schultz, H. F.; Bellstedt, F. Ind. Eng. Chem. Prod. Res. Dev. 1973, 12, 176.
6. Pretzer, W.; Kobylinski, T. Ann. N. Y. Acad. Sci. 1980, 333, 58.
7. Dale, B. E. Ind. Eng. Chem. Prod. Res. Dev. 1983, 22, 466.
8. Swodenk, W. Chem. Eng. Tech. 1983, 55, 683.
9. Deluzarche, A.; Jenner, G.; Kiennemann, A.; Samra F. A. Erobel Kohle Endgass. Petrochem. 1979, 32, 436.
10. Wegman, R.; Busby, D. C. J. Mol. Catal. 1985, 32, 125.
11. Doyle, G. J. Organomet. Chem. 1981, 13, 237.
12. Roper, M.; Lovevenich, H.; Korff, J. J. Mol. Catal. 1982, 17, 315.
13. Steinmetz, G. R.; Larkins, T. H. Organometallics 1983, 2, 1879.
14. Slocum, D. W. In Catalysis in Organic Chemistry; Jones, W. H. Ed.; Academic Press: New York, 1980; p. 245.

15. Wegman, R.; Letts, J. B. J. Mol. Catal. 1985, 33, 357.
16. Wegman, R.; Busby, D. C. J. Chem. Soc., Chem. Commun. 1986, 332.
17. Reppe, W.; Friederich, H. U.S. Patent 2 727 902, 1955.
18. Eby, R. T.; Singleton, T. C. In Applied Industrial Catalysis; Leach, B. E. Ed.; Academic Press: New York, 1983; Chap. 10.
19. Galamb, V.; Palyi, G. Coord. Chem. Rev. 1984, 59, 203.
20. Orchin, M. Acc. Chem. Res. 1981, 14, 259.
21. Ungvary, M.; Marko, L. Organometallics 1983, 2, 1608.
22. Martin, J. T.; Baird, M. C. Organometallics 1983, 2, 1073.
23. Kovacs, I.; Ungvary, F.; Marko, L. Organometallics 1986, 5, 209.
24. Wegman, R. W. Organometallics 1986, 5, 707.
25. Larkins, T. H.; Polichnowski, S. W.; Tustin, G. C.; Young, D. A. U.S. Patent 4 374 070, 1983.
26. Braca, G.; Sbrana, G.; Valentini, G.; Andrich, G.; Gregorio, G. J. Am. Chem. Soc. 1978, 100, 6238.
27. Shina, H.; Hashimoto, T. Yukagaku 1980, 29, 901.

RECEIVED August 14, 1986

## Chapter 10

# Production of Vinyl Acetate from Methanol and Synthesis Gas

Nabil Rizkalla<sup>1</sup> and Alan Goliaszewski

The Halcon SD Group, Inc., Montvale, NJ 07645

This report describes a process to produce vinyl acetate with high selectivity from exclusively methanol, carbon monoxide, and hydrogen. The simplest scheme for this process involves esterifying acetic acid with methanol, converting the methyl acetate with syn gas directly to ethylidene diacetate and acetic acid, and finally, thermal elimination of acetic acid. Produced acetic acid is recycled. Each step proceeds in high conversion and selectivity. The single step conversion of methyl acetate to ethylidene diacetate is catalyzed by either a palladium or rhodium compound, a source of iodide, and a promoter. The mechanism is described as involving the concurrent generation of acetaldehyde and acetic anhydride which subsequently react to form ethylidene diacetate. An alternative to this scheme involves independent generation of acetaldehyde by reductive carbonylation of methanol or methyl acetate, or by acetic anhydride reduction. The acetaldehyde is then reacted with anhydride in a separate step.

Mixtures of carbon monoxide and hydrogen have proven to be versatile starting materials for the chemical industry. Certain processes involving the conversion of syn gas to simple organic chemicals have been demonstrated as selective and efficient. One example is methanol, produced in high selectivities by passing carbon monoxide and hydrogen over a heterogeneous catalyst. Other examples of commercial processes are acetic anhydride and acetic acid. Patents cover other processes including acetaldehyde, ethanol, and ethylene glycol. At first glance, vinyl acetate is an unlikely candidate to be prepared exclusively from syn gas.

Most vinyl acetate is presently produced by the palladium-catalyzed reaction of acetic acid and ethylene that involves subsequent reoxidation of reduced palladium. This report describes an alternative process for vinyl acetate utilizing syn gas as feedstock, thus avoiding the necessity for ethylene (see figure 1). Of course, at this time of plummeting oil prices, a route utilizing syn gas cannot

<sup>1</sup>Current address: 415 Faletti Circle, River Vale, NJ 07675

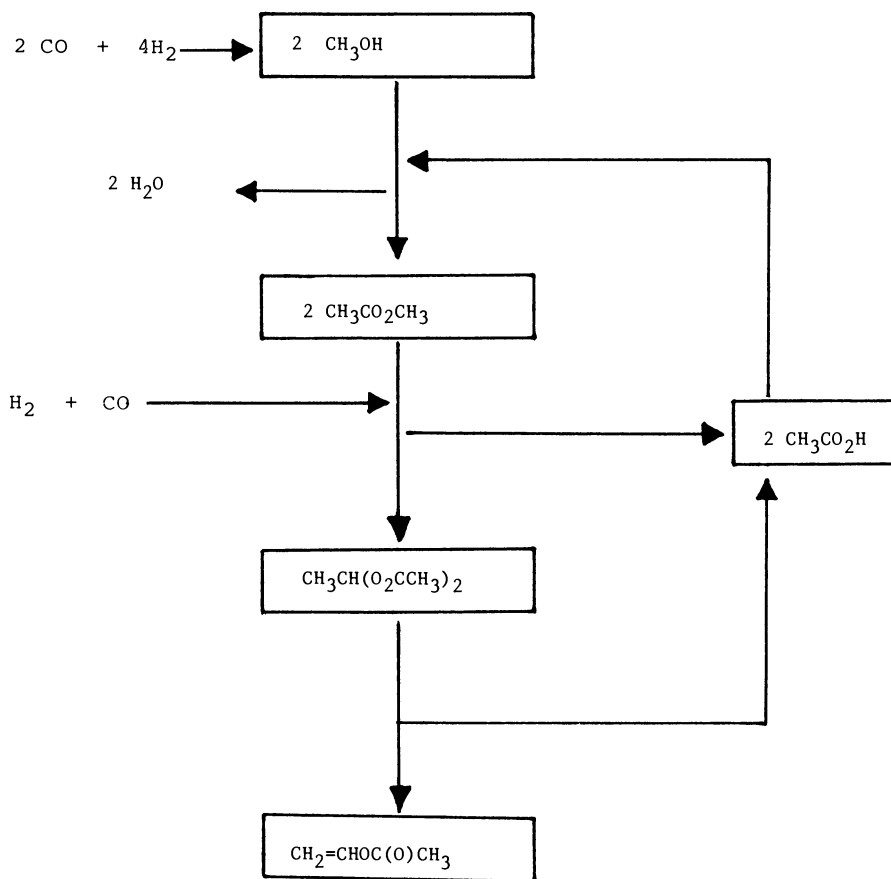
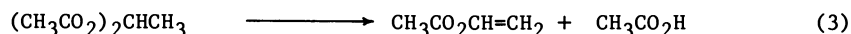
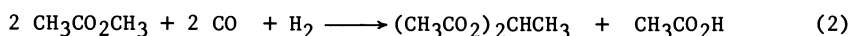
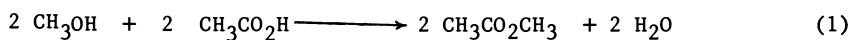


Figure 1. Vinyl Acetate from Syngas

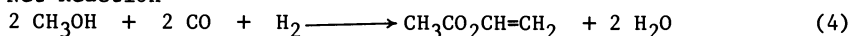
generally compete well with ethylene. However, in a future that certainly involves diminished petrochemical resources, such an alternative process should be of great value.

Considering the high selectivity and multistep capabilities of homogeneous transition metal catalysts, our attention naturally turned in this direction. A unique pathway to vinyl acetate evolved, integrating several improved reactions with a novel, metal catalyzed reductive carbonylation step. A general scheme of this alternative process is shown in Scheme I. The initial step involves esterification of acetic acid with methanol. Then ethylidene diacetate, a precursor to vinyl acetate, may be produced from methyl acetate in a single reaction with carbon monoxide and hydrogen (equation 2). In this reductive carbonylation acetic acid is co-produced. Finally, the ethylidene diacetate is converted to vinyl acetate by thermal elimination of acetic acid. Acetic acid generated in the last two steps is recycled for esterification. The net reaction expresses the advantage of this process: vinyl acetate is produced in as few as three steps exclusively from methanol and syn gas with no relevant by-products.

Scheme I. General outline for the Preparation of  
Vinyl Acetate



Net Reaction

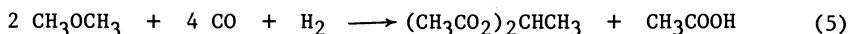


Alternatively, the transformation of methyl acetate to ethylidene diacetate may also be achieved in a multistep process. Either conversion of methyl acetate to acetic anhydride, followed by reduction to ethylidene diacetate plus acetic acid, or production of acetaldehyde directly and subsequent reaction with acetic anhydride to form ethylidene diacetate are successful. This will be examined in greater detail.

Reductive Carbonylation of Methyl Acetate

One Step Synthesis:

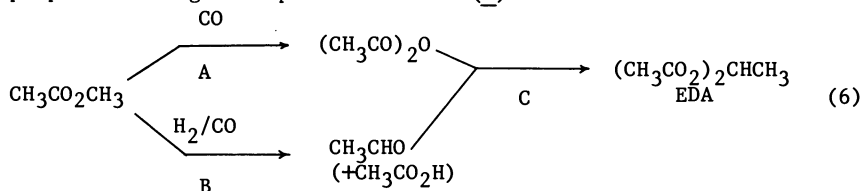
As indicated above, ethylidene diacetate (EDA) is a precursor of vinyl acetate by thermal elimination of acetic acid (equation 3). The formation of EDA in a one step reaction that involves the reductive carbonylation of methyl acetate has been achieved (equation 2) (1). Alternatively, the substrate of reductive carbonylation can be dimethyl ether instead of methyl acetate which simply integrates into the reaction an initial carbonylation step leading to EDA.



The reaction is catalyzed by a group VIII metal species, particularly that of rhodium or palladium. The initial metal species may be any variety of complexes (e.g.,  $\text{PdCl}_2 \cdot \text{Pd}$  acetate, etc.). A source of halide is necessary; iodide is especially effective. The most convenient source is methyl iodide, since it is likely a reaction intermediate. In addition, an organic promoter must be included for catalytic activity. These promoters are generally tertiary phosphines or amines. Also, chromium complexes were found to have an important promotional effect.

The catalyst components are generally dissolved in methyl acetate which acts as both reactant and solvent. Other solvents may be used and in fact, upon several batch recycles where lower boiling products are distilled off, the solvent is an ethylidene diacetate-acetic acid mixture. Any water introduced in the reaction mixture will be consumed via ester and anhydride hydrolysis, therefore anhydrous conditions are warranted. Typical batch reaction examples are presented in Table 1. There is generally sufficient reactivity when carbon monoxide and hydrogen are present at 200-500 psi. Similar results were obtained from the pilot plant using a continuous stirred tank reactor (CSTR). The reaction can also be run continuously over a supported catalyst with a feed of methyl acetate, methyl iodide, CO, and hydrogen.

In addition to small amounts of methane, acetaldehyde or acetic anhydride can be generated in substantial quantities depending on conditions. However, they are not present simultaneously in any appreciable quantity. Acetic anhydride and acetaldehyde must be competitively formed (equation 6), and subsequently react with each other to form EDA (step C). This reaction (step C) is generally catalyzed by protic acids (2-4). The reaction solution for reductive carbonylation is quite acidic; HI is an intermediate generated under reaction conditions of high alkyl iodide concentration and hydrogen pressure. The thermodynamic equilibrium of this condensation is quite favorable for diester formation; existence of an abundance of either anhydride or aldehyde in the presence of the other is not found. Yields of stoichiometric preparations are in excess of 95% (5). In fact, a plant may still be operated by Celanese which produces EDA by this reaction of acetaldehyde and acetic anhydride, each prepared through independent routes (6).



Any mechanistic scheme must account for this concurrent production of acetaldehyde and acetic anhydride. A possible mechanism for EDA formation is described in general terms by Scheme II for palladium. Methyl iodide is likely generated from methyl acetate and HI (equation 7); a portion of the iodide species in the reaction mixture certainly exists in the form of hydrogen iodide (equations 11, 12). Iodide ion tends to attack the  $\alpha$ -carbon of the alkyl portion of unhindered esters (7). Thus, methyl acetate, which would be in general inert to the metal complexes used, is converted to a reactive species which can readily oxidatively add to a palladium(0) complex. An



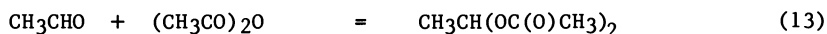
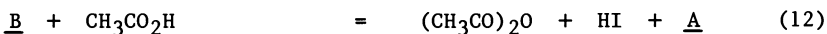
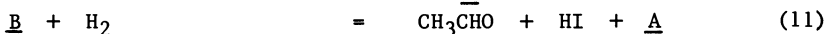
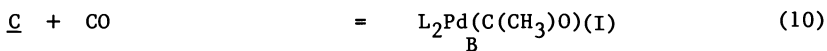
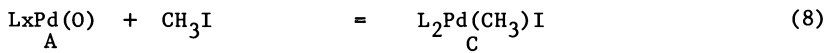
TABLE I  
REDUCTIVE CARBONYLATION OF METHYL ACETATE

Run	Catalyst Precursor (mmoles) <sup>a</sup>	%	Conversion	Products (mmoles) <sup>b</sup>		
				ethylidene diacetate	acetic anhydride	acetaldehyde
1	RhCl <sub>3</sub> (0.48), 3-picoline (3.2)	98.1	35.2	7.5	1.6	
2	RhCl <sub>3</sub> (0.48), Cr(CO) <sub>6</sub> (1.4)	62.6	12.4	24.1	1.8	
3.	RhCl <sub>3</sub> (0.48)	0	-	-	-	
4.	(PPh <sub>3</sub> ) <sub>2</sub> RhCl (0.30), PPh <sub>3</sub> (1.2)	43.3	12.4	10.3	-	
5.	(py) <sub>3</sub> RhCl <sub>3</sub> (.45)	99.9	19.2	46.4	-	
6.c	(py) <sub>3</sub> RhCl <sub>3</sub> (.45)	99.0	-	80.2	-	
7.d	RhCl <sub>3</sub> (1.4), Cr(CO) <sub>6</sub> (1.4), (Mepy) <sup>+</sup> I <sup>-</sup> (11.8)	99.9	31.8	20.9	-	
8	Pd(OAc) <sub>2</sub> (0.71), PPh <sub>3</sub> (3.8)	99.1	32.4	-	15.5	
9	Pd(PPh <sub>3</sub> ) <sub>2</sub> Cl <sub>2</sub> (0.71), PPh <sub>3</sub> (0.76)	97.5	26.5	-	26.0	
10	PdCl <sub>2</sub> (.68)	0	-	-	-	
11e	Pd(OAc) <sub>2</sub> (1.2), Cr(CO) <sub>6</sub> (9.4), PPh <sub>3</sub> (2.4)	89.6	25.4	19.8	2.0	
12	PdCl <sub>2</sub> (.71), P(n-Bu) <sub>3</sub> (3.0)	76.0	11.8	-	38.0	
13	Pd(OAc) <sub>2</sub> (.71), HMPA (5.6)	57.3	20.7	-	5.0	
14d	Pd(OAc) <sub>2</sub> (.71), PPh <sub>3</sub> (3.8), CH <sub>3</sub> Br(21)	30.7	13.4	2.6	1.3	

- a. Reaction Charge: Methyl iodide (14.1 mmole), Methyl acetate (81.0 mmole).  
 Typical Operating Conditions: 150°C; 1000 psi pressure during reaction CO/H<sub>2</sub> (1:1); 4 hr. duration.
- b. In addition to acetic acid and methane, trace quantities were found of acetone, vinyl acetate, and ethyl acetate.
- c. No hydrogen included (500 psi CO), (py=pyridine).
- d. No methyl iodide added.
- e. H<sub>2</sub> (150 psi), CO (450 psi).

ensuing CO insertion (alkyl migration) generates an intermediate metal-acyl complex (B).

Scheme II. Possible General Mechanism for Palladium Catalyzed Reductive Carbonylation



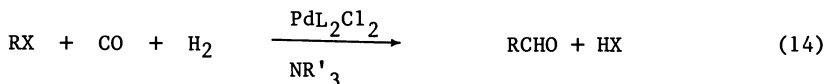
Reduction of initial palladium(II) salts to an active palladium(0) species is necessary. This may occur by base promoted (prior to HI generation) reduction with hydrogen (8-9). A more expedient reduction by added promoters offers an additional pathway (vide infra). Since similar rates and product distributions are found regardless of the nature of initial metal salt (e.g.  $\text{PdCl}_2$ ,  $\text{Pd(OAc)}_2$ , etc.), ultimately the same catalytic species for that respective metal can assumed to be formed. The reaction conditions include a relatively high iodide concentration, in which anionic palladium complexes are possible. The existence of anionic palladium complexes has been documented, especially in the presence of excess halide (e.g.  $(\text{NEt}_4)_2\text{-PdI}_4$ ,  $(\text{AsPh}_4)(\text{H(CO)PdCl}_2)$ ) (10-11). In fact, the monoanionic complexes of rhodium have demonstrated superior rates of methyl iodide oxidative addition compared to neutral complexes, (12). This may be also true for palladium. Presumably, an  $\text{SN}_2$  mode of attack is operative.

Reaction rates have first-order dependence on both metal and iodide concentrations. The rates increase linearly with increased iodide concentrations up to approximately an I/Pd ratio of 6 where they slope off. The reaction rate is also fractionally dependent on CO and hydrogen partial pressures. The oxidative addition of the alkyl iodide to the reduced metal complex is still likely to be the rate determining step (equation 8). Oxidative addition was also indicated as rate determining by studies of the similar reactions, methyl acetate carbonylation (13) and methanol carbonylation (14). The greater ease of oxidative addition for iodides contributes to the preference of their use rather than other halides. Also, a ratio of phosphorous promoter to palladium of 10:1 was found to provide maximal rates. No doubt, a complex equilibrium occurs with formation of the appropriate catalytic complex with possible coordination of phosphine, CO, iodide, and hydrogen. Such a pre-equilibrium would explain fractional rate dependencies.

Both acetaldehyde and acetic anhydride likely originated from

the same intermediate, the metal-acetyl complex (B). This species can either be reduced with hydrogen to acetaldehyde (equation 11) or proceed to form the anhydride (equation 12). For rhodium this latter pathway is currently believed to proceed by acetyl iodide formation by reductive elimination or simply by nucleophilic attack by iodide ion. Acetyl iodide rapidly reacts with acetic acid or methyl acetate (15). In fact, a rhodium catalyst system similar to the one used here is used for the production of acetic anhydride via methyl acetate carbonylation (16). The carbonylation step has been the topic of several studies (17). This acetic anhydride process has been commercialized by Tennessee Eastman utilizing Halcon/Eastman Technology.

Concurrent with acetic anhydride formation is the reduction of the metal-acyl species selectively to acetaldehyde. Unlike many other soluble metal catalysts (e.g. Co, Ru), no further reduction of the aldehyde to ethanol occurs. The mechanism of acetaldehyde formation in this process is likely identical to the conversion of alkyl halides to aldehydes with one additional carbon catalyzed by palladium (equation 14) (18). This reaction occurs with CO/H<sub>2</sub> utilizing Pd(PPh<sub>3</sub>)<sub>2</sub>Cl<sub>2</sub> as a catalyst precursor. The suggested catalytic species is (PPh<sub>3</sub>)<sub>2</sub>Pd(CO) (18). This reaction is likely occurring in the reductive carbonylation of methyl acetate, with methyl iodide (i.e. RX) being continuously generated.

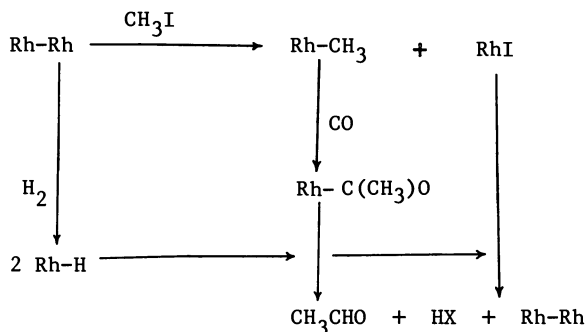


Similarly, highly selective hydrogen reductions of rhodium-acyl intermediates are known, such as in hydroformylation reactions. Rhodium phosphine complexes are highly selective with little further reduction of products to alcohols (19).

In general, the reduced metal species (e.g. L<sub>x</sub>Pd(0)) undergoes oxidative addition of methyl iodide, followed by CO insertion to form the palladium(II)-acyl complex (B). Hydrogen reduction results in acetaldehyde formation that can react with concurrently produced acetic anhydride. Reduction that occurs prior to alkyl migration results in methane formation, which is generally found as a by-product in small quantities. Undesirable quantities are generated as hydrogen pressures are increased beyond 500 psi. The hydrido-palladium-iodide complex that presumably results favors equilibrium with free HI and regenerated palladium(0) species (A). As indicated previously, methyl acetate is certainly a suitable base for HI. An analogous scheme can be suggested for rhodium (see Figure 2). Its oxidation state cycles between Rh(I) and Rh(III) with oxidative addition of methyl iodide or hydrogen alternating with eliminations of HI, acetaldehyde, or acetyl iodide.

For both rhodium and palladium there is general difficulty in defining the exact reductive process for aldehyde formation. Though the direct hydrogenation of a rhodium(I) complex by oxidative addition to form a dihydride species is commonly proposed (20), a bimolecular mechanism may better explain the chemistry involved in rhodium catalysis (see Scheme III). The bimolecular process avoids invoking the difficult oxidative addition of hydrogen to rhodium(I) complexes (21). Bimolecular routes have not been ruled out for such processes as the well-examined oxo reaction where hydrogen addition is the rate determining step (22).

Scheme III. Bimolecular Reaction Scheme for Acetaldehyde Formation



Palladium and rhodium do exhibit some distinguishing features. Rhodium has proven to be a superior carbonylation catalyst; thus it is used for commercial methyl acetate carbonylation to acetic anhydride, and it has superior rates and selectivities for oxo reactions. It is not surprising then that excess acetic anhydride is generally produced in the reductive carbonylation. With palladium, more facile formation of reduced products generally predominates (excess acetaldehyde, see Table I). Both metal species demonstrate a particular sensitivity of reaction products to hydrogen concentrations. This is indicated in Table II where the H<sub>2</sub>/CO feed ratio was varied while other conditions were held constant. Variation greatly affects EDA-acetic anhydride selectivity, permitting tuning of products. In an additional example with rhodium catalysts, reaction conditions can be geared to near complete EDA formation or to exclusive anhydride when hydrogen was excluded (see Table I, runs 1, 6).

This acute sensitivity of the EDA systems to hydrogen points out an important distinction with the well-studied rhodium-catalyzed Monsanto acetic acid process. In this system, excess water reacts with acetyl iodide generated by reductive elimination forming acetic acid and HI. When as much as a 50% hydrogen feed was used, no change in acetic acid selectivity was found (23). Hydrogen acts essentially as a simple diluent. The Monsanto catalytic species has been identified by IR as (Rh(CO)<sub>2</sub>L<sub>2</sub>)<sup>-</sup> (24). Though the catalyst components are quite similar to our case, the greatest difference in the two reactions is the presence of a protic medium, notably water. Perhaps water modifies the metal species to prevent the appropriate metal-hydride from forming by reaction with hydrogen. It is unlikely that this lack of hydrogen sensitivity reflects a more rapid consumption of the acetyl iodide by water than by acetic acid since not even traces of acetaldehyde have been reported. The difference in rates would thus have to be extraordinary. Obviously, the catalytic species for EDA formation is different than the Monsanto system.

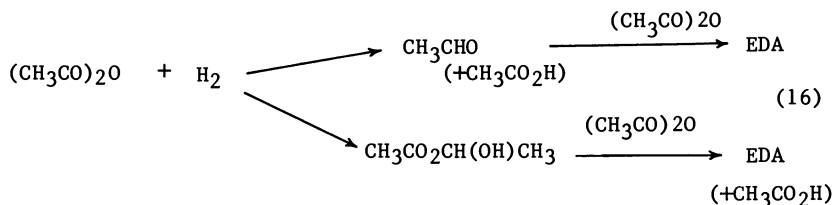
As indicated above, hydrogen has a definite influence upon the catalyst. This is manifest in several ways. (a) Small amounts of hydrogen effectively keep this same rhodium catalyst active and in solution in the carbonylation of methyl acetate. (b) The rates of

EDA formation are lower than for acetic anhydride formation by carbonylation. (c) Selective reductive chemistry occurs and rates are dependent on hydrogen partial pressure.

As indicated earlier, chromium compounds were found to be effective promoters, especially in a reduced form (metal, or carbonyl). Though having no activity when used alone, they were found to substantially decrease the induction period. This suggests their role is to reduce the initial pre-catalyst to the active form. A similar effect was postulated for chromium promotion in methyl acetate carbonylation (25). With no chromium, the difficult hydrogen reduction of the catalyst precursor probably occurs. However, evidence indicates the role of chromium may be more complex than to simply reduce induction periods. Production of EDA occurs even without the organic promoter in the presence of excess chromium (Table 1, run 2). Also, the concentration of chromium affects product distributions (see Figure 3). As chromium concentrations increase, the carbonylation function is greatly enhanced. A reaction utilizing recycled catalyst results in the same product distribution as initial catalyst charge. A more intimate interaction of metal species must be involved.

Trivalent phosphines or amines were found to be necessary for catalysis to occur (see Table 1, run 3). The predominant role of these compounds has been suggested as simply providing a greater solubility of iodide ion in less polar media (11). An example of evidence we found was that upon addition of only KI to a methyl acetate solution of appropriate rhodium or palladium complex, no reaction occurs. Subsequent addition of 6-crown-18 ether promotes EDA formation. Despite the possibility that the large excess of iodide compounds may bind all phosphines as phosphonium salts, modification at the metal center may occur. The equilibrium between metal coordination and existence as salts is difficult to ascertain. Their coordination to the metal can account for differences in phosphine performance under identical high iodide concentrations. Their coordination generally promotes the metals ability for important oxidative addition of methyl iodide or hydrogen and helps in maintaining a soluble homogeneous metal species.

An alternative scheme to simultaneous formation of acetaldehyde and acetic anhydride could entail the carbonylation of methyl acetate to acetic anhydride which is subsequently reduced to acetaldehyde and acetic acid. The reaction of acetaldehyde with excess anhydride would form EDA. In fact, Fenton has described production of EDA by the reduction of acetic anhydride using both rhodium and palladium salts as catalysts when modified with triphenylphosphine (26). Two possible mechanisms for the reduction are postulated in equation 16.



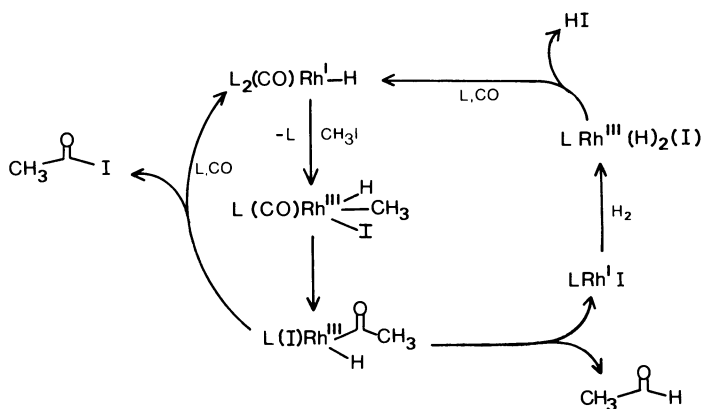


Figure 2. Simplified Scheme of Rhodium Catalyzed Generation of Acetaldehyde and Acetyl Iodide.

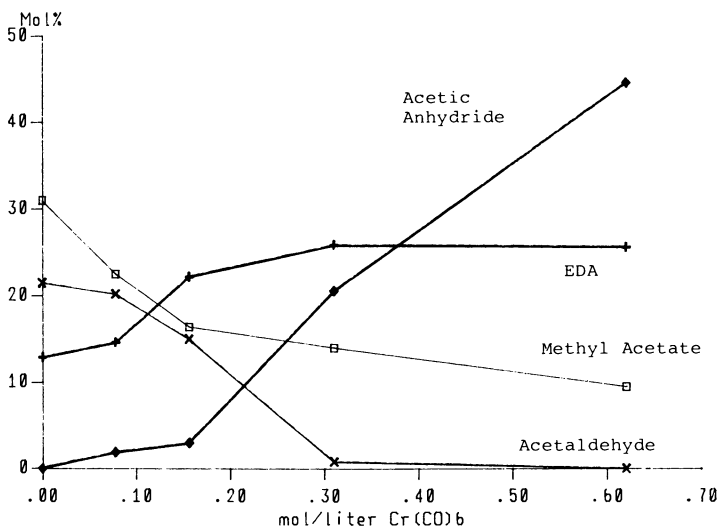


Figure 3. The Effect of Chromium Concentration on Product Distribution. All reactions charged with Pd(OAc)<sub>2</sub> (0.10 mole), ethyl iodide (0.66), methyl acetate (5.85), triphenylphosphine (0.13). Conditions: 150°C, 5 hours, 1000 psi CO/H<sub>2</sub> (1:1).

TABLE II PRODUCT SELECTIVITY WITH VARIATION OF CO/H<sub>2</sub> FEED

Example	psi		CO/H <sub>2</sub>	EDA	Acetic Anhydride	<u>(mmoles) product composition</u>		
	CO	H <sub>2</sub>				Acetaldehyde	Acetic Acid	Methyl Acetate
1	735	15	50	4.8	73.5	-	5.0	20.3
2	585	15	39	6.8	66.7	-	6.7	24.3
3 a	705	45	16	19.4	38.4	-	22.6	25.6
4 a	450	150	3	28.8	22.5	2.2	30.0	21.6

Conditions: 150°, 14 hr., Methyl Acetate (110 mmole), Pd(OAc)<sub>2</sub> (1.2), Cr(CO)<sub>6</sub> (8.2),  
Methyl iodide (8.8), PPh<sub>3</sub> (2.1)

a 9 hr. run

The reductive carbonylation conditions differ from Fenton's in having a high iodide concentration and a CO pressure of 300-500 psi. The patent indicates that CO inhibits acetic anhydride reduction. When the anhydride was placed under the reductive carbonylation conditions, EDA was produced along with methyl acetate and acetic acid. However, the rate of EDA formation was substantially lower than usual methyl acetate conversions. Also, a mechanism incorporating Fenton's reduction cannot account for excess acetaldehyde along with EDA formation. This cannot be the major path to EDA.

In addition to the successful reductive carbonylation systems utilizing the rhodium or palladium catalysts described above, a non-noble metal system has been developed (27). When methyl acetate or dimethyl ether was treated with carbon monoxide and hydrogen in the presence of an iodide compound, a trivalent phosphorous or nitrogen promoter, and a nickel-molybdenum or nickel-tungsten catalyst, EDA was formed. The catalyst is generated in the reaction mixture by addition of appropriate metallic complexes, such as 5:1 combination of bis(triphenylphosphine)-nickel dicarbonyl to molybdenum carbonyl. These same catalyst systems have proven effective as a rhodium replacement in methyl acetate carbonylations (28). Though the rates of EDA formation are slower than with the noble metals, the major advantage is the relative inexpense of catalytic materials. Chemistry virtually identical to noble-metal catalysis probably occurs since reaction profiles are very similar: by products include acetic anhydride, acetaldehyde, and methane, with ethanol in trace quantities.

#### Two-Step Reductive Carbonylation Processes

The formation of acetic anhydride by rhodium-catalyzed carbonylation of methyl acetate is a highly selective process, which is successfully practiced commercially. It is certainly a more efficient process for acetic anhydride formation than can occur as part of a one-step reductive carbonylation process. The reductive carbonylation of methyl acetate is a rather complex system involving several simultaneous reactions. This places a high demand upon the catalyst. Though it responds well, it is difficult to adjust conditions to exclusive EDA formation. Also, most selectivity loss encountered in reductive carbonylation arises from self-condensation of acetaldehyde, in situ cracking of EDA to vinyl acetate, and methane formation. These undesirable reactions are apparently catalyzed by the reaction medium. Separating and optimizing each step presumed to occur in reductive carbonylation may possibly lead to higher selectivities and therefore, higher overall efficiency. A multistep sequence involving formation of acetaldehyde, a separate carbonylation of methyl acetate to acetic anhydride, and finally combination to form EDA may represent an efficient process. The carbonylation chemistry to produce acetic anhydride is well established. The formation of acetaldehyde can be accomplished by one of the following methods.

- A. Reductive Carbonylation of Methanol. As discussed earlier, rhodium based catalysts are capable of catalyzing the reductive carbonylation of methyl acetate to ethylidene diacetate (1), as well as the carbonylation of methyl acetate to acetic anhydride (16). These reactions proceed only when the reaction environment

American Chemical Society

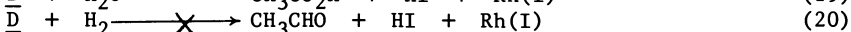
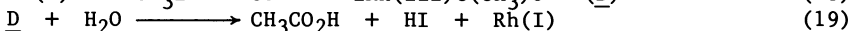
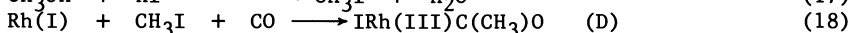
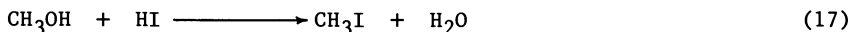
Library

1155 16th St., N.W.

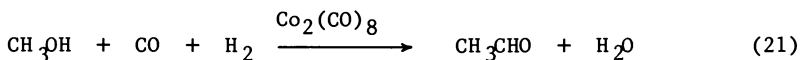
Washington, D.C. 20036



is essentially anhydrous. With rhodium catalysts, even when large amounts of hydrogen are present, protic species interfere and carbonylation processes produce only carboxylic acid derivatives. The reaction will occur with water or methanol that is part of the reaction mixture or that is produced in situ. This behavior is used to good advantage in the highly selective carbonylation of methanol to acetic acid (equations 17-19) (23).



The reductive carbonylation of methanol to acetaldehyde has been possible when catalyzed by cobalt carbonyl species. This represents a "non-ethylene" route to acetaldehyde. Though rhodium may be expected to be substantially more active than cobalt, it is undesirable since hydrogen incorporation is obviously not seen (see equation 20).



Successful cobalt carbonyl catalysts have been modified by addition of group VA compounds as ligands (29). The cobalt carbonyls, however, decompose readily upon heating. Maintenance of the active catalyst is possible by applying high CO partial pressure, generally in excess of 3000 psi (30-31). Therefore, almost all cobalt-catalyzed carbonylations report operating pressures of 3000-5000 psi. Selective reductive carbonylation may be difficult since cobalt is an effective carbonylation catalyst which is used for methanol carbonylation to acetic acid and its esters. In the presence of such a high concentration of hydrogen, cobalt can also catalyze the thermodynamically-favored homologation of methanol to ethanol, apparently by acetaldehyde reduction. Tuning the catalyst and reaction conditions to reduce selectivity losses to acetate esters on one hand and ethanol on the other proved to be a difficult task in acetaldehyde formation by reductive carbonylation.

Halcon has developed a new non-noble metal catalyst for methanol reductive carbonylation (32). It is formed under more moderate conditions (1200 psi, 120°C) and permits a selective reaction at only 1200-1800 psi of reaction pressure. Under these conditions, the catalyst's activity is comparable with noble metal catalyzed carbonylations. The conversion rate is 1.5-3.0 mol/l.hr. and acetaldehyde selectivity is 85%. In concentrated solutions, a considerable portion of product acetaldehyde (20-40%) is converted to its acetal. The acetal can be readily hydrolyzed back to acetaldehyde at 100-150° without catalyst (33). Acetal formation is actually beneficial through prevention of undesirable acetaldehyde condensation reactions.

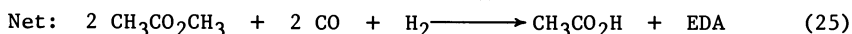
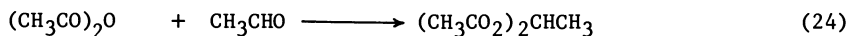
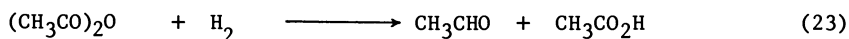
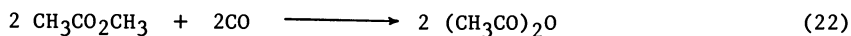
- B. Acetaldehyde From Methyl Acetate Reductive Carbonylation. A second preparation of acetaldehyde not based upon ethylene oxidation involves a process modification of the previously des-

cribed reductive carbonylation of methyl acetate (34). The reaction is run such to bias the formation of acetaldehyde relative to acetic anhydride and ethylidene diacetate. The process is performed in a "boiling reactor" where the temperature and pressure are maintained such that the reaction solvent is in a continuously boiling state. Liquid and gas reactants are fed at the bottom of the reactor while vapors are continuously removed from the top. This scheme has several advantages. Acetaldehyde is certainly the most volatile species in the reaction mixture; therefore, virtually no acetaldehyde is in the liquid phase. This enhances the selectivity by preventing EDA formation. The non-volatile catalyst remains in the reactor under a carbonylation atmosphere which maintains its activity.

The catalyst is generally a palladium compound promoted with a trivalent amine or phosphine in the presence of methyl iodide as described earlier. Systems proven to bias acetaldehyde are utilized, of course (e.g. see Table I, run 12). A yield of 85% acetaldehyde from methyl acetate is typical by this method. It can be utilized in stoichiometric addition to easily prepared acetic anhydride resulting in EDA formation. When considering that the "boiling pot" reaction by-products are recyclable acetic acid, acetic anhydride and small amounts of EDA, the yield to vinyl acetate related products is 95%.

- C. Acetaldehyde via Acetic Anhydride Reduction. Another route to ethylidene diacetate that was developed involves carbonylation of methyl acetate to acetic anhydride, of which half is hydrogenated to acetaldehyde and acetic acid (see Scheme IV). The acetaldehyde is then combined with the rest of the anhydride to form EDA. There are two process alternatives here. The acetaldehyde can be produced in excess acetic anhydride so EDA formation can occur in situ, similar to the work reported by Fenton (26). Alternatively, acetaldehyde can be isolated from acetic anhydride reduction and reacted with the anhydride in a separate step to form the desired EDA.

Scheme IV. EDA via Acetic Anhydride Reduction



Hydrogenation of acetic anhydride to acetaldehyde (equation 23) has been demonstrated utilizing cobalt carbonyl under one atmosphere of hydrogen. However, the cobalt complex is short lived. A more efficient cobalt catalyzed reaction with substantial catalyst longevity was realized at a temperature of 190°C and 3000 psi pressure CO and hydrogen. The main products were equal amounts of EDA and acetic acid. Upon investigation, this reaction was found exceptionally efficient at a more reasonable 1500 psi pressure provided that the temperature was maintained

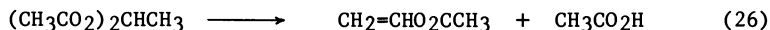
below 100°C (35). This minimum partial pressure was required to maintain the catalyst activity. The necessary CO pressure is a function of temperature. Under optimum reaction parameters, a reaction rate of 4.5 mole/liter hr. was achieved (see Table III). This rate could be increased by addition of promoters Li, Al, K, Na, or amines; however, products were now predominantly acetaldehyde and acetic acid rather than EDA. Self-condensation of the acetaldehyde is observed when its concentration exceeds 10%, but is suppressed by acetaldehyde removal from the vapor phase as it is formed.

Recovery and separation of the products were rather simple considering that the boiling point difference between the two major components is almost 100°C. Alternatively, a cold acetic anhydride scrubber was used, in which all condensable products were washed out of the effluent gas. A typical effluent contained acetaldehyde (41%), acetic acid (58%), ethyl acetate (0.8-1.0%), EDA (0.1%), and methane (trace).

The hydrogenation of acetic anhydride was also performed in the vapor phase over a supported palladium catalyst resulting in acetaldehyde and acetic acid in high yields (36). To avoid recycling, the reactor was designed for complete reaction of acetic anhydride. Minor selectivity loss was found in formation of ethyl acetate (0.5-1.5%) and methane (0.5%). Typical reaction conditions were 160-200°C, 30-100 psi, with a hydrogen-anhydride ratio of 3:1 to 10:1. A similar catalyst was used in the liquid phase (37). The simplicity and high selectivity of this process is certainly attractive.

#### Thermal Elimination of Acetic Acid from Ethylidene Diacetate

Thermal cracking of EDA (equation 26) is achieved in the presence of sulfonic acids (38) at 140°C and one atmosphere.



Alternatively, acetaldehyde and acetic anhydride are fed directly to the cracking reactor where the same sulfonic acid can catalyze the condensation of the aldehyde-anhydride mixture to EDA and the subsequent thermal elimination forming vinyl acetate. The best results are obtained when acetic anhydride is present as solvent to inhibit the competitive elimination to acetaldehyde and anhydride (see reverse of equation 2). Aldehyde degradation reactions are minimal under these conditions.

#### Conclusion

This report has described the development of a new process in which vinyl acetate is produced exclusively from methanol and syn gas with essentially no by-products. At best conditions, high conversions and selectivities are typical of the chemistry involved. Various process possibilities were described, thus permitting much flexibility for eventual development.

In the sixties, acetic acid and acetic anhydride were prepared from petrochemicals and, in particular, from inexpensive ethylene.

TABLE III COBALT CATALYZED ACETIC ANHYDRIDE REDUCTION

Charge <sup>a</sup>		H <sub>2</sub> /CO Pressure	% CO	Products (mole/mole initial anhydride) x 100			
Cobalt Carbonyl (mmole)	Acetaldehyde			EDA	acetic anhydride	acetic acid	
0.48	1500	23	2	31	33.7	36	
0.48	1500	50	0	25	51	24.9	
0.23	1500	13	0	18	63	18.8	
2.30	1230	33	10	34	5.7	50	

a. All reactions charged with 100 mmoles methyl acetate; reactions were run for 6 hrs. at 90°C.

Today acetic acid is produced mainly from methanol and carbon monoxide. This process, along with the Tennessee Eastman acetic anhydride plant using syn gas, are the current standards in the industry when considering new expansion regardless of the price of ethylene. The vinyl acetate process described here may achieve this stature if its commercial development is permitted to occur.

### General Experimental Procedures

Reductive Carbonylation, Charged to a one liter (Autoclave Engineer) Hastelloy-C autoclave, provided with a magnet-drive stirrer, a mixture of methyl acetate (81 mmole), methyl iodide (14.1 mmole), rhodium chloride (.48 mmole), and 3-picoline (3.2 mmole). The autoclave was sealed, flushed 3 times with carbon monoxide and then charged with carbon monoxide up to 300 psig followed by a charge of hydrogen up to 600 psig. The reactor was heated up with steam until the stirred mixture was 150°C. The heating period was 12 minutes. The pressure of the reactor at that point of time was 900 psig. An additional charge of 1:1 carbon monoxide to hydrogen was added to bring the reactor to the desired pressure of 1000 psig. This was considered as the zero point of time. The pressure was maintained at this level through the entire reaction duration by feeding a mixture of 1:1 carbon monoxide to hydrogen through a dual channel "Brook" mass flow meter. The progress of reaction and reaction rate were determined by monitoring the flow rate of gas through the mass flow meter and by withdrawing liquid samples periodically from the reaction mixture. The samples were quenched in cold water bath and analyzed immediately using a Varian 3700 gas chromatograph.

Acetaldehyde Via Methyl Acetate Reductive Carbonylation. The reactor and chemicals used for this reaction are very much similar to those used in preparing ethylidene diacetate. However, the reactor was provided with a pressure control "Grove" which maintained the desired reactor pressure. The pressure of the gas feed is adjusted so that the reactor pressure was slightly higher than the grove setting in order to obtain a continuous flow of gas through the reactor. The gaseous mixture leaving the grove was condensed and analyzed. The reactor temperature and pressure were kept at levels which were high enough to maintain the reactor contents in a boiling status through the entire reaction period.

Vapor Phase Hydrogenation of Acetic Anhydride. Acetic anhydride was pumped into an evaporator where it was mixed with hydrogen. The temperature of anhydride-hydrogen mixture was raised to the reaction temperature in a preheater zone, made of a 2 feet bed packed with 2 mm glass beads. The reaction took place in a 2 feet catalyst bed packed with 1 m.m. alpha-alumina coated with 0.5% Pd. The effluent was condensed and analyzed by G.C.

### Literature Cited

1. Rizkalla, N. (Halcon SD), British Patent 1538782, 1979.
2. Knoevenagel, E. Justus Liebigs Ann. Chem., 1905, 402,111.

3. Freeman, F., Karchevski, E. J. Chem., Eng. Data, 1977, 22,355.
4. Olah, G.A., Mehrotra, A. Synthesis, 1982, 962.
5. Michie, J., Miller, J. Synthesis, 1981, 824.
6. Hydrogen Process. 1965, 44, 287.
7. McMurry, J. Org. Reactions, 1976, 24, 187.
8. Brothers, P.J. Prog. Inorg. Chem., 1981, 28, 1.
9. Hallman, P., McGarvey, B., Wilkinson, G. J. Chem. Soc. A, 1968, 3143.
10. Harris, C.; Livingstone, S.; Reece, J. J. Chem. Soc. 1959, 1505.
11. Kingston, J.; Scollary, G. J. Chem. Soc., Chem. Comm. 1969, 455.
12. Hickey, C.; Maitlis, P.M. J. Chem. Soc., Chem. Comm. 1984,1609.
13. Luft, G.; Schrod, M. J. Mol. Catal., 1983, 22, 169.
14. Forster, D.; Singleton, T., J. Mol. Catal. 1982, 17, 299.
15. Hewlett, C. (Halcon International), British Patent 1468940, 1977.
16. Rizkalla, N. (Halcon International), U.S. Patent 411544, 1978.
17. Luft, G.; Schrod, M., J. Mol. Catal. 1983, 20, 175.
18. Schoenberg, A.; Heck, R.F., J. Amer. Chem. Soc. 1974, 76, 7761.
19. For review see Collman, J.; Hegedus, L., "Principles and Applications of Organotransition Metal Chemistry"; University Science Books, 1980, 427.
20. For example: Brown, C.; Wilkinson, G. J. Chem. Soc. A, 1970, 2753.
21. For general discussion, see Dickson, R.S., "Organometallic Chemistry of Rhodium and Iridium"; Academic Press, 1983, 106.
22. von Boven, M.; Alemdaroglu, N.; Penniger, J. Ind. and Eng. Chem. 1975, 15, 279.
23. Roth, J.; Craddick, J.; Hershman, A.; Paulik, F., Chemtech, 1971, 600.
24. Forster, D., J. Amer. Chem. Soc., 1976, 98, 846.
25. Schrod, M.; Luft, G., Ind. Eng. Chem. Prod. Res. Dev. 1981, 20, 649.
26. Fenton, D.M. (Union Oil), U.S. Patent 3576566, 1971.
27. Rizkalla, N. (Halcon SD), U.S. Patent 4323697, 1982.
28. Rizkalla, N. (Halcon SD), U.S. Patent 4335059, 1982.
29. Gane, B.R. (British Petroleum), European Patent, 1936.
30. Mitsubishi Gas Chemical Co. Inc., Japanese Patent 77-136111, 1976.
31. Pretzer, W.; Kobylnski, T. (Gulf), U.S. Patent 4133966, (1979).
32. Rizkalla, N. (Halcon SD), Patent Application filed in U.S.
33. Rizkalla, N. (Halcon SD), U.S. Patent 4551560, 1985.
34. Porcelli, R. V. (Halcon), U.S. Patent 4302611, 1981.
35. Rizkalla, N. (Halcon SD), British Patent 2079753, 1982.
36. Moy, D. (Halcon SD), U.S. Patent 4329512, 1982.
37. Moy, D. (Halcon SD), U.S. Patent 4356328, 1982.
38. Oxley, H.; Thomas, E.; Boyce, W. (Celanese), U.S. Patent 2425389.

RECEIVED August 14, 1986

## Chapter 11

# Production of Ethyl Acetate and Propionic Acid from Methanol and Synthesis Gas

E. Drent

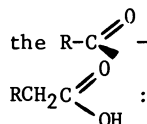
Koninklijke/Shell-Laboratorium, Amsterdam (Shell Research B.V.), Badhuisweg 3,  
1003 AA Amsterdam, The Netherlands

Rhodium-based, homogeneous catalyst systems are reported that can

be made to let the homologation of esters  $\text{R}-\text{C} \begin{array}{l} \text{=O} \\ \diagdown \\ \text{OR}' \end{array}$  occur

either at the  $-\text{OR}'$  moiety, to produce  $\text{R}-\text{C} \begin{array}{l} \text{=O} \\ \diagdown \\ \text{OCH}_2\text{R}' \end{array}$ , or at

the  $\text{R}-\text{C} \begin{array}{l} \text{=O} \\ \diagdown \\ \text{OH} \end{array}$ -moiety, to produce

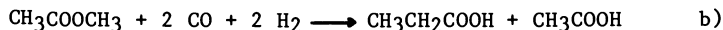


- (i) In combination with Ru, they ensure efficient homologation of esters, for example:



under mild reaction conditions (40 bar; 155 °C).

- (ii) In the absence of Ru, and with carboxylic acids as diluent/promoter they homologate esters to their next higher carboxylic acids, for example:

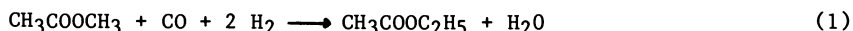


Mechanisms for both reactions are proposed, which are supported by the identification of several intermediate reactions. The role of various organic and inorganic reaction promoters is discussed. Amongst these, phosphine oxides are exceptionally efficient in that they induce high reaction rates combined with high selectivities. Reactions a) and b) potentially allow two-step, methanol/synthesis gas-based routes to ethyl acetate and propionic acid, respectively.

Methanol is an ideal starting material for the synthesis of many chemicals. It is the most important feedstock for the large-scale commercial production of acetic acid and formaldehyde. Additionally, a variety of other chemicals such as methyl esters, methyl halides and methyl ethers can be produced from it. Tennessee-Eastman's recent pioneering commercialization of a coal-based process for acetic anhydride production illustrates the growing importance of methanol as chemical feedstock.

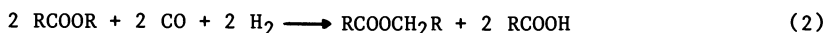
At present, methanol is (besides methane) the only chemical that can be produced with 100% selectivity from syngas, and it therefore constitutes a unique starting material for purely syngas-based industrial chemicals. This new role for methanol is also assisted by the ease of transporting it from areas where it can be cheaply produced from low-cost natural gas, coal or renewable sources such as biomass. The rising ethylene cost has given impetus to research devoted to finding routes in which ethylene can be replaced by methanol. The main emphasis has been on the homologation of methanol to ethanol (1). Homologation of substrates other than methanol has up till now been less widely studied. However, there is an increasing interest in the hydrocarbonylation of esters, as is evidenced by e.g. the development of the Halcon process (2) for the production of ethylene diacetate as a precursor for vinyl acetate.

It has been reported (3) that homogeneous ruthenium- or cobalt-iodide-based complexes catalyze the homologation of esters of carboxylic acid to their next higher homologues, for instance:



This reaction proceeds well only under rather severe conditions of pressure (> 200 bar) and temperature (> 200 °C).

We will here report on homogeneous catalyst systems which allow the homologation of esters to proceed under very mild reaction conditions, i.e. 20-60 bar and 150-160 °C, and according to two alternative stoichiometries:



and



It will be shown that Reactions 2 and 3 can be made to proceed at a high rate and with a high selectivity. Combined with simple esterification, Reactions 2 and 3 form a basis for two-step routes for the synthesis of respectively ethyl acetate and propionic acid starting from methanol and synthesis gas as the only feedstock.

### Experimental

The noble metal compounds  $\text{RhCl}_3 \cdot x \text{H}_2\text{O}$  and  $\text{RuCl}_3 \cdot x \text{H}_2\text{O}$  were purchased from Merck and Strem Chemicals. Reactants, solvents and



other chemicals were used as commercially available and were generally of p.a. quality.

All the experiments were carried out in a 300-ml Hastelloy C magnetically-stirred autoclave. After introduction of the catalyst components, feed (and solvent, if required), the autoclave was flushed with CO to remove air and then pressurized to the desired syngas pressure and CO/H<sub>2</sub> ratio. The autoclave was heated to the desired temperature in 15-20 minutes. When gas consumption took place, the working pressure was allowed to decrease and then the autoclave was repressurized depending on consumption rate. Alternatively, the working pressure was kept constant by feeding syngas of the desired composition (indicated in the tables). At the end of the experiment the autoclave was cooled and depressurized, and the liquid analyzed by conventional GLC techniques. The vented gas was analyzed for CO, H<sub>2</sub>, CH<sub>4</sub> and CO<sub>2</sub> by GC/mass spectroscopy.

The reported rates were calculated on the basis of product amounts and reaction times.

### Results and Discussion

Rhodium and ruthenium as co-catalysts in the homologation of methyl acetate to ethyl acetate. Homologation of an ester is not a simple reaction, requiring simultaneous selective carbonylation and selective hydrogenation in the presence of carbon monoxide. Although Rh complexes promoted with iodides are wellknown to be effective catalysts for the carbonylation of alcohols, ethers, and esters (4), their relatively low activity for hydrogenation in the presence of CO (and iodides) has thus far thwarted the use of Rh catalysts in alcohol and ester homologation reactions. However, certain Rh complexes, promoted by phosphines and/or pyridines are effective catalysts for the reductive carbonylation of esters to yield 1,1-diester, instead of higher homologue esters (2). On the other hand, Co and Ru complexes, promoted by iodides have been shown to be active for hydrogenation reactions and these catalysts have found application as ester homologation catalysts (3c, 5). The relatively low activity of Co and Ru complexes for carbonylation reactions has been overcome by using rather severe reaction conditions, i.e. 200 °C and > 100 bar. It was the purpose of the present study to find catalysts which, apart from being effective carbonylation catalysts, are highly active in hydrogenation-hydrogenolysis reactions in the presence of CO and would thus allow ester homologation to proceed under mild reaction conditions.

Table I shows the unique results obtained when a combination of RuCl<sub>3</sub> and RhCl<sub>3</sub>, in the presence of an iodide, is used in the homologation of methyl acetate. In particular experiments VI-IX demonstrate that the theoretical stoichiometry:



is almost completely reached. Catalysts based only on RuCl<sub>3</sub> have

a very low activity for the reductive carbonylation under the mild conditions applied (exp. I) and suffer from a lack of selectivity under more severe reaction conditions (notably  $\text{CH}_4$  formation and ether plus alcohol production increase rapidly with temperature).

Gas analysis shows that, whereas in Experiments II and III  $\text{CO}_2$  is clearly observable (from the water gas shift), no  $\text{CO}_2$  can be detected in Experiments VI-IX. In the latter experiments only a trace of  $\text{CH}_4$  (corresponding to less than 2 % based on converted methyl acetate) is found.

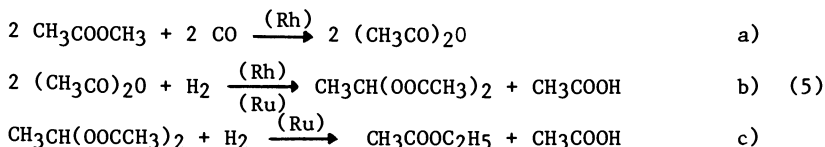
Equally notable is a change in type of by-products when  $\text{RhCl}_3$  is used as co-catalyst. In Experiments VI-IX both ethylidene diacetate (EDA) and acetic anhydride (AH) are formed as (minor) by-products. In Experiments I-III not even a trace of these products can be detected and instead alcohols and ethers are co-produced. With  $\text{RhCl}_3$ , and in the absence of  $\text{RuCl}_3$  (Exps. IV, V), EDA and AH are the main reaction products.

Experiments X-XII were performed with various other (i.e. other than  $\text{RhCl}_3$ ) co-catalysts, viz.  $\text{Pd}(\text{OAc})_2$ ,  $\text{Co}(\text{OAc})_2$  and  $\text{Mn}(\text{OAc})_2$ . With  $\text{Pd}(\text{OAc})_2$ , initially a reasonable activity (and high selectivity) is observed, but the catalyst system is not stable under the prevailing reaction conditions, resulting in Pd metal precipitation. A negligible activity is found with  $\text{Co}(\text{OAc})_2$  and with  $\text{Mn}(\text{OAc})_2$  as co-catalysts at 155 °C (Exp. XI, XII).

Our attempts to find substitutes for Ru, summarized in Table II, were unsuccessful. In all cases the low EA/AA ratio is indicative of a low selectivity, while the activity is also low (cf. exp. VIII, Table I).

Table III illustrates that the type of iodide source may have a profound effect on the course of the reaction. Both organic ( $\text{CH}_3\text{I}$ ), and inorganic iodides ( $\text{HI}$ ,  $\text{ZnI}_2$ ) can serve as iodide sources. Most inorganic iodides, other than  $\text{ZnI}_2$ , however, suffer from a lack of selectivity and are therefore less suitable for use. No activity is found in the absence of iodides.

The co-catalytic effects of  $\text{RhCl}_3$ , as evidenced by both a high activity and a high selectivity for the homologation of methyl acetate according to the stoichiometry of Reaction 4, suggest a reaction mechanism different from that postulated for the conventional Ru-catalyzed ester homologation (3). Both the products obtained with Rh alone as catalyst ((2), Table I) and the composition of the by-products formed in the Rh/Ru-catalyzed homologation are evidence of acetic anhydride and ethylidene diacetate being reaction intermediates:



Reaction 4 is then the sum of Reactions 5a-c.

Table I. Reductive Carbonylation of Methyl Acetate<sup>a</sup>

Exp. No.	Catalyst components (mmol)		Temp., °C	MeOAc conv., %	SEA <sup>b)</sup>	EA/AA <sup>c)</sup>	Other products
	RuCl <sub>3</sub>	CH <sub>3</sub> I					
I	RuCl <sub>3</sub> (0.5)	-	155	<4	-	-	
II	RuCl <sub>3</sub> (0.5)	-	190	20	45	0.3	CH <sub>4</sub> , ethers
III	RuCl <sub>3</sub> (0.5)	-	175	20	25	0.2	CH <sub>4</sub> , ethers alcohols
IV	-	RhCl <sub>3</sub> (0.5)	155	15	0	0	EDA, AH <sup>d)</sup> main products
V	-	RhCl <sub>3</sub> (0.5)	155	25	30	0.2	EDA main product
VI	RuCl <sub>3</sub> (1)	RhCl <sub>3</sub> (0.5)	155	25	91	0.50	traces EDA, AH _
VII	RuCl <sub>3</sub> (0.5)	RhCl <sub>3</sub> (1.0)	155	50	94	0.52	

VIII	do.	do.	ZnI <sub>2</sub> (30) α-picoline (3)	155	75	90	0.49	
IXe)	do.	do.	do.	155	20	85	0.43	EDA
X	RuCl <sub>3</sub> (0.35)	Pd(OAc) <sub>2</sub> (0.7)	ZnI <sub>2</sub> (30) CH <sub>3</sub> I (14) PPh <sub>3</sub> (4)	135	15*	94	0.50	-
XI	RuCl <sub>3</sub> (1)	Co(OAc) <sub>2</sub> (0.5)	CH <sub>3</sub> I (60)	155	<4	-	-	
XII	RuCl <sub>3</sub> (1)	Mn(OAc) <sub>2</sub> (0.5)	CH <sub>3</sub> I (60)	155	<4	-	-	

a) P<sub>CO</sub> = 20 bar; P<sub>H<sub>2</sub></sub> = 20 bar; pressure varies during experiment.

Intake: 0.6 mol methyl acetate.

Duration at reaction temperature: 15 h.

\* Pd precipitation

b)  $S_{EA} = \frac{2 \times \text{moles ethyl acetate produced}}{\text{moles methyl acetate converted}} \times 100 \%$

c) EA/AA = molar ratio ethyl acetate/acetic acid

d) EDA = ethylidene diacetate

AH = acetic anhydride

e) P<sub>CO</sub> = 10 bar; P<sub>H<sub>2</sub></sub> = 10 bar (constant pressure)

Table II. Reaction of MeOAc with Synthesis Gas<sup>a</sup>  
Search for substitutes for Ru

Exp. No.	Co-catalyst (mmol)	MeOAc conv., %	EA/AA <sup>b)</sup>	Other main products <sup>c)</sup>
I	CO <sub>2</sub> (CO) <sub>8</sub> (0.5)	15	0.2	ACH, EDA, AH
II	FeCl <sub>3</sub> (1)	20	0.12	do.
III	Re <sub>2</sub> (CO) <sub>10</sub> (0.5)	9	0.3	EDA, AH
IV	ZrCl <sub>4</sub> (0.5)	30	<0.1	EDA, AH, ACH + unidentified
V	H <sub>2</sub> PtCl <sub>6</sub> (0.5)	20	0.1	EDA, AH

a) Other catalyst components: 1 mmol RhCl<sub>3</sub>, 30 mmol ZnI<sub>2</sub>, 3 mmol -picoline.

T = 155 °C; PCO = 20 bar; PH<sub>2</sub> = 20 bar; t = 15 h

Intake: 0.6 mol. MeOAc

b) EA/AA = molar ratio ethyl acetate/acetic acid.

c) EDA = ethylidene diacetate, ACH = acetaldehyde, AH = acetic acid anhydride.

Table III. Homologation of Methyl Acetate to Ethyl Acetate<sup>a</sup>  
Effect of Iodide Source

Exp. No.	Iodide source (mmol)	Temp., °C	MeOAc conv., %	EA/AA <sup>b)</sup>	Other main products
I	-	160	< 1	-	-
II	ZnI <sub>2</sub> (30)	155	30	0.49	-
III	HI (50)	160	40	0.46	traces EDA, AH and PA <sup>c)</sup>
IV	CH <sub>3</sub> I (60)	160	35	0.48	do.
V	AlI <sub>3</sub> (20)	160	40	<0.1	EDA, AH
VI	LiI (30)	160	35	<0.1	EDA, AH

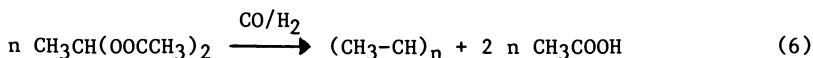
a) Catalyst: 0.5 mmol RhCl<sub>3</sub>; 1 mmol RuCl<sub>3</sub>, PCO = 20 bar, PH<sub>2</sub> = 20 bar, variable pressure, 15 h reaction time.  
Intake: 0.6 mol. methyl acetate

b) EA/AA = molar ratio ethyl acetate/acetic acid.

c) EDA = ethylidene diacetate, AH = acetic anhydride, ACH = Acetaldehyde, PA = propionic acid.

In separate experiments, we have demonstrated that Reactions 5a and 5b take place with catalysts based only on Rh. Reaction 5b is also catalyzed by Ru. The reactions proceed particularly efficiently under homologation reaction conditions when promoters such as phosphines and pyridines are present. This observation is in line with examples described in a German patent application (2).

Reaction 5c can also be separately demonstrated to take place under homologation conditions ( $\text{CO}/\text{H}_2 = 1$ ,  $T = 155\text{ }^\circ\text{C}$ ) with  $\text{Ru}/\text{CH}_3\text{I}$  (or  $\text{ZnI}_2$ ) or  $\text{Rh}/\text{Ru}/\text{CH}_3\text{I}$  (or  $\text{ZnI}_2$ ) catalysts. However, the use of neat EDA as feed results in a low selectivity to ethyl acetate. Instead, a rapid polymerization-deacetoxylation takes place:



The polymer (oily liquid) has not been fully characterized, but  $^{13}\text{C}$  and  $^1\text{H}$  NMR analyses suggest it to consist of highly branched hydrocarbons. At a lower starting concentration of EDA (e.g. 10 % (m/m) in acetic acid), ethyl acetate yields of more than 95 % can be obtained. Reactions 5b, c can also be combined in a single reaction step under syngas reaction conditions ( $\text{CO}/\text{H}_2 = 1$ ) with  $\text{Ru}/\text{CH}_3\text{I}$  (or  $\text{ZnI}_2$ ) catalysts resulting in high ethyl acetate yields (>90 %) directly from acetic anhydride.

Reactions 5b, c are particularly well catalyzed by  $\text{Ru}/\text{HBr}$  catalysts (7). Unfortunately, HBr is less suitable (than HI) as a promoter for overall reaction 4 because it promotes reaction 5a less effectively.

Reaction 5a does not proceed to any significant extent under our reaction conditions with catalyst based on Ru alone, thus explaining the low overall activity of Ru for Reaction 4.

For Reaction 4 to proceed selectively it will be necessary that Reaction 5c proceeds faster than, or concerted with, Reactions 5a, b so that no substantial build-up of EDA can take place and hence Reaction 6 will be prevented. Thus, we interpret the exceptional behaviour of  $\text{ZnI}_2$ ,  $\text{CH}_3\text{I}$ , and HI as iodide promoters in the sense that they allow a high hydrogenolysis-hydrogenation activity of the Ru function in the catalyst system. Whereas the hydrocarbonylation function of Rh (Reactions 5a, b) is promoted by a variety of iodides, it appears that the hydrogenolysis function of Ru (Reaction 5c) is very sensitive to the nature of the iodide source used, as evidenced by a low ethyl acetate/acetic acid product ratio obtained with iodides such as  $\text{AlI}_3$  and  $\text{LiI}$ .

Table IV shows that ester homologation is not limited to methyl acetate. A symmetric ester,  $\text{R}-\text{C} \begin{array}{l} \text{=O} \\ \diagdown \\ \text{OR} \end{array}$ , can be selectively converted to

the next higher homologue and its parent carboxylic acid. For example, homologation of ethyl propionate yields selectively propyl propionate and co-product propionic acid in a ratio of 1:2. Homologation of a symmetric branched ester, isopropyl isobutyrate, yields two esters, n- and iso-butyl isobutyrate and surprisingly almost exclusively isobutyric acid as co-product. This is probably due to isomerization of the isopropyl moiety during carbonylation. As can be expected on the

Table IV. Homologation of Various Esters<sup>a</sup>

Exp. No.	Ester (1% conversion)	Temp., °C	Time, h	Products		Σ Esters/Σ Acids (m/m)
				Esters	Acids	
I	$\text{CH}_3\text{CH}_2-\overset{\text{O}}{\parallel}{\text{C}}-\text{OC}_2\text{H}_5$ (30)	160	15	$\text{CH}_3\text{CH}_2-\overset{\text{O}}{\parallel}{\text{C}}-\text{OC}_3\text{H}_7$	$\text{CH}_3\text{CH}_2-\overset{\text{O}}{\parallel}{\text{C}}-\text{OH}$	~ 0.5
II	$\text{CH}_3-\overset{\text{O}}{\parallel}{\text{C}}-\overset{\text{O}}{\parallel}{\text{C}}-\text{CH}_3$ $\text{H} \quad \text{H} \quad \text{H}$	160	5	$\text{CH}_3-\overset{\text{O}}{\parallel}{\text{C}}-\overset{\text{O}}{\parallel}{\text{C}}-\text{OCH}_2\text{CH}_2\text{CH}_2\text{CH}_3$ (3) $\text{H} \quad \text{H} \quad \text{H}$ $\text{CH}_3-\overset{\text{O}}{\parallel}{\text{C}}-\overset{\text{O}}{\parallel}{\text{C}}-\text{O}-\text{CH}_2-\overset{\text{O}}{\parallel}{\text{C}}-\text{CH}_3$ (1) $\text{H} \quad \text{H} \quad \text{H}$	$\text{CH}_3-\overset{\text{O}}{\parallel}{\text{C}}-\overset{\text{O}}{\parallel}{\text{C}}-\text{OH}$ $\text{H} \quad \text{H}$ $\text{CH}_3\text{CH}_2\text{CH}_2-\overset{\text{O}}{\parallel}{\text{C}}-\text{OH}$ (trace)	~ 0.5
III	$\text{CH}_3-\overset{\text{O}}{\parallel}{\text{C}}-\text{OC}_2\text{H}_5$ (35)	170	15	$\text{CH}_3\text{CH}_2-\overset{\text{O}}{\parallel}{\text{C}}-\text{OC}_2\text{H}_5$ (4) $\text{CH}_3-\overset{\text{O}}{\parallel}{\text{C}}-\text{OC}_3\text{H}_7$ (1)	$\text{CH}_3-\overset{\text{O}}{\parallel}{\text{C}}-\text{OH}$ (1) $\text{CH}_3\text{CH}_2-\overset{\text{O}}{\parallel}{\text{C}}-\text{OH}$ (2.5)	~ 0.5
IV	$\text{CH}_3\text{CH}_2-\overset{\text{O}}{\parallel}{\text{C}}-\text{OCH}_3$ (60)	160	15	$\text{CH}_3\text{CH}_2-\overset{\text{O}}{\parallel}{\text{C}}-\text{OC}_2\text{H}_5$ (1) $\text{CH}_3-\overset{\text{O}}{\parallel}{\text{C}}-\text{OC}_3\text{H}_7$ (1.5) $\text{CH}_3\text{CH}_2-\overset{\text{O}}{\parallel}{\text{C}}-\text{OC}_3\text{H}_7$ (3) + methyl acetate/ethyl acetate	$\text{CH}_3-\overset{\text{O}}{\parallel}{\text{C}}-\text{OH}$ (1) $\text{CH}_3\text{CH}_2-\overset{\text{O}}{\parallel}{\text{C}}-\text{OH}$ (2.2)	~ 0.5

a) Catalyst: 1 RhCl<sub>3</sub>; 0.5 RuCl<sub>3</sub>; 30 ZnI<sub>2</sub>, 3 α-picoline ( ) = approximate molar ratios, 50 ml ester feed, CO/H<sub>2</sub> = 1/2 (60 bar).

basis of Reaction equations 5a-c, asymmetric esters,  $R_1-C \begin{array}{l} \text{O} \\ \parallel \\ \text{OR}_2 \end{array}$ , are

converted to two types of higher homologue esters and two coproduced acids, mixed anhydrides and 1,1-diesters now being the intermediates. For example, homologation of methyl propionate yields ethyl propionate and propyl acetate together with acetic acid and propionic acid. Transesterification and consecutive homologation lead to further products, e.g. propyl propionate.

A notable difference in reactivity between the various esters is observed, e.g. methyl esters and isopropyl esters give a much faster reaction than ethyl esters.

Search for effective organic promoters. Selective and active catalysts for Reaction 4 should not only be effective carbonylation catalysts, but also be highly effective in hydrogenation-hydrogenolysis reactions in the presence of CO. The most obvious parameters affecting activity and selectivity include: Rh/Ru ratio, partial CO and H<sub>2</sub> pressures, temperature, solvent type, and type of iodide promoter.

We will here describe some remarkable effects on reaction rate and selectivity that are observed when organic ligands are added to the catalyst system. Table V shows the effects of phosphine and pyridines. Comparison of Experiments I and II demonstrates a relatively weak promoting effect on the reaction rate when  $\alpha$ -picoline is added to a ZnI<sub>2</sub>-promoted catalyst system. The selectivity remains practically unchanged. Remarkably different results are obtained with CH<sub>3</sub>I as the iodide source (Exp. III and IV):  $\alpha$ -picoline exerts a strong promoting effect on the reaction rate, but the selectivity to ethyl acetate is greatly reduced, mainly due to polymer formation (Reaction 6). In terms of Reactions 5a-c this means that picoline strongly promotes hydrocarbonylation (Reactions 5a, b; Rh function), but at the same time inhibits hydrogenolysis (Reaction 5c; Ru function). Therefore, we applied small quantities of picoline (and pyridine) with respect to Ru (Exps. V, VI) and surprisingly observed besides restored selectivity, also retention of a strong promoting effect on the overall homologation reaction. This suggests that picolines function as co-catalysts in the catalytic hydrocarbonylation cycle, thus increasing the turnover frequency of the latter. Similar effects are observed with triphenylphosphine (Exps. VII, VIII). At phosphine/Ru < 1 both a high activity and a high selectivity can be maintained, while at phosphine/Ru > 1 the catalytic system becomes unselective, producing mainly polymer, EDA and AA. The effects demonstrated with  $\alpha$ -picoline and triphenylphosphine are exemplary for a wide variety of trivalent phosphorus and nitrogen compounds such as amines, amides, ureas, alkylphosphines, etc. Numerous attempts have been made to find compounds which promote both the hydrocarbonylation and the hydrogenolysis (Ru), for example by incorporating sterically hindered amines and phosphines to prevent complexation of the ligands with Ru. However, these attempts were all unsuccessful.



Table V. Homologation of Methyl Acetate to Ethyl Acetate<sup>a</sup>  
Effect of Organic Promoters

Exp. No.	Catalyst composition (mmol)	Temp., °C	Org. promoter (mmol)	MeOAc conv. rate, mol/(mol Rh.h)	S <sub>EA</sub> <sup>b)</sup>
I	RhCl <sub>3</sub> (1.0) RuCl <sub>3</sub> (0.5) ZnI <sub>2</sub> (30)	155	-	20	94
II	do.	155	α-picoline (3)	30	90
III	RhCl <sub>3</sub> (0.5) RuCl <sub>3</sub> (1.0) CH <sub>3</sub> I (60)	160	-	44	91
IV	do.	155	α-picoline (3)	160 <sup>c)</sup>	32
V	do.	160	α-picoline (0.1)	100	93
VI	do.	160	pyridine (0.1)	100	92
VII	RhCl <sub>3</sub> (0.25) RuCl <sub>3</sub> (1.0) CH <sub>3</sub> I (60)	160	PØ <sub>3</sub> (1)	125	75
VIII	do.	160	PØ <sub>3</sub> (0.5)	70	87

a) 25 ml methyl acetate, 25 ml acetic acid; time 5 h; P = 60 bar (constant)  
CO/H<sub>2</sub> = 1/2 (initially); gas feed CO/H<sub>2</sub> = 1/1

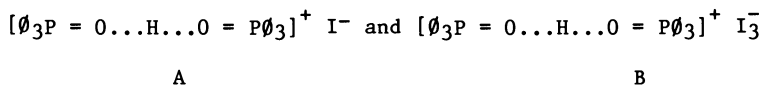
b)  $S_{EA} = \frac{2 \times \text{moles of ethyl acetate produced}}{\text{moles of methyl acetate converted}} \times 100 \%$

c) 2 h reaction time

As a potential class of compounds we came to consider phosphine oxides, reasoning that pentavalent phosphorus compounds are certain not to interact strongly with Ru.

Comparison of Experiment I with Experiments II and III in Table VI reveals a very strong rate increase (by more than a factor of 10) when triphenylphosphine oxide (TPO) is added to the catalyst. At the same time, the selectivity to ethyl acetate remains high. Comparison of Experiments II and III suggests that the homologation rate is approximately proportional to the applied TPO concentrations. Triphenylphosphinesulfide (TPS) behaves differently: at concentrations higher than the ruthenium concentration, only traces of ethyl acetate are produced and instead a selective reaction to acetic anhydride and ethylene diacetate is observed (Exp. IV). This again points to interference with the hydrogenolysis function (Ru), probably due to the complexing properties of the sulphide ion. At lower concentrations, ( $[TPS] \gg [Ru]$  and  $[TPS] < [Ru]$ ), again a high selectivity to ethyl acetate is obtained (Exp. V). Qualitatively, the same phenomena are observed with pyridine N-oxide. The relatively high hydrocarbonylation activity and selectivity to EDA are striking (Exp. VI). From NMR analysis it is clear that under the reaction conditions no reduction of phosphine oxide or pyridine oxide (to phosphine or pyridine, respectively) takes place.

NMR analysis ( $^1H$  and  $^{31}P$ ) of the reaction media and elemental analysis of crystals isolated from the reaction medium revealed the unique capacity of the phosphine oxide to form a hydrogen-bond (bridge) and behave as a cationic species:

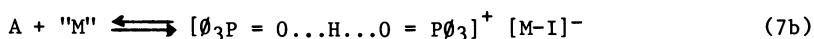


Complexes A and B can be simply prepared by passing HI into a solution of TPO in acetic acid at room temperature. Crystals of complex A form immediately and can be isolated by filtration. The suggested composition of complex A follows from NMR and elemental analysis. On standing of the filtrate (in air) further crystals of composition B are formed. Similar complexes were isolated with pyridine N-oxide.

Utilization of the free compounds A and B instead of TPO indeed led to the same promoting effect. These observations suggest that the effect is primarily due not to direct interaction between the active metal center and the oxide, but to the generation of a high concentration of strongly nucleophilic iodide ions:

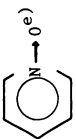
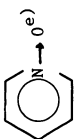


which in turn generate anionic metal centers:



Anionic metal species are then assumed to be the active catalyst.

Table VI. Homologation of Methyl Acetate to Ethyl Acetate<sup>a</sup>  
Effects of Pentavalent Phosphorus and Nitrogen Compounds

Exp. No.	Catalyst components (mmol)	Promoter (mmol)	MeOAc conv. rate, mol/(mol Rh.h)	SEA <sup>b)</sup>	SAH <sup>b)</sup>	SEDA <sup>b)</sup>
I	RhCl <sub>3</sub> (0.5) RuCl <sub>3</sub> (1)	-	44	94	3	3
II	RhCl <sub>3</sub> (0.125) RuCl <sub>3</sub> (1)	O=P <sub>3</sub> <sup>c)</sup> (4)	475	91	4	3
III	do.	O=P <sub>3</sub> <sup>c)</sup> (2)	250	92	3	3
IV	do.	S=P <sub>3</sub> <sup>d)</sup> (4)	160	<3	65	30
V	do.	S=P <sub>3</sub> <sup>d)</sup> (0.5)	300	88	8	4
VI	RhCl <sub>3</sub> (0.1) RuCl <sub>3</sub> (1.0)		115	<3	18	78
VII	do.		300	90	4	5

a) 25 ml methyl acetate, 25 ml acetic acid; time 5 h; P = 60 bar (constant); CO/H<sub>2</sub> = 1/2 (initially); gas feed CO/H<sub>2</sub> = 1/1; CH<sub>3</sub>I 60 mmol, Temp. = 160 °C.

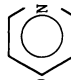
b) SEA =  $\frac{2 \times \text{moles of ethyl acetate produced}}{\text{moles of methyl acetate converted}} \times 100 \%$

SAH =  $\frac{\text{moles of acetic anhydride produced}}{\text{moles of methyl acetate converted}} \times 100 \%$

SEDA =  $\frac{2 \times \text{moles of ethylidene diacetate produced}}{\text{moles of methyl acetate converted}} \times 100 \%$

c) O=P<sub>3</sub> = triphenylphosphine oxide

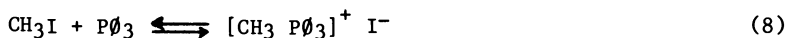
d) S=P<sub>3</sub> = triphenylphosphine sulfide

e)  = pyridine N-oxide

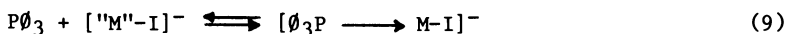
Such an explanation could also hold for the dependence of reaction selectivity (and activity) on the type of cation in the iodide promoter, as shown in Table III. The role of anionic Ru complexes and the effects of various iodide salts in syngas reactions have been elucidated by Dombek et al. (8).

The effects of TPO (and PO) could thus be attributed to their shifting of the equilibria between the various metal complexes towards anionic species.

Such an explanation is very similar to that of phosphine promotion, however, with the essential difference that free phosphine in equilibrium reactions such as



is able to complex directly to the active metal center:



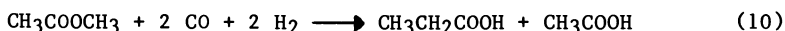
which may prevent or modify interaction of substrates (CO, H<sub>2</sub>, etc.) with the metal center, leading to a reduced activity. Thus, for complexing ligands such as phosphines and pyridines the generation of anionic complexes may in general be counteracted by a ligand-poisoning effect. In particular, the hydrogenolysis function (Ru) appears to be extremely sensitive to such complexation (even with e.g. TPS and PO).

An additional promoting effect of nucleophilic iodide species generated by application of both phosphines, pyridines and their oxides in carbonylation catalysis (Reaction 5a) may occur by their enhancement of iodide transfer through the "organic catalytic cycle": for instance, a phosphonium iodide generates, in reaction with methyl acetate, a phosphonium acetate plus CH<sub>3</sub>I; the latter is then participating in the Rh-based catalytic cycle to yield CH<sub>3</sub>C(=O)I, which in turn reacts with the phosphonium acetate to yield acetic anhydride and phosphonium iodide, etc. Such an explanation is in line with mechanistic studies by Polichnowski (6) of the role of inorganic iodides in Rh-catalyzed methyl acetate carbonylation.

In separate experiments, we have demonstrated that TPO also promotes hydrogenolysis by Ru (7), although the effects are weaker than for the Rh-catalyzed hydrocarbonylation of esters. The use of alkylphosphine oxides and their role in Ru-catalyzed syngas reactions have also been reported by Warren and Dombek (8b).

TPO as catalyst promoter may have important consequences. It will allow either a considerable reduction of the Rh inventory or a reduction of iodide promoter, thus leading to significantly reduced costs of a potential process.

Homologation of esters to higher-homologue carboxylic acids. As a spin-off of our work on ester homologation to higher-homologue esters we found that homologation of esters can also proceed to produce higher-homologue carboxylic acids, for instance:

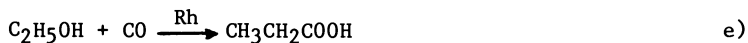
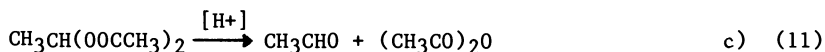
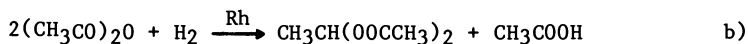
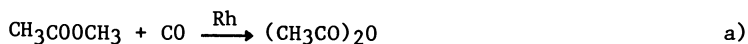


It will be shown that the mechanism of this reaction is very much related to that depicted by Equation 5.

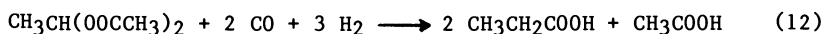
Relevant experimental results are summarised in Table VII. When using RhCl<sub>3</sub>/CH<sub>3</sub>I catalyst and acetic acid as reaction solvent, propionic acid can be produced; however, a high degree of dilution by acetic acid appears essential (see Exps I, II and III). At a high CH<sub>3</sub>I/CH<sub>3</sub>COOCH<sub>3</sub> ratio, CH<sub>3</sub>I also takes part in a fast reaction, resulting in homologation to C<sub>2</sub>H<sub>5</sub>I (Exp. III).

Acids considerably promote homologation to propionic acid. This applies not only to the weaker acids used as essential solvents, but also to added stronger acids (e.g. p-toluenesulphonic acid) (Exp. IV). Triphenylphosphine oxide promotes the generation of high yields of propionic acid, accompanied by (next to acetic acid) relatively small quantities of next higher homologue carboxylic acids (iso- + n-butyric acid) (Exp. V). Even at a low CH<sub>3</sub>I concentration, a high propionic acid yield is obtained (Exp. VI). As shown in Experiment VII, RuCl<sub>3</sub> is practically inactive for the reaction.

The above observations are best explained by a sequence of reactions similar to Reactions 5:



Reactions 11a-e add up to Reaction 10. Reactions 11a-b have been shown above to be catalyzed by Rh/CH<sub>3</sub>I. Reaction 11c, i.e. acid-catalysed pyrolysis of EDA to acetaldehyde and acetic anhydride, is well documented (9). Both reaction 11d, hydrogenation of aldehyde, and Reaction 11e, carbonylation of alcohols, are of course well known. The reaction sequence is in agreement with the fact that EDA and AH, especially in short-duration experiments, are detected as by-products. Acetaldehyde is also observed in small quantities, but no ethanol is found. Possibly, Reactions 11d and 11e occur concertedly. We have separately demonstrated that both EDA and AH are suitable feeds to produce propionic acid under homologation reactions conditions. We thus demonstrated



which is composed of Equations 11b + 2x11c + 11d + 11e, and



which is composed of Equations 11b + 11c + 11d + 11e.

Table VII. Homologation of Methyl Acetate to Propionic Acid<sup>a</sup>

Exp. No.	Catalyst (mmol)	Methyl acetate intake, mol	Temp., °C	pb), bar	Propionic acid <sup>c</sup> yield, %	By-products <sup>d</sup>
I	RhCl <sub>3</sub> (1) CH <sub>3</sub> I (30)	0.2	145	40	33	EDA, EA, AA
II	do.	0.4	160	40	trace	EDA
III	do.	0.1	145	40	40	EI, EA, AA
IV	RhCl <sub>3</sub> (1) CH <sub>3</sub> I (30) p-toluenesulphonic acid (3)	0.1	150	60	60	EI, AA 5-10 % iso- + n-butyric acids
V	RhCl <sub>3</sub> (1) CH <sub>3</sub> I (15) (Pφ <sub>3</sub> ) <sub>2</sub> O <sup>e</sup> (4)	0.1	160	60	78	AA + 10-15 % iso- + n-butyric acids
VI	RhCl <sub>3</sub> (1) CH <sub>3</sub> I (7.5) (Pφ <sub>3</sub> ) <sub>2</sub> O <sup>e</sup> (4)	0.1	160	60	72	AA + 10-15 % iso- + n-butyric acids
VII	RuCl <sub>3</sub> (1) <sup>f</sup> CH <sub>3</sub> I (30) p-toluenesulphonic acid (3)	0.1	155	40	trace	-

a) 35 ml acetic acid as reaction solvent; in all experiments 100 % methyl acetate conversion (time 15 h).

b) CO/H<sub>2</sub> = 1/1 (pressure drops during experiment).

c) Propionic acid yield =  $\frac{\text{moles of propionic acid produced}}{\text{moles of methyl acetate converted}} \times 100\%$

d) EDA = Ethylidene diacetate;

AA = Acetic acid in all cases major by-product;

EA = Ethyl acetate;

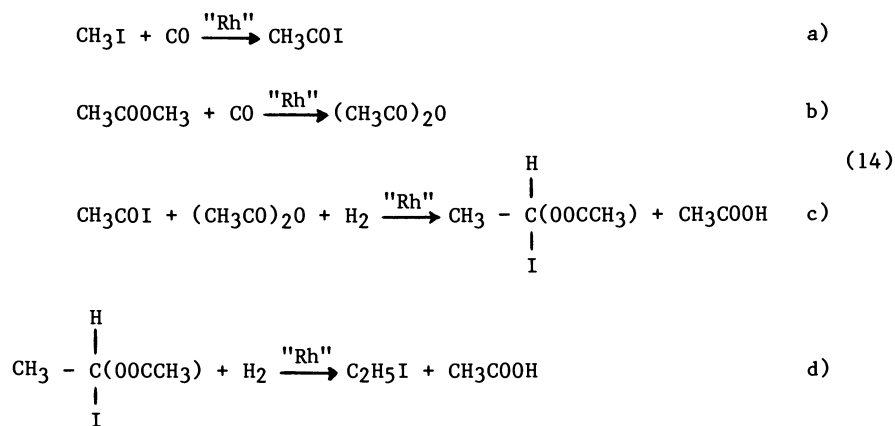
EI = Ethyl iodide

e) (Pφ<sub>3</sub>)<sub>2</sub>O = triphenylphosphine oxide

f) low conversion of methyl acetate

For both reactions a RhCl<sub>3</sub>/CH<sub>3</sub>I/TPO catalyst in acetic acid as reaction solvent affords propionic acid in more than 80 % yield according to the respective stoichiometries of Equations 12 and 13. Although acetic acid is present in excess in the reaction medium, it does not participate in the homologation as reactant. Only traces of propionic acid are produced in the absence of methyl acetate, ethylidene diacetate or acetic anhydride under our reaction conditions. Homologation of carboxylic acids has been reported by Knifton (10) to require more severe reaction conditions (220 °C, > 100 bar).

At a relatively high CH<sub>3</sub>I/CH<sub>3</sub>COOCH<sub>3</sub> ratio (≥ 0.5) homologation of CH<sub>3</sub>I to C<sub>2</sub>H<sub>5</sub>I proceeds rapidly. In the absence of methyl acetate, however, no CH<sub>3</sub>I homologation occurs. This can be explained by a mechanism similar to that represented by Equation 5:

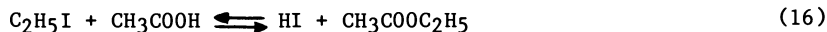


Reactions 14a-d add up to:



Analysis of the reaction products by <sup>13</sup>C NMR confirms the presence of minor quantities of α-iodoethyl acetate (CH<sub>3</sub>COOCHICH<sub>3</sub>), thus adding credence to the postulated Reaction sequence 14a-d.

Reaction 15 also plays a minor role in the homologation of methyl acetate to ethyl acetate (Reaction 4). However, when acetic acid is used as a reaction solvent, C<sub>2</sub>H<sub>5</sub>I never builds up to a significant concentration because of the equilibrium:



Reaction 10 is not limited to methyl acetate but can be generally applied. Table VIII shows some results with various starting esters and alkanolic acid solvents. In Experiments I and II the parent acid of the ester is different from the acid solvent. Transesterification reactions lead to two different starting esters and acids. Homologa-

Table VIII. Homologation of Various Esters to <sup>a</sup> Higher Homologue Carboxylic Acids

Exp. No.	Starting ester	Alkanoic acid solvent	Products
I	$\begin{array}{c} \text{O} \\ \parallel \\ \text{CH}_3\text{C} \\ \backslash \\ \text{OCH}_3 \end{array}$	$\begin{array}{c} \text{O} \\ \parallel \\ \text{CH}_3\text{CH}_2\text{C} \\ \backslash \\ \text{OH} \end{array}$	$\begin{array}{c} \text{O} \\ \parallel \\ \text{CH}_3\text{C} \\ \backslash \\ \text{OH} \end{array} \quad (4)$
			$\begin{array}{c} \text{O} \\ \parallel \\ \text{CH}_3\text{CH}_2\text{C} \\ \backslash \\ \text{OH} \end{array} \quad (-)$
			$\text{CH}_3-\text{CH}_2\text{CH}_2\text{C} \begin{array}{c} \text{O} \\ \parallel \\ \backslash \\ \text{OH} \end{array} \quad (1.2)$
			$\begin{array}{c} \text{CH}_3 \\   \\ \text{CH}_3-\text{C}-\text{C} \begin{array}{c} \text{O} \\ \parallel \\ \backslash \\ \text{OH} \end{array} \\   \\ \text{H} \end{array} \quad (1.0)$
II	$\begin{array}{c} \text{O} \\ \parallel \\ \text{CH}_3\text{CH}_2\text{C} \\ \backslash \\ \text{OCH}_3 \end{array}$	$\begin{array}{c} \text{O} \\ \parallel \\ \text{CH}_3\text{C} \\ \backslash \\ \text{OH} \end{array}$	$\begin{array}{c} \text{O} \\ \parallel \\ \text{CH}_3\text{C} \\ \backslash \\ \text{OH} \end{array} \quad (-)$
			$\text{CH}_3\text{CH}_2-\text{C} \begin{array}{c} \text{O} \\ \parallel \\ \backslash \\ \text{OH} \end{array} \quad (26)$
			$\text{CH}_3\text{CH}_2\text{CH}_2-\text{C} \begin{array}{c} \text{O} \\ \parallel \\ \backslash \\ \text{OH} \end{array} \quad (1.1)$
			$\begin{array}{c} \text{CH}_3 \\   \\ \text{CH}_3-\text{C}-\text{C} \begin{array}{c} \text{O} \\ \parallel \\ \backslash \\ \text{OH} \end{array} \end{array} \quad (1.0)$

--Continued on next page

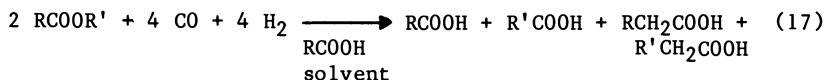


Table VIII---Continued

Exp. No.	Starting ester	Alkanoic acid solvent	Products
III	$\text{CH}_3\text{CH}_2\text{C}(\text{O})\text{OCH}_3$	$\text{CH}_3\text{CH}_2\text{C}(\text{O})\text{OH}$	$\text{CH}_3\text{C}(\text{O})\text{OH}$ (7) $\text{CH}_3\text{CH}_2\text{C}(\text{O})\text{OH}$ (-) $\text{CH}_3\text{CH}_2\text{-CH}_2\text{-C}(\text{O})\text{OH}$ (6) $\text{CH}_3\text{-C}(\text{O})\text{OH}$ (4.5)
IV	$\text{CH}_3\text{CH}_2\text{-C}(\text{O})\text{OC}_2\text{H}_5$	$\text{CH}_3\text{CH}_2\text{-C}(\text{O})\text{OH}$	$\text{CH}_3\text{CH}_2\text{-C}(\text{O})\text{OH}$ (-) $\text{CH}_3\text{-CH}_2\text{-CH}_2\text{-C}(\text{O})\text{OH}$ (7) $\text{CH}_3\text{-C}(\text{O})\text{OH}$ (5)

- a) 35 ml alkanoic acid solvent; 160 °C, 60 bar (CO/H<sub>2</sub> = 1)  
 Catalyst: 1 mmol RhCl<sub>3</sub>, 15 mmol CH<sub>3</sub>I, 4 mmol O=P(0)<sub>3</sub>; 7.5 ml ester feed.  
 Ester conversion in all cases ≥ 60%, product acid yield 60-80%.  
 ( ) = relative concentration  
 (-) = not determined.

tion of each ester yields its higher homologue and parent acid via Reaction 10, thus resulting in a complicated acid mixture. Experiment III shows an example of a "mixed" starting ester,  $R-C\overset{O}{\parallel}OR'$ , in its parent acid solvent. Even here, a complicated mixture of products arises, because now mixed anhydrides and 1,1-diesters (see Reactions 11) are intermediates. Thus Reaction 10 can be generally represented by:



With  $R, R' \geq C_2$  two isomers  $RCH_2COOH$  (i.e. normal + iso) are produced.

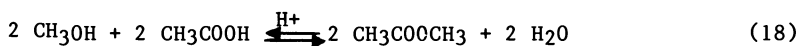
Experiment IV represents another example of a symmetric ester,  $R-C\overset{O}{\parallel}OR$ , in its parent acid solvent; apart from n/i-isomer formation, no complications arise.

In all cases relatively small quantities (10-15%) of "further" higher homologue acids are coproduced. This is attributed to the transesterification of "next" higher homologue product acids with starting ester in the course of the reaction. The products of transesterification are in turn homologated to their next higher homologues, etc.

We have thus made plausible that, basically, the mechanism of homologation to higher homologue carboxylic acids is the same as that of homologation to higher homologue esters, the difference being that whereas in the latter reaction intermediate EDA is hydrogenated to ethyl acetate, in the former reaction the EDA is pyrolysed, followed by hydrocarbonylation of intermediate acetaldehyde. Depending on the experimental conditions and the type of catalyst system used either reaction can take place with high selectivity.

Possible applications of ester-homologation reactions. The co-production of acetic acid and ethyl acetate according to Reaction 4 may find some interesting applications:

(i) Combination of homologation with esterification:



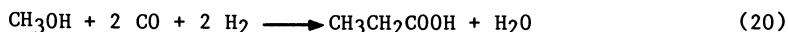
yields:



i.e. a two-step route to ethyl acetate from methanol and synthesis gas. It is interesting to note that such a process requires one process step less than conventional commercial esterification routes based on ethylene and methanol.

Various combinations of Reaction 19 with e.g. transesterification (with methanol) or hydrogenation give access to ethanol, acetic acid and/or methyl acetate.

- (ii) The co-production of propionic acid and acetic acid via Reaction 10 may also be combined with esterification Reaction 18, resulting in:



Reactions 19 and 20 demonstrate the possibility of replacing ethylene by methanol as a base chemical in routes to industrial chemicals.

### Conclusions

We have shown that ester homologation can proceed via two different stoichiometries, yielding either a higher homologue ester or a higher homologue carboxylic acid. For both reaction routes Rh species are essential components in the catalyst system in that they yield intermediate hydrocarbonylation products, which can be selectively converted either to higher homologue esters or to higher homologue carboxylic acids. Thus a Ru-assisted, Rh-based catalyst system promoted with suitable organic or inorganic compounds yields a higher homologue ester and a coproduced parent carboxylic acid of the starting ester in high yield and under mild reaction conditions. Such a homologation stoichiometry differs from that of conventional Co- or Ru-based catalyst systems, which yield H<sub>2</sub>O and/or CO<sub>2</sub> as by-product.

The activity of the Rh-catalysts is strongly promoted by phosphine oxides, which phenomenon is attributed to the generation of anionic Rh species which are responsible for the hydrocarbonylation of the ester, yielding 1,1-diester as intermediates. Hydrogenolysis of these intermediates is catalyzed by the Ru species under mild conditions and may proceed with high selectivity. This compares very favourably with Co- or Ru-catalyzed homologation, which requires direct hydrogenation of intermediate acyl complexes and calls for severe reaction conditions.

In the absence of Ru and using carboxylic acids as a reaction diluent/promoter, esters are homologated to their higher homologue carboxylic acids with coproduction of the parent carboxylic acid of the starting ester. Intermediate 1,1-diester are then efficiently converted to higher carboxylic acids by pyrolysis-hydrocarbonylation reactions, proceeding under the same mild reaction conditions. The presented chemistry offers methanol/syngas-based two-step-routes to such valuable chemicals as ethyl acetate and propionic acid.

### Acknowledgments

The author is grateful to Mr. W. Jager for his able technical assistance and to Drs. A.L. Farragher, G.T. Pott, J.A.M. van Broekhoven, J.C. van Ravenswaay Claasen and R.L. Wife for their support and interest.

### Literature Cited

- (a) Slocum, D.W. In "Catalysis in Organic Synthesis"; Jones, W., Ed.; Academic Press: New York, 1980; p. 245;
- (b) Wender, I. Catal. Rev.-Sci Eng. 1976, 14, 97;

- (c) Bahrmann, H.; Cornils, B. In "New Syntheses with Carbon Monoxide"; Falbe, J., Ed.; Springer-Verlag. Berlin, 1980; p. 226;
- (d) R per, M.; Loevenich, H. In: "Catalysis in C<sub>1</sub>-Chemistry"; Reidel Publ.: Dordrecht, 1983; p. 105;
- (e) Braca, G.; Sbrana, G. In "Aspects of Homogeneous Catalysis", Reidel Publ., Vol. V, 1984; p. 241.
2. (a) German Patent Application 2 610 035 to Halcon (1976);  
(b) German Patent Application 2 856 791 to Halcon (1979).
3. (a) Braca, G.; Sbrana, G.; Valentini, G.; Andrich, G.P.; Gregorio, G.J.  
J. Am. Chem. Soc. 1978, 100, 6238;  
(b) Braca, G.; Sbrana, G.; Valentini, G.; Cini, M.J. J. Mol. Catal. 1982, 17, 323;  
(c) German Patent Application 2 731 962 to Imhausen Chemie GmbH (1979);  
(d) European Patent Application 37184 to Rhone-Poulenc Ind. (1980).
4. Forster, D. Adv. Organomet. Chem. 1979, 17, 255.
5. (a) Braca, G.; Paladini, L.; Sbrana, G.; Valentini, G.; Andrich, G.; Gregorio, G. Ind. Eng. Chem., Prod. Res. Dev. 1981, 20, 115;  
(b) Braca, G.; Sbrana, G.; Valentini, G.; Andrich, G.; Gregorio, G.  
Fund. Res. Homogeneous Catal. 1979, 3, 221;  
(c) Braca, G.; Gunani, G.; Raspolli, A.M.; Sbrana, G.; Valentini, G.  
Prod. Res. Dev. 1984, 23, 409;
6. Polichnowski, S.W. J. Chem. Educ. 1986, 63, 206.
7. European Patent Application 117 575 (1984) to Shell Internationale Research Maatschappij B.V.
8. (a) Dombek, B.D. J. Organomet. Chem. 1983, 250, 467;  
(b) Warren, B.; Dombek, B. J. Catal. 1983, 79, 334.
9. Kirk-Othmer, "Encyclopedia of Chemical Technology"; Interscience. New York, 1965; 2nd ed. VIII, p. 410.
10. (a) Knifton, J. Hydrocarbon Process. 1981, 60, 113;  
(b) Knifton, J. J. Mol. Catal. 1981, 11, 91.

RECEIVED July 15, 1986

## Chapter 12

# Vapor-Phase Carbonylation of Dimethyl Ether and Methyl Acetate with Supported Transition Metal Catalysts

Tsutomu Shikada, Kaoru Fujimoto, and Hiro-o Tominaga

Department of Synthetic Chemistry, Faculty of Engineering, The University of Tokyo, Hongo, Bunkyo-ku, Tokyo 113, Japan

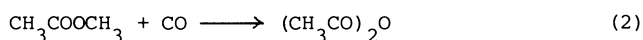
It was found that a nickel-activated carbon catalyst was effective for vapor phase carbonylation of dimethyl ether and methyl acetate under pressurized conditions in the presence of an iodide promoter. Methyl acetate was formed from dimethyl ether with a yield of 34% and a selectivity of 80% at 250°C and 40 atm, while acetic anhydride was synthesized from methyl acetate with a yield of 12% and a selectivity of 64% at 250°C and 51 atm. In both reactions, high pressure and high CO partial pressure favored the formation of the desired product. In spite of the reaction occurring under water-free conditions, a fairly large amount of acetic acid was formed in the carbonylation of methyl acetate. The route of acetic acid formation is discussed. A molybdenum-activated carbon catalyst was found to catalyze the carbonylation of dimethyl ether and methyl acetate.

The synthesis of acetic acid (AcOH) from methanol (MeOH) and carbon monoxide has been performed industrially in the liquid phase using a rhodium complex catalyst and an iodide promoter (1-4). The selectivity to acetic acid is more than 99% under mild conditions (175°C, 28 atm). The homogeneous rhodium catalyst is also effective for the synthesis of acetic anhydride (Ac<sub>2</sub>O) by the carbonylation of dimethyl ether (DME) or methyl acetate (AcOMe) (5-13). However, rhodium is one of the most expensive metals, and its' proved reserves are quite limited. It is highly desirable, therefore, to develop a new catalyst as a substitute for rhodium.

We have already reported that nickel supported on activated carbon exhibits an excellent activity for the vapor phase carbonylation of methanol in the presence of methyl iodide (MeI) at moderate pressures (14-16). In addition, corrosive attack of iodide compounds on reactors is expected to be minimized in the vapor phase system.

We have tried to explore the catalytic capabilities of

transition metals supported on activated carbon for the carbonylation of dimethyl ether and methyl acetate (17-19). It was found that nickel and molybdenum gave methyl acetate from dimethyl ether and acetic anhydride from methyl acetate with high selectivities. In the present work, catalytic features of nickel-activated carbon (Ni/A.C.) and molybdenum-activated carbon (Mo/A.C.) for the carbonylation of dimethyl ether and methyl acetate were studied together with the effects of several factors that controlled the rate of carbonylation.



### Experimental

Nickel-activated carbon catalysts were prepared by impregnating commercially available activated carbon granules (Takeda Shirasagi C, 20-40 mesh) with aqueous solutions of nickel chloride or nickel acetate, followed by drying in air at 120°C for 24 h and then activating in a stream of hydrogen at 400°C for 3 h. Molybdenum-activated carbon catalysts were prepared by the same procedure but using an aqueous solution of ammonium molybdate and activating in flowing hydrogen at 450°C for 3 h.

A continuous-flow reactor with a fixed catalyst bed was employed at pressurized conditions. Gaseous dimethyl ether was supplied to the reactor at its vapor pressure with carbon monoxide while liquid reactants such as methyl acetate, methyl iodide, and water were fed with microfeeders. Methyl acetate used in this experiment was dehydrated by Molecular Sieve 5A before use. A part of the reaction mixture was sampled with a heated syringe and was analyzed by gas chromatography.

The product yields were calculated by the following equation.

$$\text{Yield} = (nr_p/2r_R)100 \quad (3)$$

where  $n$  is the number of methyl groups in a molecule,  $r_p$  is the formation rate of product (mol/g·h), and  $r_R$  is the feed rate of dimethyl ether or methyl acetate (mol/g·h).

### Results and Discussion

Carbonylation of Dimethyl Ether on Ni/A.C. Catalysts. The main product of this reaction was methyl acetate. Small amounts of acetic acid, acetic anhydride, methane and CO<sub>2</sub> were formed as by-products. Figure 1 shows the product yields and the selectivity to methyl acetate as a function of reaction temperature. The yield of methyl acetate increased with a rise in the temperature up to 250°C and then decreased, while those of acetic acid and methane increased to lower the selectivity to methyl acetate. A trace amount of acetic anhydride was formed at around 250°C. Figure 2 shows the effect of operational pressure on the product yields and the selectivity to methyl acetate. Methyl acetate was formed with a yield of 14.2% and a selectivity of 95.3% at 10 atm. The yield of methyl acetate increased monotonically with an increase in the

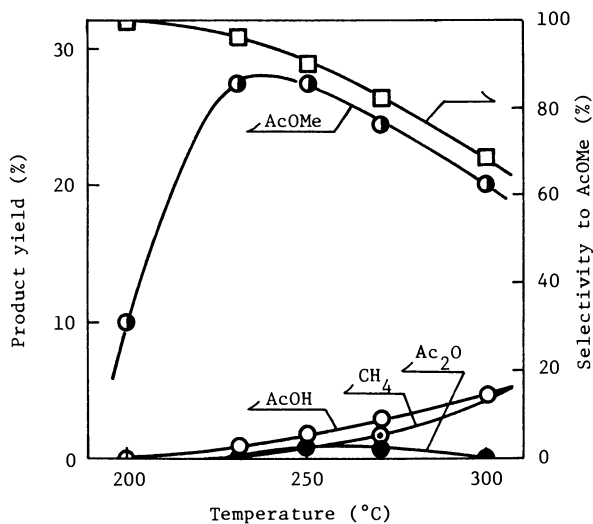


Figure 1. Effect of reaction temperature on DME carbonylation. 2.5wt%Ni/A.C., 10 atm, W/F (Weight of catalyst/Flow rate)=5 g·h/mol, CO/DME/MeI = 100/9.5/1.

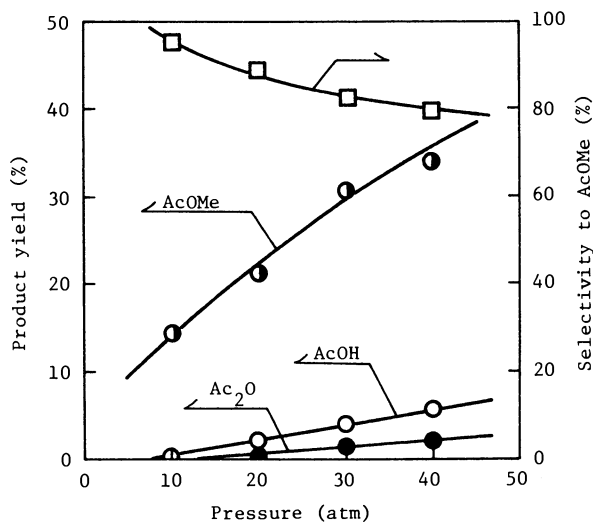


Figure 2. Effect of reaction pressure on DME carbonylation. 2.5wt%Ni/A.C., 250°C, W/F=2.5 g·h/mol, CO/DME/MeI=60/9.5/1.0.

pressure, while its selectivity decreased gradually. Small amounts of acetic acid and acetic anhydride were found in the products and their selectivities increased with increasing pressure suggesting that they were formed successively from methyl acetate. The fact that higher pressure is suitable for the formation of acetic anhydride agrees with the results in the carbonylation of methyl acetate mentioned later.

Table I shows the effects of MeI/DME and CO/DME ratios in the feed gas on product yields. With increasing MeI/DME ratio both methyl acetate yield and selectivity increased. The yield of methyl acetate increased with an increase in the CO/DME ratio whereas its selectivity decreased. In the case of methanol carbonylation on Ni/A.C. catalyst, the product yield and selectivity were strongly affected by CO/MeOH ratio but not by MeI/MeOH ratio (14-16). The promoting effect of methyl iodide on the methanol carbonylation reached a maximum at a very low partial pressure, that is 0.1 atm or lower. However, both CO/DME and MeI/DME ratios were important for regulating the product yield and selectivity of the dimethyl ether carbonylation. This suggests that the two steps, namely, the dissociative adsorption of methyl iodide on nickel (Equation 4) and the insertion of CO (Equation 5) are slow in the case of dimethyl ether reaction.

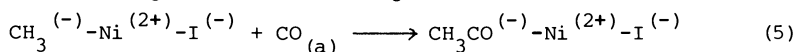
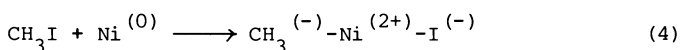


Figure 3 shows the effect of partial pressure of water on the rate of dimethyl ether carbonylation. It is apparent from Figure 3 that the reaction is markedly accelerated by added water. One possible explanation for this is the hydrolysis of dimethyl ether to methanol and its subsequent carbonylation. However, the contribution of the hydrolysis is quite small as shown in Figure 3. Therefore, the carbonylation of dimethyl ether via methanol should be negligible. The role of water for the reaction is not clarified yet.

Carbonylation of Methyl Acetate on Ni/A.C. Catalysts. Table II shows the catalytic activities of nickel and platinum group metals supported on activated carbon for the carbonylation of methyl acetate. Ruthenium, palladium, or iridium catalysts showed much lower activity for the synthesis of acetic anhydride than the nickel catalyst. In contrast, the rhodium catalyst, which has been known to exhibit an excellent carbonylation activity in the homogeneous system (1-13), showed nearly the same activity as the nickel catalyst but gave a large amount of acetic acid.

Figure 4 shows the effect of operational pressure on the reaction. The yield of acetic anhydride increased with an increase in the pressure. The selectivity to acetic anhydride was low at 30 atm because of a fairly high selectivity to AcOH. Figure 5 shows the effect of CO/AcOMe ratio in the feed at an operational pressure of 15 atm. When the ratio was 1, little acetic anhydride was formed. However, acetic anhydride comprised one of the main products when the CO/AcOMe ratio was raised up to 10. Thus, high operational pressure and high CO partial pressure were found to be advantageous for the synthesis of acetic anhydride.



Table I. Effects of MeI/DME and CO/DME Ratios on Carbonylation of Dimethyl Ether<sup>a</sup>

Feed		Product yield (%)				CO <sub>2</sub> /CH <sub>4</sub> <sup>b</sup>	Selectivity to AcOMe (%)
MeI/DME <sup>b</sup>	CO/DME <sup>b</sup>	AcOMe	Ac <sub>2</sub> O	AcOH	CH <sub>4</sub>		
0.04	2.4	11.3	0.1	1.2	0.3	1.4	87.6
0.09	2.4	17.6	0.7	1.9	0.1	0.8	86.7
0.17	2.4	28.6	0.2	2.2	0.6	1.5	90.5
0.09	1.0	11.6	0.1	0.6	0.4	0.6	91.3
0.09	4.2	27.2	0.5	3.5	0.2	1.7	81.9

<sup>a</sup>Catalyst : 10 wt% Ni/A.C., reaction conditions : temperature, 250°C; pressure, 11 atm; W/F, 9.8 g·h/mol. <sup>b</sup>Molar ratio.

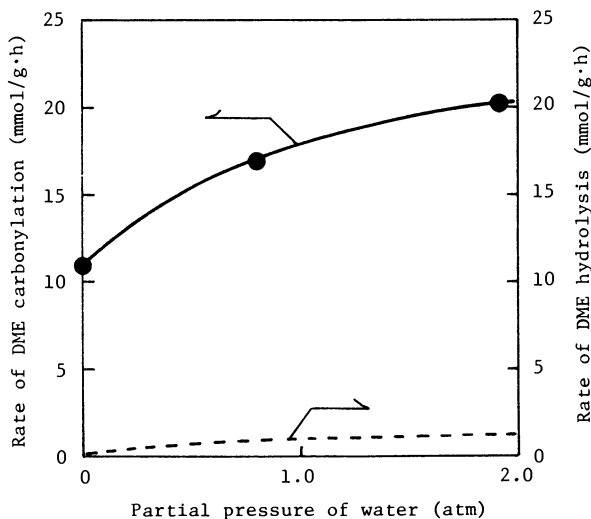


Figure 3. Effect of partial pressure of water on DME carbonylation. 2.5wt%Ni/A.C., 250°C, P<sub>total</sub>=10 atm (P<sub>DME</sub>=0.7 atm, P<sub>CO</sub>=3.9 atm, P<sub>MeI</sub>=0.3 atm, N<sub>2</sub> balance); dotted curve : CO free condition.

Table II. Activities of supported metal catalysts

Catalyst element <sup>b</sup>	Product yield (%)				CO <sub>2</sub> /CH <sub>4</sub> <sup>c</sup>
	Ac <sub>2</sub> O	AcOH	MeOH	CH <sub>4</sub>	
Ni	10.8	9.9	2.1	2.6	1.1
Ru	1.9	4.4	0.9	1.6	2.0
Pd	2.1	3.5	tr	0.3	-
Ir	3.0	4.5	tr	0.1	-
Rh	9.4	13.1	1.2	0.8	0.9

<sup>a</sup>Reaction conditions : temperature, 250°C; pressure, 15 atm; W/F, 10 g·h/mol, CO/AcOMe/MeI, 100/9/1 molar ratio. <sup>b</sup>2.5 wt% metal/A.C. <sup>c</sup>Molar ratio.

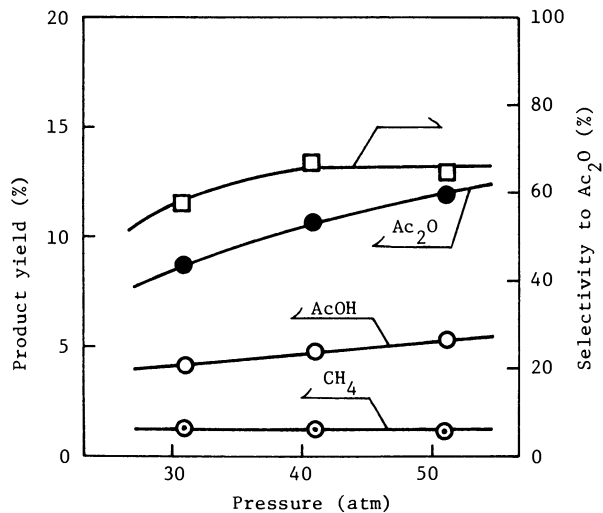


Figure 4. Effect of pressure on AcOMe carbonylation. 10wt%Ni/-A.C., 250°C, W/F=10 g·h/mol, CO/AcOMe/MeI=108/19/1.

Figure 6 shows the TPR spectra of adsorbed CO on nickel. The CO was desorbed mostly as the molecular form, whereas the amounts of desorbed carbon dioxide and methane were quite small. Thus, most of the CO adsorbed on nickel is in an undissociated state, and the extent of its adsorption is fairly weak, as the desorption is completed below 200°C. In contrast, the adsorption of methyl acetate on nickel is stronger than those of other reactants or products, as evaluated from the retention time in the nickel-activated carbon column shown in Table III. This fact suggests that most of the nickel is covered by methyl acetate and reaction products, and the coverage of adsorbed CO is quite low under the reaction conditions when the partial pressure of CO is close to that of methyl acetate. The carbonylation is therefore accelerated by increasing the CO/AcOMe ratio which increases the coverage of CO adsorbed competitively with methyl acetate.

As mentioned above, not only acetic anhydride but a large amount of acetic acid is formed in the carbonylation of methyl acetate on Ni/A.C. catalyst. For the formation of acetic acid from methyl acetate, molecular hydrogen or water is needed and would have to be formed during the reaction. It has been reported that a large amount of acetic acid is also formed in the liquid phase carbonylation of methyl acetate with a homogeneous rhodium complex catalyst (20). In this catalyst system, a carbonaceous compound is precipitated in the solution after the reaction. This fact suggests that the formation of acetic acid in the present system may be attributed to hydrogenation or hydrolysis of methyl acetate or acetic anhydride by hydrogen or water which is formed from a part of methyl acetate or acetic anhydride and which is accompanied by carbon formation.

Table IV shows the reactivities of raw materials and products on a nickel-activated carbon catalyst and the effect of hydrogen on the reactions. When carbon monoxide and hydrogen were introduced into the catalyst, no product was formed. Thus, the hydrogenation of CO does not proceed at all. When methyl iodide was added to the above-mentioned feed, 43% of the methyl iodide was converted to methane. In the presence of methyl iodide small amounts of methane, methanol, and acetic acid were formed from methyl acetate, while small amounts of methane and acetic acid were also formed from acetic anhydride. Hydrogen fed with methyl acetate accelerated the formation of methane and acetic acid remarkably.

Figure 7 shows the results of methyl acetate carbonylation in the presence of water. Methanol and dimethyl ether were formed up to 250°C suggesting that hydrolysis of methyl acetate proceeded. With increasing reaction temperature, the yield of acetic acid increased remarkably, while those of methanol and dimethyl ether decreased gradually. Figure 8 shows the effects of partial pressures of methyl iodide, CO, and methyl acetate in the presence of water. The rate of acetic acid formation was 1.0 and 2.7 order with respect to methyl iodide and CO, respectively. Thus, the formation of acetic acid from methyl acetate is highly dependent on the partial pressure of CO. This suggests that acetic acid is formed by hydrolysis of acetic anhydride (Equation 6) which is formed from methyl acetate and CO rather than by direct hydrolysis of methyl acetate.

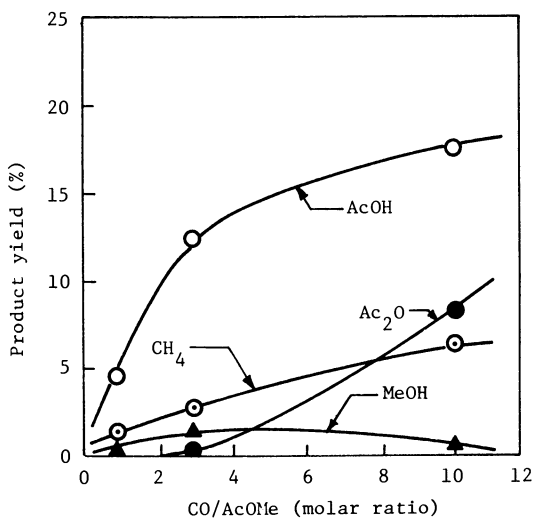


Figure 5. Effect of CO/AcOMe ratio in feed gas. 2.5 wt% Ni/A.C., 275 C, 15 atm, W/F = 10 g·h/mol, MeI/AcOMe = 1/10 (17). Reproduced with permission from reference 17. Copyright 1983, Elsevier Science.

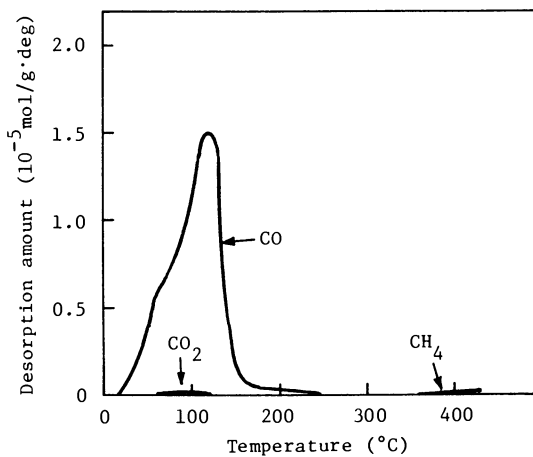


Figure 6. TPR spectra of adsorbed CO on 2.5 wt% Ni/A.C. catalyst. Heating rate : 400°C/h, H<sub>2</sub> flow rate : 100 cm<sup>3</sup>/g min.

Table III. Relative Retention Time of Reactant and Product Materials on 2.5 wt% Nickel-Activated Carbon<sup>a</sup>

Material	Retention time <sup>b</sup> (s)
CO	0
MeOH	2
MeI	36
AcOH	46
Ac <sub>2</sub> O	57
AcOMe	70

<sup>a</sup>Temperature, 200°C; pulse amount, 0.1 mol/mol of Ni.

<sup>b</sup>Normalized on the basis of the effluent time of N<sub>2</sub>.

Table IV. Reactions of Raw materials and Products<sup>a</sup>

Feed (molar ratio)	W/F (g·h/mol)	Product yield (%)			
		Ac <sub>2</sub> O	AcOH	MeOH	CH <sub>4</sub>
CO/H <sub>2</sub> (100/25)	8.9	-	-	-	0 <sup>b</sup>
CO/H <sub>2</sub> /MeI (100/25/1)	8.9	-	-	-	43.0 <sup>c</sup>
AcOMe/MeI/N <sub>2</sub> (10/1/100)	10.0	-	2.3 <sup>d</sup>	1.5 <sup>d</sup>	2.0 <sup>d</sup>
Ac <sub>2</sub> O/MeI/N <sub>2</sub> (10/1/100)	10.0	-	4.9 <sup>e</sup>	-	0.2 <sup>e</sup>
CO/AcOMe/MeI/H <sub>2</sub> (100/9/1/25)	8.2	1.2 <sup>d</sup>	45.1 <sup>d</sup>	-	33.7 <sup>d</sup>

<sup>a</sup>Catalyst : 2.5 wt% Ni/A.C., reaction conditions : temperature, 250°C; pressure, 11 atm. <sup>b</sup>CO base. <sup>c</sup>MeI base. <sup>d</sup>AcOMe base.

<sup>e</sup>Ac<sub>2</sub>O base.

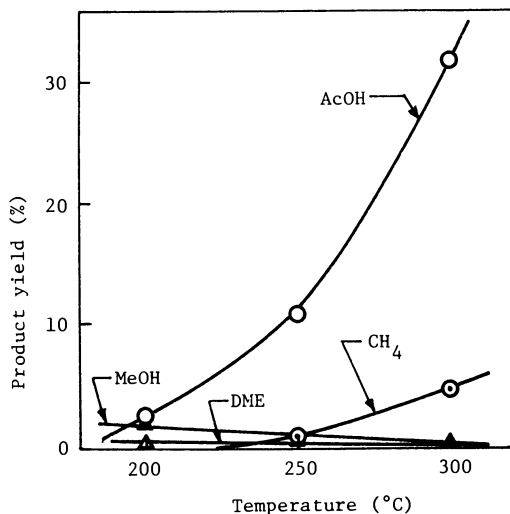


Figure 7. Carbonylation of AcOMe in the presence of water. 2.5wt%Ni/A.C., 11 atm, W/F=10 g·h/mol, CO/AcOMe/MeI/H<sub>2</sub>=29/9/1/4.5.

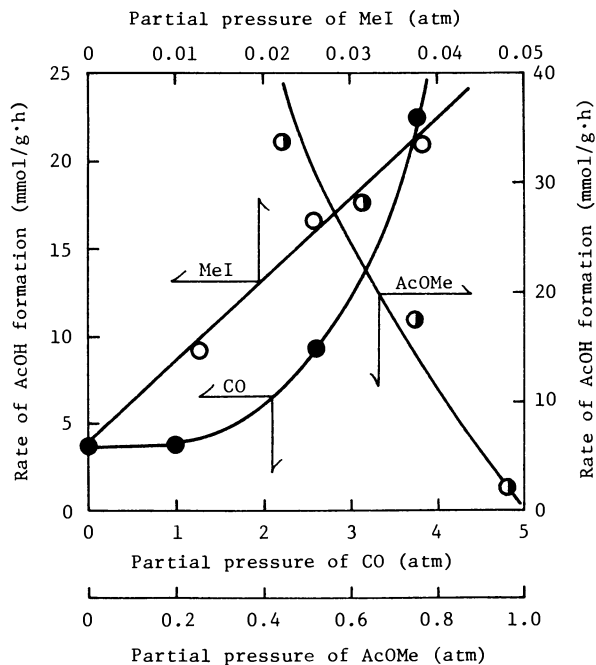
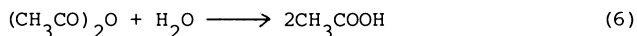


Figure 8. Effect of partial pressures of CO, MeI and AcOMe on the rate of AcOH formation in the presence of water. 2.5wt%Ni/A.C., 250°C, 10 atm, (●)  $P_{AcOMe}=0.6$  atm;  $P_{MeI}=0.01$  atm;  $P_{H_2O}=0.6$  atm, (○)  $P_{AcOMe}=0.6$  atm;  $P_{CO}=2.8$  atm;  $P_{H_2O}=0.6$  atm, (◐)  $P_{CO}=7.4$  atm;  $P_{MeI}=0.02$  atm;  $P_{H_2O}=1.8$  atm.



On the other hand, the reaction order with respect to methyl acetate was -1.7. The strong self-inhibition effect of methyl acetate should be noted, because of stronger adsorption of methyl acetate on Ni/A.C. than other reactants.

Carbonylation of Dimethyl Ether and Methyl Acetate on Mo/A.C. Catalyst. In this section, the carbonylation of dimethyl ether and methyl acetate on Mo/A.C. catalyst was investigated. To our knowledge, molybdenum has never been reported to catalyze carbonylation reactions.

Table V shows the results obtained for the carbonylation of dimethyl ether and methyl acetate with molybdenum catalysts supported on various carrier materials. In the case of dimethyl ether carbonylation, molybdenum-activated carbon catalyst gave methyl acetate with a yield of 5.2% which was about one-third of the activity of nickel-activated carbon catalyst. Silica gel- or  $\gamma$ -alumina-supported catalyst gave little carbonylated product. Similar results were obtained in the carbonylation of methyl acetate. The carbonylation activity occurred only when molybdenum was supported on activated carbon, and it was about half the activity of nickel-activated carbon catalyst.

Figure 9 shows the product yields as a function of operational pressure in the carbonylation of methyl acetate. The yield of acetic anhydride increased monotonically with increasing pressure, while that of methane was almost unchanged. The yield of acetic acid increased up to 30 atm and then decreased above that pressure. Acetic anhydride was formed with a yield of 15% and a selectivity of 83% at 45 atm, indicating that high operational pressure was favorable for the selective formation of acetic anhydride on the Mo/A.C. catalyst.

Table V. Carbonylation Activities of Supported Molybdenum and Nickel-Activated Carbon Catalysts<sup>a</sup>

Reactant <sup>b</sup>	Catalyst <sup>c</sup>	Temp (°C)	Press. (atm)	Product yield (%)				CO <sub>2</sub> /CH <sub>4</sub> <sup>d</sup>
				AcOMe	Ac <sub>2</sub> O	AcOH	CH <sub>4</sub>	
DME	Mo/A.C.	300	11	5.2	0	0	2.7	0.1
DME	Mo/SiO <sub>2</sub>	300	11	0.6	0	0	0.2	0.1
DME	Mo/ $\gamma$ -Al <sub>2</sub> O <sub>3</sub>	300	11	0.4	0	0	1.1	0.1
DME	Ni/A.C.	300	11	15.2	tr	7.4	3.2	0.8
AcOMe	Mo/A.C.	250	15	-	4.5	6.6	1.3	0.4
AcOMe	Mo/SiO <sub>2</sub>	250	15	-	0	0	0.1	-
AcOMe	Mo/ $\gamma$ -Al <sub>2</sub> O <sub>3</sub>	250	15	-	0	0	tr	-
AcOMe	Ni/A.C.	250	15	-	10.3	9.9	2.6	0.5

<sup>a</sup>W/F, 10 g·h/mol. <sup>b</sup>CO/DME/MeI, 240/100/9 molar ratio; CO/AcOMe/MeI, 100/9/1 molar ratio. <sup>c</sup>Metal loading, 2.5 wt%. <sup>d</sup>Molar ratio.

Reproduced with permission from reference 18. Copyright 1985, The Chemical Society of Japan.

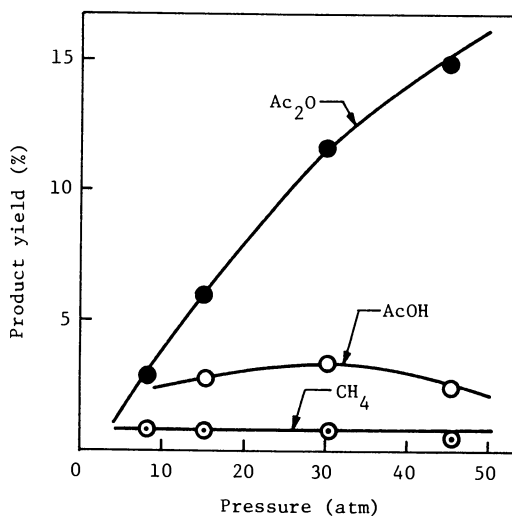


Figure 9. Effect of pressure on AcOME carbonylation. 2.5 wt% Mo/A.C., 250 C, W/F = 10 g·h/mol, CO/AcOME/MeI = 100/9/1 (18). Reproduced with permission from reference 18. Copyright 1985, The Chemical Society of Japan.

#### Literature Cited

1. Paulik, F. E.; Roth, J. F. *Chem. Commun.* 1968, 1578.
2. Roth, J. F.; Craddock, J. H.; Hershman, A.; Paulik, F. E. *Chemtech* 1971, 600.
3. Grove, H. D. *Hydrocarbon Process.* 1972, 51, 76.
4. Foster, D. *Adv. Organomet. Chem.* 1979, 17, 255.
5. Rizkalla, N. German Patent 2 610 036, 1976.
6. Sherwin, M. B. *Hydrocarbon Process.* 1981, 60, 79.
7. Schrod, M.; Luft, G. *Ind. Eng. Chem. Prod. Res. Dev.* 1981, 20, 649.
8. Kawabata, Y.; Pittman, C. U., Jr. 43rd Annual Meeting of the Chemical Society of Japan, Tokyo, April 1981, Preprints 4D10.
9. Ehrler, J. L.; Juran, B. *Hydrocarbon Process.* 1982, 61, 109.
10. Layman, P. L. *Chem. Eng. News* 1982, 60(48), 9.
11. Aquilo, A.; Alder, J. S.; Freeman, D. N.; Voorhoeve, R. J. H. *Hydrocarbon Process.* 1983, 62, 57.
12. Luft, G.; Schrod, M. *J. Mol. Catal.* 1983, 20, 175.
13. Schrod, M.; Luft, G. *J. Mol. Catal.* 1983, 22, 169.
14. Fujimoto, K.; Shikada, T.; Omata, K.; Tominaga, H. *Ind. Eng. Chem. Prod. Res. Dev.* 1982, 21, 429.
15. Fujimoto, K.; Omata, K.; Shikada, T.; Tominaga, T. *Ind. Eng. Chem. Prod. Res. Dev.* 1983, 22, 436.



16. Omata, K.; Fujimoto, K.; Shikada, T.; Tominaga, H. Ind. Eng. Chem. Prod. Res. Dev. 1985, 24, 234.
17. Shikada, T.; Fujimoto, K.; Miyauchi, M.; Tominaga, H. Appl. Catal. 1983, 7, 361.
18. Shikada, T.; Yagita, H.; Fujimoto, K.; Tominaga, H. Chem. Lett. 1985, 547.
19. Shikada, T.; Yagita, H.; Fujimoto, K.; Tominaga, H. Ind. Eng. Chem. Prod. Res. Dev. 1985, 24, 521.
20. Kawabata, Y.; Hayashi, T.; Mori, K.; Ogata, I. 45th Annual Meeting of the Chemical Society of Japan, Tokyo, April 1982, Preprints 4K12.

RECEIVED September 8, 1986

## Chapter 13

# Ammoxidation of Methanol to Hydrogen Cyanide

## Binary Oxide Catalysts and Mechanistic Aspects

J. R. Ebner, J. T. Gleaves, T. C. Kuechler, and T. P. Li

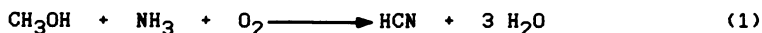
Monsanto Chemical Company, St. Louis, MO 63167

Hydrogen cyanide can be obtained in high yields by the ammoxidation of methanol using silica supported FeMo oxide or MnP oxide catalysts. The yields of HCN observed in small fluid bed reactors approach 90%. These catalysts have been studied by XRD, vibrational spectroscopy, TPR and TAP (Temporal Analysis of Products - a pulsed microreactor embedded in a vacuum chamber that allows direct monitoring of reaction intermediates and the microscopic reaction kinetics). The FeMo oxide catalyst is composed of a single phase,  $\text{Fe}_2(\text{MoO}_4)_3$ . Two  $\text{Mn}^{2+}$  phases were found to be present in the MnP oxide catalyst, the pyrophosphate,  $\text{Mn}_2\text{P}_2\text{O}_7$ , and the orthophosphate,  $\text{Mn}_3(\text{PO}_4)_2$ . Methanol, ammonia, and hydrogen reduced the FeMo oxide catalyst at temperatures below  $300^\circ\text{C}$ , whereas the MnP oxide system was found to be unreactive up to  $500^\circ\text{C}$ . In the presence of ammonia and methanol under anaerobic conditions, the FeMo oxide catalyst produced HCN, and the MnP oxide produced methylamine. The methylamine was found to be oxidized selectively to HCN in the presence of molecular oxygen. The Mars van Krevelen redox mechanism is operational only for the FeMo oxide system, and we suggest a surface activated oxo species is formed with the MnP oxide system.

Hydrogen cyanide is an important building block chemical for the synthesis of a variety of industrially important chemicals, such as 2-hydroxy-4-methylthiobutyric acid, adiponitrile, nitrilotriacetic acid, lactic acid, and methyl methacrylate. The primary commercial routes to hydrogen cyanide are the reaction of methane and ammonia under aerobic (Andrussow Process) or anaerobic conditions (Degussa Process), or the separation of hydrogen cyanide as a by-product of the ammoxidation of propylene (1). The ammoxidation of methanol could represent an attractive alternate route to HCN for a number of reasons. First, on a molar basis, the price of methanol has become close to that of methane as world methanol capacity has increased. However, an accurate long term pricing picture for these two raw

materials is difficult to obtain. Second, shipment of methanol and ammonia for on-site production of HCN in areas where cheap natural gas is not available could offer both a cost and safety advantage.

The ammoxidation of methanol as a route to HCN according to



was originally suggested by Andrussov (2), and Distillers has early patents on the use of silica supported molybdenum oxides and antimony tin oxides (3,4). This is an exothermic reaction with an estimated heat release of about 83 kcal/mole. More recently, Japanese companies have reported improved multicomponent systems (5,6). The primary focus of our investigations has been development of fluid bed catalyst technology. Fluid bed operation offers the advantage of running under isothermal conditions, and the capability of running with potentially explosive reaction mixtures. In addition, it was attractive because we could utilize idle acrylonitrile fluid bed reactors and gain an economic advantage. However, fluid bed operation puts great physical demands on the catalyst in that it must fluidize well and possess good attrition resistance. These factors, as well as chemical performance, are important in final catalyst selection. A large number of molybdenum based binary oxides, such as bismuth, cobalt, nickel and iron, and phosphorous based binary oxides, including manganese, nickel, cobalt, boron, iron, bismuth, zinc, copper, vanadium, uranium, aluminum, and chromium, were studied. These studies led ultimately to the development of an iron molybdenum oxide catalyst and a manganese phosphorus oxide catalyst capable of ammoxidizing methanol in high yields (7,8). To develop a better understanding of these two catalyst systems, we also conducted a more fundamental study using a variety of techniques, focusing primarily on discerning the role of oxygen in the reaction.

With many metal oxide catalysts, the substrate molecule is oxidized by the lattice oxygen of the catalyst, and the reduced catalyst is reoxidized by molecular oxygen according to the well-known Mars Van Krevelen redox mechanism (9). Alternatively, the oxide may activate molecular oxygen directly resulting in a surface oxo species, such as  $\text{O}^-$ ,  $\text{O}_2^-$ , or  $\text{O}_2^{2-}$ , which is responsible for abstraction of hydrogen from C-H bonds (10-12). The iron molybdenum oxide catalyst used commercially for the oxidation of methanol to formaldehyde has been studied extensively, and is a well established example of the Mars Van Krevelen redox mechanism (13-15). This catalyst is a mixture of two compounds,  $\text{Fe}_2(\text{MoO}_4)_3$  and  $\text{MoO}_3$ , and these compounds have been shown to have the same intrinsic catalytic properties (15). In addition to establishing the redox mechanism, studies have clearly established the following: 1) methoxy groups are important surface species formed by dissociative adsorption of methanol; 2) the rate determining step in the formation of formaldehyde is breaking of the C-H bond of the surface methoxy group; and 3) the estimated number of surface active sites for  $\text{Fe}_2(\text{MoO}_4)_3$  is about  $2.1 \times 10^{14}$  sites/cm<sup>2</sup> (16). On the other hand, the manganese phosphorus oxide system, which is our favored catalyst for commercialization, will be shown in this paper to be an example of the latter mechanism.

We have found very little literature on the use of MnP oxide

for oxidation or amoxidation catalysis. Moffat has published a general review of phosphate compounds used for catalysis, and common catalytic reactions mentioned for metal phosphates (Mn systems are not mentioned) include dehydration and dehydrogenation of alcohols, alkylations, aminations of alcohols, and oxidative dehydrogenations (17). Specifically, nickel and tin phosphorus oxide catalysts have been reported to be effective for the latter reaction class (18,19). To our knowledge, our study represents the first fundamental work on the manganese phosphorus oxide system.

### Experimental Methods

TPD,TPR. Adsorption and temperature programmed desorption studies of the reactant gases were conducted using a Mettler TA-1 thermoanalyzer equipped with a quartz furnace with capabilities for the controlled addition of reactive atmospheres, and interfaced to allow mass spectral analysis of the off-gas (20). In a typical experiment 100 - 200 mg of catalyst was saturated with a stream of reactant gas (90% helium/10% reactant) at room temperature, brought to equilibrium in a helium atmosphere, and then heated at a rate of 10° C per minute. Temperature programmed reduction (TPR) experiments using a 3% hydrogen/argon gas mixture were conducted using dynamic flow through a fixed bed reactor according to the experimental concepts of Robertson, et. al. (21).

TAP. Mechanistic studies were conducted using the Monsanto designed TAP (Temporal Analysis of Products) reactor system schematically shown in Figure 1 (22). The TAP apparatus consists of a 1.25 cm long and 0.64 cm diameter stainless steel tube catalytic reactor embedded in a differentially pumped vacuum system operating at 10<sup>-7</sup> torr. The reactor is connected to two high speed pulsed molecular beam valves produced by Newport Corporation, and a continuous bleed valve. The pulsed valves admit a triangular shaped pulse of reactant molecules of variable intensity (10<sup>13</sup> to 10<sup>19</sup> molecules per pulse) with a width (FWHM) of about 150 microseconds. As a reference point, when pulsing 10<sup>15</sup> molecules per pulse to a 10 m<sup>2</sup>/gram catalyst, the molecules in a single pulse address approximately 1/10000 of the available surface area. Experiments in this study required only a single pulsed valve. The molecular species exiting the microreactor travel essentially a collision free path through the reactor chamber and differential chamber (10<sup>-8</sup> torr) to the detector chamber (10<sup>-9</sup> torr) which contains a UTI 100C quadrupole mass spectrometer interfaced to a PARC 4203 signal averager for real time detection. In a typical experiment a catalyst charge consisting of 0.5 cc of 500 micron diameter catalyst particles is loaded into the microreactor and the system is evacuated. An inert gas blended with the reactant gas is then pulsed through the catalyst bed which is maintained at the desired reaction temperature. The product spectrum is obtained by monitoring individual mass peaks and plotting their intensity versus time. Since almost all species produce multiple fragment peaks, care must be exercised in not choosing mass peaks which are composites of two or more products. After all the product curves are collected a composit spectrum can be plotted and the relative time behavior of the various products and reactants can be compared. An

inert gas curve is collected to obtain the flow characteristics through the catalyst bed, and we find that in general this flow can best be described by Knudsen type diffusion. Average reactor residence times for a non-interacting molecule are 3 to 5 milliseconds. This technique allows direct detection of desorbing reaction intermediates, examination of adsorption/desorption properties of molecular species of interest, and a direct measure of the sequence of events in the catalytic process.

Activity measurements. Activity and selectivity measurements were performed at 10 psig in a 14-mm internal diameter glass fluid bed reactor using 25 grams of 90 to 38 micron catalyst particles. A reactant mixture of approximately 18 volume % O<sub>2</sub>, 7 volume % NH<sub>3</sub> and 7 volume % CH<sub>3</sub>OH and the balance of helium was fed to the catalyst, and temperature and contact time were varied to find the optimum yield of HCN. Optimum reaction temperatures were found to range from 425° to 475°C with contact times of 3 to 5 seconds (calculated at STP). Fixed bed reactor studies produced similar results. The yields reported in this paper are based on carbon fed, unless otherwise noted. More details on catalyst performance can be found in our patents (7,8).

Other characterization. Powder X-ray diffraction patterns were obtained on finely ground (below 325 mesh) samples with a Scintag PAD II system using CuK radiation, a high-purity germanium detector maintained at 77°K and single channel analyzer. Fourier-transform infrared (FTIR) studies were conducted using a Nicolet 7199 spectrometer. Laser Raman Spectra were acquired by illuminating the spinning sample powder (ca 5000 rpm) with 100 to 200 milliwatts of 514.5-nm radiation obtained from a Coherent Radiation CR-3 argon ion laser. The Raman spectra were recorded with a Spex Ramalog 5 system, and peak positions calculated from the spectra are considered to be accurate to within 2 cm<sup>-1</sup>.

## RESULTS AND DISCUSSION

The FeMo Oxide Catalyst. There have been extensive studies on the preparation of FeMo oxide catalysts, and these have been recently discussed in the literature (15). The preparation of the FeMo oxide catalyst best suited for ammoxidation of methanol is as follows: i) 683 grams (1.69 mol) of Fe(NO<sub>3</sub>)<sub>3</sub>·9H<sub>2</sub>O is dissolved in 1400 ml of distilled water and added to it is a solution of 365 grams (2.54 mol) of MoO<sub>3</sub> in 345 ml of 29% aqueous ammonia to yield a viscous brown precipitate. It is important that the pH of the reaction mixture be between 2.0 and 2.3 after the addition is complete, and it may successfully be adjusted to this range with 29% aqueous ammonia, if required. Further, we found rapid addition of 90% of the moly solution minimizes slurry viscosity problems. ii) The reaction mixture is maintained at 95-100 °C until the brown precipitate turns bright yellow. iii) The precipitate is filtered and washed with two liters of distilled water. iv) The yellow filter cake is combined with 1250 grams of Nalco #2327 40% silica sol (pH adjusted to 2.0 with 70% HNO<sub>3</sub>), ball milled to improve dispersion, concentrated by heating, and spray dried. The catalyst is calcined for 2 hours at 760°C to produce a fluidizable catalyst

of stoichiometry  $\text{Fe}_{0.67}\text{MoO}_4 \cdot 50 \text{ wt}\% \text{ SiO}_2$  with commercially viable bulk density and attrition rate for a fluid bed process. DTA studies showed that during the calcination step the amorphous bright yellow silica supported solid undergoes a  $200^\circ\text{C}$  dehydration followed by an exothermic conversion to ferric molybdate at  $370^\circ\text{C}$ . Although no further events are seen in the DTA, we find it to be beneficial to performance to complete the calcination at  $760^\circ\text{C}$  to reduce the surface area to less than  $10 \text{ m}^2/\text{gram}$ .

The iron molybdenum oxide catalyst was structurally characterized by XRD and vibrational spectroscopy (IR and Raman). The preferred catalyst is found to be composed of a single crystalline phase,  $\text{Fe}_2(\text{MoO}_4)_3$ . The laser Raman spectrum of the catalyst is illustrated in Figure 2 with a reference spectrum for  $\text{MoO}_3$  showing no free  $\text{MoO}_3$  is present in the catalyst. This is in contrast to the commercial methanol to formaldehyde catalyst which does contain free  $\text{MoO}_3$ . In fact, we realized no benefit for methanol ammonoxidation on adding excess  $\text{MoO}_3$ . When evaluated in a fluid bed reactor at  $435^\circ\text{C}$ , 10 psig, a contact time of 5 gram sec/cc (W/F: grams of catalyst divided by total gas flow at STP in cc/sec) with a feed composition of 7.0% methanol, 7.2% ammonia, 18% oxygen and the balance helium, a 86% yield of HCN was obtained at 98%  $\text{CH}_3\text{OH}$  conversion. The non-selective pathways lead to CO and  $\text{CO}_2$ , and the HCN selectivity on ammonia is generally greater than 95%. Calcination of the catalyst at a substantially lower temperature, such as  $550^\circ\text{C}$ , results in a lowering of yield to ca. 73%. A calcination temperature within  $50^\circ\text{C}$  of the designated value is not deleterious to performance. Raising the feed concentration to 11%  $\text{CH}_3\text{OH}$ , 11%  $\text{NH}_3$  and 16%  $\text{O}_2$  results in a yield loss of 3-5%.

The MnP Oxide Catalyst. Reviewing the literature, one finds that the MnP binary oxide system has a rich solid state chemistry, but very little is published on the catalytic properties of the system. The preferred catalyst for methanol ammonoxidation is prepared as follows: i) To 5527 grams of a vigorously stirring aqueous solution containing 50% by weight  $\text{Mn}(\text{NO}_3)_2$  (15.45 mol) is added a solution containing 1424 grams of 85 wt%  $\text{H}_3\text{PO}_4$  (12.35 mol) and 741 grams of Nalco #2327 40 wt% silica sol. ii) The reaction mixture is maintained near  $100^\circ\text{C}$  while the volume is slowly reduced to ca. 3 liters. During this step brown  $\text{NO}_2$  gas evolves, and the solution changes color from pink to greenish-brown indicative of oxidation of  $\text{Mn}^{2+}$  to  $\text{Mn}^{3+}$ . iii) After cooling the reaction mixture an additional 4314 grams of silica sol is added. (The two step silica addition resulted in higher catalyst activity and more consistent bulk density and attrition rate.) iv) The reaction mixture is ball milled and then spray dried to give a fluidizable material. v) The catalyst is calcined for 2 hours at  $925^\circ\text{C}$  to give a catalyst with ca.  $35 \text{ m}^2/\text{gram}$  surface area and a stoichiometry of  $\text{Mn}_{1.25}\text{PO}_x \cdot 50 \text{ wt}\% \text{ SiO}_2$ . DTA studies of the calcination reveal that the hydrated manganese orthophosphate precursor undergoes a two step endothermic dehydration at 150 and  $400^\circ\text{C}$ . The endotherm at  $460\text{-}475^\circ\text{C}$  results from solid state chemistry leading to formation of ortho- and pyrophosphate compounds through evolution of water and oxygen. Well defined crystalline phases are present when the calcination temperature exceeds  $600^\circ\text{C}$  (weak endotherm  $580\text{-}600^\circ\text{C}$ ).

The manganese phosphorous oxide catalyst has been prepared with

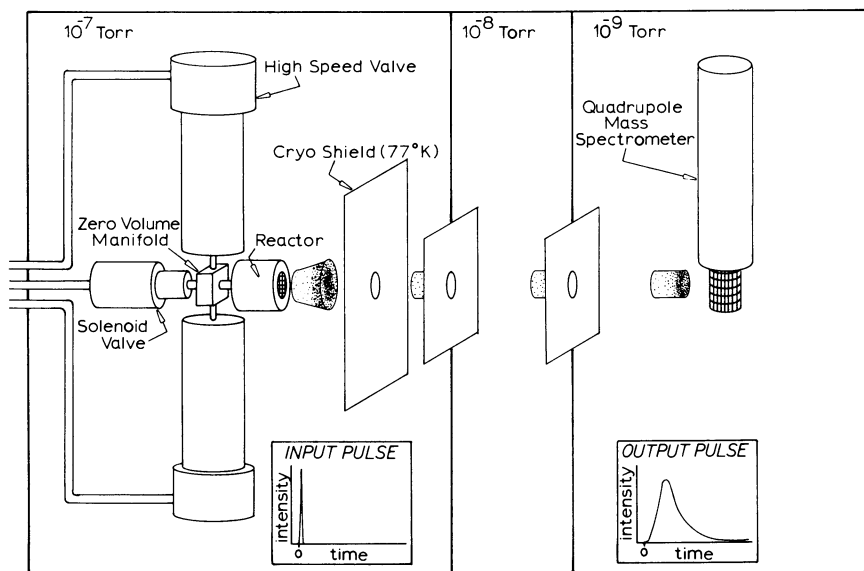


Figure 1. Schematic of the TAP (Temporal Analysis of Products) reactor system used for fundamental catalyst studies.

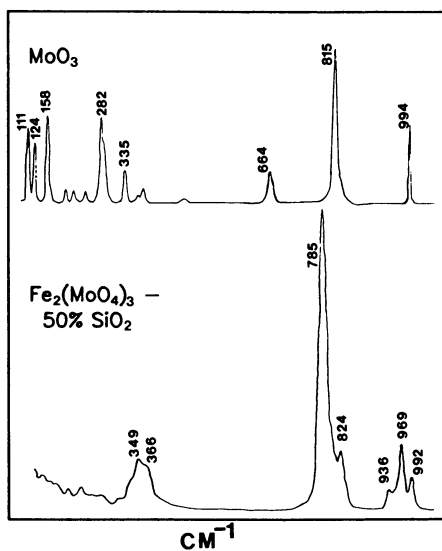


Figure 2. Laser Raman spectra of  $\text{MoO}_3$  and the preferred iron molybdenum oxide catalyst.

ratios of Mn/P ranging from 0.5 to 1.5, with 1.25 being preferred. Over this range of stoichiometry, XRD studies show two compounds are present, an orthophosphate phase with the graftonite structure (23),  $Mn_3(PO_4)_2$ , and a pyrophosphate phase,  $Mn_2P_2O_7$ . The XRD pattern of the preferred catalyst is shown in Figure 3, and the yield versus composition curve obtained under conditions described in the experimental section is given in Figure 4. In summary, we observe high HCN yields when the pyrophosphate compound is present in the catalyst, reduced yields in the presence of excess phosphorous, and inactivity over the pure orthophosphate. Mn/P ratios above 1.5 result in catalysts that burned methanol to carbon oxides because of the presence of free manganese oxides. The HCN selectivity based on ammonia is 100%. A study in the fluid bed reactor of the dependence of HCN yield on  $O_2/CH_3OH$  ratio showed the HCN yield decreases with decreasing  $O_2$  concentration in the feed. For example, we found the yield to be stable at  $O_2/CH_3OH$  ratios greater than 2, and decline to a value of 76% at a 1.26  $O_2/CH_3OH$  ratio. Although a kinetic study was not undertaken, these results clearly indicate an oxygen order dependence ( $CH_3OH$  concentration was kept constant).

The structure of the active component, manganese pyrophosphate, has been reported in the literature (24). It is layer like with planes of octahedrally coordinated  $Mn^{2+}$  ions being separated by planes of pyrophosphate anions ( $P_2O_7^{4-}$ ). Examination of models of this compound gave calculated Mn-Mn thru space distances of 3.26 and 3.45 angstroms, a metal-metal distance close to that found for binuclear dibridged peroxo- and superoxo- complexes of cobalt (25).

TAP Microreactor and TPROX Studies. In an examination of the role of oxygen in the reaction, it is useful to decouple the redox reactions. In separate TAP experiments we pulsed a 50-50 blend of methanol and argon to  $Mn_2P_2O_7 \cdot 50 \text{ wtx } SiO_2$  and  $Fe_2(MoO_4)_3 \cdot 50 \text{ wtx } SiO_2$ . Each pulse contained approximately  $10^{15}$  molecules of methanol. As previously discussed in the experimental section on TAP, because the number of available sites far exceeds the number of reactant molecules, this pulsed experiment is an extremely sensitive method for determining the involvement of surface  $O^{2-}$  in a redox mechanism. The FeMo oxide catalyst produced formaldehyde for over 100,000 pulses in experiments conducted at 450°C. Total oxygen consumption from the oxide was greater than the calculated amount for a surface monolayer, and thus lattice oxide migration to the surface occurred. In the case of the MnP catalyst, methanol oxidation was not observed at reaction temperatures from 350 to 500°C, even with the initial pulses.

Pulsing an equimolar mixture of methanol and ammonia to the FeMo catalyst at 450°C resulted in HCN formation. In a parallel experiment with the MnP catalyst, reaction was also observed, but analysis of the TAP mass-time curves showed that a nucleophilic substitution reaction occurred resulting in methylamine formation. Even including oxygen in the gas pulse mixture did not result in clearly detectable HCN over the MnP catalyst. This can be understood by an examination of the temporal curve in Figure 5. It shows the oxygen gas exits the TAP reactor prior to the formation of significant quantities of methylamine intermediate. Pulsing an equimolar mixture of methylamine and oxygen results in a facile conversion to HCN. Studies using the combined pulse/flow reactor



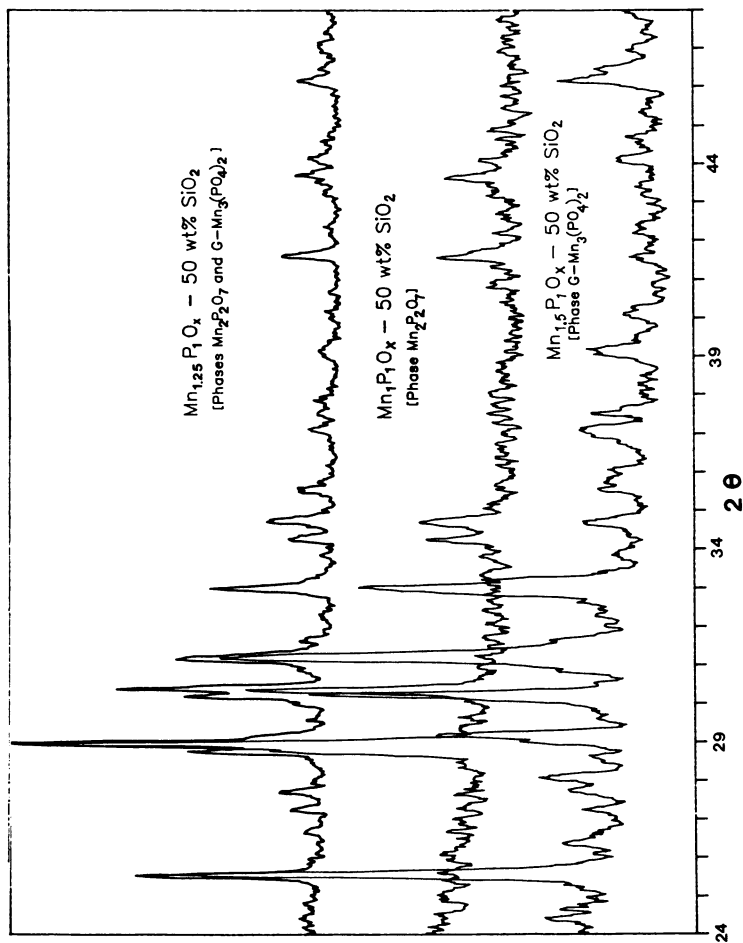


Figure 3. XRD patterns of the preferred manganese phosphorus oxide catalyst, manganese pyrophosphate, and manganese orthophosphate.

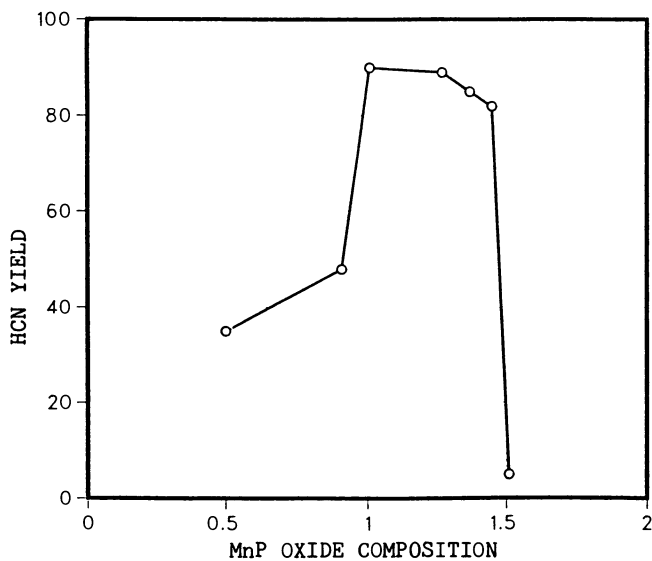


Figure 4. Maximum attainable HCN yield versus composition of the MnP oxide on silica catalyst.

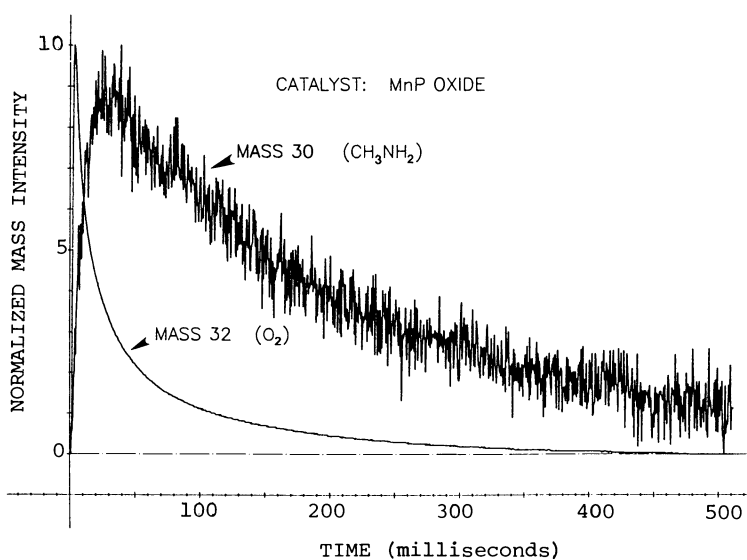


Figure 5. TAP mass intensity versus time curve comparing the time sequence of formation of methylamine versus the diffusion of reactant oxygen.

allowed continual dosing of the surface with oxygen while pulsing methanol and ammonia, and only in this case is HCN formed (Figure 6). These experiments point to the importance of gas phase oxygen with the MnP oxide catalyst.

The reducibility of the catalyst systems was further examined using temperature programmed reduction with a 3% hydrogen/argon gas mixture. The TPR curves shown in Figure 7 illustrate the MnP oxide catalyst is not readily reduced at reaction temperatures. In contrast, the FeMo oxide catalyst begins to reduce at 250°C, and the rate of reduction is fast at temperatures of methanol ammoxidation activity (425°-475°C). The poor lability of lattice oxygen for the MnP oxide catalyst provides additional evidence for a non-redox process.

Temperature Programmed Desorption Studies. Methanol adsorption/desorption studies of ferric molybdate are reported in the literature (26). The salient features of these studies parallel our findings for the silica supported FeMo catalyst. These are as follows: First, there are two desorption peaks, one at 98°C attributed to adsorbed methanol and one at 275°C attributed to the decomposition of methoxy groups to formaldehyde (Figure 8). Second, the skewing of the methanol desorption peak on the high temperature side is attributed to the recombination of the methoxy groups with available H from surface hydroxy groups to form methanol. This has been unambiguously established in the previous study (26) using deuterated methanol. Third, because of the oxidation of methanol to formaldehyde, there is a net weight loss due to reduction of the catalyst, and exposure to oxygen restores the initial state of the catalyst. The total amount of oxygen removed resulted in a calculated surface oxide concentration of  $9 \times 10^{13}$  oxide sites/cm<sup>2</sup>.

Analogous methanol adsorption/desorption experiments conducted with the supported manganese pyrophosphate catalyst gave the following results: 1) A single desorption peak centered at 100°C is observed (Figure 8). 2) Mass spectral analysis indicates the desorption product is methanol. 3) The final weight of the sample is unchanged from the initial weight, consistent with absence of oxidation products during the desorption cycle. These results further support our hypothesis that the MnP oxide catalyst does not possess labile surface oxide species for oxidation chemistry.

Ammonia adsorption/desorption experiments were also conducted over both catalyst systems in a microbalance system not interfaced with a mass spectrometer. The desorption curves obtained after saturating the surface with ammonia and equilibrating in helium are shown in Figure 9. The weight loss spectrum of the FeMo oxide catalyst sample shows a high temperature shoulder and the MnP oxide catalyst does not. FTIR studies of the FeMo catalyst were conducted under an ammonia atmosphere. The strongly bound ammonia species seen in Figure 10 is identified as ammonium ion by the characteristic ammonium bending mode at 1450 cm<sup>-1</sup> (17). The formation of ammonium ions on the surface by reaction of ammonia with surface hydroxyls is consistent with our FTIR results on the catalyst in N<sub>2</sub> which show the presence of surface hydroxyls up to 400°C. The surface ammonium species disappears completely from the surface by 350°C, and we believe this species accounts for the high temperature shoulder observed in the TPD experiment. We found no

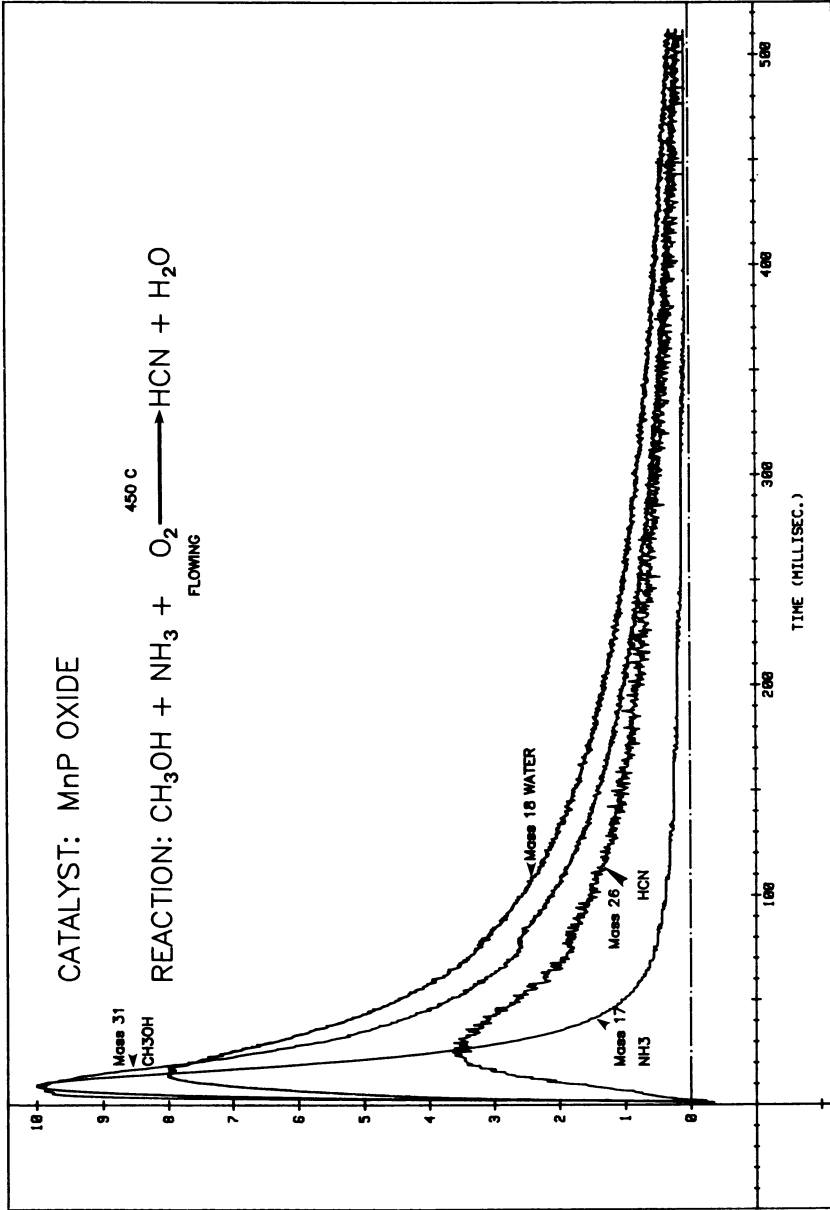


Figure 6. TAP mass intensity versus time curve showing the time sequence of HCN formation when continually flowing oxygen and pulsing a methanol/ammonia blend.

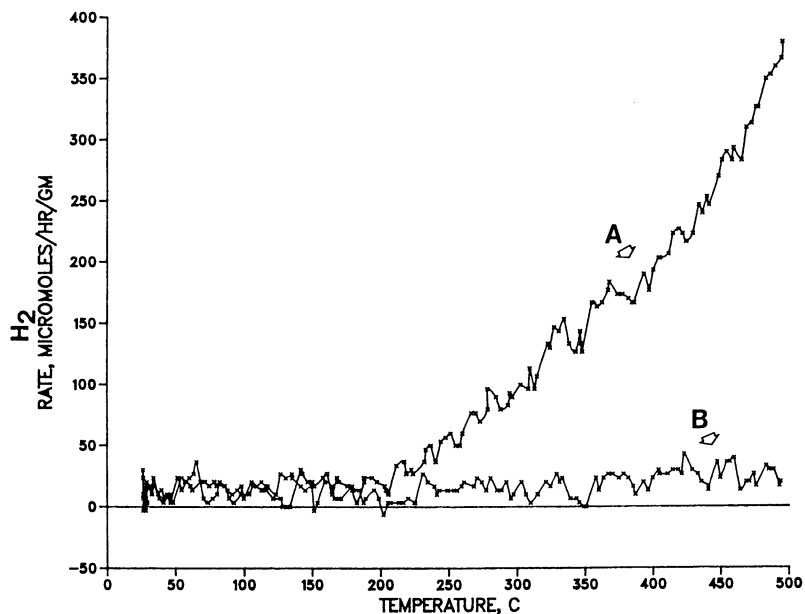


Figure 7. Temperature Programmed Reduction curves for the ferric molybdate (A) and the manganese pyrophosphate (B) catalysts.

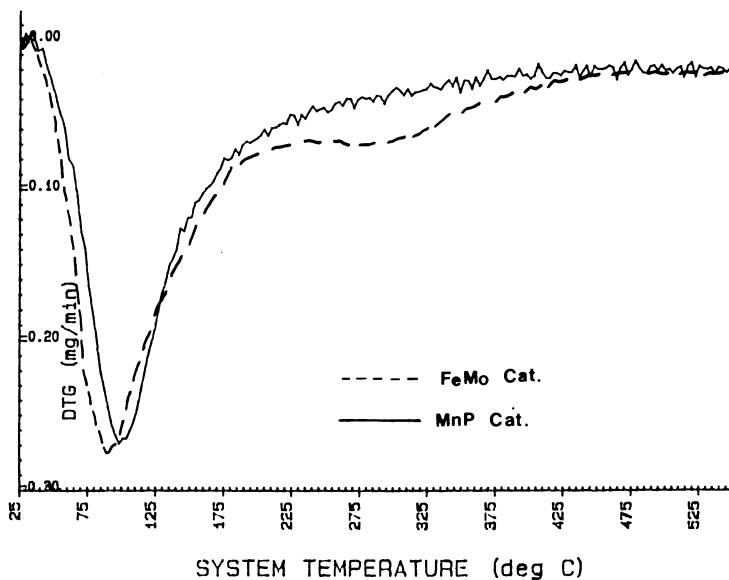


Figure 8. Temperature Programmed Desorption of methanol from the ferric molybdate (dashed line) and the manganese pyrophosphate (solid line) catalysts determined gravimetrically.

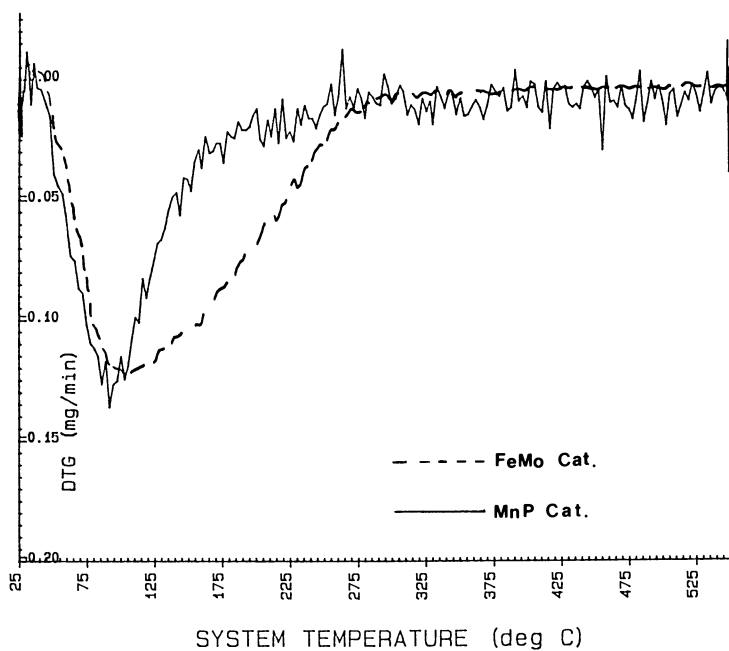


Figure 9. Temperature Programmed Desorption of ammonia from the ferric molybdenum (dashed line) and the manganese pyrophosphate (solid line) catalysts determined gravimetrically.

spectroscopic evidence for the surface imido (=NH) group generally proposed in ammoxidation mechanisms with molybdate catalysts (28). As with methanol desorption, a net weight loss was observed for the FeMo catalyst after ammonia desorption. This was caused by oxidation of the ammonia substrate to nitrogen and consequent catalyst reduction. The relative number of oxygen atoms removed was ca. 20% less than with methanol surface reduction.

### Conclusions

Reaction Mechanism. Our current proposal for the mechanism of ammoxidation of methanol to HCN over the two catalyst systems discussed is shown in Figure 11. The experimental data presented strongly indicates the ferric molybdate catalyst operates by a Mars Van Krevelen redox mechanism in the formation of HCN. This mechanism is not applicable in the case of the manganese phosphate catalyst. Two possibilities exist: (1) a Rideal mechanism in which an activated surface methylamine or methanol species reacts with gas phase oxygen, or (2) a mechanism involving formation of a surface activated molecular oxygen species capable of selective oxidation. Although we do not have sufficient evidence to distinguish these two possibilities, we prefer the latter. It is quite plausible that the surface Mn<sup>2+</sup> sites activate molecular oxygen to form a Mn<sup>3+</sup> superoxo or a dinuclear Mn<sup>3+</sup> bridged peroxy species which could lead to cleavage of the O<sub>2</sub> bond to form O<sup>-</sup> species. The O<sup>-</sup> species is believed to be very selective for C-H bond cleavage (10). Mn<sup>3+</sup> pyrophosphate is a well known low temperature oxidant (27). In our proposed mechanism we indicate this activated oxygen as O<sup>+</sup>, but we do not imply that this is necessarily a monoatomic oxygen species.

Based on literature reports for molybdate catalysts (28), ammoxidation of the surface molybdenum oxo species occurs resulting in surface -NH groups. We propose for the molybdate catalyst that the bound methoxy reacts with the -NH to give a CH<sub>3</sub>NH surface species which is dehydrogenated to HCN with surface lattice oxygen. Using literature precedent for bound -NH<sub>2</sub> groups on phosphate catalysts (17), we propose for the pyrophosphate catalyst that the methoxy groups can react with -NH<sub>2</sub> to form methylamine which can desorb, or, in the presence of an activated oxo species, undergo oxydehydrogenation to HCN.

Process Economics. The last economic evaluation of this technology was done during the latter part of 1985. In considering conversion of an acrylonitrile plant to exclusive production of HCN, the methanol technology is far superior to the Andrussow process. However, as can be seen from the data in Table I, the manufacture of HCN in a new 30 M lb/yr plant has only a slight economic advantage over the Andrussow process. Since one of the key variables in the analysis is price of methanol versus methane, and since there is currently considerable volatility in the pricing of these two carbon raw materials, a grassroots plant would be a marginal proposition. This is not true of the retrofit scenario.

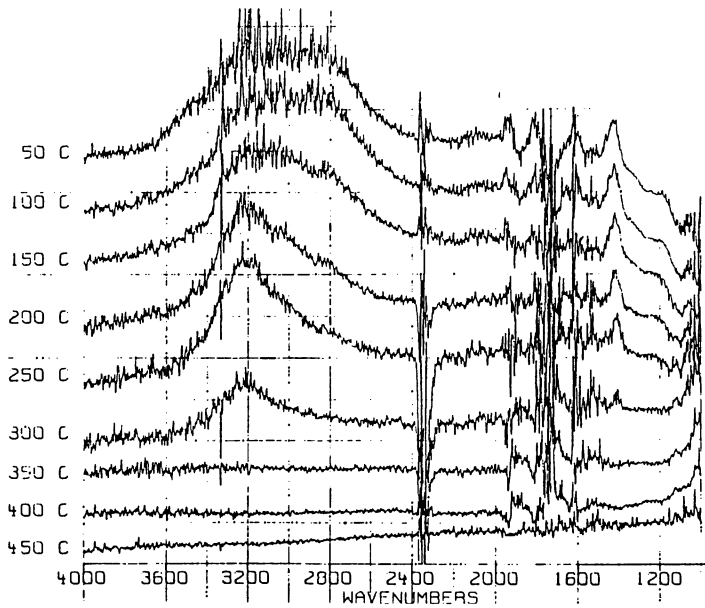


Figure 10. FTIR difference spectra showing adsorbed ammonia species on the iron molybdenum oxide catalyst as a function of temperature. The catalyst and vapor phase ammonia vibrational bands have been subtracted out.

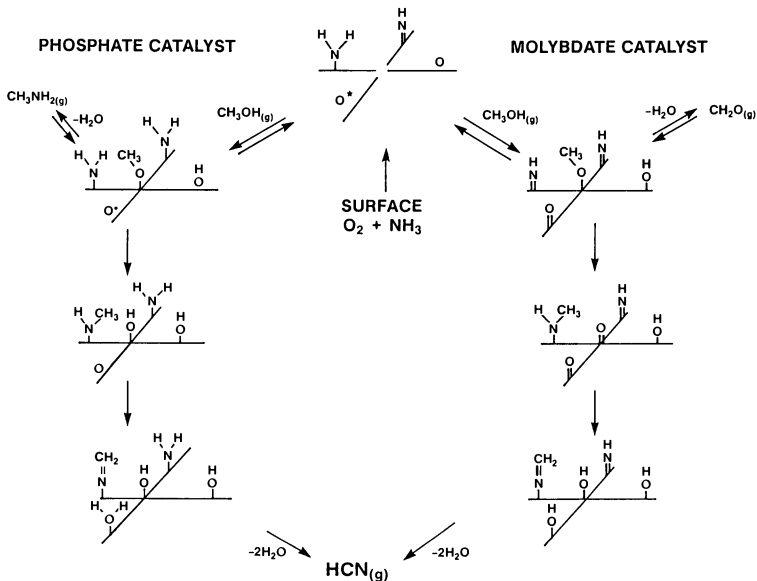


Figure 11. Mechanistic proposal for the amoxidation of methanol to HCN over the ferric molybdate and the manganese pyrophosphate catalysts.



Table I. Economic Comparison of the Two HCN Processes

Cost Element	Andrussow \$/lb HCN	Methanol \$/lb HCN
Natural Gas (\$5/M Btu)	0.10	
Methanol (\$0.40/gal)		0.09
Ammonia	0.05	0.05
Capital Related Costs (Capital)	0.17 (\$23M)	0.16 (\$21M)
Other Manufacturing Costs	0.03	0.02
<b>Total Manufacturing Cost</b>	<b>0.35</b>	<b>0.32</b>

### Acknowledgments

The authors are thankful for the able assistance of the chemical technicians Warren Biest, Sue Opfer, William Andrews, and Fred Strauser. Also, the TGA work of David Chan and Joe Bullock, TPR runs by Claire Schosser, spectroscopy studies by John Freeman, XRD studies by Frank May and economic analysis by Jim Allman are greatly appreciated.

### Literature Cited

- Jenks, W. R. In "Kirk-Othmer Encyclopedia of Chemical Technology"; M. Grayson, Ed.; John Wiley & Sons: New York, 1979; Vol. VII, pp. 307-319.
- Andrussow, L. U.S. Patent 2 006 981, 1935.
- Bellringer, F. J. British Patent 718 112, 1954.
- Bellringer, F. J. British Patent 913 816, 1962.
- Shiraishi, T.; Ichihashi, H.; Kato, F. U.S. Patent 3 911 089, 1975.
- Nitto Chemical Japanese Patent 51 10200, 1976.
- Ebner, J. R. U.S. Patent 4 425 260, 1984.
- Ebner, J. R., U.S. Patent 4 457 905, 1984.
- Mars, R.; van Krevelen, D.W. Chem. Eng. Sci. Suppl. 1954, 3, 41.
- Lunsford, J. H. In "Catalytic Materials"; Whyte, T. E., Jr.; Dalla Betta, R. A.; Derouane, E. G.; Baker, R. T. K., Eds.; ACS SYMPOSIUM SERIES No. 248, American Chemical Society: Washington, D.C., 1984; pp. 127-142.
- Boreskov, G. K. In "Catalysis-Science and Technology"; Anderson, J. R.; Boudart, M., Eds.; Springer-Verlag: Berlin Heidelberg New York, 1982; Vol. III, pp. 39-137.
- Che, M.; Tench, A.J. In "Advances in Catalysis"; Eley, D. D.; Pines, H.; Weisz, P. B., Eds.; Academic Press, Inc.: New York, 1982; pp 78-133.
- Pernicone, N. J. Less Common Metals 1974, 36, 289.
- Machiels, C. J.; Sleight, A. W. Proc. of the Fourth International Conference on the Chemistry and Uses of Molybdenum, Climax Molybdenum Co.: Ann Arbor, Mich., 1982, p. 411.

15. Machiels, C. J.; Chowdhry, U.; Harrison, W. T. A.; Sleight, A. W. In "Solid State Chemistry of Catalysis"; Grasselli, R. K.; Brazdil, J. F., Eds.; ACS SYMPOSIUM SERIES No. 279, American Chemical Society: Washington, D.C., 1985; pp. 103-119.
16. Sleight, A. W. Presented At 187th ACS National Meeting, St. Louis, Mo. 1984.
17. Moffat, J. B. In "Topics in Phosphorous Chemistry"; Grayson, M.; Griffith, E. J., Eds.; John Wiley & Sons: New York, 1980; Vol. X, pp. 285-340.
18. Nolan, G. J.; Doane, E. P.; Hogan, R. J. U.S. Patent 3 501 548, 1970.
19. Bertus, B. J. U.S. Patent 3 972 954, 1976
20. Yuen, H. K.; Mappes, G. W.; Grote, W.A. Thermochemica Acta 1982, 52, 143.
21. Robertson, S. D.; McNicol, B. D.; de BAAS, J. H.; Kloet, S. C.; Jenkins, J. W. J. Catal. 1975, 37, 424.
22. Ebner, J. R.; Gleaves, J. T., patent filed 1984.
23. Calvo, C. Amer. Mineral. 1968, 53, 742.
24. Stefanidis, T.; Nord, A. Acta Cryst. 1984, C40, 1995.
25. Martell, A. Chem. Rev. 1984, 84(2), 137.
26. Cheng, W. H.; Chowdhry, U.; Ferretti, A.; Firment, L. E.; Groff, R. P.; Machiels, C. J.; McCarron, E. M.; Ohuchi, F.; Staley, R. H.; Sleight, A. W. Proc. of the 2nd Symposium of the Industry-University Cooperative Chemistry Program, Texas A&M University: College Station, Texas 1984, pp. 165-181.
27. Fadnis, A. G.; Kulshrestha, S. K. React. Kinet. Catal. Lett. 1982, 19(3-4), 267.
28. Burrington, J. D.; Kartisek, C. T.; Grasselli, R. K. J. Catal. 1984, 87, 363.

RECEIVED July 15, 1986

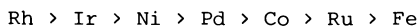
## Chapter 14

# Catalytic Features of Carbon-Supported Group VIII Metal Catalysts for Methanol Carbonylation

Kaoru Fujimoto, Kohji Omata, Tsutomu Shikada, and Hiro-o Tominaga

Department of Synthetic Chemistry, Faculty of Engineering, The University of Tokyo,  
Hongo, Bunkyo-ku, Tokyo 113, Japan

The catalytic activities of group VIII metals supported on activated carbon for methanol carbonylation were in the order as follows:



A plot of the relation between the catalytic activity and the affinity of the metals for halide ion resulted in a volcano shape. The rate determining step of the reaction was discussed on the basis of this affinity and the reaction order with respect to methyl iodide. Methanol was first carbonylated to methyl acetate directly or via dimethyl ether, then carbonylated again to acetic anhydride and finally quickly hydrolyzed to acetic acid. Overall kinetics were explored to simulate variable product profiles based on the reaction network mentioned above. Carbon monoxide was adsorbed weakly and associatively on nickel-activated-carbon catalysts. Carbon monoxide was adsorbed on nickel- $\gamma$ -alumina or nickel-silica gel catalysts more strongly and, in part, dissociatively. Methanol carbonylation over nickel-activated carbon was shown to be a structure-insensitive reaction.

Carbonylation of methanol to form acetic acid has been performed industrially using carbonyl complexes of cobalt (1) or rhodium (2) and iodide promoter in the liquid phase. Recently, it has been claimed that nickel carbonyl or other nickel compounds are effective catalysts for the reaction at pressure as low as 30 atm (3,4). For the rhodium catalyst, the conditions are fairly mild (175°C and 28 atm) and the product selectivity is excellent (99% based on methanol). However, the process has the disadvantages that the proven reserves of rhodium are quite limited in both location and quantity and that the reaction medium is highly corrosive. It is highly desirable, therefore, to develop a vapor phase process, which is free from the corrosion problem, utilizing a base metal catalyst. The authors have already reported that nickel on activated carbon exhibits excellent catalytic activity for the carbonylation of

methanol and its derivatives at low pressure in the presence of methyl iodide promoter (5-7).

In the present work some of the catalytic features of nickel and other group VIII metals for methanol carbonylation and the role of activated carbon as carrier were studied.

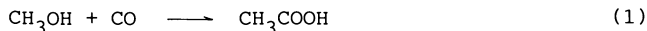
### Experimental

Catalysts were prepared by impregnating a commercially available granular activated carbon (Takeda Shirasagi C, charcoal base, activated with steam, specific surface area 1200 m<sup>2</sup>/g, particle size 20-40 mesh) and other commercially available ones with metal nitrates and chlorides in aqueous solution. The catalysts were dried in air at 120 °C for 24 h and then reduced in flowing hydrogen at 400 °C for 3 h. The metal content in the catalyst was 2.5 wt% (as the metal). The reference catalysts were prepared by the same procedure but using γ-alumina (Tokaikonetsu TKS 99651), silica gel (Davison ID), graphite or carbon black (Ketjen black EC, 950 m<sup>2</sup>/g) as the carriers.

A continuous-flow reactor with a fixed catalyst bed was employed under pressurized conditions. The reactor was made of stainless steel with an inner diameter of 6 mm. All products and unreacted feed materials were withdrawn in the gaseous state from the reactor through a heated pressure let-down valve. A quantitative analysis of the products was carried out by gas chromatography. The time factor, which corresponds to contact time, is expressed by W/F, where W is the weight of catalyst (g) and F is the total flow rate of feed (mol/hr). Chemisorption of H<sub>2</sub>, CO and methyl iodide (MeI) were measured by a conventional glass vacuum system.

### Results and Discussion

Effect of Support Materials. The carbonylated products were methyl acetate (AcOMe) and acetic acid (AcOH) as Equations 1 and 2.



Other products were dimethyl ether (DME), methane and carbon dioxide. The data in Table I show that high yields of carbonylated products were produced with nickel catalysts supported on activated carbon and carbon black. Other nickel catalysts gave mainly methane and dimethyl ether. It is clear that a carbonaceous carrier is essential for the appearance of carbonylation activity for the nickel catalyst. The role of the carbonaceous carrier will be discussed later.

Activities of Group VIII Metal Catalysts. Methanol conversions to methyl acetate and acetic acid on group VIII metals supported upon activated carbon are illustrated in Figure 1. The yield was calculated as methanol conversion to acetyl group. For each catalyst, acetic acid formation is predominant at high temperature while methyl acetate has a point of maximum yield.

Table I. Effect of supported materials for carbonylation of methanol<sup>a</sup>

Carrier <sup>b</sup>	Temp(°C)	Conversion of MeOH(%)	Product Yield (%)			
			CH <sub>4</sub>	DME	AcOME	AcOH
A.C.	257	82.8	1.7	14.9	58.2	8.0
A.C.	300	95.8	3.0	2.1	21.6	69.1
C.B. <sup>c</sup>	250	54.7	0.1	4.3	43.3	7.0
G. <sup>d</sup>	256	6.1	0.1	4.8	1.2	0
γ-Al <sub>2</sub> O <sub>3</sub>	293	99.1	0.7	96.2	2.2	0
SiO <sub>2</sub>	290	1.9	0.4	0.4	1.1	0
TiO <sub>2</sub>	292	13.3	0	13.3	0	0

<sup>a</sup>Reaction conditions : pressure = 11 atm, CO/MeOH/MeI = 20/19/1, W/F = 10 g·h/mol. <sup>b</sup>2.5wt% Ni/carrier. <sup>c</sup>Carbon black, CO/MeOH/MeI = 100/19/1, W/F = 5 g·h/mol. <sup>d</sup>Graphite.

The turn over frequency (TOF) and the activity of carbonylation are defined by Equations 3 and 4, respectively.

$$\text{TOF} = (Y_{\text{AcOH}} + Y_{\text{AcOME}}/2) \times F_{\text{MeOH}} / M / 100 \text{ (h}^{-1}\text{)} \quad (3)$$

$$\text{ACTIVITY} = T_{10}^{-1} \text{ (K}^{-1}\text{)} \quad (4)$$

where  $Y_{\text{AcOME}}$  and  $Y_{\text{AcOH}}$  are the yields of methyl acetate and acetic acid from methanol in mol%, respectively.  $F_{\text{MeOH}}$  is the feed rate of methanol (mmol/g·h) and  $M$  is the amount of supported metal (mmol/g).  $T_{10}$  indicates the temperature where TOF of the catalyst is 10 h<sup>-1</sup>. The order of the catalytic activity evaluated from Equation 4 is as follows:

$$\text{Rh} > \text{Ir} > \text{Ni} > \text{Pd} > \text{Co} > \text{Ru} > \text{Fe} \quad (5)$$

Halide Promoter. A halide promoter, such as methyl iodide, is essential for the carbonylation of methanol for liquid and vapor phase catalysts. As reported in Table II, the reaction order of methyl iodide is 0.7 for Rh and decreases according to Rh > Ru > Pd > Ni. The variation in reaction order may be due to the metal-halide affinity.

Table II. Reaction order with respect to methyl iodide

Catalyst <sup>a</sup>	Reaction order
Rh	0.7
Ru	0.6
Pd	0.3
Ni	0.1

<sup>a</sup> 2.5 wt% metal/activated carbon.

In Figure 2 the activity defined by the Equation 4 is plotted as a function of the affinity, where the affinity of the metal for halogen is defined by the Equation 6.

$$\text{AFFINITY} = \Delta H_f(\text{Cl})/\text{ON} \quad (6)$$

where  $\Delta H_f(\text{Cl})$  is the standard enthalpy of formation of metal chloride and ON is the oxidation number of the compound. The value corresponds to the heat of formation of one metal-chloride bond. Although the affinity level is represented as the enthalpy of formation of metal chloride because of the lack of data for the iodide system, the TPD spectra of methyl iodide proved to be well consistent with the concept shown in Figure 2. Namely, the order of peak temperature of methyl iodide desorption was  $\text{Ru} > \text{Pd} > \text{Rh}$ .

The relation between the activity and the affinity represents a volcano shape. With the metals located on the left hand side of the maximum, i.e., Ru, Pd, and Rh, the oxidative addition of methyl iodide to the metal should be slow because of their weak affinity for halide ion. This step could determine the rate of methanol carbonylation and lead to a high reaction order in methyl iodide. Although the rate of oxidative addition should be high for the metals located on the right hand side of the plot, since they have a strong affinity for halide ion, methyl iodide might adsorb too strongly and suppress the adsorption of other reactants which could retard other steps. Therefore, the more strongly methyl iodide is adsorbed, the lower the activity. A metal with high halide affinity should exhibit low reaction order with respect to methyl iodide; this is in agreement with the value of 0.1 for the Ni/A.C. catalyst and 0.7 for the Rh/A.C. catalyst (Table II).

Stability of Catalytic Activity of Nickel-Activated Carbon. In Figure 3 are shown the changes in the activity and the product selectivity of a Ni/A.C. catalyst. It is clear from the figure that the activity and the selectivity are fairly stable for several hundreds of hours. After 500 hours, the carbonylated products totaled 18,000 moles per mole of supported nickel.

Accumulation of Iodide Ion in the Catalyst. As has been indicated, methyl iodide is strongly adsorbed on the reduced Ni/A.C. catalysts. Figure 4 shows the transient responses of methyl iodide and methyl acetate effluence from Ni/A.C. and  $\text{NiI}_2/\text{A.C.}$  catalyst during the initial period of the reaction. For the Ni/A.C. catalyst, the effluence of methyl acetate reached a steady state level fairly quickly, whereas the breakthrough of the methyl iodide effluence requires about 90 minutes. On the other hand, a large amount of methyl iodide effuses from the bed of  $\text{NiI}_2/\text{A.C.}$  catalyst very early during the reaction and then reaches a steady state level, which is equal to the inlet level. The total amount of iodide ion trapped in the catalyst (after correction for the amount trapped by activated carbon itself) corresponded to the amount of atomic nickel for both catalysts. The phenomena mentioned above suggested that the chemical species of nickel in the catalyst reaches a particular state

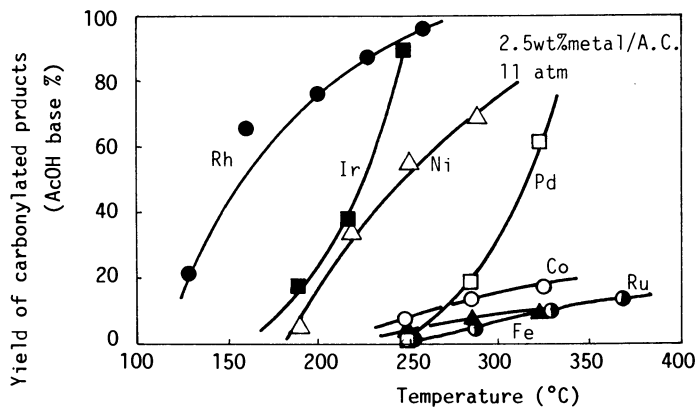


Figure 1. Activity of group VIII metals supported on activated carbon for methanol carbonylation:W/F=5 g·h/mol; CO/MeOH/MeI=100/19/1.

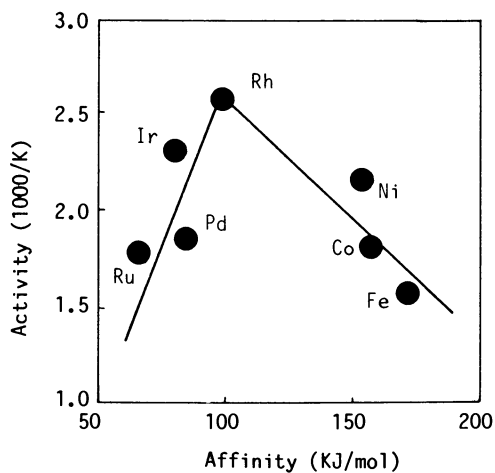


Figure 2. Activity as a function of halide affinity:the same experiment as in Figure 1.

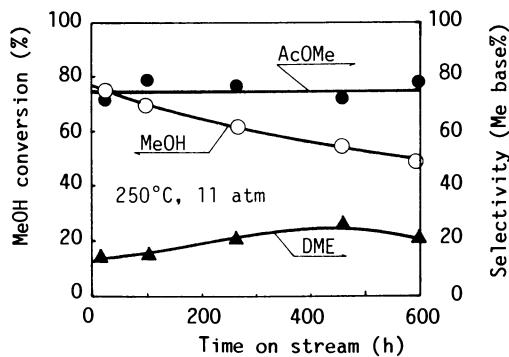


Figure 3. Catalytic activity and product selectivity as a function of time on stream:  $W/F=5 \text{ g}\cdot\text{h}/\text{mol}$ ;  $\text{CO}/\text{MeOH}/\text{MeI}=40/19/1$ .

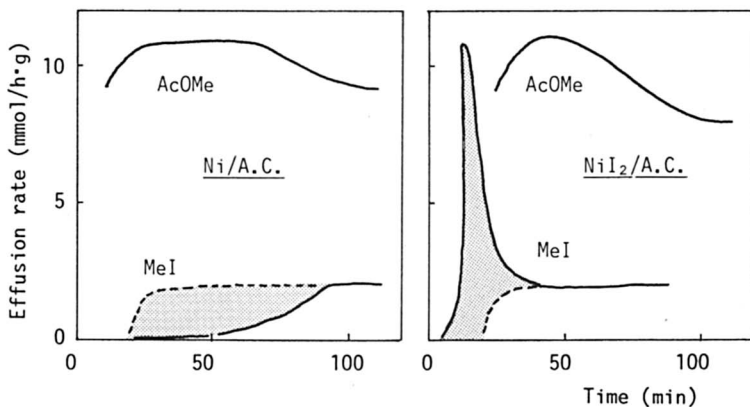


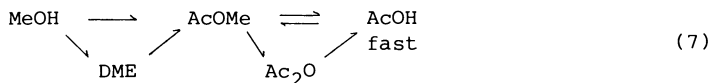
Figure 4. Transient response: Ni loading, 10wt% as metal; 250°C; 10 atm.



during the reaction which contains one iodide atom bonded to one nickel atom, irrespective of its starting state.

Operational Factors Controlling Rate and Selectivity of Carbonylation. In Figures 5 and 6 are shown the effects of reaction temperature and of CO/MeOH feed gas ratio on catalytic performances. Methanol conversion increased monotonically with an increase in the temperature and was 99% at 300°C. The yield of methyl acetate reached a maximum level at 250°C and then decreased. Acetic acid yield increased with increasing temperature and was 95% at 300°C. It should be noted that the yield of DME was 2.7% or less and that its yield was almost zero at 300°C. As already pointed out by the present authors, DME and methyl acetate are converted successively to methyl acetate and acetic acid, respectively (6,7). A high reaction temperature should accelerate the successive reaction. The mole ratio of CO/MeOH also exhibited marked effects on the rate and the selectivity. With an increase in the CO/MeOH ratio, the methanol conversion and the acetic acid selectivity increased while the selectivities to DME and methane decreased. In Figure 5 are shown selectivity-conversion curves for methyl acetate, acetic acid and DME. The figures indicate clearly that methyl acetate and DME are the primary products and that acetic acid is produced successively from them.

Reaction Network. As has been already pointed out (6,7), the reaction path of the present system can be expressed as follows:



Rate parameters of all unit reactions were determined by a differential reaction technique and are summarized in Table III for the Ni/A.C. catalyst. For methyl acetate formation, the reaction orders with respect to methyl iodide, methanol and carbon monoxide are 0.1, 0.6 and 0.7, respectively, which are remarkably different from those for the rhodium catalyst (1.0, 0 and 0, respectively) (2). The low reaction order with respect to methyl iodide is consistent with the strong affinity of halide anion to nickel.

The computer simulation based on the rate equations gave a satisfactory agreement with the experimental data with the correction that methyl acetate, which is adsorbed strongly on the catalyst, suppresses the methanol carbonylation (Figure 6).

Effect of Carrier Material on the Character of Adsorbed CO on Nickel. It is clear from the data in Table I that the carbonaceous carrier material is essential for catalysis. The results of H<sub>2</sub> adsorption and CO adsorption are given in Table IV. The amount of chemisorbed H<sub>2</sub> was far less than that of CO for every sample, and thus the ratio of chemisorbed CO to H<sub>2</sub> was very much higher than 1.0. It should be also noted that the amount of chemisorbed CO is greater than total Ni loaded on activated carbon, which indicates that more than one molecule of CO is adsorbed on each surface Ni atom.

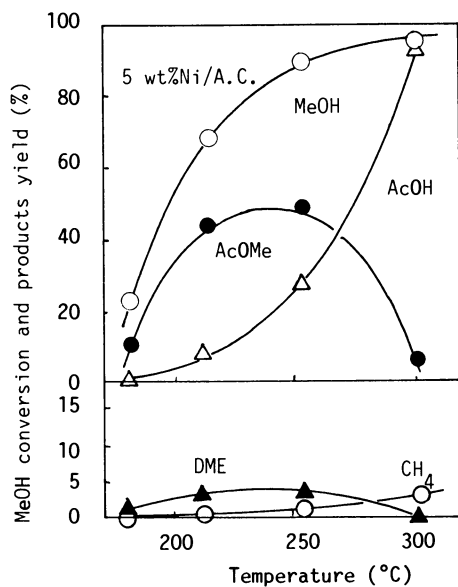


Figure 5. Effect of temperature on methanol carbonylation: W/F=5 g·h/mol; CO/MeOH/MeI=100/19/1; 10 atm.

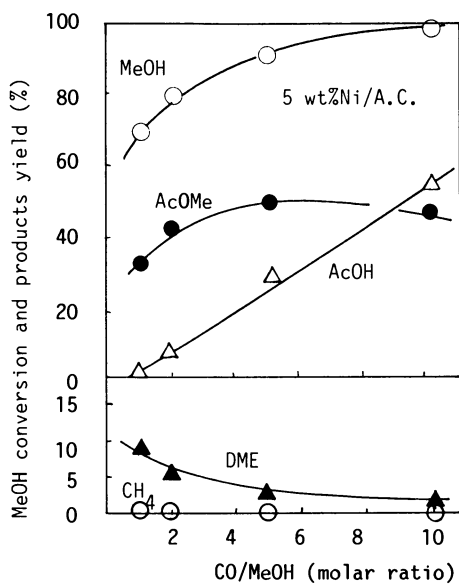


Figure 6. Effect of CO/MeOH ratio on methanol carbonylation: W/F=5 g·h/mol; MeOH/MeI=19/1; 250°C; 10 atm.

Table III. Experimental rate equation for methanol carbonylation catalyzed by Ni-activated carbon

reaction path	reaction order	rate constant <sup>a</sup>
2MeOH + CO → AcOMe + H <sub>2</sub> O	$P_{MeI}^{0.1} P_{MeOH}^{0.6} P_{CO}^{0.7}$	9
2MeOH → DME + H <sub>2</sub> O	$P_{MeI}^{0.6} P_{MeOH}^{1.2}$	11
DME + CO → AcOMe	$P_{MeI}^{0.5} P_{DME}^{0.6} P_{CO}^{0.5}$	15
AcOMe + H <sub>2</sub> O → AcOH + MeOH	$P_{H_2O}^{0.3} P_{AcOMe}^{0.7}$	11
AcOH + MeOH → AcOMe + H <sub>2</sub> O	$P_{AcOH}^{0.3} P_{MeOH}^{0.9}$	35
AcOMe + H <sub>2</sub> O + CO → 2AcOH	$P_{MeI}^{1.0} P_{CO}^{2.7} P_{AcOMe}^{-1.7}$	15

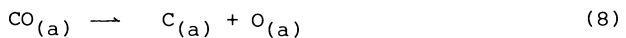
<sup>a</sup> mmol/h·g of catalyst atm<sup>x</sup>, where x is the sum of the reaction order.

TABLE IV. Chemisorption of H<sub>2</sub>, CO and MeI on nickel

Carrier <sup>a</sup>	H <sub>2</sub> uptake <sup>b</sup> (μmoles/g)	CO uptake <sup>b</sup> (μmoles/g)	H/Ni <sup>c</sup>	CO/Ni	MeI/Ni <sup>d</sup>
A.C.	6.7	677 <sup>e</sup>	0.03	1.59	0.70
SiO <sub>2</sub>	37	206	0.17	0.48	-
Al <sub>2</sub> O <sub>3</sub>	7.2	237	0.03	0.56	-

<sup>a</sup> 2.5wt% Ni/carrier. <sup>b</sup> Measured at 0°C. <sup>c</sup> atomic ratio  
<sup>d</sup> Measured at 250°C. <sup>e</sup> CO uptake at 80 Torr.

Figure 7 shows the results of TPR of CO adsorbed on nickel supported on activated carbon, γ-alumina and silica gel, respectively. For Ni/γ-Al<sub>2</sub>O<sub>3</sub> and Ni/SiO<sub>2</sub>, only CO was desorbed at low temperature and methane (and CO<sub>2</sub>) were formed at higher temperature. In the case of Ni/A.C., however, almost all of adsorbed CO was desorbed below 150°C. It has been generally accepted that the first step of methane formation by hydrogenation of CO is the dissociation of C-O bond (Equation 8) (8). The resultant C<sub>(a)</sub> and O<sub>(a)</sub> then react with either hydrogen or CO as shown in Equation 8 to 11.



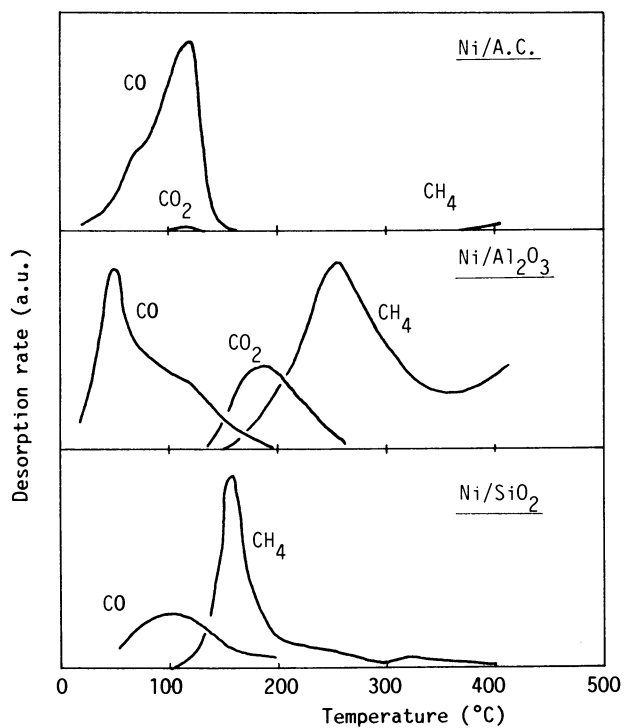


Figure 7. TPR profiles of adsorbed CO on nickel: Ni loading, 2.5wt% as metal; in flowing hydrogen; 400°C/h.

Thus, it is clear that on the Ni/ $\gamma$ - $Al_2O_3$  catalyst or the Ni/ $SiO_2$  catalyst a large fraction of adsorbed CO is in the dissociated or nearly dissociated form. On the Ni/A.C. catalyst CO is adsorbed non-dissociatively and the bond between nickel and CO is weak, as suggested from the low temperature desorption spectrum. In contrast to Ni/ $\gamma$ - $Al_2O_3$  and Ni/ $SiO_2$ , the C-O bond dissociation (Equation 8) hardly proceeds on the Ni/A.C. and therefore the formation of methane (Equation 9) or  $CO_2$  (Equation 10) is small. The suppression of  $H_2$  adsorption on Ni/A.C. suggests that a unique interaction with activated carbon exists. The large chemisorption of CO and its TPR spectrum indicate the formation of subcarbonyl. The molecular CO bonded weakly on nickel should play an important role in the carbonylation of methanol.

Since methyl iodide is adsorbed strongly on the Ni/A.C. catalyst even at  $250^\circ C$ , the number of surface nickel atoms can be determined by measuring the chemisorption at the temperature. The data in Table IV and Figure 8 show that the dispersion of nickel decreases with increasing nickel loading from 90% (1 wt%) to 22% (10wt%). However, the turn over frequency of the carbonylation is independent of the Ni loading, indicating that this reaction is a structure insensitive reaction.

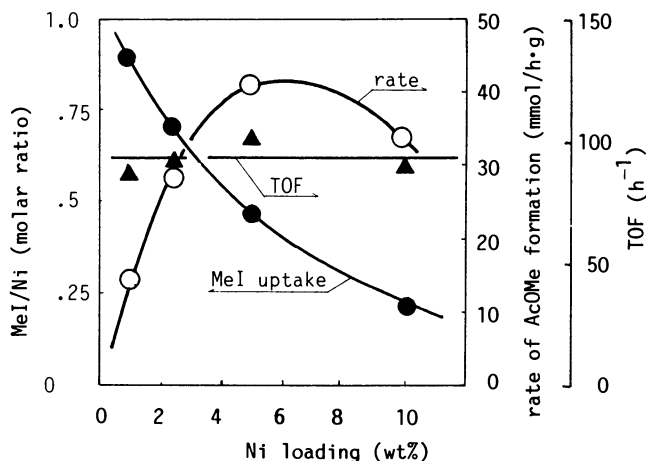


Figure 8. Effect of nickel loading on adsorption of methyl iodide and TOF: reaction conditions,  $250^\circ C$ , 10 atm,  $P_{CO}=4$  atm,  $P_{MeOH}=2$  atm,  $P_{MeI}=0.6$  atm: adsorption, at  $250^\circ C$ .

Literature Cited

1. Hohenschutz, H.; von Kutepow, N.; Himmele, W. Hydrocarbon process. 1966, 45, 141.
2. Roth, J.F.; Craddock, J.H.; Hershman, A.; Paulik, F.E. Chemtech 1971, 600.
3. Rizkalla, N.; Naglieri, A.N. German Patent 2 749 955, 1978.
4. Issiki, T.; Kijima, Y.; Miyauchi, Y. Japan Kokai 79-59211, 1979.
5. Fujimoto, K.; Shikada, T.; Omata, K.; Tominaga, H. Ind. Eng. Chem. Prod. Res. Dev. 1982, 21, 429.
6. Shikada, T.; Fujimoto, K.; Miyauchi, M.; Tominaga, H. Appl. Catal. 1983, 7, 361.
7. Omata, K.; Fujimoto, K.; Shikada, T.; Tominaga, H. Ind. Eng. Chem. Prod. Res. Dev. 1985, 24, 234.
8. Zagli, A.E. J. Catal. 1979, 56, 435.

RECEIVED July 29, 1986

## Chapter 15

# Chemical and Catalytic Properties of Ruthenium Carbonyl Iodide Systems during Reactions on Oxygenated Substrates

Giuseppe Braca, Anna Maria Raspolli Galletti, and Glauco Sbrana

Department of Chemistry and Industrial Chemistry, University of Pisa,  
Via Risorgimento 35, 56100 Pisa, Italy

The chemical and spectroscopic properties of the acid hydride  $\text{HRu}(\text{CO})_3\text{I}_3$  and of the ion-pairs of the  $[\text{Ru}(\text{CO})_3\text{I}_3]^-$  anion are reported and their role in the catalytic carbonylation and homologation reactions on oxygenated substrates are discussed.

Singular characteristics of the ruthenium catalysts are the capability of direct activation of different substrates (alcohols, ethers, formic, orthoformic and other carboxylic acid esters) at a low iodine concentration, and a high flexibility toward carbonylation and/or homologation processes for the substrates used. The catalytic activity of the ruthenium catalysts moreover do not strongly decrease, as occurs with Co or Rh systems, by passing from methyl to higher oxygenated alkyl derivatives.

Homologation reactions on alcohols-formic esters produce a mixture of oxygenates rich in acetates suitable for use in gasoline with interesting antiknock and combustion properties.

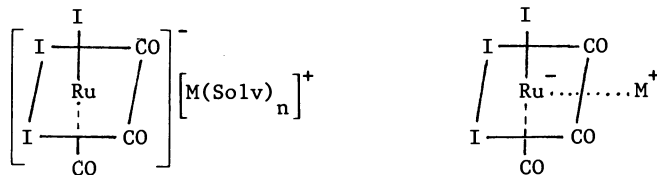
Monometallic ruthenium, bimetallic cobalt-ruthenium and rhodium-ruthenium catalysts coupled with iodide promoters have been recognized as the most active and selective systems for the hydrogenation steps of homologation processes (carbonylation + hydrogenation) of oxygenated substrates : alcohols, ethers, esters and carboxylic acids (1,2). While the ruthenium component is important and essential, the reasons for its behaviour are not always well understood. We will give some accounts of the chemical and catalytic properties of the ruthenium tricarbonyl triiodide species,  $[\text{Ru}(\text{CO})_3\text{I}_3]^-$ , which is often the sole derivative detected in catalytic solutions under reaction conditions. This will contribute to a better understanding of the aspects of the catalytic behaviour and of the scope of catalytic capabilities.

Chemical and spectroscopic properties of  $[\text{Ru}(\text{CO})_3\text{I}_3]^-$  species

The essential requirement for ruthenium catalysts to be active in homologation reactions of oxygenated substrates is the presence of an iodide promoter which may be  $\text{I}_2$ , HI, an alkyl or metal iodide, or a quaternary ammonium or phosphonium iodide (3). With alkali iodides as promoters, ion-pairs of the  $[\text{fac-Ru}(\text{CO})_3\text{I}_3]^-$  anion are formed in the catalytic solution of the homologation reactions starting from different precursors :  $\text{Ru}(\text{Acac})_3$ ,  $\text{Ru}_3(\text{CO})_{12}$ ,  $\text{Ru}(\text{CO})_4\text{I}_2$  etc. (4).

The addition of a selective crown-ether to a methyl acetate-acetic acid solution of the potassium salt of the anion results in the separation of the crystalline derivative  $[\text{K-18-crown-6}][\text{Ru}(\text{CO})_3\text{I}_3]$ . Its X-ray structure indicates the formation of a contact ion-pair where the complexed cation  $[\text{K-18-crown-6}]^+$ , shaped as "an overturned umbrella", is connected to the anion through three bridging iodine atoms. This arrangement allows the potassium ion to interact with other possible ligands in a direction perpendicular to the plane containing the crown-ether.

The I.R. spectra in solution of  $\text{MRu}(\text{CO})_3\text{I}_3$  salts ( $\text{M} = \text{Li, Na, K, Cs}$  and  $\text{PPh}_4$ ) show evidence of the formation of solvent separated (A) and tight ion-pairs (B).



A : Solvent separated ion-pair

B : Tight ion-pair

These species show different promoting effects on the activity and selectivity of the homologation of methyl acetate with  $\text{CO} + \text{H}_2$  (carbonylation to acetic acid, homologation to ethyl acetate and hydrogenation to methane) (5).

The formation and the spectroscopic properties of the  $[\text{Ru}(\text{CO})_3\text{I}_3]^-$  species can be easily studied in different solvents by reacting  $\text{Ru}(\text{CO})_4\text{I}_2$  directly with the iodide promoters (HI, NaI etc.). Thus the hydrido species  $\text{HRu}(\text{CO})_3\text{I}_3$ , which up to now was not well characterized, has been obtained in concentrated solutions in different solvents at room temperature from  $\text{Ru}(\text{CO})_4\text{I}_2$  and gaseous or aqueous HI. ( Mass spectrum :  $\text{M/e} : 567 (\text{M}^+)$ ;  $539 (\text{M}^+-\text{CO})$ ;  $511 (\text{M}^+-2\text{CO})$ ;  $483 (\text{M}^+-3\text{CO})$ ).

As a pure compound it is a red-brown oil, unstable at room temperature, that under vacuum or by addition of water rapidly decomposes releasing HI.



The I.R. and <sup>1</sup>H-NMR spectra of solutions of HRu(CO)<sub>3</sub>I<sub>3</sub> give new insight on its properties:

- it is a strong acid : a signal of a non-acidic hydride in the <sup>1</sup>H-NMR spectrum between 0 and -30δ is not observed; the protonic resonance appears at 1.4δ in anhydrous hexadeuteroacetone and is strongly broadened by addition of stoichiometric amounts of water;
- the ionic character of HRu(CO)<sub>3</sub>I<sub>3</sub> is also indicated by changes in its I.R. spectrum (ν<sub>CO</sub>) in different solvents (Table I): in hydrocarbon solution or in weakly-donating solvents (i.e. AcOH-AcOMe solutions), two bands at 2105-2102 and 2035-2025 cm<sup>-1</sup>, typical of tight ion-pair (B), are present; in oxygenated solvents (THF, diisopropyl ether) the bands are shifted to lower frequencies, 2098 and 2025 cm<sup>-1</sup>, as occurs for solvent separated ion-pairs (A); the addition to THF of small amounts of water, having a higher solvating capacity for H<sup>+</sup>, causes a further lowering of the frequencies to 2092 and 2022 cm<sup>-1</sup>; finally the addition to a THF solution of aniline results in the formation, by protonation of the basic solvent, of a non-solvated anilinium salt [(PhNH<sub>2</sub>)<sup>+</sup>[Ru(CO)<sub>3</sub>I<sub>3</sub>]<sup>-</sup> (tight ion-pair).

Table I. I.R. spectra of [Ru(CO)<sub>3</sub>I<sub>3</sub>]<sup>-</sup> species

	I.R. frequencies ν <sub>CO</sub> (cm <sup>-1</sup> )				
	Benzene	THF anhydrous	THF aqueous	THF+ aniline	AcOH + AcOMe
HRu(CO) <sub>3</sub> I <sub>3</sub>	2105 2035	2098 2025	2092 2022	2102 2032	2102 2025
KRu(CO) <sub>3</sub> I <sub>3</sub>	-	2102 <sup>a)</sup> 2033	2095 <sup>b)</sup> 2022	-	2098 <sup>a+b)</sup> 2085 <sup>sh</sup> 2027
[Li(Solv) <sub>n</sub> ] <sup>+</sup> [Ru(CO) <sub>3</sub> I <sub>3</sub> ] <sup>-</sup>	-	2092 <sup>b)</sup> 2021	-	-	-
[Co] <sup>2+</sup> [Ru(CO) <sub>3</sub> I <sub>3</sub> ] <sub>2</sub> <sup>-</sup>	-	2100 <sup>a)</sup> 2032	-	-	2097 <sup>a+b)</sup> 2085 <sup>sh</sup> 2027

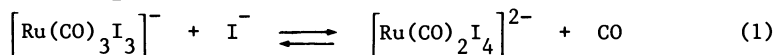
a) Tight ion-pair; b) Solvent separated ion-pair

The predominance of the ruthenium iodocarbonyl over the cobalt carbonyl species in the bimetallic Co-Ru systems is evidenced by the I.R. spectra of the catalytic solutions of the methyl acetate homologation with cobalt and ruthenium catalysts used in about the same concentration or with an excess of ruthenium. The latter compositions actually show the highest activity for the homologation

of methanol to ethanol (6,7) and of methyl acetate to ethyl acetate (8,9). These solutions do not contain the cobalt component as a carbonyl derivative when the cobalt is supplied either as  $\text{CoI}_2$  or as  $\text{Co}_2(\text{CO})_8$ . All cobalt is present as  $\text{Co}^{2+}$ , forming a tight ion-pair with  $[\text{Ru}(\text{CO})_3\text{I}_3]^-$ : in this form cobalt acts as a strong Lewis acid which accelerates the kinetics of the homologation processes (5,9,10). The same tight ion-pair is formed also when  $\text{Co}_2(\text{CO})_8$  is added at room temperature to a THF solution of the solvent separated ion-pair  $[\text{Li}(\text{THF})_n]^+[\text{Ru}(\text{CO})_3\text{I}_3]^-$ .

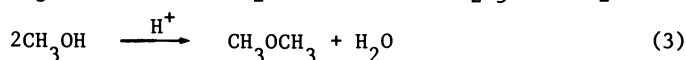
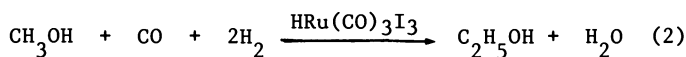
The cobalt is present as a carbonyl derivative and can be directly active in the hydrocarbonylation steps of the process only when a large excess of cobalt is used in the presence of phosphine ligands and iodide promoters (Co/Ru : 10/1). In this case the ruthenium is probably mainly involved in the hydrogenation of the aldehydes and their acetals to alcohols (6).

The picture is different for the bimetallic ruthenium-rhodium systems: both metals in the presence of iodide promoters and CO give anionic iodocarbonyl species, namely  $[\text{Ru}(\text{CO})_3\text{I}_3]^-$  and  $[\text{Rh}(\text{CO})_2\text{I}_2]^-$ , but the range of I, CO concentration and temperature in which the anions exist and are catalytically active in carbonylation reactions is different.  $[\text{Ru}(\text{CO})_3\text{I}_3]^-$  species in fact are extensively transformed at high temperature and low carbon monoxide pressure by an excess of  $\text{I}^-$  (i.e. I/Ru : 50) into catalytically inactive  $[\text{Ru}(\text{CO})_2\text{I}_4]^{2-}$  ( $\nu_{\text{CO}}$  : 2047, 1990  $\text{cm}^{-1}$  in THF (11)) (eq. 1), whereas  $[\text{Rh}(\text{CO})_2\text{I}_2]^-$  can work in the carbonylation process only in the presence of a large excess of  $\text{I}^-$  (I/Rh : 100-1000) which prevents reduction to metal (12) (for instance at 150 °C rhodium(I) carbonyl halides,  $[\text{Rh}(\text{CO})_2\text{X}_2]^-$ , without  $\text{CH}_3\text{I}$  under a  $\text{CO}/\text{H}_2$  pressure of 10 MPa are completely reduced to metal).



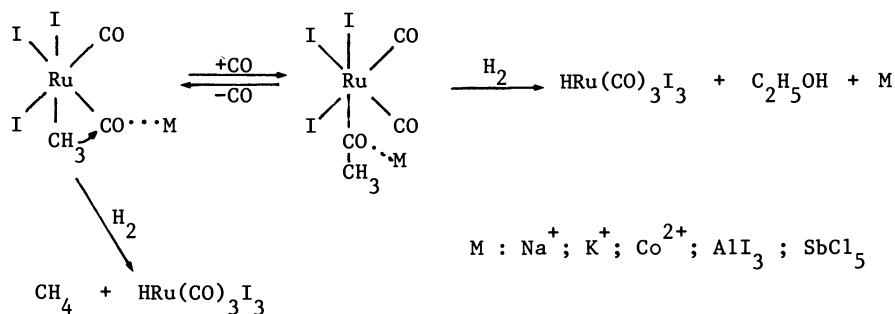
### Role of $[\text{Ru}(\text{CO})_3\text{I}_3]^-$ species in the homologation processes

Methanol homologation - The strong acid hydride  $\text{HRu}(\text{CO})_3\text{I}_3$ , present in the catalytic ruthenium iodide solutions for the methanol homologation, is able to directly protonate the substrate and produce the methyl and successively the acetyl intermediates for the homologation to ethanol (eq. 2). It also catalyzes etherification to dimethyl ether (eq. 3).



The side reaction of hydrogenolysis of the methyl-ruthenium intermediate to methane also become predominant when the carbonyl insertion-methyl migration step of the process (Scheme 1) proceeds at a low rate. To reduce this drawback some Lewis acid promoters (i.e. metal alkali cations, classical Lewis acids such as  $\text{AlI}_3$ ,  $\text{SbCl}_5$  etc.)

which strongly accelerate the formation of the acetyl intermediate can be conveniently added to the catalytic system.



**Scheme 1** Lewis acid assisted evolution of alkyl and acyl ruthenium carbonyl iodide intermediates.

Accordingly the best results in the methanol homologation are obtained by a compromise between the concentration of the protonic and Lewis acid components of the catalytic system and the hydrogen and carbon monoxide partial pressures (Table II)

**Table II.** Methanol homologation with ruthenium catalysts

Catalytic system	MeOH			Selectivity, %				
	Conv. %	h	EtOH	Me <sub>2</sub> O	MeOEt + Et <sub>2</sub> O	AcOMe + AcOEt	Heavy prod.	CH <sub>4</sub> + C <sub>2</sub> H <sub>6</sub>
Ru/CH <sub>3</sub> I 1/4.5	66	8	8.0	65.0	7.0	10.0	traces	10.0
Ru/CH <sub>3</sub> I/NaI 1/2/8	64	8	24.0	26.0	14.0	13.0	1.0	22.0
Ru/KI/18-crown-6 1/10/10 ether	11.5	8	6.0	21.0	28.7	15.3	traces	28.9

Reaction conditions : Ru(Acac)<sub>3</sub> : 1.5x10<sup>-2</sup> mol/l; T : 200 °C;  
P : 15 MPa; H<sub>2</sub>/CO : 1/1

Thus mixtures containing methyl iodide, which generates the protonic acids, HI and HRu(CO)<sub>3</sub>I<sub>3</sub>, and ionic iodides (NaI, KI), which provide the Lewis acid (K<sup>+</sup>, Na<sup>+</sup>), give the highest yields of ethanol and the highest reaction rates (Table II) analogously to that found with cobalt-ruthenium catalysts (Ru/Co : 2; I<sup>-</sup>/Co : 5) (13) .

In the case of bimetallic ruthenium-rhodium catalysts on the contrary it is more difficult to balance the conditions required for the optimum performance of both metal species : either the formation

of  $[\text{Rh}(\text{CO})_2\text{I}_2]^-$  species is favoured (Ru/Rh/I : 1/0.1/100 ;  $\text{CH}_3\text{I}/\text{KI}$  : 1) and the carbonylation reaction to acetyl derivatives (acetic acid + methyl acetate) is the main reaction as occurs in the Monsanto process (Table III ; runs 1 and 2), or  $[\text{Ru}(\text{CO})_3\text{I}_3]^-$  is predominant (Ru/Rh/I : 1/0.1/10 ;  $\text{CH}_3\text{I}$  sole iodide promoter) and the situation is that typical for monometallic ruthenium catalysts (Table III ; runs 5 and 6). For intermediate conditions, both the carbonylation and the homologation reactions are observed.

Table III. Methanol homologation with ruthenium-rhodium catalysts

Run	Catalytic system	Selectivity, %							
		MeOH Conv. %	EtOH	Me <sub>2</sub> O	MeOEt + EtOEt	AcOMe + AcOH	AcOEt	Heavy Prod.	CH <sub>4</sub> + C <sub>2</sub> H <sub>6</sub>
1	Rh/CH <sub>3</sub> I : 1/100 <sup>a)</sup>	100	-	-	-	99	-	-	traces
2	Ru/Rh/I : 1/0.1/100 CH <sub>3</sub> I/KI : 1/1	100	-	-	-	90.0	-	-	10.0
3	Ru/Rh/I : 1/0.1/20 CH <sub>3</sub> I/KI : 1/1	95	2.0	19.4	3.6	60.0	8.0	-	7.0
4	Ru/Rh/I : 1/0.1/22 CH <sub>3</sub> I	97	2.0	-	3.7	67.3	16.0	-	11.0
5	Ru/Rh/I : 1/0.1/10 CH <sub>3</sub> I/NaI : 1/8 <sup>b)</sup>	62	23.0	21.0	15.0	17.0	1.0	1.0	22.0
6	Ru/I : 1/10 CH <sub>3</sub> I/NaI : 1/4	64	24.0	26.0	14.0	11.0	2.0	1.0	22.0

Reaction conditions : Catalysts : Ru charged as Ru(Acac)<sub>3</sub>, Rh as RhCl<sub>3</sub>·3H<sub>2</sub>O ; Ru + Rh : 0.74 mmol ; MeOH : 0.7 mol  
AcOH : 0.07 mol ; T : 200 °C ; P : 15 MPa ; CO/H<sub>2</sub> : 1/1 ; Time : 8 h ;

a) P : 40 MPa ; CO/H<sub>2</sub> : 1 ; T : 180 °C

b) Ru charged as Ru(CO)<sub>4</sub>I<sub>2</sub> ; MeOH : 0.7 mol.

Higher alcohols homologation - The carbonylation and homologation of higher aliphatic alcohols strongly differs from that of methanol in two respects : reaction rate and product distribution. A dramatic decrease of catalytic activity was observed passing from methanol to ethanol and higher straight and branched chain primary homologs in the carbonylation and homologation reactions in the presence of cobalt and rhodium catalysts (reactivity ratio in the homologation with Co/I catalysts (1) : methanol/ethanol = 42 ; with Co/I/P catalysts (14) : methanol/ethanol = 11, methanol/n-butanol = 12; reactivity ratio in the carbonylation with Rh/I catalysts (15) : methanol/ethanol = 18.5).

The formation of different isomers is often observed with

secondary and tertiary alcohols caused by a dehydration of the alcohol to an olefin followed by hydroformylation to the isomeric aldehydes and hydrogenation to the homologous alcohols (14).

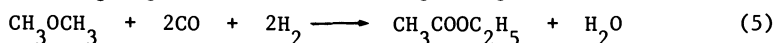
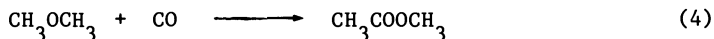
With the  $[\text{Ru}(\text{CO})_3\text{I}_3]^-$  systems no strong decrease of the catalytic activity is observed passing from methanol to higher primary alcohols (reactivity ratio in the homologation with Ru/I catalysts : methanol/ethanol = 1.5; methanol/n-butanol = 0.5; methanol/i-butanol = 1.1) , but only a variation in the selectivity towards carbonylation, homologation, and hydrogenation products (selectivity ratio to carbonylation/homologation/hydrogenation products : for methanol = 0.24/1/1.8; for n-butanol = 3.8/1/1.9 ; for i-butanol = 2.8/1/2.5) (Table IV).

In the case of secondary and tertiary alcohols the strong acid  $\text{HRu}(\text{CO})_3\text{I}_3$  causes a very rapid dehydration of the substrates to olefins which have been found in very large amount in the reaction mixtures together with their oligomerization products.

The isomer aldehydes are completely hydrogenated to alcohols which are partially dehydrated to ethers and carbonylated to esters. The straight chain alcohols and their ether and ester derivatives comprise 50 % of the products resulting from homologation of 2-butanol. This isomer ratio is quite analogous to that observed in the synthesis of esters from olefins, CO and alcohols (16).

The unique behaviour of the ruthenium iodocarbonyl catalysts allows the production of mixtures of oxygenates rich in esters by the carbonylation and homologation of mixtures of methanol with higher alcohols (methyl fuel, M.A.S. etc.). Thus, for instance, using a 1/1 methanol/i-butanol mixture, the reaction at long times leads to the prevalent formation of mixed esters (isobutyl acetate + methyl isovalerate) coming from the crossed reaction of the two alcohols. Ethers initially formed in high amounts by acid catalysis are successively activated and consumed in carbonylation and homologation reactions (Figure 1).

Carbonylation and homologation of ethers - The carbonylation and homologation of dimethyl ether to methyl and ethyl acetate (eqs. 4 and 5) in methyl acetate-acetic acid solution are considerably affected by the acidity of the reaction medium and by the nature of the iodide promoter which determines the concentration of  $\text{HRu}(\text{CO})_3\text{I}_3$ .



The highest conversions of the substrates are obtained, analogous to methanol homologation, with HI as promoter. This assures a high concentration of  $\text{HRu}(\text{CO})_3\text{I}_3$  . The best selectivities to ethyl acetate + acetic acid and the lowest formation of hydrocarbons are obtained with NaI, which generates  $\text{NaRu}(\text{CO})_3\text{I}_3$  and supplies the Lewis acid  $\text{Na}^+$

Table IV. Higher alcohols carbonylation and homologation with ruthenium catalysts

Alcohol (mmol)	MeOH (800)	EtOH (370)	n-BuOH (375)	i-BuOH (370)	sec-BuOH (370)	ter-BuOH (370)						
Conversion, %	84	82	96	64	86	96						
Products of a)	meq.	Sel.%	meq.	Sel.%	meq.	Sel.%	meq.	Sel.%				
Carbonylation b)	16	2.4	42	14.0	135	37.5	58	24.5	18 i)	5.5	-	-
Homologation c)	66	9.8	13	4.0	35	9.7	21	8.8	130 i)	40.8	18 j)	5.0
Hydrogenolysis d)	123	18.3	37	12.0	67	18.5	51	21.5	88	27.7	85	24.0
Etherification e)	456	67.7	181	60.0	62	17.1	54	23.0	11	3.3	8	2.2
Esterification f)	12	1.8	30	10.0	62	17.2	41	17.4	3	1.0	-	-
Dehydration g)	-	-	-	-	-	-	6	2.4	69	21.7	61	17.2
Isomerization h)	-	-	-	-	-	-	6	2.4	-	-	-	-
Other reactions k)	-	-	-	-	-	-	-	-	-	-	183	51.6

Reaction conditions : Alcohol/Ru(Acac)<sub>3</sub> : 840; CH<sub>3</sub>I/Ru : 10; T : 200 °C; P : 15 MPa; CO/H<sub>2</sub> : 1/1

a) Equivalents of alkyl groups of the substrate involved in the indicated reactions.

b) Esters and acids from simple carbonylation reactions; c) Alcohols, ethers and esters with higher homologous alkyl groups. d) Hydrocarbons from hydrogenolysis of the alcohol and its homologs. e) Ethers from dehydration of the substrate. f) Esters of the reagent alcohol. g) Olefins from dehydration of the alcohols. h) Isomeric alcohols. i) Isomer products (linear/branched : 50/50 - 60/40). j) Only 2-methyl butanol; k) Dimers and trimers of i-butene.

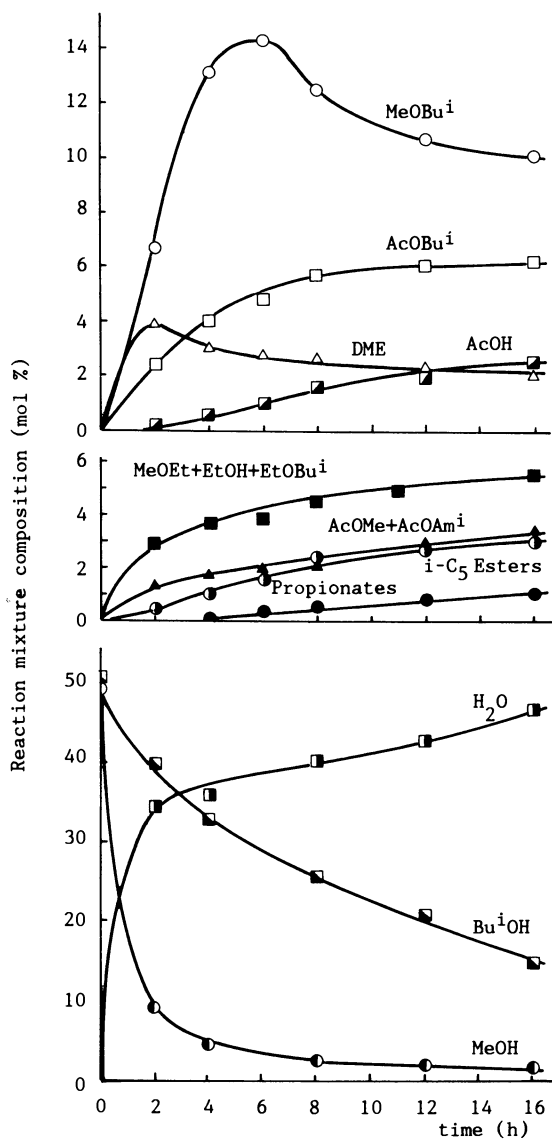


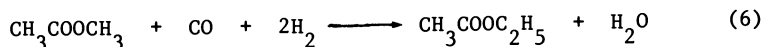
Figure 1. Carbonylation and homologation of a methanol-*i*-butanol mixture.

Reaction conditions : Ru(Acac)<sub>3</sub> :  $1.2 \times 10^{-2}$  M ; CH<sub>3</sub>I/Ru : 10 ;  
 MeOH : 3 mol ; *i*-BuOH : 3 mol ; T : 200°C ; P : 15 MPa ;  
 H<sub>2</sub>/CO : 1.

(4). An analogous behaviour has been observed with bimetallic Ru-Co catalysts (8).

For ethers of higher alcohols, activity comparable to that of dimethylether is observed with the  $[\text{Ru}(\text{CO})_3\text{I}_3]^-$  catalysts, where simple carbonylation is favoured over homologation (1).

Methyl acetate homologation - Our recent work on the effect of formation of ion-pairs in the homologation of methyl acetate to ethyl acetate (eq. 6) has clarified the role played by  $\text{HRu}(\text{CO})_3\text{I}_3$  and  $\text{M}^+[\text{Ru}(\text{CO})_3\text{I}_3]^-$  salts (M = alkali metal) (5,10).



$\text{HRu}(\text{CO})_3\text{I}_3$  and/or other strong acids favour the activation of the substrate and increase the reaction rate but do not favour the carbonylation steps of the process. Thus the prevailing reactions are the hydrogenation of the acetyl groups to ethyl derivatives and of methyl groups to methane. In the presence of  $\text{M}^+[\text{Ru}(\text{CO})_3\text{I}_3]^-$  salts and particularly when the cation is less solvated or selectively complexed by a specific crown-ether, the carbonylation steps of the process are favoured.

Thus a decrease in the formation of hydrocarbons and etherification and further homologation products is observed with selectivities to ethyl acetate + acetic acid as high as 93 % with a  $\text{TN}_{50\% \text{ conv}}$  of about  $0.027 \text{ sec}^{-1}$  (Table V).

Table V. Performances of different promoters of the  $[\text{Ru}(\text{CO})_3\text{I}_3]^-$  species in the homologation of methyl acetate to ethyl acetate

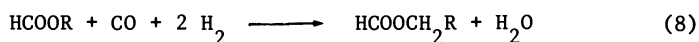
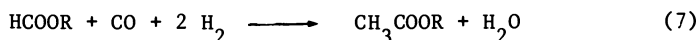
Promoter	$\text{CH}_3\text{I}$	KI	$\text{HPF}_6/\text{KI}$	KI/18-crown-6 ether	$\text{AlI}_3$
Time, h	26.0	24.0	8.0	10.0	8.0
AcOMe conv. %	84.6	80.5	47.4	80.4	77.5
$\text{TN}_{50\% \text{ conv.}}$ , $\text{s}^{-1}$	0.01	0.01	0.008	0.027	0.018
<u>Reaction products</u>	Sel.%	Sel.%	Sel.%	Sel.%	Sel.%
$\text{C}_1 + \text{C}_2$ alcohols and ethers	8.7	0.3	3.3	traces	5.0
AcOH	3.1	61.3	46.4	63.0	33.1
AcOEt	51.8	22.6	41.7	27.9	40.7
Heavy products	10.0	traces	0.7	traces	8.3
Hydrocarbons	24.4	7.9	15.8	9.1	12.7

Reaction conditions :  $\text{Ru}(\text{Acac})_3$  :  $3.6 \times 10^{-3}$  mol; I/Ru : 10; AcOMe : 1.8 mol; AcOH : 1.8 mol; T : 200 °C; P : 12 MPa;  $\text{H}_2/\text{CO}$  : 2/1.



Upon the addition of Lewis (i.e. AlI<sub>3</sub>) and protonic non-complexing acids (i.e. HPF<sub>6</sub>) promoters to [Ru(CO)<sub>3</sub>I<sub>3</sub>]<sup>-</sup> catalysts, improvements in selectivity to valuable products (acetic acid + ethyl acetate) and in reaction rate are observed. This is believed to be due to an acceleration by acids of the alkyl migration-carbonyl insertion step of the process, as discussed in detail in a recent paper (10).

Formic esters homologation - Ruthenium catalysts based on [Ru(CO)<sub>3</sub>I<sub>3</sub>]<sup>-</sup> species are sole Group VIII metal systems able to hydrogenate and homologate the formyl group of formic esters to methyl and acetyl derivatives without causing an extensive decarbonylation of the formyl moiety (eqs.7,8) (17).



HRu(CO)<sub>3</sub>I<sub>3</sub>, produced by addition of suitable iodide promoters, i.e. CH<sub>3</sub>I or AlI<sub>3</sub> + HPF<sub>6</sub>, in this case seems essential to the activation of the substrate and for the hydrogenation of the formyl moiety to methyl derivatives (Fig. 2). On the other hand, iodide promoters which act also as Lewis acids (i.e. AlI<sub>3</sub>) favour the formation of products derived from carbonylation and homologation of the alkyl part of the formic ester.

These results also demonstrate the ability of the ruthenium carbonyl iodide systems to activate both the alkyl and the acyl part of the formates. The same is true for esters of higher carboxylic acids where new esters of higher homologous acids and alcohols are produced.

The carbonylation-homologation reaction may also be carried out on a mixture of alcohols and their formates. For instance, at a very high conversion of the reagents, methanol-methyl formate and i-butanol-i-butyl formate produce a mixture of oxygenates particularly rich in acetates that are useful as octane improvers for gasoline (Fig. 3).

A large amount of the water is produced in the homologation, etherification and esterification reactions, but the water is only slightly soluble in the oxygenates mixture and it spontaneously separates thus facilitating the separation of the reaction products.

Ethyl orthoformate homologation - The special ability of the [Ru(CO)<sub>3</sub>I<sub>3</sub>]<sup>-</sup> species for activating oxygenated substrates is also well evidenced by the homologation of ethyl orthoformate at lower temperatures (130 - 170 °C) (18).

A large variety of products coming from different activation paths of the substrate have been observed (Scheme 2) :

- diethoxymethane, CH<sub>2</sub>(OEt)<sub>2</sub>, methyl derivatives (MeOH, MeOEt etc.) and methane, are formed by a step-wise hydrogenation of the HC≡ moiety of the ester;

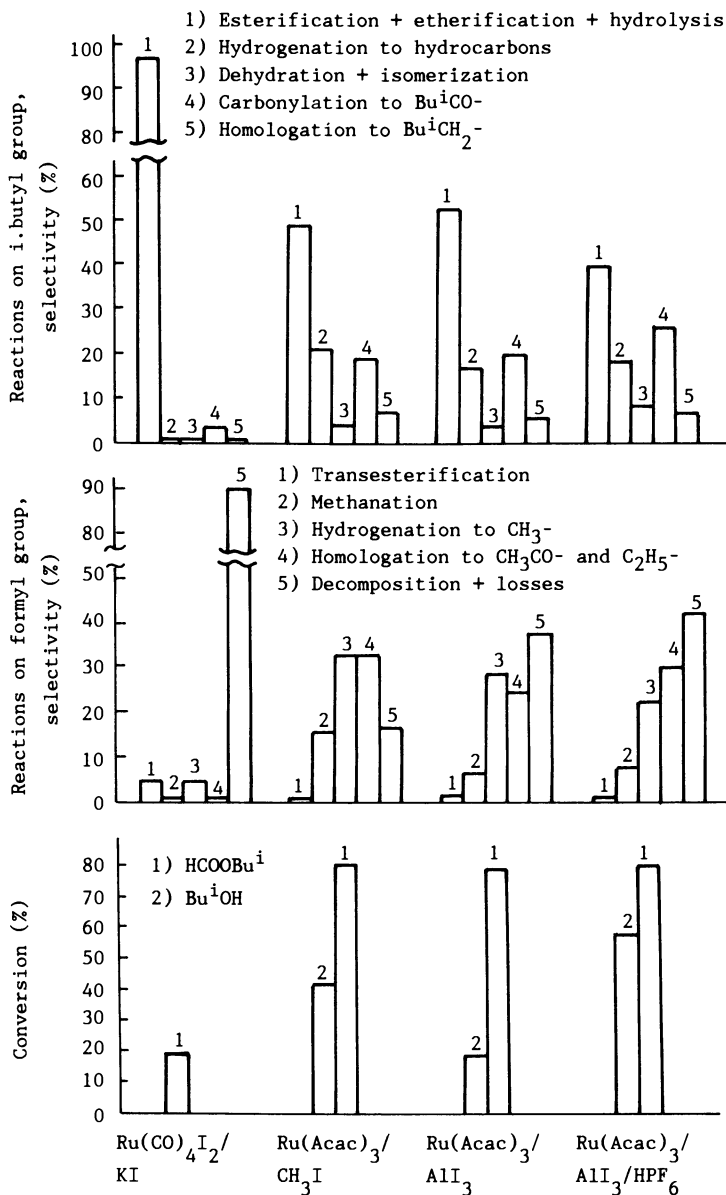


Figure 2. Homologation of mixtures of *i*-butyl formate-*i*-butanol. Reaction conditions : Catalyst conc. : 0.012 M; I/Ru : 10;  $\text{HCOO}^i\text{Bu}$  : 0.14 mol; *i*-BuOH : 0.18 mol; T : 200°C; P : 15 MPa;  $\text{H}_2/\text{CO}$  : 1; Time : 8 h.

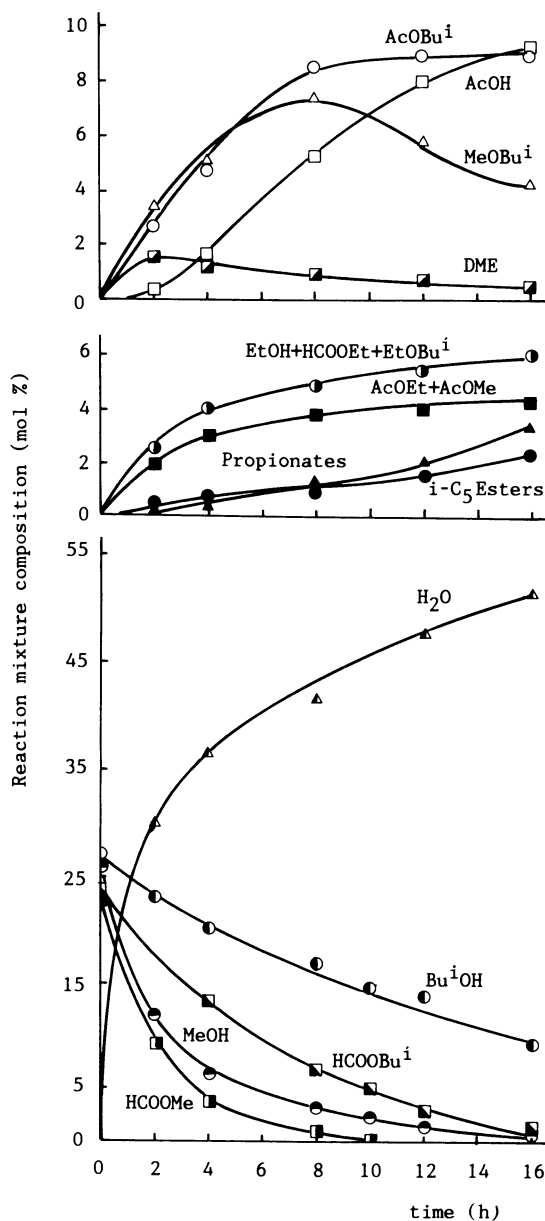
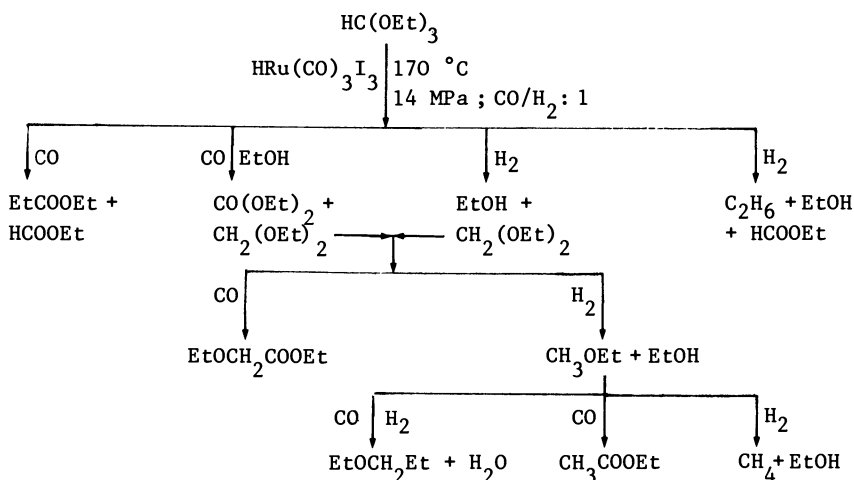


Figure 3. Carbonylation and homologation of methanol-methyl formate, i-butanol-i-butyl formate mixture.

Reaction conditions : see Figure 1; MeOH : 0.8 mol; HCOOMe : 0.71 mol; i-BuOH : 0.83 mol; HCOOiBu : 0.75 mol.

- propionic esters and n-propyl derivatives come from carbonylation and homologation of the ethyl moiety;
- diethyl carbonate comes from the carbonylation of the ethoxy group;
- ethoxyacetic and acetyl derivatives come from a further carbonylation of diethoxymethane and methyl derivatives respectively.

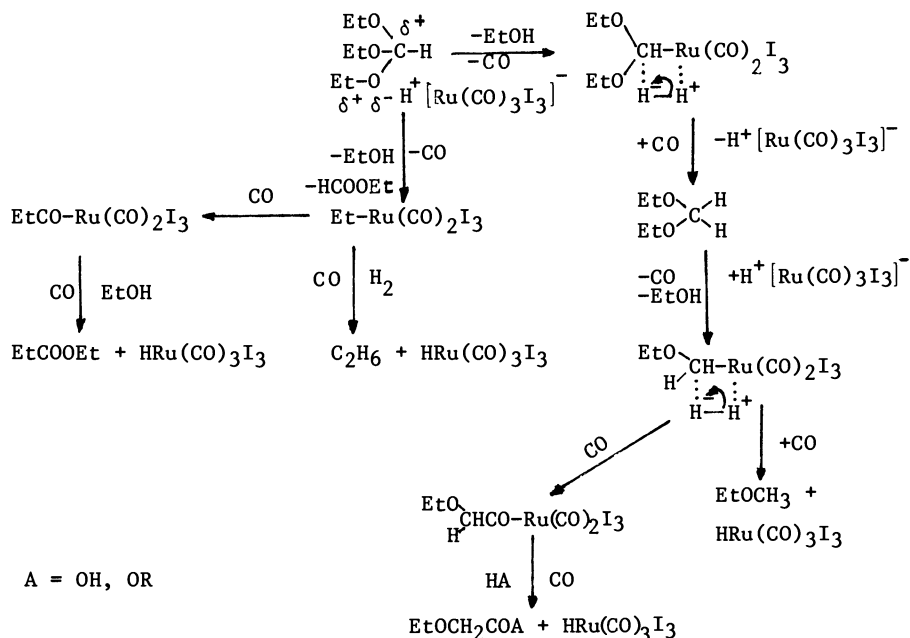
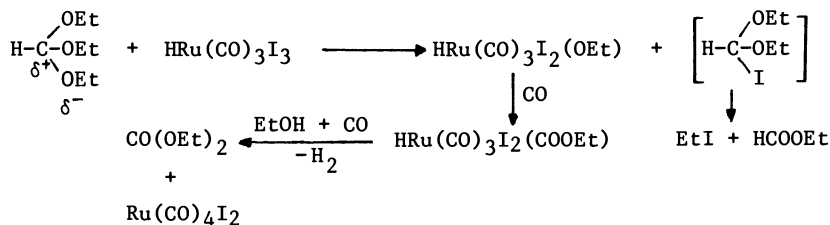


Scheme 2 - Homologation of ethyl orthoformate

Diethoxymethane is the main product obtained at lower temperature (130 °C), whereas methyl ethyl ether, methanol, ethyl propionate and ethoxyacetic derivatives predominate at higher temperature (170 °C). Diethylcarbonate, always present among the reaction products, is obtained, however, only in low yields (2-3%).

The behaviour of the ruthenium catalysts is quite different from that previously reported for cobalt carbonyl catalysts, which give a mixture of aldehydes and their acetals by formylation of the alkyl group of the orthoformate (19). The activity of rhodium catalysts, with and without iodide promoters, is limited to the first step of the hydrogenation to diethoxymethane and to a simple carbonylation or formylation of the ethyl groups to propionates and propionaldehyde derivatives (20).

In this case, the presence of the acid  $\text{HRu(CO)}_3\text{I}_3$ , as depicted in Scheme 3, also seems to play an essential role in the activation of the C-O bond of the different ether derivatives and in the evolution of the alkyl and acyl intermediates toward hydrogenation and carbonylation products. The formation of diethyl carbonate may be related to the substitution of an  $\text{I}^-$  by an  $\text{EtO}^-$  group in  $\text{HRu(CO)}_3\text{I}_3$  promoted by the  $[\text{CH(OEt)}_2]^+$  base. The ethoxy intermediate is then carbonylated to an ethoxycarbonyl derivative and transformed into diethyl carbonate by a nucleophilic attack by ethanol (Scheme 4).

Scheme 3 - Activation of ethyl orthoformate by  $\text{H}^+ [\text{Ru}(\text{CO})_3 \text{I}_3]^-$ Scheme 4 - Formation of diethyl carbonate from ethyl orthoformate catalyzed by  $\text{HRu}(\text{CO})_3 \text{I}_3$ 

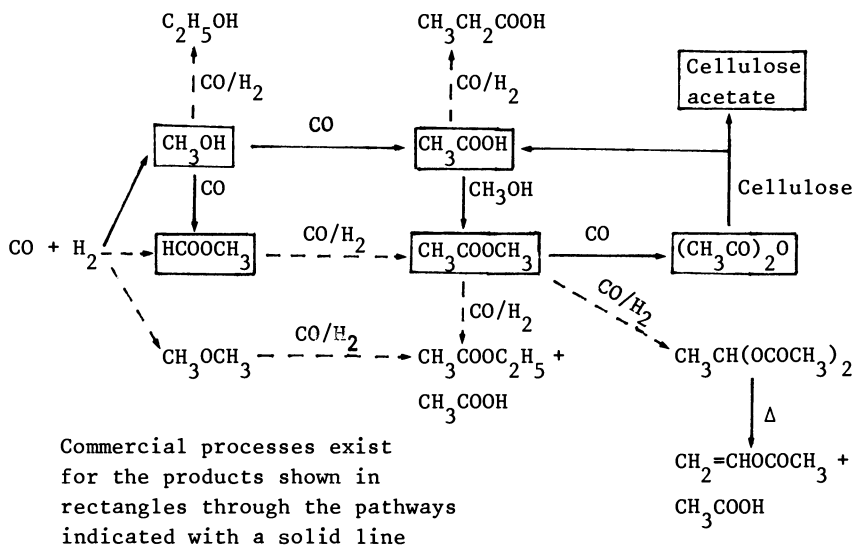
### Conclusions

In comparison with the other Group VIII metal derivatives, Ni, Co, Rh, active in CO + H<sub>2</sub> reactions on oxygenated substrates, the ruthenium iodocarbonyl systems show the following attractive catalytic properties:

- they are the most active catalysts for homologation reactions (carbonylation + hydrogenation or hydrogenation + carbonylation) of ethers and esters; the activity and the selectivity of the catalysts can be varied and directed towards the desired products by adding proton or Lewis acid and suitable phosphines or N-bases;

- they need a lower content of iodide promoter (Ru/I : 1/5-15), in contrast to rhodium catalysts (Rh/I : 1/100-1000), which can be supplied even as a saline iodide;
- the ruthenium catalytic solutions for homologation reactions are particularly stable and can be recycled, after separation of the reaction products, without any loss of catalytic activity;
- they catalyze the WGSR (water gas shift reaction) (21) consuming part of the water produced in the homologation reaction and increasing the  $H_2$  content in the gases.

Industrial development of homologation processes for dimethyl ether, methyl formate, methyl acetate and acetic acid is likely only if they are integrated into a comprehensive plant for the production of  $C_2$  derivatives from syn-gas (Scheme 5).



Scheme 5 - Alternative paths to  $C_2$  chemicals starting from  $CO + H_2$

#### Acknowledgments

The present work was carried out under the research programs Progetti Finalizzati "Chimica Fine e Secondaria" and "Energetica II" of C.N.R.

#### Literature Cited

1. Braca, G.; Sbrana, G. In "Aspects of Homogeneous Catalysis"; Ugo, R. Ed.; Reidel Pu.:Dordrecht, 1984; Vol. 5, pp. 241-337.
2. Röper, M.; Loevenich, H. In "Catalysis in  $C_1$  Chemistry"; Keim, W. Ed.; Reidel Pu.:Dordrecht, 1983; pp. 105-135.

3. Braca, G.; Sbrana, G.; Valentini, G.; Andrich, G.; Gregorio, G. In "Fundamental Research in Homogeneous Catalysis"; Tsutsui, M. Ed.; Plenum : New York, 1979; Vol III, p.221.
4. Braca, G.; Paladini, L.; Sbrana, G.; Valentini G.; Andrich, G.; Gregorio, G. Ind. Eng. Chem. Prod. Res. Dev. 1981, 20, 115.
5. Raspolli Galletti, A. M.; Braca, G.; Sbrana, G.; Marchetti, F. J. Mol. Catal. 1985, 32, 291.
6. Doyle, G. J. Mol. Catal. 1983, 18, 251.
7. Hidai, M.; Orisaku, H.; Ue, M.; Koyasu, Y.; Kodoma, T.; Uchida, Y. Organometallics 1983, 2, 292.
8. Jenner, G.; Kheradmand, H.; Kiennemann, A.; Deluzarche, A. J. Mol. Catal. 1983, 18, 61.
9. Gauthier-Lafaye, J.; Perron, R. Eur. Pat. Appl. 31 784, 1981.
10. Braca, G.; Raspolli Galletti, A. M.; Sbrana, G.; Zanni, F. J. Mol. Catal. 1986, 34, 183.
11. Colton, R.; Farthing, R. H. Aust. J. Chem. 1971, 24, 903.
12. Forster, D.; Singleton, T. C. J. Mol. Catal. 1982, 17, 299.
13. Gauthier-Lafaye, J.; Perron, R. Eur. Pat. Appl. 22 038, 1980.
14. Pretzer, W.R.; Habib, M.M. Proc. Symp. on Catalytic Conversion of Syngas and Alcohols, 17th Middle Atlantic Regional Mtg., Am. Chem. Soc., 1983.
15. Hjortkjaer, J.; Jorgensen, J. C. J. Mol. Catal. 1978, 4, 199.
16. Sbrana, G.; Braca, G.; Piacenti, F.; Marzano, G.; Bianchi, M. Chim. Ind. (Milan) 1972, 54, 117.
17. Braca, G.; Guainai, G.; Raspolli, A. M.; Sbrana, G.; Valentini, G. Ind. Eng. Chem. Prod. Res. Dev. 1984, 23, 409.
18. Braca, G.; Raspolli Galletti, A. M.; Sbrana, G.; Lazzaroni, R. J. Organomet. Chem. 1985, 289, 107.
19. Piacenti, F.; Bianchi, M. In "Organic Syntheses via Metal Carbonyls"; Wender, I.; Pino, P. Eds.; Wiley : New York, 1979; Vol. II, pp. 1-41.
20. Braca, G.; Raspolli Galletti, A. M.; Sbrana G.; Lazzaroni, R. Proc. 12th Int. Conf. Organomet. Chem., Vienna, 1985; p. 383.
21. Braca, G.; Sbrana, G.; Valentini, G.; Barberini, C. Cl Mol. Chem. 1984, 1, 9.

RECEIVED July 29, 1986

## Chapter 16

# Alcohol Synthesis from Carbon Oxides and Hydrogen on Palladium and Rhodium Catalysts

### Study of Active Species

A. Kiennemann, J. P. Hindermann, R. Breault, and H. Idriss

Laboratoire de Chimie Organique Appliquée, UA 469, Ecole Nationale Supérieure de Chimie, 1, rue Blaise Pascal, 67008 Strasbourg, France

Palladium and rhodium based catalysts, which yield methanol and ethanol from synthesis gas respectively, were selected for a mechanistic study. Chemical trapping showed a correlation between formyl species and the catalytic activity, indicating that these species probably are reaction intermediates. The role of the support on the activity and on the nature of the products was elucidated by chemical trapping of formyl, methoxy and formate species on palladium catalysts, and of formyl and acetate on rhodium catalysts. The rhodium catalysts were also studied by probe molecule experiments ( $C_2H_4$ ,  $CH_3CHO$ ) and by FT-IR spectroscopy (chemisorption of CO).<sup>3</sup> From these observations a mechanism is proposed for the synthesis of oxygenates on palladium and rhodium catalysts.

The synthesis of alcohols for chemical feedstock and/or gasoline octane boosters from synthesis gas has attracted much attention in recent years. At present, methanol is industrially the most important oxygenated product owing to its 99% selectivity when using a high pressure gas mixture ( $CO$ ,  $CO_2$ ,  $H_2$ ) and copper containing catalysts (1,2). However, intensive research is being carried out on the direct synthesis of higher alcohols: ethanol for organic synthesis purposes (3-5), a  $C_1$  to  $C_5$  alcohols mixture as an additive to gasolines (6).

Copper based catalysts have long been considered as the only effective methanol synthesis catalysts. However, Poutsma et al. (7) showed that palladium catalysts were active in methanol synthesis from  $CO-H_2$ . This latter metal had been previously considered as either almost inactive or active only for methane formation (8). Furthermore it is now known that both activity and selectivity can change drastically with the support. Vannice (9) observed that the methanation activity of a  $Pd/Al_2O_3$  was enhanced eighty and forty times compared to palladium black or  $Pd/SiO_2$  (or  $Pd/TiO_2$ ) respectively. The support effect on the selectivity was pointed out by many authors even at atmospheric pressure when the reaction temperature



did not limit the methanol production thermodynamically. For instance, Ichikawa (10), Bell (11), Poels (12), Vannice (13) and Ramarosan (14) showed that palladium supported on rare earth oxides had an excellent methanol selectivity in CO-H<sub>2</sub> or CO<sub>2</sub>-H<sub>2</sub> reactions. Tamaru et al. (15), starting from M<sub>2</sub>PdCl<sub>4</sub> (M ≡ Na, Li, K), supplied evidence of the importance of the precursor and concluded that an intimate contact between the metal and the promotor was necessary to achieve a good selectivity.

The works of Bhasin (5) and Ichikawa (10) with rhodium catalysts pointed out that interesting changes can occur in the reaction products :

- mainly hydrocarbons were the products with pure metal or when Rh is deposited on an inert support.
- methanol was formed with Rh/MgO
- ethanol was produced by addition of a second element (Fe, Mn, Zr...) to Rh-silica or when a rare earth oxide is used as a support.

The role of the support on the selectivity is still the object of many discussions, and different factors have been invoked to explain the selectivity changes :

- particle size effects (7, 16-18)
- acidity or basicity of the support (19)
- structure of active sites
- stabilization of intermediates by an intimate contact between metallic particles and promotor ions (15, 20).
- activation of the carbon monoxide by the interaction of its oxygen end with the support (21-24)
- the so-called strong metal support interaction (S.M.S.I.)
- stabilization of the metal in a higher oxidation state.

The last explanation for methanol formation, which was proposed by Ponec et al. (12,26), seems to be well supported by experimental and theoretical results. They established a correlation between the methanol activity and the concentration of Pd<sup>4+</sup>, most probably Pd<sup>4+</sup>. Furthermore, Anikin et al. (27) performed ab initio calculations and found that a positive charge on the palladium effectively stabilizes formyl species. Metals in a non-zero valent state were also proposed by Klier et al. (28) on Cu/ZnO/Al<sub>2</sub>O<sub>3</sub>, by Apai (29) on Cu/Cr<sub>2</sub>O<sub>3</sub> and by Somorjai for rhodium catalysts (30). Recently results were obtained with different rhodium based catalysts which showed the metal was oxidized by an interaction with the support (Rh-0) (on Rh/Al<sub>2</sub>O<sub>3</sub>) by EXAFS (31-32) and by FT-IR (33) and on Rh/MgO by EXAFS (34). The oxidation of the rhodium was promoted by the chemisorption of carbon monoxide (32, 34).

To obtain more information about the role of the support, it is necessary to investigate the reaction mechanisms over the various catalysts more thoroughly. One approach to the study of the reaction mechanism is the identification of reactive surface species by means of chemical trapping. This method has been fully described earlier (35-36) and only an outline will be given here.

A species chemisorbed on the surface of a catalyst will react if brought in contact with an appropriate reagent, for example an alkylating agent. The product, thus formed, can be identified by using gas chromatography. In the case of formyl species, when methyl- or ethyl iodide are used as trapping agents, acetaldehyde or

propionaldehyde, respectively, are obtained. The presence of formyl moieties can be confirmed by water treatment and the resulting formaldehyde detected by the method of Soukup ((37). On rhodium catalysts the chemical trapping was performed with  $\text{CD}_3\text{I}$  to distinguish between acetaldehyde as a reaction product or resulting from the chemical trapping experiments.

The methoxy species was detected by a reaction with acetic acid, ethyl iodide or water (or ethanol) giving methyl acetate, methyl ethyl ether or methanol, respectively. Formates were determined using dimethylsulfate (DMS).

The reproducibility and precision of the measurements are around 15% for formyl and 10% for formate and methoxy species.

### Results and discussions

#### Palladium catalysts

$\text{CO-H}_2$  reactions. We studied the concentration of surface species as a function time. The catalysts, which were the same as those used by Ponc (26) in his experiments, showed a correlation between activity and concentration of  $\text{Pd}^{n+}$  species. From batch experiments we obtained the following results :

- formyl moieties formed instantly and their concentration diminished rapidly with time.
- conversely the concentration of the methoxy species increased only slowly.
- there was a good correlation between methanol activity and the concentration of formyl and methoxy species for catalysts with different amounts of "MgO" or palladium (38).
- the concentration of formate was always very low on these catalysts and no correlation was found between their surface concentration and the methanol activity.

The rate of increase in the concentration of the surface species versus the reaction temperature was studied:

- formyl species were present at room temperature whereas methoxy entities appeared only at temperatures higher than 50°C.
- as the temperature increased the formyl concentration diminished slowly to reach a quasi-stationary state at the reaction temperature. Additionally, there was a regular increase of the methoxy up to 195-200°C. At that temperature, methanol began to be detected in the gas phase. At 215°C the methoxy concentration decreased sharply.

These results suggest clearly that, on palladium catalysts, formyl and methoxy species are reaction intermediates in the methanol synthesis from  $\text{CO-H}_2$ . No significant changes were observed in the concentration of formate species, thus they are believed to play no role in the methanol synthesis on these catalysts.

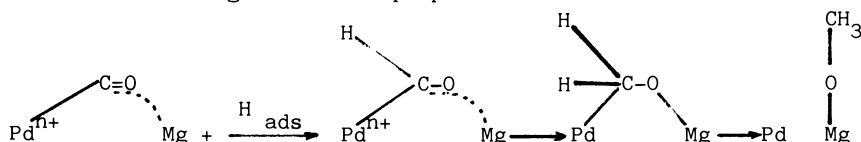
The formation of formyl species can be favored by different factors :

- a positive charge on the metal can attract the 5  $\sigma$  electrons of the carbon monoxide more efficiently. This creates a positive charge on the carbon atom which favors the formation of the formyl moiety with a stabilizing effect. The same conclusions were drawn by Anikin et al. (27) from ab-initio calculations on palladium systems.

Furthermore, Ponec's results (26) strongly support this interpretation.

- Shriver et al. (39) have shown that the presence of a Lewis acid strongly enhances the rate of methyl migration in metal carbonyls. Recently, theoretical calculations by Blyholder displayed a stabilization of formyl species by interaction of  $\text{Li}^+$  (40) with the 4 electrons of CO (mainly on the oxygen). This interaction also results in an increase in the positive charge on the carbon atom. In the chemical trapping experiments, with respect to the evolution of the formyl and methoxy species, we observed a delay between the formation of formyls and the appearance of methoxy moieties. This effect brought us to consider another intermediate between them.

The following scheme was proposed :



Most of the species included in this scheme have previously been characterized by chemical trapping and by I.R. spectroscopy (41) except for the adsorbed formaldehyde.

Indeed, on  $\text{Pd}/\text{SiO}_2$  adsorbed formaldehyde was characterized with dimethyl- or diethylsulfate in the form of formaldehyde dimethyl or diethyl acetal, respectively. The highest concentration of formaldehyde ( $10^{-7}$  mol. (g of cat) $^{-1}$ ) was observed when only CO was added to the prerduced Pd catalyst (42). With an excess of hydrogen as well as on more active magnesium containing catalyst, only trace amounts of adsorbed formaldehyde were detected. Its low concentration on these catalytic surfaces may result from rapid conversion of adsorbed formaldehyde into methoxy moieties (Table I).

In the methanol synthesis, a fast hydrogenation of the adsorbed formaldehyde would overcome arguments invoking any thermodynamic limitation to its formation. Formaldehyde adsorbed through both the oxygen and the carbon ends has been characterized in homogeneous catalysis (43), on oxide surfaces (44) and more recently on ruthenium metal (45).

Table I. Chemical Trapping Experiments

Catalysts	Reagent	Temperature (°C)	Trapping reagent	Products <sup>a</sup>
2%Pd/SiO <sub>2</sub>	CO	140	MeOH	CH <sub>2</sub> (OCH <sub>3</sub> ) <sub>2</sub>
	CO	110	MeOH	CH <sub>2</sub> (OCH <sub>3</sub> ) <sub>2</sub>
	CO + 2H <sub>2</sub>	110	MeOH	traces of
				CH <sub>2</sub> (OCH <sub>3</sub> ) <sub>2</sub>
	CO	110	EtOH	CH <sub>2</sub> (OC <sub>2</sub> H <sub>5</sub> ) <sub>2</sub>
	CO <sub>2</sub>	130	MeOH	CH <sub>2</sub> (OCH <sub>3</sub> ) <sub>2</sub>
	CO <sub>2</sub>	130	DMS	CH <sub>2</sub> (OCH <sub>3</sub> ) <sub>2</sub>
	CO <sub>2</sub> + H <sub>2</sub>	130	MeOH	CH <sub>2</sub> (OCH <sub>3</sub> ) <sub>2</sub>
H <sub>2</sub>	110	MeOH	-	

<sup>a</sup>Detected amounts were  $1 - 2 \times 10^{-7}$  mol (g catalyst) $^{-1}$

CO<sub>2</sub>-H<sub>2</sub> reaction. The results were somewhat different than those obtained with CO-H<sub>2</sub> :

- the reaction started at a lower temperature (185°C instead of 200°C)
- the selectivity was not the same : 50% CH<sub>4</sub>, 50% CH<sub>3</sub>OH compared to a minimum of 90% CH<sub>3</sub>OH with CO-H<sub>2</sub>.
- although the reaction starts at a lower temperature, the activity was much lower than with CO-H<sub>2</sub> at 215°C.
- the detected species on Pd-MgO/SiO<sub>2</sub> were the same : formyl, methoxy and adsorbed formaldehyde.
- formates, which could be expected in a higher concentration by activation of CO<sub>2</sub> on hydride sites, were detected only after ten hours and their concentration remained low.
- as with CO-H<sub>2</sub> an excellent correlation was found between the total activity (CH<sub>4</sub> + CH<sub>3</sub>OH) and the concentration of formyl and methoxy (fig. 1). Nevertheless, with CO, the maximum activity and surface species concentration was observed for the catalyst containing 0.5% of MgO instead of 1% of MgO. This could point to different catalytically active sites.

The change in selectivity when using CO<sub>2</sub> instead of CO is not well understood. Either the active sites differ, as mentioned above, or the chemisorption of CO<sub>2</sub> is weaker, thus promoting hydrogen chemisorption and the hydrogenative power of the catalyst. The correlation between formyl species and methane suggests that the former are intermediates in the methanation of CO<sub>2</sub>.

With CO<sub>2</sub>-H<sub>2</sub>, the formyl species developed slower than with CO-H<sub>2</sub>, and the maximum concentration was obtained after 5 hrs (compared to 15 minutes with CO-H<sub>2</sub>). The concentration decreased afterwards (fig. 2). Methoxy species followed the same behavior, but formates appeared only after 5 hrs.

The same behavior was observed in temperature experiments. Formyls, which were present at room temperature, increased until the reaction temperature was reached (190°C). Methoxy moieties were not detectable at temperatures lower than 100°C (50°C with CO-H<sub>2</sub>). It appeared as though the formation of C<sub>1</sub> oxygenates was inhibited with CO<sub>2</sub>-H<sub>2</sub>. The formation of formyls was slower and that of methoxy entities in reactions started at a higher temperature.

Different hypotheses can be formulated for the reaction mechanisms :

- the reverse water-gas shift reaction produces some CO and subsequently the reaction proceeds as with CO-H<sub>2</sub>. Assuming this mechanism, how could one explain the lower reaction temperature, the difference in selectivity and the different evolution of the surface moieties ? (fig.1 and 2).
- the reaction follows a pathway through formates. Since formates appeared after the formation of formyls and showed the same behavior as the methoxy species, the formation of formates through a Tischenko type reaction seems more probable.

The formation of formyl entities from CO<sub>2</sub> can be explained by two different mechanisms :

- from an equilibrium with a formate. This formate could be of a special type like the one proposed by Hattori (46)

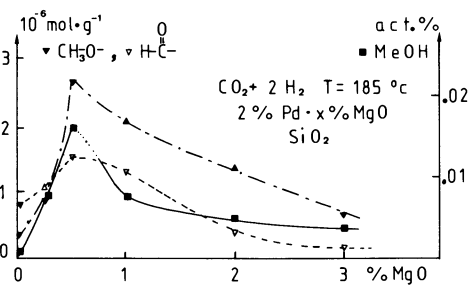


Figure 1. Correlation of catalytic activity with concentration of formyl and methoxy species as a function of % of MgO.

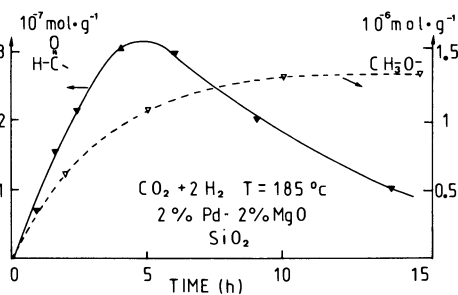
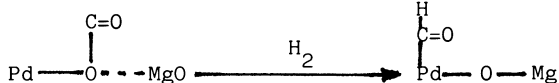


Figure 2. Evolution with time of methoxy and formyl species over  $2\% \text{ Pd} \cdot 2\% \text{ MgO} \cdot \text{SiO}_2$  catalyst.



- from a direct reaction with  $\text{CO}_2^-$  moiety



The intermediacy of a  $\text{CO}_2^-$  species has been proposed on a Cu catalyst by Chinchén et al. (2). Furthermore, a chemisorbed  $\text{CO}_2$  of special type has been observed by X-Ray and I.R. spectroscopies (47).

Here, the sites where  $\text{CO}_2$  is hydrogenated are not necessarily an oxidized palladium atom.  $\text{Pd}^{n+2}$  could be the site where methoxy is formed whereas methane is produced on  $\text{Pd}^0$ .

**Rhodium catalysts.** The study of the mechanism with rhodium catalysts is somewhat more complicated since the carbon-carbon bond formation is added. We will discuss the two points developed for palladium, the roles of the support and the formyl species.

Two types of catalysts,  $\text{Rh}/\text{SiO}_2$  and  $\text{Rh}-\text{CeO}_2/\text{SiO}_2$ , were used. The reactivity tests (185°C, 1 atm.) showed that the presence of cerium affected the activity and also the selectivity of  $\text{Rh}/\text{SiO}_2$  catalysts. The total conversion (calculated as mole per cent of  $\text{CO}$  converted) after 8 hours on stream was 3.8% on  $\text{Rh}/\text{SiO}_2$  and 1.9% on the cerium containing catalyst. What is most striking is that the selectivity to oxygenates shifted from 6 to 71% by the addition of cerium. On  $\text{Rh}/\text{SiO}_2$ , acetaldehyde was obtained as the major oxygenated product whereas on  $\text{Rh}-\text{CeO}_2/\text{SiO}_2$  catalysts ethanol was the most abundant product.

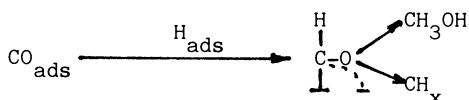
Results of chemical trapping of the formyl species on these catalysts showed a higher concentration of formyl moieties on  $\text{Rh}/\text{SiO}_2$  than on cerium containing catalysts (Table II).

Table II. Concentration of formyl species on different  $\text{Rh}-\text{Ce}/\text{SiO}_2$

Catalyst	Experimental concentration of formyl species $10^7 \text{ mole g}^{-1} \text{ cat.}$	Calculated concentration of formyl species $10^7 \text{ mole g}^{-1} \text{ cat.}$
5%Rh-0%Ce/ $\text{SiO}_2$	78 <sup>a</sup>	78 <sup>b</sup>
5%Rh-0.5%Ce/ $\text{SiO}_2$	41	41 <sup>b</sup>
5%Rh-2%Ce/ $\text{SiO}_2$	32	32
5%Rh-5%Ce/ $\text{SiO}_2$	47	50

a the standard deviation is 15% ; b used to evaluate the rate constants.

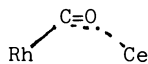
As in the case of palladium catalysts, formyl species can be assumed to be transformed either into hydrocarbons (on Rh<sup>0</sup>) or into oxygenates (on Rh<sup>n+</sup>). The rates of these transformations can be calculated from the activities of two catalysts having different selectivities and their formyl concentrations. Once the rates are known, an expected concentration can be evaluated from the activity of a given catalyst. The calculated results are in good agreement with the experimentally determined formyl concentration (Table II). This suggests that formyl species are key intermediates both to hydrocarbons and to oxygenates. The first part of the mechanism for oxygenates formation would be the same as in methanol synthesis.



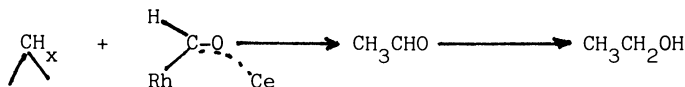
To better understand the role of the cerium in shifting the selectivity to ethanol we studied the Rh-CeO<sub>2</sub>/SiO<sub>2</sub> catalysts by means of F.T.-I.R. spectroscopy and probe molecules.

The addition of cerium has an influence on the CO chemisorption as observed by F.T.-I.R. spectroscopy. CO is adsorbed in linear (2070 cm<sup>-1</sup>) and bridged configurations (1910 cm<sup>-1</sup>) on Rh/SiO<sub>2</sub> catalysts (48). When cerium was present we observed new absorption bands (2100 cm<sup>-1</sup> and 2030 cm<sup>-1</sup>). According to literature data (33), these new adsorption bands can be attributed to twin CO on oxidized Rh (Rh<sup>+</sup>). Another band was observed at 1725 cm<sup>-1</sup>. A first explanation for this new band might be from an electronic transfer from the support to the metal, thus reducing the adsorption frequency of the carbon monoxide (enhanced backdonation). This was already observed in the case of potassium addition to metals (49-53). Furthermore, on Pd/CeO<sub>2</sub> catalysts, Le Normand by XPS (54) reported a partial reduction of the support and showed an electronic transfer from the support to the metal. This new band can also originate from an interaction of the oxygen of the adsorbed carbon monoxide with a Lewis acid site near the rhodium atom. Horwitz and Shriver recently published a review on complexes containing such carbon monoxide ligands (55).

On Rh-CeO<sub>2</sub>/SiO<sub>2</sub> catalysts, this interaction can be depicted as



Ichikawa (56) also observed the lowering of the CO adsorption frequency on Rh-Mn/SiO<sub>2</sub> catalysts and ascribed it to this type of interaction. Recently, Blyholder et al. (40), by theoretical calculations, showed that such interaction of the oxygen atom with Lewis acid centers would have a stabilizing effect on the formyl species. This stabilization could cause the high selectivity to oxygenates by a reaction pathway like the following (57).

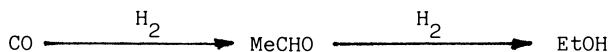


A comparable mechanism was also proposed by Keim (58) from homogeneous catalysis results.

The possibility of ethanol formation by such a reaction pathway was tested by different probe molecule experiments. As can be seen in figure 3 the introduction of acetaldehyde in the CO+H<sub>2</sub> flow on a Rh/CeO<sub>2</sub> catalyst enhanced the ethanol formation. The same experiment with Rh/SiO<sub>2</sub> left all the other products including ethanol unchanged. These results are in agreement with those observed recently by Bell et al. on Rh/La<sub>2</sub>O<sub>3</sub> (59).

Acetaldehyde is chemisorbed strongly on cerium oxide containing catalysts. This could result from the formation of acetate species on the support. Bidentate acetates were observed from the adsorption of acetaldehyde on cerium oxide by F.T.I.R. spectroscopy (1579 and 1466 cm<sup>-1</sup>) and also by chemical trapping (60).

The reduction of acetaldehyde to ethanol could be explained by its chemisorption near rhodium particles and the action of spill over hydrogen. On Rh/La<sub>2</sub>O<sub>3</sub>, Bell has observed that at low residence times acetaldehyde is the primary product whereas at longer residence times the formation of ethanol becomes the dominant process. They concluded that this pattern is characteristic of the sequential reaction process :



Analogous results have been obtained with our Rh-CeO<sub>2</sub>/SiO<sub>2</sub> catalysts (60), suggesting that acetaldehyde is a possible intermediate in ethanol synthesis on rhodium catalysts.

The addition of ethylene to a CO-H<sub>2</sub> flow on a Rh-CeO<sub>2</sub> catalyst (fig. 4), which should enhance the surface concentration of C<sub>2</sub>H<sub>x</sub> groups increased the formation of propanol and propionaldehyde and decreased the ethanol and acetaldehyde production.

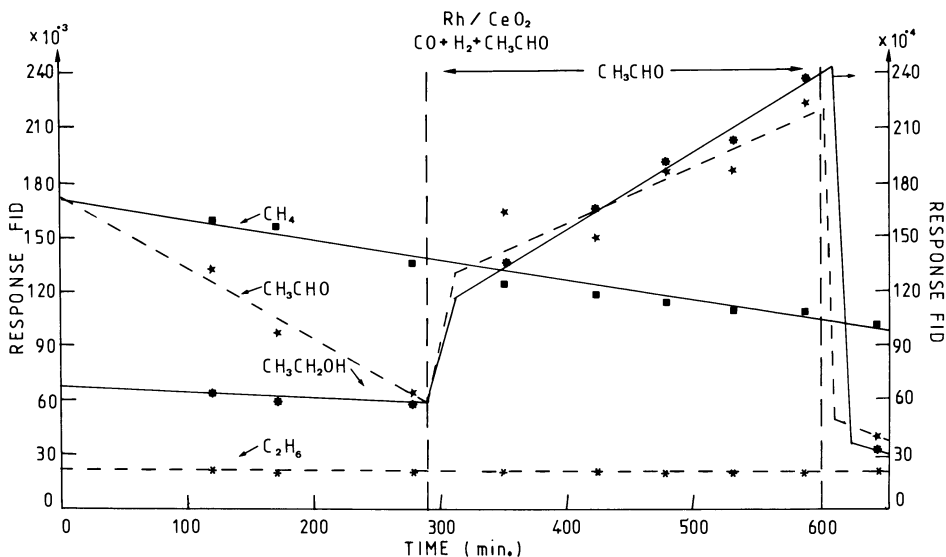


Figure 3. Effect of acetaldehyde as a probe molecule.



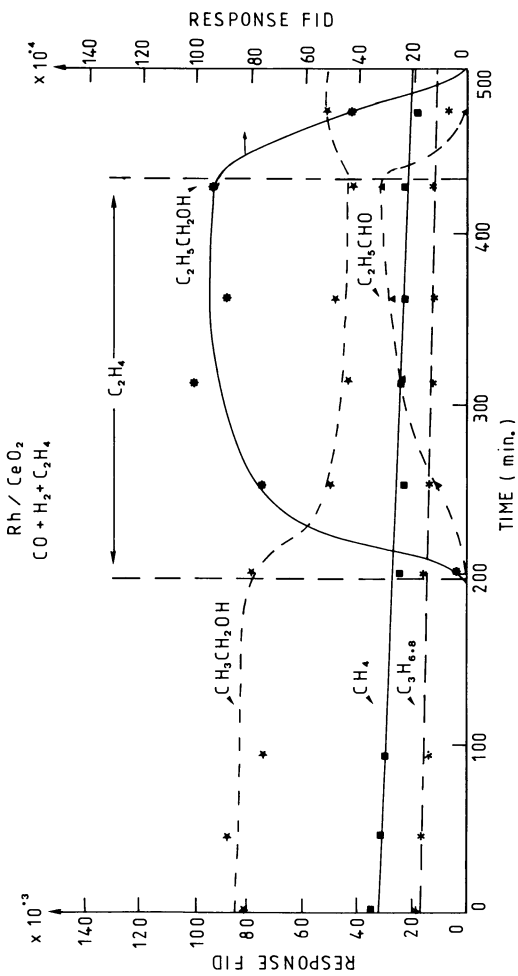


Figure 4. Effect of ethylene as a probe molecule.

Conclusions

Chemical trapping was shown to be a very useful tool in the study of reaction mechanisms. The results thus obtained combined with those by F.T.I.R. spectroscopy have pointed out :

- the importance of the formyl species as key intermediates on both metals
- the presence of adsorbed formaldehyde on methanolation catalysts
- the possible role of acetaldehyde in ethanol synthesis on rhodium catalysts
- the presence of a new band in the F.T.I.R. spectra of adsorbed carbon monoxide ( $1725\text{ cm}^{-1}$ ) which we attributed to the interaction of the oxygen with a Lewis acid site. This CO species could be the intermediate in the alcohols formation.

Acknowledgments

We are deeply indebted to Ms S. Libs and Miss E. Schleiffer for their numerous chromatographic analysis.

Literature Cited

1. Klier, K., In "Catalysis of Organic Reactions"; Moser, W.R., Ed.; CHEMICAL INDUSTRIES, 1981; Vol. V, p. 195.
2. Chinchon, G.C.; Denny, P.J.; Parker, D.G.; Short, G.D.; Spencer, M.S.; Waugh, K.C.; Whan D.A. In "The Activity of Cu/ZnO/Al<sub>2</sub>O<sub>3</sub> Methanol Synthesis Catalysts"; ACS SYMPOSIUM ON METHANOL SYNTHESIS CATALYSTS, Division of Fuel Chemistry; American Chemical Society : Philadelphia, 1984.
3. Ichikawa, M.; Bull. Chem. Soc. Jap., 1978, 51, 2268.
4. Ichikawa, M.; Bull. Chem. Soc. Jap., 1978, 51, 2273.
5. Bhasin M.M.; Bartley, W.J.; Ellgen P.C.; Wilson T.P.; J. Catal. 1978, 54, 120.
6. Courty, P.; Durand, D.; Freund, E.; Sugier, A. J. Mol. Catal. 1982, 17, 241.
7. Poutsma, M.L.; Eleck, L.F.; Ibarbia, P.A.; Rabo, J.A. J. Catal. 1978, 52, 157.
8. Vannice, M.A.; Catal. Rev. Sci. Eng., 1976, 4, 271.
9. Vannice, M.A.; Garten, R.L.; Ind. Eng. Chem. Prod. Res. Dev. 1979, 18, 186.
10. Ichikawa, M., Chemtech. 1982, 674.
11. Bell, A.T.; Ryndin, Y.S.; Hicks, H.F.; Yermakov, Y.I. J. Catal. 1981, 70, 287.
12. Poels, E.K.; Van Broekhoven, E.H.; Van Barneveld, W.A.A.; Ponc, V. React. Kinet. Catal. Lett. 1981, 18, 223.
13. Vannice, M.A.; Mitchell, M.D. Ind. Eng. Chem. Fundam. 1984, 23, 88.
14. Ramarosan, E.; Kieffer, R.; Kiennemann, A. J. Chim. Phys. 1982, 79, 759.
15. Kikuzono, Y.; Kagami, S.; Naito, S.; Onishi, T.; Tamaru, K. Farad. Discuss. 1982, 72, 135.
16. Doering, D.L.; Poppa, H.; Dickinson, J.T.; J. Catal., 1982, 73, 104.

17. Ichikawa, M.; Poppa, H.; Boudart, M. A.C.S. SYMPOSIUM SERIES, Mater. Relat. Struct. React. 1984, 248, 439.
18. Ponec, V. Personal communication.
19. Fajula, F.; Anthony, R.G.; Lunsford, J.H. J. Catal., 1982, 73, 237.
20. Sudhakar, C.; Vannice, M.A. J. Catal., 1985, 95, 227.
21. Hindermann, J.P.; Deluzarche, A.; Kieffer, R.; Kiennemann, A. Can. J. Chem. Eng., 1983, 61, 21.
22. Ichikawa, M.; Fukushima, T. J. Phys. Chem., 1985, 89, 1564.
23. Sachtler, W.M.H.; Shriver, D.F.; Hollenberg, W.B.; Lang, A.F. J. Catal., 1985, 92, 428.
24. Ichikawa, M.; Lang, A.J.; Shriver, D.F.; Sachtler, W.M.H. J. Am. Chem. Soc., 1985, 107, 7216.
25. Orita, H.; Naito, S.; Tamaru, K. J. Chem. Soc. Chem. Comm. 1984, 994.
26. Driessen, J.M.; Poels, E.K.; Hindermann, J.P.; Ponec, V. J. Catal., 1983, 82, 26.
27. Anikin, N.A.; Bagatur'Yants, A.A.; Zchidomirov, G.M.; Kazanskii, V.B. Russian J. Phys. Chem. 1983, 573, 393.
28. Herman, R.G.; Klier, K.; Simmons, G.W.; Finn, B.P.; Bulko, J.P. J. Catal., 1979, 56, 407.
29. Apai, G.B.; Monnier, J.R.; Hanrahan, M.J. J. Chem. Soc. Chem. Comm., 1984, 212
30. Watson, P.R.; Somorjai, G.A. J. Catal., 1982, 74, 282
31. Van Zon, J.B.A.D.; Koningsberger, D.C.; Sayers, D.E.; Van't Blik, H.F.J.; Prins, R.; J. Chem. Phys., 1984, 80, 3914
32. Koningsberger, D.C.; Van Zon, J.B.A.D.; Van't Blik, H.F.J.; Visser, G.J.; Prins, R.; Mansour, A.N.; Sayers, D.E.; Short, D.R.; Katzer, J.R.; J. Phys. Chem. 1985, 89, 4075
33. Solymosi, F.; Pasztor, M. J. Phys. Chem. 1985, 89, 4789
34. Emrich, R.J.; Mansour, A.N.; Sayers, D.E.; Mc Millan, S.T.; Katzer, J.R. J. Phys. Chem., 1985, 89, 4261
35. Deluzarche, A.; Hindermann, J.P.; Kieffer, R.; Cressely, J.; Stupfler, R.; Kiennemann, A. Spectra 2000, 1982, 75(100) 27
36. Hindermann, J.P.; Kiennemann, A.; Kieffer, R.; Deluzarche, A. J. Mol. Catal. 1985, 31, 225
37. Soukup, J.; Scarpellius, R.S.; Danielczik, E. Anal. Chem. 1964 36, 2255
38. Hindermann, J.P.; Kiennemann, A.; Chakor-Alami, A.; Kieffer, R. Proc. 8th Int. Cong. Catal., 1984, Vol. II, p. 163
39. Richmond, T.G.; Basolo, F.; Shriver, D.F. Inorg. Chem. 1983, 21, 1272
40. Blyholder, G.; Zhao, K.; Lawless, M. Organometallics 1985, 4, 2170
41. Saussey, J.; Lavalley, J.C.; Rais, T.; Chakor-Alami, A.; Hindermann, J.P.; Kiennemann, A. J. Mol. Catalysis 1984, 26, 159
42. Hindermann, J.P.; Schleiffer, E.; Idriss, H.; Kiennemann, A. J. Mol. Catalysis 1985, 33, 133
43. Wolczanski, P.T.; Threlkel, R.S.; Berkaw, J.F. J. Am. Chem. Soc., 1979, 101, 208
44. Lamotte, J.; Lavalley, J.C.; Druet, E.; Freund, E. J. Chem. Soc. Faraday Trans 1, 1983, 79, 2219
45. Anton, A.B.; Parmeter, J.E.; Weinberg, W.H. J. Am. Chem. Soc. 1985, 107, 5558

46. Hattori, H.; Wang, G.W. Proc. 8th Int. Cong. Catal. 1984, Vol. III, p. 219
47. Aresta, M.; Nobile, C.F.; Albano, V.G.; Forni, M.; Manassero, M. J. Chem. Soc. Chem. Comm. 1975, 636
48. Rice, C.A.; Worley, S.D. J. Chem. Phys., 1981, 74, 6487
49. Weimer, J.J.; Umbach, E. Physical Review B. 1984 30 (8), 4863
50. Somerton, C.F.; Mc Conveille, D.P.; Woodruff, D.P.; Guder, D.E.; Richardson, N.V. Surf. Sci. 1984, 138, 31
51. Hoffmann, M.; Hrbek, J.; De Paola, R.A. Chem. Phys. Lett. 1984, 106, 83
52. Crowell, J.E.; Garfunkel, E.L.; Somorjai, G.A. Surf. Sci. 1982, 121, 303
53. Kiskinova, M.P.; Pirug, G.; Bonzel, H.P. Surf. Sci. 1983, 133, 321
54. Le Normand, J.F., Ph.D. Thesis, University Louis Pasteur, Strasbourg, France
55. Horwitz, C.P.; Shriver, D.F. Adv. Organomet. Chem. 1984, 23, 219
56. Ichikawa, M.; Fukushima, T. J. Phys. Chem. 1985, 89, 1564
57. Breault, R.; Hindermann, J.P.; Kiennemann, A.; Laurin, M. Stud. Surf. Sci. Catal., 1984, 19, 489
58. Hackenbuch, J.; Keim, W.; Röper, M.; Schutz, H. J. Mol. Catal. 1984, 26, 129
59. Underwood, R.P.; Bell, A.T. Appl. Catal. 1986, 21, 157
60. Breault R., unpublished results.

RECEIVED August 14, 1986

## Author Index

- Avidan, A. A., 34  
 Braca, Giuseppe, 220  
 Breault, R., 237  
 Busby, David C., 125  
 Chang, C. D., 34  
 Courty, Ph., 42  
 Drent, E., 154  
 Dry, Mark E., 18  
 Ebner, J. R., 189  
 Forestiere, A., 42  
 Fujimoto, Kaoru, 176, 208  
 Galletti, Anna Maria  
     Raspolti, 220  
 Gilhooley, K., 108  
 Gleaves, J. T., 189  
 Goliaszewski, Alan, 136  
 Gould, R. M., 34  
 Hindermann, J. P., 237  
 Idriss, H., 237  
 Kane, S. E., 34  
 Kawata, N., 42  
 Keim, W., 1  
 Kesling, Jr., H. S., 77  
 Kiennemann, A., 237  
 Knifton, John F., 98  
 Kuechler, T. C., 189  
 Letts, John B., 125  
 Li, T. P., 189  
 Ohno, T., 42  
 Omata, Kohji, 208  
 Raimbault, C., 42  
 Rigby, S., 108  
 Rizkalla, Nabil, 61, 136  
 Sbrana, Glauco, 220  
 Shikada, Tsutomu, 176, 208  
 Socha, R. F., 34  
 Tominaga, Hiro-o, 176, 208  
 Wegman, Richard W., 125  
 Whyman, R., 108  
 Winstanley, D., 108  
 Yoshimoto, M., 42

## Subject Index

- A
- Acetaldehyde  
   bimolecular reaction scheme  
     formation, 143  
   chemisorbed on cerium oxide  
     containing catalysts, 245  
   effect as a probe molecule, 245  
   formation  
     ethers as solvents, 130  
     mechanism, 128-130, 141-142  
     methods, 148  
     via acetic anhydride  
       reduction, 150-151  
     via dimethyl carbonate, 131  
     via dimethyl ketals, 131  
     via methyl acetate reductive  
       carbonylation, 152  
   homologation of methanol, 9-11  
   mechanism, 126  
   methyl acetate reductive  
     carbonylation, 149-150  
   reduction to aldehyde, 245  
   reductive carbonylation of methyl  
     esters, 132  
   rhodium-catalyzed generation, 147f
- Acetaldehyde--Continued  
   role in ethylidene diacetate  
     formation, 139-141  
   selectivity with catalyst use, 127  
   synthesis by reductive  
     carbonylation, 125-134  
   temperature effect on methanol  
     carbonylation route, 127
- Acetic acid  
   carbonylation of methanol, 149, 209  
   carbonylation of methyl acetate, 182  
   feedstock, 155  
   formation via methyl acetate, 71, 144  
   generation as function of  
     catalyst composition, 99  
   iodide role in selective  
     synthesis, 104-106  
   Monsanto process, 143  
   production  
     via carbonylation, 62  
     via nickel-catalyzed methanol  
       carbonylation, 61-75  
     via synthesis gas, 5, 98-106  
   reduction to ethanol, 5  
   role of cobalt carbonyl in  
     carbonylation, 104  
   solvent for methyl acetate  
     homologation, 170

## Author Index

- Avidan, A. A., 34  
 Braca, Giuseppe, 220  
 Breault, R., 237  
 Busby, David C., 125  
 Chang, C. D., 34  
 Courty, Ph., 42  
 Drent, E., 154  
 Dry, Mark E., 18  
 Ebner, J. R., 189  
 Forestiere, A., 42  
 Fujimoto, Kaoru, 176, 208  
 Galletti, Anna Maria  
     Raspolti, 220  
 Gilhooley, K., 108  
 Gleaves, J. T., 189  
 Goliaszewski, Alan, 136  
 Gould, R. M., 34  
 Hindermann, J. P., 237  
 Idriss, H., 237  
 Kane, S. E., 34  
 Kawata, N., 42  
 Keim, W., 1  
 Kesling, Jr., H. S., 77  
 Kiennemann, A., 237  
 Knifton, John F., 98  
 Kuechler, T. C., 189  
 Letts, John B., 125  
 Li, T. P., 189  
 Ohno, T., 42  
 Omata, Kohji, 208  
 Raimbault, C., 42  
 Rigby, S., 108  
 Rizkalla, Nabil, 61, 136  
 Sbrana, Glauco, 220  
 Shikada, Tsutomu, 176, 208  
 Socha, R. F., 34  
 Tominaga, Hiro-o, 176, 208  
 Wegman, Richard W., 125  
 Whyman, R., 108  
 Winstanley, D., 108  
 Yoshimoto, M., 42

## Subject Index

- A
- Acetaldehyde  
   bimolecular reaction scheme  
     formation, 143  
   chemisorbed on cerium oxide  
     containing catalysts, 245  
   effect as a probe molecule, 245  
   formation  
     ethers as solvents, 130  
     mechanism, 128-130, 141-142  
     methods, 148  
     via acetic anhydride  
       reduction, 150-151  
     via dimethyl carbonate, 131  
     via dimethyl ketals, 131  
     via methyl acetate reductive  
       carbonylation, 152  
   homologation of methanol, 9-11  
   mechanism, 126  
   methyl acetate reductive  
     carbonylation, 149-150  
   reduction to aldehyde, 245  
   reductive carbonylation of methyl  
     esters, 132  
   rhodium-catalyzed generation, 147f
- Acetaldehyde--Continued  
   role in ethylidene diacetate  
     formation, 139-141  
   selectivity with catalyst use, 127  
   synthesis by reductive  
     carbonylation, 125-134  
   temperature effect on methanol  
     carbonylation route, 127
- Acetic acid  
   carbonylation of methanol, 149, 209  
   carbonylation of methyl acetate, 182  
   feedstock, 155  
   formation via methyl acetate, 71, 144  
   generation as function of  
     catalyst composition, 99  
   iodide role in selective  
     synthesis, 104-106  
   Monsanto process, 143  
   production  
     via carbonylation, 62  
     via nickel-catalyzed methanol  
       carbonylation, 61-75  
     via synthesis gas, 5, 98-106  
   reduction to ethanol, 5  
   role of cobalt carbonyl in  
     carbonylation, 104  
   solvent for methyl acetate  
     homologation, 170

Acetic acid--Continued  
synthesis

- cobalt-carbonyl catalyzed
    - carbonylation, 105f
    - competing secondary reactions, 106
    - iodide effect on yield, 103f
    - routes, 7
    - ruthenium effect on yield, 101f
    - typical reaction profile, 101f
    - via methanol, 176
    - via methyl formate, 11
  - thermal elimination from ethylidene diacetate, 151
  - U.S. demand, 98
  - use in vinyl acetate production, 138
- Acetic anhydride**
- carbonylation of methyl acetate, 182
  - cobalt-catalyzed reduction, 147t
  - formation mechanism from methyl acetate carbonylation, 141-142
  - methyl acetate homologation byproducts, 159
  - reaction intermediates in methyl acetate homologation, 159
  - rhodium-catalyzed carbonylation of methyl acetate, 148
  - role in formation of ethylidene diacetate, 139-141
  - synthesis, 11, 176
  - vapor-phase hydrogenation, 152
- Acetonitrile, synthesis, 6**
- Acetyl iodide**
- hydrolysis, 74
  - rhodium-catalyzed generation, 147f
- Acids**
- Fischer-Tropsch reactions, 19
  - promoter ability, 168
- Activity**
- carbonylation, relationship to affinity of metal for halogen, 211
  - function of halide affinity, 212f
  - function of time on stream, 213f
  - group VIII metals supported on activated carbon, 212f
- Activity measurements, use in ammoxidation of methanol, 192**
- Activity of carbonylation, definition, 210**
- Adipic acid**
- comparative raw materials, 80t
  - hydrolysis to dimethyl adipate, 86
  - precursor in ARCO process, 82
  - preparation, 78
  - raw materials for the ARCO process, 80
  - uses, 78
  - world-scale plant, 87
- Affinity, metal for halogen, 211**

**Alcohols**

- Fischer-Tropsch reactions, 19
  - high-yield requirements in Fischer-Tropsch process, 30
  - homologation, 225-226
  - motor fuel properties of bench-fractionated, 53
  - production
    - Fischer-Tropsch process, 30-32
    - optimization in reaction section, 48
    - process development, 48-53
    - via synthesis gas, 42-58
    - synthesis from carbon oxides and hydrogen, 237-246
    - synthesis on copper-cobalt based catalysts, 43-48
- Aldol condensation, minimization in adipic acid synthesis, 85**
- Alkenes**
- long-chain, 29-30
  - production maximization, 29
  - short-chain, 29
  - temperature effect on production, 29
- Alkyl halides, formation of five-coordinate nickel intermediate via oxidative addition, 73-74**
- Amines, role in methyl acetate carbonylation catalysis, 144**
- Ammonia, Fischer-Tropsch process, 32-33**
- Ammoxidation, methanol to hydrogen cyanide, 189-204**
- Arge reactors**
- Fischer-Tropsch synthesis, 21
  - selectivities obtained, 28
- Argon, Fischer-Tropsch process, 33**
- Aromatics, Fischer-Tropsch process, 32**
- Azeotropic distillation process, alcohol dehydration, 53**
- B
- Butadiene**
- conversion, optimum catalyst system, 90
  - oxycarbonylation, 79, 81t, 89t
  - use in adipic acid production, 78-79
- Butene, use in adipic acid preparation, 79**
- Butyl formate butanol, homologation, 231f**
- Byproducts**
- carbonylation of dimethyl ether, 177
  - vinyl acetate production, 138

## C

- $C_1$ - $C_4$  hydrocarbon separation,  
Fischer-Tropsch process, 28
- $C_2$  chemicals, alternative paths, 235
- Carbon dioxide  
byproducts of alcohol  
synthesis, 46-48  
Fischer-Tropsch process, 33  
formation in the Fischer-Tropsch  
process, 19
- Carbon monoxide  
adsorption on nickel, 182  
decomposition of methyl formate, 11  
effect on nickel-catalyzed methanol  
carbonylation, 69  
Fischer-Tropsch process, 4  
hydrogenation, 5,24t,115t  
inhibition of acetic anhydride  
reduction, 148  
oxygen interaction on rhodium  
catalysts, 244  
partial pressure, inhibition of  
methanol carbonylation  
catalyst, 73  
reduction to ethylene glycol, 5  
role in alkene production via  
Fischer-Tropsch process, 29  
selectivity during  
hydrogenation, 108
- Carbon monoxide oxidation, role in  
adipic acid synthesis, 83
- Carbonylation  
dimethyl ether, 177-179  
ethers, 226-229  
general reaction to adipic and  
sebacic acid, 83  
higher aliphatic alcohols, 225  
methanol, 7,128  
operational factors controlling rate  
and selectivity, 214  
see also Reductive carbonylation
- Carboxylic acids  
homologation of esters, 167-173  
production  
Fischer-Tropsch process, 30-32  
via synthesis gas, 100t
- Catalysts
- cobalt iodide and ruthenium roles  
in acetic acid  
production, 102-106
  - copper-cobalt based, 43-48
  - effect on methanol  
carbonylation, 66-69
  - Fischer-Tropsch process, 24
  - fluid-bed study of olefin  
production, 35
  - propionic acid formation, 168-170
  - reductive carbonylation of  
methanol, 126
  - rhodium systems, 154

## Catalysts--Continued

- sebacic acid synthesis, 90
  - transition metals, 176-186
  - see also Group VIII metal catalysts,  
Molybdenum-activated carbon  
catalysts, Nickel-activated  
carbon catalysts, Rhodium-  
ruthenium catalysts, Ruthenium  
trichloride
- Catalytic activity, correlation with  
concentration of formyl  
species, 242f
- Cerium, role in selectivity to  
ethanol, 244
- Cesium  
addition to rhodium-ruthenium  
catalysts, 110  
effect on rhodium-ruthenium catalyst  
system, 111t  
promoter similarity to  
triethylamine, 112
- Chain growth, Fischer-Tropsch  
synthesis, 4,26
- Chemical trapping, identification of  
reactive surface species, 238-239
- Chromium, promotion in methyl acetate  
carbonylation, 144
- Coal, chemical production interest, 1
- Coal gasifiers, comparison with Lurgi  
reactors, 21
- Cobalt  
catalyst for reductive carbonylation  
of methanol, 126  
role in acetic acid  
catalysts, 102-106  
role in ruthenium carbonyl iodide  
catalyst, 223
- Cobalt carbonyl, catalysis of methanol  
reductive carbonylation, 149
- Cobalt-ruthenium catalysts,  
predominance of the ruthenium  
iodocarbonyl, 222-223
- Copper-cobalt based catalysts,  
performances, 48,237
- Cyclohexanone, dehydration agents, 85

## D

- Dehydration agent, role in adipic acid  
production, 80
- Diethyl carbonate, formation, 234
- Dimethoxy ketals, reductive  
carbonylation, 131
- Dimethyl adipate, hydrolysis to adipic  
acid, 86
- Dimethyl carbonate  
oxidation carbonylation of  
methanol, 9  
reductive carbonylation, 131



- Dimethyl ether
  - carbonylation on molybdenum-activated carbon catalyst, 186
  - effect of partial pressure on carbonylation, 179
  - effect of reaction temperature on carbonylation, 180f
  - vapor-phase carbonylation with supported transition metal catalysts, 176-186
- Dimethyl oxalate, hydrolysis role in adipic acid synthesis, 83-84
- Dimethyl sebacate, recovery in sebacic acid synthesis, 93
- Direct conversion, synthesis gas, 2,4

## E

- Economics, alcohol production from natural gas, 57
- Ester homologation, 161-163,174
- Esterification, combination with homologation, 173
- Esters
  - applications of homologation reactions, 173-174
  - homologation, 155
- Ethanol
  - acetic acid production, 61
  - fermentation routes, 125-126
  - formation via rhodium catalysts, 245
  - synthesis gas production, 5
- Ethene, production from ethanol, 5
- Ethers, carbonylation and homologation, 226-229
- Ethyl acetate
  - ethylidene diacetate as feedstock, 161
  - production from methanol and synthesis gas, 1,154-174
  - triethylamine as a source, 112
- Ethyl orthoformate, homologation, 230-234
- Ethylene
  - effect as a probe molecule, 246f
  - use in vinyl acetate production, 136-138
- Ethylene glycol, rhodium-catalyzed synthesis, 6
- Ethylene glycol esters
  - experimental description in production study, 109-110
  - materials used in production study, 109
  - pressure-dependence studies of catalyst system, 112-115
  - ruthenium-rhodium catalysts use, 108-123

- Ethylene glycol esters--Continued
  - temperature-dependence studies on catalyst system, 115
- Ethylidene diacetate
  - formation mechanism, 139-141
  - formation via methyl acetate, 138
  - low selectivity to ethyl acetate, 161
  - nonmetal catalyst system for formation, 148
  - palladium-catalyzed reductive carbonylation, 141
  - reaction intermediates in methyl acetate homologation, 159
  - sensitivity to hydrogen, 143
  - use in vinyl acetate production, 138

## F

- Fischer-Tropsch process
  - chemicals produced, 18-33
  - composition of chemicals in water phase, 31t
  - generalized mechanism, 4,24-25
  - mechanism, 25f
  - overall process scheme, 19
  - primary and secondary reactions, 19
  - product selectivity control, 24-28
  - synthesis gas production, 19-21
  - work-up of oxygenates, 31
- Fischer-Tropsch reactors, 21-28
- Fixed-bed reactors, 22f
- Fixed-fluid bed (FFB) reactor, Fischer-Tropsch synthesis, 21
- Fluid-bed catalyst, advantage, 190
- Fluid-bed reactor, 23f,34-39,193
- Formaldehyde
  - characterization on palladium catalysts, 240
  - derived chemicals, 12t
  - feedstock, 155
  - indirect synthesis gas conversions, 12-13
- Formic esters, homologation, 230
- Formyl species, intermediates to synthesis gas products, 244
- Fourier transform infrared (FTIR) spectroscopy, rhodium-ruthenium catalyst system, 117,121

## G

- Group VIB metals, effect on methanol carbonylation, 65t
- Group VIII metal catalysts, activities, 209-210

## H

- Heat of reaction, MTO process, 39
- Homologation  
 active catalysts for  
 hydrogenation, 220  
 alcohols, 225-226  
 definition, 9  
 esters and carboxylic acids, 167-173  
 ethers, 226-229  
 formic esters, 230  
 methanol, 223-225  
 methyl acetate, 229-230  
 methyl iodide, 170  
 summary, 9
- Hydrocarbonylation, route to adipic acid, 78
- Hydrogen  
 effect on catalysts in vinyl acetate formation, 143  
 nickel-catalyzed effect on nickel-catalyzed methanol carbonylation, 69  
 role in alkene production via Fischer-Tropsch process, 29
- Hydrogen activation, role in reduction of carbon monoxide, 122
- Hydrogen cyanide  
 economic comparison of two processes, 204t  
 primary commercial routes, 189  
 synthesis use, 189
- Hydrogen-carbon monoxide ratio, effect on chemical synthesis, 2-4
- Hydrogenation, acetic anhydride to acetaldehyde, 150-151
- 2-Hydroxypyridine, role in nickel-catalyzed methanol carbonylation, 66
- 8-Hydroxyquinoline, role in nickel-catalyzed methanol carbonylation, 66

## I

- Indirect conversion, synthesis gas, 2,6
- Iodide  
 effect on carbonylation and homologation of ethers, 225-229  
 effect on methanol carbonylation rate, 68f  
 promoter formula, 221  
 role in acetic acid catalysts, 102-106  
 role in selective acetic acid synthesis, 104-106
- Iodide promoters, 161

## Iron

- basicity of surface, 26  
 role in Fischer-Tropsch reaction, 24
- Iron-molybdenum oxide catalyst  
 characterization, 192-193  
 FTIR studies, 198,203f  
 laser Raman spectra, 196f  
 mechanism, 202  
 temperature-programmed desorption studies, 198-202
- Isoparaffin, micro fluid-bed and large pilot plant yield, 40f
- Isothermicity, fluid-bed reactor, 35

## K

- Ketal, regeneration in adipic acid synthesis, 85
- Ketones, production in Fischer-Tropsch process, 30-32

## L

- Leaving group, preference, 90
- Lewis acid, enhanced rate of methyl migration in metal carbonyls, 240
- Lithium salts, role in nickel-catalyzed methanol carbonylation, 63-64
- Lurgi rectisol process, 19

## M

- Manganese-phosphorus oxide catalyst  
 chemistry, 190,193-195  
 laser Raman spectra, 196f  
 maximum attainable hydrogen cyanide yield, 197f  
 XRD studies on catalyst, 195
- Mars Van Krevelen redox mechanism, 190
- Metal-activated carbon catalysts, features for methanol carbonylation, 208-218
- Methane  
 production via Fischer-Tropsch process, 28  
 reforming reaction, 21
- Methanol  
 ammoxidation to hydrogen cyanide, 189-204  
 chemicals synthesized, 8t  
 conversion to hydrocarbons, 34  
 dehydrogenation to methyl formate, 11

Methanol--Continued

- effect of reaction variables in carbonylation, 129t
- effect on carbonylation, 66
- effect on methanol carbonylation rate, 67f
- ethene synthesis, 2
- formation, correlation of methanol activity with palladium ion, 238
- homologation, 9,223-225
- ideal starting material, 155
- importance, 237
- mechanistic proposal for ammoxidation, 203f
- nonnoble metal catalyst for reductive carbonylation, 149
- products, 7
- reductive carbonylation, 125-134,148
- role in vinyl acetate, 136-152
- synthesis gas production, 5
- use of solvents in reductive carbonylation, 133
- yearly production, 6
- Methanol carbonylation
  - advantages of nickel catalysis, 74-75
  - effect of carbon monoxide, 69,70t,215f
  - effect of catalyst concentration, 66-69
  - effect of hydrogen, 69-71
  - effect of methanol, 66
  - effect of supported materials, 210t
  - effect of temperature, 215f
  - effect of water, 71-72
  - nickel-catalyzed, general
    - experimental procedure, 75
  - promoters of nickel-catalyzed, 63-64
  - rate equation for nickel-activated carbon catalysis, 214t
  - reaction intermediate pathways, 72-74
  - Repe system, 62t
  - rhodium-catalyzed, 62
- Methanol homologation, ruthenium catalysts, 224t
- Methanol-methyl formate, carbonylation and homologation, 232f
- Methanol-to-gasoline (MTG) process, conversion to hydrocarbons, 34
- Methanol-to-light olefins (MTO) process, 37-39
- Methanol-to-light olefins (MTO) reactors, temperature profiles, 38
- Methyl 2,4-pentadienoate, synthesis, 88-90
- Methyl acetate
  - acetaldehyde formation role, 132
  - adsorption on nickel, 182
  - carbonylation
    - molybdenum-activated carbon catalyst, 186

Methyl acetate--Continued

- presence of water, 182,187f
- products from methanol, 209
- via methanol, 127-128
- via nickel-activated carbon catalysts, 179
- effect of reaction temperature on carbonylation, 180f
- homologation, 156-163,229-230
- mechanism of formation in methanol carbonylation, 128
- reductive carbonylation, 133t,138-148
- suppression of methanol carbonylation, 130,216
- use in vinyl acetate production, 138
- Methyl acetate carbonylation, chromium promotion, 144
- Methyl esters, reductive carbonylation, 125-134
- Methyl ether, vapor-phase carbonylation with supported transition metal catalysts, 176-186
- Methyl formate, 11-12
- Methyl iodide
  - homologation, 170
  - methanol carbonylation role, 209
  - nickel-activated carbon catalyst, 182
  - promoters, 163
  - reaction order of catalysts, 210t
- Methyl ketals, reductive carbonylation, 125-134
- Methyl-2,4-pentadienoate, dimerization, 90-91, 92t
- Molybdenum-activated carbon catalysts, 177

## N

- Natural gas
  - chemical production interest, 1
  - economics of alcohol production, 57
- Nickel
  - catalysis of methanol carbonylation, 62,70,208-209
  - catalyst activity affected by carbon monoxide, 69,70t
  - chemisorption, 216t
  - effect on methanol carbonylation rate, 68f
  - role in Fischer-Tropsch reactions, 24
  - TPR profiles of adsorbed carbon monoxide, 217f
- Nickel-activated carbon
  - accumulation of iodide ion in the catalyst, 211-214

- Nickel-activated carbon--Continued  
 stability of catalytic activity, 211
- Nickel-activated carbon catalysts  
 carbon monoxide spectra of  
 adsorbed, 185f  
 carbonylation of dimethyl  
 ether, 177-179  
 character of adsorbed carbon  
 monoxide on nickel, 216  
 preparation, 177  
 reactivities of raw materials and  
 products, 182,184t  
 TPR of adsorbed carbon monoxide, 216
- Nitrogen-containing bases, promoters  
 of composite catalyst systems, 112
- Nylon 6,6, production via dimethyl  
 adipate, 86
- O
- Oils, uses, 30
- Olefin  
 Fischer-Tropsch reactions, 19  
 micro fluid-bed and large pilot  
 plant yield, 39f  
 production  
 fluid-bed studies, 34-39  
 methanol conditions, 37  
 yield dependence on  
 propane-propene ratio, 37-39
- Organic ligands, effects on reaction  
 rate, 163
- Oxalate esters, synthesis from alcohol  
 and carbon monoxide, 7-9
- Oxamides, synthesis, 9
- Oxidation carbonylation, route to  
 adipic and sebacic acids, 77-94
- P
- Palladium  
 oxidation by copper, 84  
 role in methyl acetate  
 carbonylation, 139
- Palladium catalysts  
 carbon monoxide and hydrogen  
 reactions, 239  
 characterization of adsorbed  
 formaldehyde, 240  
 comparison to rhodium as  
 catalyst, 143  
 methanol synthesis, 237  
 methyl acetate homologation, 159  
 recovery in ARCO adipic acid  
 process, 86  
 reduction for aldehyde  
 formation, 142
- Palladium catalysts--Continued  
 temperature effect on alcohol  
 synthesis, 239  
 use in ethylidene diacetate  
 formation, 141
- Paraffin, micro fluid-bed and large  
 pilot plant yield, 40f
- Penta-2,4-dienoate, 82,88
- Phenols, Fischer-Tropsch process, 32
- Phosphine  
 effects on reaction rate, 163  
 promotion problems, 167  
 role in nickel-catalyzed methanol  
 carbonylation, 63-64,74
- Phosphine oxides, promoter  
 ability, 165
- Phosphines, role in methyl acetate  
 carbonylation catalysis, 144
- Phosphorus-nickel ratio, effect on  
 methanol carbonylation rate, 67f
- Picoline, 163
- Polymethylene, synthesis, 4
- Pressure, effect on acetaldehyde  
 production, 127
- Promoter synergism, role in  
 nickel-catalyzed methanol  
 carbonylation, 63-64
- Promoters  
 acetaldehyde production, 132  
 nickel-catalyzed methanol  
 carbonylation, 63  
 rhodium-ruthenium catalyst  
 system, 113t  
 role in methyl acetate  
 carbonylation, 139
- Propene  
 common uses, 29  
 production from ethanol, 5
- Propionic acid, production from  
 methanol and synthesis  
 gas, 154-174
- Propylene, produced at MTO  
 conditions, 37
- Pyridines, effects on reaction  
 rate, 163
- R
- Reductive carbonylation  
 methanol, 148-149  
 methyl acetate, 133t,140t
- Rhodium, role in methyl acetate  
 carbonylation, 139
- Rhodium catalysts  
 carbon monoxide and hydrogen  
 reactions, 243-245  
 carbonylation, effect of  
 hydrogen, 69-70  
 comparison to palladium as  
 catalyst, 143

- Rhodium catalysts--Continued  
 concentration of formyl species in synthesis gas reactions, 243t  
 methanol carbonylation, 62  
 methanol selectivity, 238  
 reduction for aldehyde formation, 142  
 systems, 154  
 use, 176
- Rhodium-acyl intermediates, selective hydrogen reductions, 142
- Rhodium-ruthenium catalysts  
 cesium addition, 111t  
 concentration-dependence studies, 115-117  
 FTIR spectrum, 117-121  
 influence of the promoter on the product selectivity, 117  
 methyl acetate homologation, 156-163  
 optimum performance concentrations, 224  
 pressure-dependence studies, 112-115  
 reaction with iodide and carbonyl groups, 223  
 rhodium concentration, 110  
 temperature-dependence studies, 115-117
- Ruthenium, role in acetic acid catalysts, 102-106
- Ruthenium carbonyl iodide catalysts  
 alkyl and acyl intermediates in methanol homologation, 224  
 chemical and spectroscopic properties, 221  
 ethyl orthoformate homologation, 230-234  
 formic esters homologation, 230  
 IR spectra, 221-222  
 methyl acetate homologation, 229-230  
 performances of different promoters, 229t  
 primary alcohols, 226  
 production oxygenates rich in esters, 226  
 reactions on oxygenated substrates, 220-235  
 role in the homologation processes, 223  
 secondary and tertiary alcohols, 226
- Ruthenium catalysts  
 contact charge effect upon acetic acid production, 99  
 higher alcohols carbonylation and homologation, 227t  
 methanol homologation, 224t  
 observed reactions, 225  
 requirements, 221
- Ruthenium-cobalt catalysts, iodide effect on acetic acid production, 102
- Ruthenium-cobalt halide bimetallic combinations, catalysis of acetic acid, 99-106
- Ruthenium-melt catalysis, 98
- Ruthenium trichloride, catalyst in methyl acetate homologation, 156-159
- S
- Sasol, process scheme, 20f
- Schultz-Flory distribution, alcohol synthesis on copper-cobalt based catalysts, 46
- Sebacic acid  
 coproduct of ARCO adipic acid process, 87  
 declining U.S. market, 78  
 electrolytic route, 87  
 oxidative environment role in ARCO process, 84  
 process, catalysts, 90  
 production from dimethyl sebacate, 93  
 uses, 78
- Selectivity  
 change after carbon monoxide and carbon dioxide use as feedstocks, 241  
 effect of temperature, 26t  
 Fischer-Tropsch process, 27f  
 hydrogenation of carbon monoxide, 108  
 methyl acetate carbonylation, 146t  
 role of support, 238
- Slurry-phase reactor, Fischer-Tropsch synthesis, 21
- Sulfur, Fischer-Tropsch process, 32
- Synergism  
 catalyst activity of rhodium-ruthenium systems, 122  
 catalyst metals in ethylene glycol production, 110
- Synthesis gas  
 acetaldehyde production, 132  
 arguments in favor of research, 2  
 commercial and near-commercial processes, 17-95  
 composition determination, 2  
 developmental processes, 97-205  
 direct conversion, 4  
 feedstock for chemicals, 1-14  
 Fischer-Tropsch process, 19-21  
 indirect conversion, 6-9  
 new technical insights, 207-249  
 production of ethyl acetate and propionic acid, 154-174  
 production of formyl species, 239-240  
 reactions with ammonia, 6  
 reactions with crude oil derivatives, 14t

Synthesis gas--Continued

- role in production of vinyl acetate, 136-152
  - routes to industrial chemicals, 2
  - selective generation of acetic acid, 98
  - sources, 42
  - use, 3t
  - vinyl acetate production, 139f
- Synthol reactors
- Fischer-Tropsch synthesis, 21
  - selectivities obtained, 28

## T

- Tars, Fischer-Tropsch process, 32
- Temperature
  - effect on acetaldehyde production, 127
  - effect on alcohol synthesis, 239
  - effect on hydrogen-carbon dioxide feedstocks, 241
  - effect on methanol carbonylation reactions, 214
- Temperature-programmed desorption
  - ammonia, 201f
  - methanol, 200f
  - methanol ammoxidation, 198-202
- Temperature-programmed reduction, ferric molybdate and manganese pyrophosphate catalysts, 200f
- Temporal analysis of products (TAP) reactor
  - mass intensity vs. time curve, 199f
  - methanol ammoxidation, 195-198
  - system description, 191
  - system used for fundamental catalyst studies, 191f
- Tetrabutylphosphonium bromide, use in acetic acid production, 102
- Tetraglyme, solvent for acetaldehyde formation, 131
- Thermoanalyzer, use in ammoxidation study, 191
- Tin, role in nickel-catalyzed methanol carbonylation, 64
- Transesterification, dimethyl sebacate, 93

- Triethylamine
  - effect on rhodium-ruthenium catalyst systems, 117
  - promoter similarity to cesium, 112
- Trimethylorthoformate
  - dehydration agent use in adipic acid synthesis, 85
  - synthesis, 85
- Triphenylphosphine, promoter
  - ability, 163
- Triphenylphosphine oxide, promoter
  - ability, 165
- Triphenylphosphinesulfide, promoter
  - ability, 165
- Triphenylstannide anion, formation of nickel-carbonyl complexes, 74
- Turnover frequency (TOF),
  - definition, 210

## V

- Vinyl acetate
  - common production reaction, 136
  - obtained via ethylidene diacetate, 7
  - production via methanol and synthesis gas, 136-152
- 4-Vinylcyclohexene,
  - dicarbonylation, 86

## W

- Water
  - byproducts of alcohol synthesis, 46-48
  - effect on methanol carbonylation, 71-72
  - partial pressure effect on rate of dimethyl ether carbonylation, 179
- Waxes, uses, 30

## X

- X-ray diffraction, use in ammoxidation of methanol, 192

*Production and indexing by Keith B. Belton  
Jacket design by Pamela Lewis*

*Elements typeset by Hot Type Ltd., Washington, DC  
Printed and bound by Maple Press Co., York, PA*